

RICE UNIVERSITY

**Impact Loading and Functional Tissue Engineering
of Articular Cartilage**


by


Roman M. Natoli


A THESIS SUBMITTED
IN PARTIAL FULFILLMENT OF THE
REQUIREMENTS FOR THE DEGREE

Doctor of Philosophy

APPROVED, THESIS COMMITTEE


Kyriacos Athanasiou, Committee Chair
Karl F. Hasselmann Professor
Department of Bioengineering


Jane Grande-Allen, Associate Professor
Department of Bioengineering


Michael Gustin, Professor
Department of Biochemistry and Cell Biology

HOUSTON, TEXAS

OCTOBER 2008

UMI Number: 3362374

INFORMATION TO USERS

The quality of this reproduction is dependent upon the quality of the copy submitted. Broken or indistinct print, colored or poor quality illustrations and photographs, print bleed-through, substandard margins, and improper alignment can adversely affect reproduction.

In the unlikely event that the author did not send a complete manuscript and there are missing pages, these will be noted. Also, if unauthorized copyright material had to be removed, a note will indicate the deletion.



UMI Microform 3362374

Copyright 2009 by ProQuest LLC

All rights reserved. This microform edition is protected against unauthorized copying under Title 17, United States Code.

ProQuest LLC
789 East Eisenhower Parkway
P.O. Box 1346
Ann Arbor, MI 48106-1346

Abstract

Impact Loading and Functional Tissue Engineering of Articular Cartilage

by

Roman M. Natoli

This thesis presents two advances for alleviating the problem of articular cartilage degeneration: mitigating degradative changes that follow mechanically induced injuries and growing functional neo-cartilage for diseased tissue replacement. Experiments demonstrate that cartilage subjected to a single, non-surface disrupting 1.1 J (Low) impact experiences sufficient degeneration over 4 weeks to become functionally equivalent to tissue subjected to a single, surface disrupting 2.8 J (High) impact. By 24 hrs post High impact, cell death and sulfated glycosaminoglycan (sGAG) release increased, changes in gene expression distinguished injured from adjacent tissue, and compressive stiffness decreased. In contrast, Low impacted tissue did not show decreased compressive stiffness until 4 weeks, revealing that Low impacted tissue experiences a delayed biological response.

Post-injury treatment with the polymer P188, growth factor IGF-I, or matrix metalloproteinase inhibitor doxycycline partially ameliorated cell death and sGAG loss, two detrimental changes that occurred following either Low or High impact. With 1 week of treatment after Low impact, P188 reduced cell death 75% and IGF-I decreased sGAG release 49%. Following High impact, doxycycline treatment reduced 1 and 2 week sGAG release by 30% and 38%, respectively.

As a novel method for engineering functional replacement tissue to use in cases of established disease, the GAG degrading enzyme chondroitinase ABC (C-ABC) improved the tensile integrity of articular cartilage constructs grown with a scaffold-less approach. C-ABC application increased ultimate tensile strength and tensile stiffness, reaching values of 1.4 and 3.4 MPa, respectively. Moreover, construct collagen concentration was ~22% by wet weight. Though C-ABC temporarily depleted sGAG, by 6 weeks no significant differences in compressive stiffness remained. Furthermore, chondrocyte phenotype was maintained, as constructs contained collagen type II, but not collagen type I. Decorin decreased following C-ABC treatment, but recovered during subsequent culture. The known ability of decorin to control collagen fibrillogenesis suggests a putative mechanism for C-ABC's effects.

Diseased articular cartilage heals poorly. For patients, the last resort is total joint replacement, though its associated morbidity and the limited lifespan of its results drive the need for alternate treatment strategies. Decreasing degradative changes post-injury and increasing functional properties of engineered cartilage are two significant improvements.

Acknowledgements

This thesis is not so much an event; it was a process. Further, the past 4.5 years at Rice University it took to create this work are a personal coming of age story, only partly contained within the research written herein. For the personal and academic support, guidance, and successes/failures, I owe a debt of gratitude much greater than can be expressed, and to many more people than can be listed, in this section.

I would first like to thank my thesis advisor, Dr. Kyriacos Athanasiou, for his unwavering mentorship, healthy perspective on life, and generous praise and support. I also thank the other members of my thesis committee, Dr. Michael Gustin and Dr. Jane Grande-Allen for their insightful comments on my research progress at varied points along the way. Additional thanks to Dr. Jane Grande-Allen for sharing her lab space and graduate students with me from time to time.

I have only accomplished the work in this thesis by standing on the broad shoulders of those before me. Sincere thanks to all the members of the Rice Musculoskeletal Bioengineering laboratory past, present, and future. To the past members, thank you for laying a solid foundation for me to build upon. To the present members, thank you for the ever present push and pull that makes our collective research the unique contribution that it is. To the future members, thanks for the reminder to do things "right," since it is you all that will be moving forward from where I leave off. Particular thanks to Dr. Corey Scott for the boot-camp in cartilage impact research, Dr. Jerry Hu for showing me that wandering

stories do have a point, and Dr. Chris Revell for imparting to me some degree of attention to detail. To Drs. Gwen Hoben and Dierdre Anderson and the soon to be Dr. Najmuddin Gunja, I could not have made this journey without you all. To Mr. Donald Responte and Mr. Gidon Ofek, thanks for working with me on certain projects. You all provided the energy and courage needed to carry on, energy and courage I hope you all will keep as you finish your own courses of study.

Over the past years I have also had the great pleasure of working with several extremely bright undergraduate students: Mr. Todd Blumberg, Mr. Ben Lu, Ms. Stacey Skaalure, Ms. Shweta Bijlani, and Mr. Ke Xun Chen. Thank you for your hard work and long hours, and for the steadfast questioning that kept me on my game. Additionally, thanks specifically to several graduate students from the Grande-Allen and Raphael laboratories for helping me out along the way. Thank you to Valhalla for providing a reasonable outlet from the laboratory and for the cross-disciplinary, cross-generation, and cross-cultural relationships and conversations only you can provide.

I would also like to offer special thanks to the Baylor College of Medicine MSTP program. Thank you to the co-directors for career mentorship. Thank you also to the other members of my MSTP class. Our solidarity has been a firm support during these years. Thank you to Dr. Scott Basinger for the heartfelt, straightforward, and poignant conversations we have had. Thank you to Kathy Crawford, MSTP program administrator, for all that you have done to help me make it to this day. Your efforts do not go unnoticed.

I believe that a person is only as good as the support around himself or herself, and that we are a product of the many relationships we form. I have been unbelievably blessed in this way. Thank you to Ms. Leah MacDougal; I am forever changed by you. Thank you to my college roommates (the “brothers 321”) who remain some of my closet friends and biggest fans. Thanks also to Mr. Ankur Nagaraja and Dr. Nick Snively; you two are one of a kind people. A very special thank you to Ms. Eileen Meyer, for keeping me running with your many meals and for making me “+ n” smarter.

Finally, to all of my family, I know the time I work and the distance between us keeps us from sharing many moments, but know that you all are *a/ways* in my heart and on my mind. Mom, Dad, Delena, Mark, Nona, and Pa, thank you so much for allowing me the freedom to make the choices and take the route I have. Thanks also to my aunts, uncles, and cousins, whose e-mails and phone calls at various times have been precisely what I needed. Last but not least, as the Psalmist said, “What a glorious Lord! He who daily bears our burdens also gives us our salvation.” For teaching me the lessons of humility, patience, and steadfastness through my research, thank you Lord.

- Roman M. Natoli

Table of Contents

Abstract	ii
Acknowledgements	iv
Table of Contents	vii
List of Tables	xiii
List of Figures	xiv
Introduction and Background	1
Global objective and specific aims	1
Articular cartilage: Basic biology and function	4
Osteoarthritis: The burden and its relation to injury	7
Cartilage injury, impact, and molecular biology post-impact	9
Tissue engineering	12
Overview of thesis chapters	16
Chapter 1: Injurious loading of articular cartilage: Mechanical and biological responses and post-injury treatment	19
Abstract	19
Introduction	20
Mechanical response of articular cartilage to mechanical injury	22
<i>Analytical and computational models</i>	<i>22</i>
<i>Contact and surface damage</i>	<i>25</i>
<i>Mechanical properties of articular cartilage measured during injurious loading</i>	<i>28</i>
<i>Perspectives on modeling the mechanical behavior of articular cartilage during injury</i>	<i>31</i>
Biological response of articular cartilage to mechanical injury	32
<i>In vivo investigations</i>	<i>33</i>
<i>- Proteoglycan loss, surface fibrillation, and inflammation</i>	<i>33</i>
<i>- Changes in mechanical properties and subchondral bone thickening</i>	<i>34</i>
<i>In vitro investigations</i>	<i>36</i>
<i>- Cell death</i>	<i>36</i>
<i>- Proteoglycan release and synthesis</i>	<i>41</i>
<i>- Decreased tissue stiffness</i>	<i>42</i>
<i>Perspectives on the biological response of articular cartilage from different models of mechanical injury</i>	<i>44</i>
Interventions following mechanically-induced cartilage injury	45
<i>Interventions targeting cell death</i>	<i>45</i>
<i>Interventions targeting sGAG release and others</i>	<i>49</i>
Conclusions	51

Chapter 2: Temporal effects of impact on articular cartilage cell death, gene expression, matrix biochemistry, and biomechanics	58
Abstract.....	58
Introduction	59
Materials and methods.....	62
<i>Tissue harvest and articular cartilage impact</i>	<i>62</i>
<i>Explant culture and processing.....</i>	<i>63</i>
<i>Viability staining.....</i>	<i>64</i>
<i>RNA isolation and qRT-PCR</i>	<i>65</i>
<i>Biochemical characterization.....</i>	<i>66</i>
<i>Creep indentation biomechanical properties</i>	<i>67</i>
<i>Statistical analysis</i>	<i>68</i>
Results.....	69
<i>Impact measurements.....</i>	<i>69</i>
<i>Gross morphology and cell viability.....</i>	<i>69</i>
<i>qRT-PCR.....</i>	<i>71</i>
<i>Biochemistry.....</i>	<i>73</i>
<i>Biomechanics</i>	<i>74</i>
Discussion	75
 Chapter 3: P188 reduces cell death and IGF-I reduces GAG release following single-impact loading of articular cartilage	 91
Abstract.....	91
Introduction	92
Materials and methods.....	95
<i>Articular cartilage tissue harvest.....</i>	<i>95</i>
<i>Impact of articular cartilage</i>	<i>96</i>
<i>Explant and culture of articular cartilage.....</i>	<i>96</i>
<i>Explant processing</i>	<i>98</i>
<i>Gross morphology and cell viability</i>	<i>98</i>
<i>GAG release to media</i>	<i>99</i>
<i>Creep indentation biomechanical testing.....</i>	<i>100</i>
<i>Statistical analysis</i>	<i>100</i>
Results.....	101
<i>Compression protocol.....</i>	<i>101</i>
<i>Gross morphology</i>	<i>102</i>
<i>GAG release to media</i>	<i>102</i>
<i>Cell viability.....</i>	<i>103</i>
<i>Biomechanical properties</i>	<i>104</i>
Discussion	105
 Chapter 4: Effects of doxycycline on articular cartilage GAG release and mechanical properties following impact.....	 118
Abstract.....	118
Introduction	119
Materials and methods.....	122
<i>Articular cartilage tissue harvest.....</i>	<i>122</i>

<i>Impact of articular cartilage</i>	122
<i>Explant and culture of articular cartilage</i>	123
<i>Histology</i>	124
<i>GAG release to media</i>	124
<i>Creep indentation biomechanical testing</i>	124
<i>Statistical analysis</i>	125
Results.....	126
<i>Histology</i>	126
<i>GAG release</i>	126
<i>Biomechanical properties</i>	128
Discussion	129

Chapter 5: Collagens of articular cartilage: structure, function, and their importance in tissue engineering141

Abstract.....	141
Introduction	141
Biology of articular cartilage collagens.....	143
<i>Types of collagen</i>	143
- <i>Collagen II</i>	143
- <i>Collagen IX</i>	144
- <i>Collagen XI</i>	144
- <i>Collagen VI</i>	145
- <i>Collagen I</i>	145
- <i>Collagen X</i>	146
<i>Collagen crosslinks</i>	146
<i>Collagen fibrillogenesis</i>	148
<i>Ultrastructure of articular cartilage</i>	149
- <i>Organization of collagen</i>	149
- <i>Ultrastructure development</i>	151
<i>Collagen interactions with other matrix molecules</i>	152
<i>Collagen-cell interactions</i>	152
<i>Summary</i>	153
Collagen mechanics: theoretical, computational, and experimental insights	154
<i>Fibrillar and molecular stiffness of collagen</i>	154
<i>Theoretical and computational models incorporating the effects of collagen</i>	155
- <i>Fiber reinforced continuum models</i>	155
- <i>Other models incorporating features of the collagen network</i>	158
<i>Experimental findings identifying the varied roles of collagen in mechanics</i>	159
- <i>Effects of collagen amount, orientation, and intrinsic viscoelasticity on tensile properties</i>	159
- <i>Effects of crosslinking on tensile properties</i>	160
- <i>The role of collagen in compression</i>	161
<i>Summary</i>	163
Experimental methods for collagen assessment.....	163
<i>General collagen assessment</i>	164

<i>Immunohistochemistry (IHC) and enzyme-linked immunosorbent assays (ELISAs)</i>	165
<i>Electron microscopy</i>	166
- <i>Scanning electron microscopy (SEM)</i>	167
- <i>Transmission electron microscopy (TEM)</i>	168
<i>Assessing collagen orientation</i>	169
<i>Assessing collagen inhomogeneity</i>	170
<i>Crosslink assessment</i>	170
<i>Summary</i>	171
Role of collagen in articular cartilage tissue engineering	172
<i>Significance of collagen in tissue engineering</i>	172
<i>Engineering the collagen network</i>	172
- <i>Collagen scaffolds for tissue engineering</i>	172
- <i>Collagen content</i>	173
- <i>Crosslinking</i>	175
- <i>Network organization</i>	177
<i>Summary</i>	177
Conclusions	178
 Chapter 6: Chondroitinase ABC treatment results in increased tensile properties of self-assembled tissue engineered articular cartilage	185
Abstract	185
Introduction	186
Materials and methods	188
<i>Chondrocyte isolation, self-assembly, and culture</i>	188
<i>Gross morphology, histology, and IHC</i>	189
<i>Biochemical analysis</i>	190
<i>Creep indentation testing</i>	191
<i>Tensile testing</i>	192
<i>Statistical analysis</i>	192
Results	192
<i>Gross characteristics</i>	192
<i>Histology and IHC</i>	193
<i>sGAG content, cell number, and percent water</i>	193
<i>Total collagen and collagens type I and type II ELISAs</i>	194
<i>Biomechanics</i>	194
Discussion	195
 Chapter 7: Effects of multiple chondroitinase ABC applications on tissue engineered articular cartilage	206
Abstract	206
Introduction	207
Materials and methods	209
<i>Chondrocyte isolation and culture</i>	209
<i>C-ABC treatment and construct processing</i>	210
<i>Gross morphology, histology, and immunohistochemistry (IHC)</i>	211
<i>Biochemical analysis</i>	212

<i>Creep indentation testing</i>	213
<i>Tensile testing</i>	214
<i>Statistical analyses</i>	214
Results.....	215
4 week experiment	215
6 week experiment	217
Discussion	219
Conclusions and Future Directions	227
Mechanical injury of articular cartilage: Tissue's temporal response and amelioration of degradative changes	227
Tissue engineering of articular cartilage: Increased functional properties with chondroitinase ABC	231
Future Directions	235
References	239
Appendix 1: <i>In situ</i> mechanical properties of the chondrocyte cytoplasm and nucleus	285
Abstract.....	285
Introduction	286
Materials and methods.....	287
Results.....	288
Discussion	289
Appendix 2: Validation, pilot, and supplemental data for various articular cartilage impact experiments	295
Introduction	295
Methods	296
<i>Compression device fabrication and validation</i>	296
<i>Doxycycline pilot experiment</i>	296
<i>FACE analysis of culture media post-injury</i>	297
Results.....	297
<i>Compression device fabrication and validation</i>	297
<i>Doxycycline pilot experiment</i>	298
<i>FACE analysis of culture media post-injury</i>	298
Summary	298
Appendix 3: Mechanical properties of immature bovine articular cartilage and mechanical testing of self-assembled articular cartilage constructs	303
Introduction	303
Methods	304
<i>Tissue acquisition and mechanical testing of cartilage explants</i>	304
<i>Generation of self-assembled constructs for mechanical testing</i>	305
<i>Construct compressive testing</i>	306
<i>Construct tensile testing to failure</i>	307
<i>Construct stress-relaxation tensile testing</i>	308

<i>Statistics</i>	309
Results	310
<i>Tissue explants</i>	310
<i>Construct creep indentation testing</i>	310
<i>Construct tensile testing to failure</i>	311
<i>Construct stress-relaxation tensile testing</i>	311
Discussion	311
Appendix 4: Transmission electron microscopy images of self-assembled constructs	321
Introduction	321
Methods	321
<i>Tissue processing of self-assembled constructs</i>	321
<i>Transmission electron microscopy</i>	322
Results	322
Discussion	323

List of Tables

Table 1-I: Post-injury interventions affecting cell death	54
Table 1-II: Post-injury interventions affecting glycosaminoglycan release, tissue stiffness, and progenitor cells	55
Table 2-I: qRT-PCR target gene primers and probes and dyes and quenchers	83
Table 2-II: Impact measurements for the Low and High levels	84
Table 2-III: Data for tissue matrix biochemical content.....	84
Table 3-I: Gross morphology grading scale	113
Table 3-II: Tissue permeability and Poisson's ratio as measured by creep indentation	114
Table 4-I: Tissue permeability and Poisson's ratio as measured by creep indentation	136
Table 5-I: Zonal variation in collagen fibril characteristics, collagen content, and mechanical properties	180
Table 5-II: Select studies showing effects of mechanical stimulation on collagen in tissue engineered cartilage	180
Table 6-I: Construct thickness, diameter, and total wet weight	201
Table 7-I: Construct GAG and collagen content normalized to wet weight	223
Table A1-I: Effect of Poisson's ratio combinations on cytoplasmic and nuclear stiffnesses for the initial coarse search.....	292
Table A3-I: Mechanical properties of immature bovine articular cartilage	316

List of Figures

Figure I-1: Thesis overview	3
Figure I-2: Articular cartilage structure	5
Figure I-3: Tissue engineering process	15
Figure 1-1: Framework for mechanical injury of living tissues	56
Figure 1-2: Different models used for mechanical injury of articular cartilage	57
Figure 2-1: Cell viability staining	85
Figure 2-2: Quantification of cell viability	86
Figure 2-3: Temporal profile of gene expression	87
Figure 2-4: 24 hr gene expression	88
Figure 2-5: Cumulative sGAG release	89
Figure 2-6: Tissue compressive stiffness	90
Figure 3-1: Tissue response immediately post-injury	115
Figure 3-2: Tissue response 24 hrs post-injury	116
Figure 3-3: Tissue response 1 week post-injury	117
Figure 4-1: Experimental timeline	137
Figure 4-2: Histology	138
Figure 4-3: Cumulative sGAG release data	139
Figure 4-4: Compressive stiffness	140
Figure 5-1: Hierarchical structure of a collagen fiber	181
Figure 5-2: Development of tissue-level collagen anisotropy	182
Figure 5-3: Split-lines	183
Figure 5-4: Mechanical models of articular cartilage incorporating collagen	184
Figure 6-1: Gross morphology and histology	202
Figure 6-2: Construct sGAG concentration and compressive stiffness	203
Figure 6-3: Collagen type II production	204
Figure 6-4: Construct tensile properties	205
Figure 7-1: Histology and IHC	224
Figure 7-2: 4 week biomechanical properties	225
Figure 7-3: 6 week biomechanical properties	226
Figure C-1: Model of articular cartilage's response to injury and treatment post-impact	230
Figure C-2: Growth of tissue engineered articular cartilage	234
Figure A1-1: Axisymmetric finite element model of chondrocyte and nucleus	293
Figure A1-2: Cost function (δ_{RMS}) plots	294
Figure A2-1: Compression device design and validation data	300
Figure A2-2: sGAG release data from doxycycline pilot	301
Figure A2-3: Data for HA release post-impact injury	302
Figure A3-1: Aggregate modulus resulting from different tare/test loads	317
Figure A3-2: Representative data for tensile test to failure	318
Figure A3-3: Construct tensile properties at different strain rates	319
Figure A3-4: Stress-relaxation of a self-assembled construct	320
Figure A4-1: Representative TEM images	325
Figure A4-2: Select TEM image showing a collagen fiber	326

Introduction and Background

Global objective and specific aims

The purpose of the work contained in this thesis was to identify and develop ways to slow or prevent injured articular cartilage from becoming diseased and to grow replacement cartilage with enhanced functional properties for use in situations of established disease. Based on this global objective, three specific aims were employed. In the first specific aim, articular cartilage injury was simulated *ex vivo* using impact experiments, and the temporal response of the tissue was characterized. The main hypothesis was that a low level of injury, given enough time, could become similar to a high level of injury. Using results from the first aim, the second aim employed targeted interventions in the form of poloxamer 188 (P188), insulin-like growth factor I (IGF-I), and doxycycline (an inhibitor of matrix degrading enzymes) for the treatment of cell death and sulfated glycosaminoglycan (sGAG) loss post-impact. The hypothesis was that these treatments could mitigate prominent degradative changes characterized in specific aim one, potentially leading to preserved tissue functionality, as measured by compressive stiffness.

From the other direction, tissue engineering is a potential solution in the case of established articular cartilage disease, but creating constructs with mechanical properties sufficient to function in the demanding *in vivo* loading environment remains a challenge. Hence, in the final specific aim of this work, chondroitinase ABC (C-ABC), a GAG degrading enzyme, was investigated as a

novel technique for increasing the tensile properties of tissue engineered articular cartilage. The hypotheses were that C-ABC treatment would increase construct tensile properties without permanently destroying GAG content and compressive properties, and that decorin has a potential role in increasing the tensile integrity.

Figure I-1 depicts the overall approach of this thesis. The results of this work demonstrate that Low impacted (1.1 J) articular cartilage experiences a delayed biological response, experiencing degradation similar in to High impacted (2.8 J) tissue at 4 weeks. Further, the interventions P188, IGF-I, and doxycycline were able to partially mitigate cell death and sGAG loss from the tissue post-injury. Finally, C-ABC application increased the tensile integrity of tissue engineered constructs, making it an innovative, counter-intuitive approach for functional articular cartilage tissue engineering.

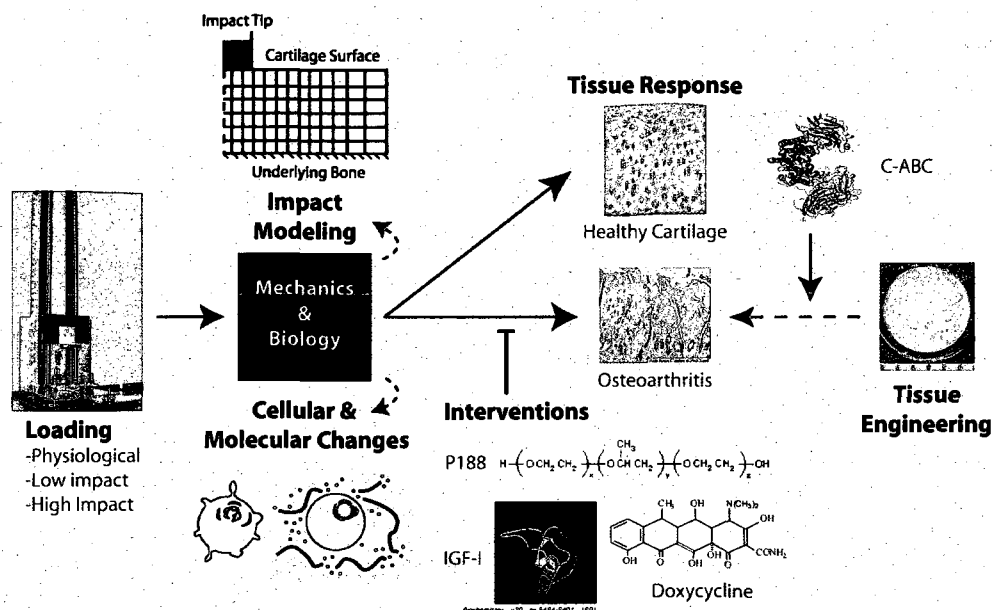


Figure I-1: Overall concept of this thesis. Articular cartilage is constantly subjected to loading, be it physiologic or pathologic, e.g., impact overloading. The tissue then responds to loading both mechanically and biologically. This unknown response is depicted by the central “black box.” Based on the tissue’s response, cartilage can go down a pathway by which healthy tissue is maintained or a pathway leading to joint disease, such as osteoarthritis. In terms of articular cartilage injury research, it is desirable to understand what determines the responses that occur within the “black box.” The immediate mechanical response can be understood through analytical and computational models, whereas understanding the biological response can be achieved through cellular and molecular biological approaches. This thesis focuses on the biological response, an example of which is cell death. What we learn from the biological response can then become targets for interventions to prevent the pathway leading to diseased tissue. P188, IGF-I, and doxycycline are the particular treatments studied in this thesis. Finally, tissue engineering can be used to grow tissue that may one day be used to replace diseased tissue. In this thesis, chondroitinase ABC (C-ABC) was used as a novel strategy to increase the tensile properties of engineered constructs, which brings us one step closer to growing replacement tissue with sufficient mechanical properties to function in the native loading environment experienced by articular cartilage.

Articular cartilage: Basic biology and function

Articular cartilage is a special type of hyaline cartilage that lines the articulating surface of bones. It is a tissue devoid of vasculature, nerves, and lymphatics.²³⁰ Articular cartilage tissue consists of its sole resident cell type, chondrocytes, and the extracellular matrix (ECM) they produce (Fig. I-2A). Though essential for tissue maintenance, chondrocytes make up only 1-5% of the tissue by volume.²³⁰ Further, they are thought to be post-mitotic. The remaining ECM is largely composed of collagen and proteoglycans (Fig. I-2B). The collagen is primarily type II, but trace amounts of other collagens (i.e., types VI, IX, and XI) can also be found.²⁶³ In terms of proteoglycans, the most abundant species is aggrecan, but others known as small leucine-rich proteoglycans, such as decorin, biglycan, and fibromodulin, are also present. These small proteoglycans play important roles in organizing the ECM. For example, decorin has been shown to decrease the amount of collagen incorporated into fibrils during fibrillogenesis and to limit fibril diameter.¹³⁵ The two main sGAG chains attached to proteoglycans found in cartilage are keratan and chondroitin sulfate.²³⁰ Additionally, there are dermatan and heparan sulfates. Cartilage also contains a significant amount of hyaluronic acid, a non-sulfated GAG. Hyaluronic acid binds proteoglycans through link proteins (Fig. I-2C), and proteoglycans electrostatically bind to the collagen type II fibers.²⁶³ However, the solid portion of cartilage tissue is only ~15-40% of the wet weight, of which 15-22% is collagen type II and 4-7% is proteoglycan. The rest of cartilage is predominantly water, constituting 60-85% of its total weight.³⁴⁹

Figure I-2: Articular cartilage structure

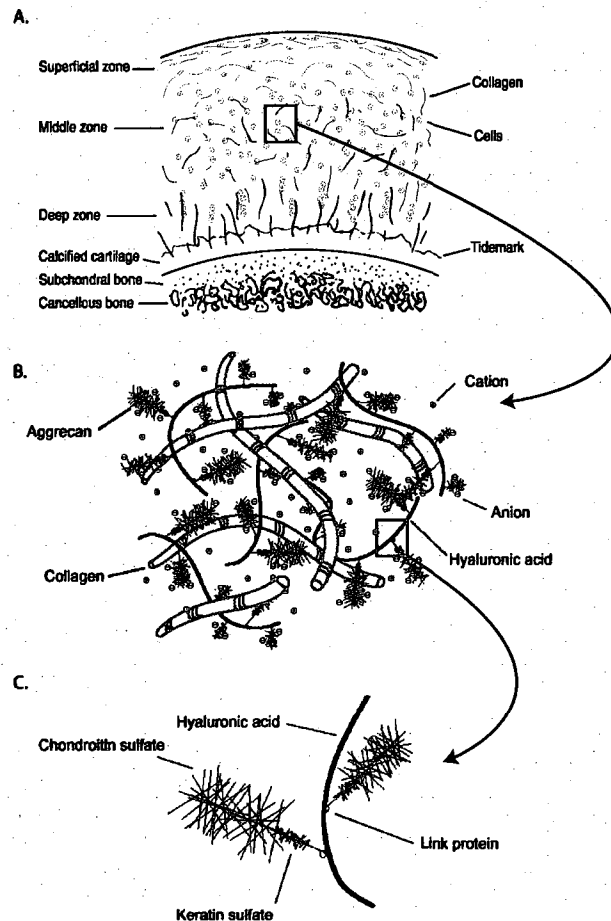


Figure I-2: This figure was adapted from *Structure and Function of Articular Cartilage*, by Hu and Athanasiou.²³⁰ This figure depicts important features of articular cartilage from the tissue level down to the molecular level. Articular cartilage is described in terms of its zonal arrangement, consisting of the superficial, middle, and deep zones (A). The predominant characteristic defining each zone is collagen orientation, which, classically, is parallel to the articulating surface in the superficial zone, randomly oriented in the middle zone, and perpendicular to the subchondral bone in the deep zone. Additionally, the zones have distinctive biochemical content and biomechanical properties. The extracellular matrix of articular cartilage, which is completely inundated by water, is predominantly composed of collagen type II and aggrecan (B). Another important component of the extracellular matrix is hyaluronic acid (C), which forms a backbone that the core protein of aggrecan connects to via link protein. The sulfated glycosaminoglycan side chains of aggrecan are chondroitin and keratin sulfate.

The structure of cartilage directly contributes to the description of it as a biphasic material. Being composed of a solid matrix inundated by a fluid, both consolidation³³³ and mixture theories³⁴⁶ have been extensively used to describe its behavior. Based on the linear biphasic theory,³⁴⁷ three material properties describe articular cartilage in compression. These properties are the aggregate modulus (measure of tissue's compressive stiffness), permeability (measure of resistance to fluid flow), and Poisson's ratio (ratio of lateral to axial deformation). In terms of tensile mechanical properties, articular cartilage has been described using linear elasticity,²⁷⁴ from which Young's modulus (measure of tensile stiffness) and Poisson's ratio can be determined. Additionally, ultimate tensile strength (maximum stress achieved before failure) is measured. Unlike standard engineering materials, it is difficult to define values for the material properties of articular cartilage. This difficulty occurs because the material properties vary from joint to joint, by location within a joint, as a function of depth within the tissue, from species to species, in healthy versus diseased states, as a function of hormone status, and dependent upon age of the tissue, to name a few.^{17,29,100,146,230,274,349,471,493,494,501} The tissue is frequently subjected to a multitude of loading conditions, such as tension and compression. Predominantly, it is held that the collagen network governs the tissue's tensile behavior, while proteoglycans are responsible for the compressive behavior.

The combined biochemical structure and mechanical characteristics of cartilage allow it to perform its functions, but they are also responsible for tissue failure in disease. The normal function of articular cartilage is to provide wear

resistance, a smooth, frictionless surface for joint movement, and to bear and distribute loads. Unfortunately, the avascular, aneural, alymphatic characteristics of cartilage, coupled with the paucity of chondrocytes, cause it to be a tissue largely incapable of repairing itself after damage.²⁴¹ The difficulty associated with treating cartilage injury has been documented for centuries.²³⁹ Following injury, cartilage forms mechanically inferior fibrocartilage-like tissue,^{87,190} which is unable to perform the required functions. Fibrocartilage typically has more collagen type I and contains less GAGs. These biochemical changes lead to changes in the tissue's mechanical properties.^{68,442} The repair tissue ultimately breaks down, and a vicious cycle of degeneration ensues leading to the degenerative joint disease known as osteoarthritis (OA).

Osteoarthritis: The burden and its relation to injury

OA is a significant problem worldwide, especially in developed countries. In western nations, it is estimated that up to 2.5% of the GNP is spent on arthritis,⁴⁰⁶ and, in the United States, \$65 billion are spent annually.²⁴⁹ Thus, the economic burden of this disease to society is great. Further, there are complicated medico-legal issues surrounding this disease, such as time to disease development in personal injury suits.⁵⁰⁹ While these are important considerations, the ultimate burden of OA is borne by the patient. It is estimated that 10% of the world's population aged 60 years or more has OA,⁷⁷ making it a leading cause of disability.⁶⁶ OA is also associated with some of the poorest quality of life issues,⁴⁰⁶ particularly in terms of pain and physical function. With

respect to these issues, patients fare less well than those with gastrointestinal disorders, chronic respiratory diseases, and cardiovascular conditions.

Clinically, OA is divided into two types: primary (absence of a known cause for joint degeneration) and secondary.⁷⁷ It is believed that a majority of secondary OA is attributable to traumatic joint injury that may have occurred years previously.^{75,322,416} These cases are known as post-traumatic OA. For example, the Clearwater OA study showed a 7.7 relative risk ratio for developing OA in individuals reporting a history of knee injury.⁴⁹⁰ Impact injuries, such as those that happen during motor vehicle collisions, falls, and sporting incidents, have been implicated in the development of post-traumatic OA, though the precise pathophysiology is not fully understood.^{66,102}

To reproduce these observations, investigators have begun to employ impact-induced injury models.^{373,460} In one *in vivo* study, canine patellofemoral joints were impacted and changes were followed for six months. Initially there was only fracture in the calcified zone of cartilage; however, by six months, surface fissuring, proteoglycans loss, expression of inflammatory markers, and cell cloning were evident, suggesting progression to arthritic like degeneration.⁴⁶⁰ More recently, *in vitro* impact has also reproduced changes reminiscent of OA.²⁴² Further study of impact-induced cartilage injury is important for understanding its pathology. This thesis investigates early responses (4 weeks or less) of articular cartilage to two levels of impact injury.

The major pathways of degeneration in cartilage leading to OA are cell death,³ matrix breakdown,^{276,321} and inflammation.^{124,221} While work done thus far

provides clues into the pathogenesis of OA, more extensive investigation is necessary. In one study qRT-PCR was used to study nine genes in regions of normal and osteoarthritic cartilage, from which it was determined that there is a possible phenotypic shift in the tissue.⁵¹⁷ Moreover, two studies have employed microarray technology to identify changes in osteoarthritic cartilage. Zhang et al.⁵²³ used microarray analysis to show that beta-2 microglobulin up-regulates 20 genes in OA chondrocytes. Another group showed through cluster analysis that genes regulating collagen synthesis and cell proliferation were co-expressed, suggesting a possible wound response.⁴²⁷ These types of studies allow for a big picture of cartilage biology to be formed, providing essential data needed for identifying potential disease markers or targets for intervention.

Cartilage injury, impact, and molecular biology post-impact

In one classification of articular cartilage injuries, Buckwalter⁷⁵ describes a rubric based on 1) damage to joint surface that does not cause visible disruption, 2) mechanical disruption limited to the cartilage (partial thickness defect), and 3) disruption affecting both cartilage and the subchondral bone (osteochondral fracture). This is an important distinction because it is known that partial thickness articular cartilage defects are much less likely to have any healing response.³² The impact experiments performed in this thesis pertain only to the first two of the classifications in order to better understand and address cartilage specific injury.

To begin to understand the nature of cartilage impact biology, one must first understand what range of forces and time scales are experienced during

everyday physical activity. In a review of all techniques used to determine forces in the human knee, Komistek et al.²⁸⁵ determined that during walking/running, peak forces range from 1.9 to 7.2 times body weight. For a 70 kg person, this would correspond to ~140 to 4900 N. Taking the medial tibial plateau to have an area of 1670 mm²,⁵⁰² this corresponds to a maximum stress of ~3 MPa. During normal activities, like running, time to peak force is on the order of 30 ms, leading to a stress rate of 100 MPa/s. One can expect that impact injuries occur on a time scale an order of magnitude smaller, resulting in stress rates of 1000 MPa/s. Based on data such as these, Aspden et al.²⁶ put forth a definition for impact loading as time to peak load on the order of ms plus one of the following: 1) stress rate greater than 1000 MPa/s, 2) strain rate greater than 500 s⁻¹, or 3) loading rates in excess of 100 kN/s. The impact experiments performed in this thesis were designed to meet this definition.

Impact loading of articular cartilage leads to tissue injury and degeneration through effects on the chondrocytes and ECM, as well as gross tissue failure.⁴³⁰ Cartilage function is believed to deteriorate as a result of chondrocyte death,⁵² changes in the tissue's biochemical content,³²⁵ and weakening of the tissue's biomechanical properties, particularly the compressive stiffness.^{150,293,431} However, the majority of cartilage explant studies have investigated these changes only at early time points post-injury, leaving the chronology of these changes unknown. While the above studies underscore the detrimental effects that impact loading can produce, to further understand and eventually prevent post-traumatic OA, we need better temporal characterization of the molecular

changes and biomechanical behavior of articular cartilage post-impact loading. In particular, information is needed with regard to impact loading regimes that do not cause gross identifiable damage to help understand possible causes of 'idiopathic', or primary, OA.

Additionally, little work investigating gene expression following mechanical injury of articular cartilage has been performed. In one study, Lee et al.³⁰³ applied a single injurious compression to bovine cartilage explants and looked at gene expression profiles of 24 genes over the course of 24 hrs with qRT-PCR. They found increased expression of matrix degrading enzymes (MMP-3 and ADAMTS-5) and an endogenous inhibitor of such enzymes (TIMP-1). Further, clustering analysis revealed five groups of genes with distinct temporal expression patterns. In another gene expression study, a bovine cDNA microarray revealed several changes between control and injuriously compressed tissue 3 hrs post-injury, most notable of which was down-regulation of IGF-I. They also revealed increased matrix metalloproteinase-3 (MMP-3) expression, but decreased MMP-9, MMP-13, and Aggrecanase-1 expression.⁹⁴ Following a cyclical loading injury protocol, the canine Affymetrix gene chip was used to identify 172 genes with increased or decreased expression levels compared to uninjured controls. One gene, MIG-6, had never before been identified in cartilage.⁸³ Last, in a recent study the cartilage of porcine patellae was loaded at 25 mm/s and then cultured whole for 2 weeks. In contrast to previous work, MMP-3 had decreased expression in the injured tissue.²³ These studies highlight differences that could be resulting from various loading regimens, time post-injury, and/or species.

Further characterization of temporal gene expression profiles may aid in the discovery of clinical tools to prevent or manage post-traumatic OA. In this thesis, temporal gene expression is examined up to 4 weeks post-impact. While preventing and managing OA is desirable, some patients (e.g., those who are non-compliant or whose physician contact is limited or inconsistent) will invariably develop the disease. In such cases, cartilage replacement products and procedures are attractive.

Tissue engineering

The goal of articular cartilage tissue engineering is to grow replacement tissue with biochemical content and resulting biomechanical properties that will enable it to function in the demanding loading environment encountered when implanted in a joint. The need for replacing tissue that principally performs biomechanical functions has led to the field of functional tissue engineering.⁸⁵ In this approach, it is no longer enough for constructs to resemble the biological aspects of the tissue being engineered; they must also obtain suitable mechanical function.

To grow replacement tissue, the classical tissue engineering paradigm includes scaffolds, cells, bioactive agents, and bioreactors.¹⁴⁴ The scaffolds used for articular cartilage repair are many and varied, including autologous, natural, and synthetic scaffolds.¹⁷⁷ However, scaffold design and implementation are laden with challenges such as biocompatibility, need for enough mechanical integrity to withstand native loading conditions, and ideal degradation properties, whereby the scaffold disappears at a similar rate to which new tissue is

produced. Cell source is also an important consideration. Native, primary articular chondrocytes are limited in supply due to the relative acellularity of the tissue, but passaging of primary articular chondrocytes induces dedifferentiation.^{123,225,456} This problem has led to investigations of mesenchymal stem cells,²³³ embryonic stem cells,²⁸³ and cells isolated from the dermis¹²⁷ for use in articular cartilage tissue engineering, as these cell sources have advantages of availability and self-renewal, though identifying suitable differentiation regimens for these cells is a current challenge.¹⁴⁴ Finally, the purpose of bioactive agents and bioreactors is to motivate cells to produce and organize the ECM they produce, leading to increased biomechanical functionality. The effects of several types of mechanical stimulation (an example of bioreactors) and growth factors (an example of bioactive agents) have been reviewed elsewhere.^{120,121} During *in vitro* culture, cell seeded scaffolds are combined with bioactive agents and cultured under various bioreactor conditions to generate a tissue engineered construct with properties approaching native articular cartilage.

Recently, with the advent of the self-assembly process, our laboratory has departed from the classical tissue engineering paradigm by eliminating the use of a scaffold.²³¹ Though not the only form of scaffold-less articular cartilage tissue engineering,^{180,382,456} self-assembly has proven to be a significant advance. It has been shown that the self-assembly process is driven by N-cadherin expression and recapitulates several salient features of articular cartilage maturation, such as pericellular localization of collagen type VI.³⁷⁵ Though most commonly

employed with 5.5 million cells per construct, it has been shown that 3.75 million cells are sufficient in self-assembly for forming mechanically robust constructs, with sGAG and collagen content greater than that in agarose encapsulation and scaffold based systems.⁴⁰⁹ Self-assembly has also been undertaken in the presence of biomechanical stimulation^{143,232} and growth factor treatment,^{143,145} with the most exciting finding being an aggregate modulus (compressive stiffness) of 248 kPa, Young's modulus (tensile stiffness) of 2 MPa, sGAG content normalized to wet weight of 9.6%, and collagen content normalized to wet weight of 15.3%.¹⁴³ Self-assembly has also been used for tissue engineering of the knee meniscus,^{226,227} where it demonstrated the capability to be formed into the unique meniscus shape.³⁵

Though the self-assembly process has had numerous successes, insufficient tensile properties and collagen content are a well recognized hurdle for any articular cartilage tissue engineering approach.^{176,267,369,504} Hence, methods for increasing collagen content and tensile properties are desirable. Figure I-3 shows the current articular cartilage tissue engineering paradigm employed in our laboratory. Using primary immature bovine articular chondrocytes, this thesis investigates use of the matrix modifying enzyme C-ABC as an original methodology for increasing tensile properties of self-assembled tissue engineered articular cartilage constructs.

Figure I-3: Tissue engineering process

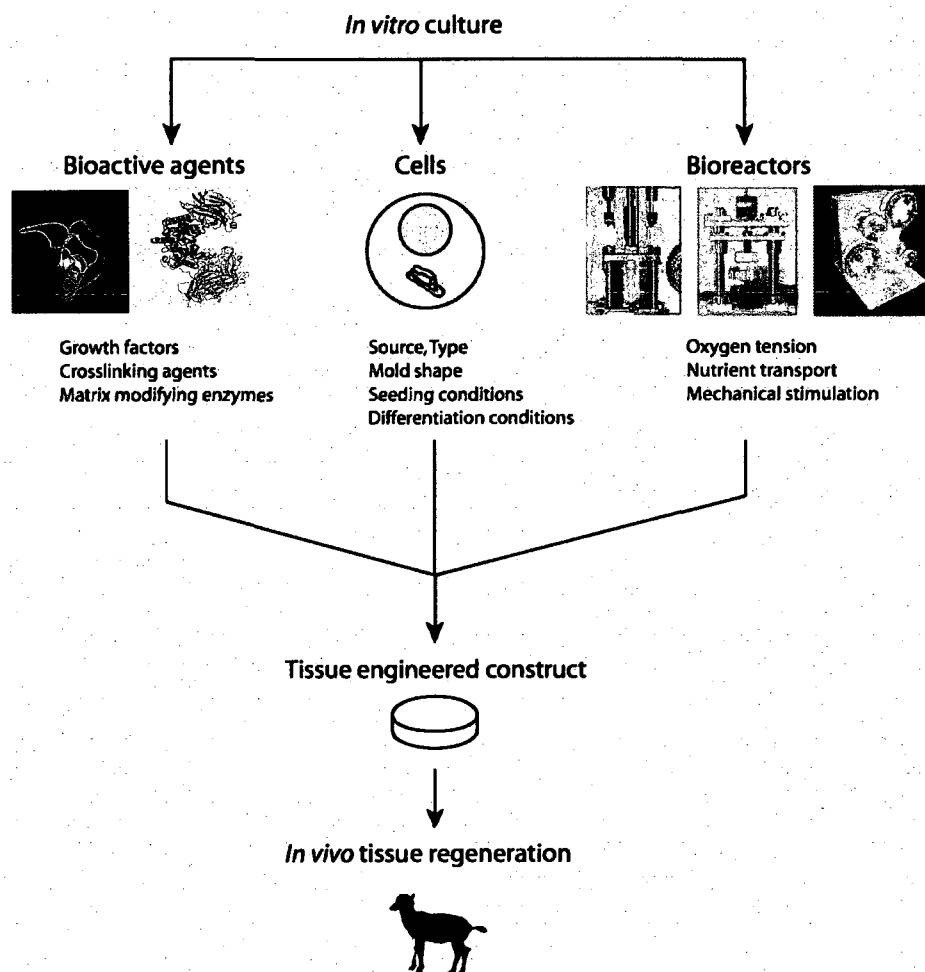


Figure I-3: A tissue engineering paradigm without scaffolds. This figure is modified from *Paradigms of Tissue Engineering with Applications to Cartilage Regeneration*, by Elder and Athanasiou.¹⁴⁴ During *in vitro* culture, cells are combined with bioactive agents and cultured under various bioreactor conditions. The net effect of these three components is generation of a functional tissue engineered construct with enhanced biochemical content and biomechanical properties approaching those of native articular cartilage. This thesis uses primary immature bovine articular chondrocytes in the self-assembly process.²³¹ Furthermore, a particular bioactive agent, the glycosaminoglycan degrading enzyme C-ABC, is investigated for the purposes of increasing construct tensile properties. Ultimately, these constructs will be implanted into animal models for *in vivo* regeneration of articular cartilage. Contingent upon success, clinical trials can be commenced.

Overview of thesis chapters

The above discussion was a brief introduction to articular cartilage, OA, impact injuries as a model for post-traumatic OA, and the tissue engineering approach. The remainder of this thesis provides more in depth review of salient literature, and the specific details and outcomes of studies concerning my global objective: *developing ways to slow or prevent injured tissue from becoming diseased and growing functional replacement cartilage for potential use in situations of established disease.*

In the first chapter, a detailed review of the articular cartilage mechanical injury field is presented, including a discussion of the post-injury treatment studies that have been published to date. Chapter 2 then describes a study characterizing the temporal effects of articular cartilage impact on cell death, gene expression, matrix biochemical content, and compressive biomechanical properties. Chapters 3 and 4 look at intervention strategies for ameliorating the degenerative changes characterized in Chapter 2. Chapter 3 presents an investigation of P188, IGF-I, and their combination for decreasing cell death in, and sGAG loss from, the injured tissue. Chapter 4 investigates the effects of doxycycline, an MMP inhibitor, on sGAG loss and compressive biomechanical properties post-injury. Collectively, Chapters 1-4 contain the work of this thesis pertaining to slowing degradative changes in an attempt to prevent injured tissue from becoming diseased.

Regarding cases of established disease, Chapters 5-7 contain the work of this thesis directed toward growing functional replacement cartilage. Chapter 5

contains a comprehensive review of the collagens of articular cartilage and methods to assess them, ending with a discussion of state of the art articular cartilage tissue engineering efforts with respect to the collagen network. Chapters 6 and 7 then describe a novel approach to increasing engineered articular cartilage collagen concentration and tensile properties using C-ABC. Chapter 6 describes a study where the work with C-ABC done in articular cartilage explants²¹ is extended to tissue engineering in a scaffold-less, serum-free system. Chapter 7 builds upon the results of Chapter 6, demonstrating that multiple C-ABC treatments lead to further increased construct tensile properties, that sGAG and compressive stiffness recover with longer culture time post-treatment, and suggesting that decorin may be part of the mechanism by which C-ABC causes an increase in tensile properties.

Additionally, there are several appendices at the end of this thesis. The first appendix is a short communication investigating the *in situ* mechanical properties of the chondrocyte's nucleus and cytoplasm using a finite element analysis approach. The discovery that the cytoplasm and nucleus have compressive stiffnesses more similar to each other than previously reported suggests that mechanical forces experienced at the tissue level may be directly imparted to the nucleus of the chondrocyte. Appendix 2 gives validation data for the compression protocol used in the P188/IGF-I study (Chapter 3), pilot data supporting the choice of doxycycline concentrations used in Chapter 4, and fluorophore assisted carbohydrate electrophoresis data showing hyaluronic acid is not released post-impact. Appendix 3 concerns the mechanical testing of self-

assembled tissue engineered articular cartilage constructs in both tension and compression, and the testing of immature bovine articular cartilage for comparison with results from tissue engineering studies. Finally, Appendix 4 provides transmission electron microscopy images supporting the first C-ABC study (Chapter 6).

Chapter 1: Injurious loading of articular cartilage: Mechanical and biological responses and post-injury treatment*

Abstract

Mechanical injury of many tissues initiates disease processes. In this review, a framework for mechanical injury to living tissues is discussed using articular cartilage as a model system. The framework separates the mechanical and biological responses of tissue to injury. The mechanical response is governed by the tissue's biomechanical behavior and sets off mechanotransductive pathways. These pathways then determine the biological response. Mechanical overload of articular cartilage can lead to post-traumatic osteoarthritis. The mechanical response of cartilage to injury has been studied by both analytical and computational models of injurious loading, joint contact, and surface fissure initiation and propagation. This work has identified shear and tensile stresses as important mechanical parameters governing articular cartilage failure in response to mechanical injury. Further, measurement of material properties of cartilage during impact loading has shown that the tissue is significantly stiffer than predicted from quasi-static testing. With respect to the biological response, cell death and sulfated glycosaminoglycan (sGAG) release due to matrix breakdown are early degradative changes that lead to decreased tissue function. These biological sequelae have also been the subject of targeted intervention strategies post-injury. Some success has been found for decreasing

*Chapter to be submitted as Natoli RN and Athanasiou KA, "Mechanical Injury of Living Tissues: Lessons from Articular Cartilage."

cell death and sGAG loss using various bioactive agents. These treatments may be useful stating points for mechanical injury of other tissues.

Introduction

Studying mechanical injury of any living tissue is a complicated problem due to two dichotomies. The first is between the internal and external mechanical systems (Fig. 1-1). The internal system is the tissue, while the external system is the device, etc. that is used to create the mechanical insult. Experimentally, investigators are able to control variables in the external system, but the internal system comes pre-defined. Another way of putting this is that researchers control the boundary conditions of the mechanical problem. However, the tissue's mechanical response occurs internally, dependent upon such factors as tissue material properties and anisotropies.

The other dichotomy is separation of the mechanical and biological responses (Fig. 1-1). The mechanical response of a tissue is immediate and is governed by the tissue's biomechanical behavior. The combination of the tissue's tolerance criteria and severity of the mechanical insult determines whether the tissue will fail. Based on the mechanical response, mechanotransduction pathways are set in motion that initiate the biological response. This response may be beneficial, leading to healing of the injury, or it may be detrimental, resulting in further tissue degradation. These two dichotomies provide a simple, elegant framework for designing and interpreting studies involving mechanical injury to tissues.

With respect to articular cartilage, osteoarthritis (OA) can result from mechanical injury. OA causes significant pain and suffering to individual patients, and the economic burden of this disease for society is great.⁵¹⁹ For example, the United States realizes in excess of \$65 billion per year in medical costs and lost wages.²⁴⁹ Conservatively, it is estimated that 1 in 8 American adults over the age of 25 have clinically manifested OA,^{300,301} making it one of the leading causes of disability in the United States.⁶⁶ Further, when looking at a smaller age range, it is estimated that 10% of people in the world over age 60 have OA.⁷⁷ OA is clinically divided into two types: primary (cases with no known cause) and secondary (cases with identifiable cause). Known as post-traumatic OA, a majority of secondary OA is attributable to traumatic joint injury that may have occurred years previously.^{75,322,416} Mechanical injuries, such as those that happen during motor vehicle collisions, falls, and sports injuries, have been implicated in the development of post-traumatic OA, though the precise pathophysiology is not yet fully understood.^{66,102,377}

Mechanical injury of articular cartilage, such as impact overloading, has emerged as a useful model for post-traumatic OA, particularly of the early degenerative changes.^{66,430} In an early study, Thompson et al.⁴⁶⁰ demonstrated that a single 2170 N transarticular load applied to the canine patellofemoral joint *in vivo* leads to osteoarthritic changes by 6 months. Much later, by comparison with samples from horses diagnosed with OA, it was validated that *in vitro* impact of articular cartilage explants also causes osteoarthritic like changes.²⁴² This review discusses what research has uncovered pertaining to the mechanical and

biological responses of articular cartilage to mechanical injury and the post-injury treatment studies published to date. Additionally, areas for future research are identified, in the hope that the burden of post-traumatic OA can be reduced. The lessons learned may provide insight into the mechanical injury of other tissues.

Mechanical response of articular cartilage to mechanical injury

Analytical and computational models

Understanding the mechanical response of cartilage during injury is essential to identifying the reasons for tissue failure. To this end, the tissue's material response has been modeled during mechanical injury to ascertain metrics that can predict structural damage. While finite element models (FEMs) have been used extensively to study cartilage biomechanics, relatively few have looked at mechanical injury.⁴⁹⁸

Early approaches to modeling mechanical injury of articular cartilage used isotropic, linear elastic models for the tissue. In one study, dynamic loading of the rabbit tibiofemoral joint was assessed.¹² Using a parametric approach, plane strain contact elements were used to examine the effects of tibial displacement rate, bone density, and cartilage and bone material properties. When experimental data obtained from a load cell implanted in the rabbit's tibia were compared to the FEM output, some agreement emerged. The study demonstrated that resultant force magnitude was sensitive to these parameters, but that stress patterns were not. Further, the computed stresses were within damage thresholds previously identified through experiment, and increased

shear in the deep cartilage at the model's periphery was consistent with experimental findings of fissuring at that level.¹² To ascertain if a dynamic formulation was necessary to study rabbit tibiofemoral joint impact, the same model was used to examine stress waves.¹³ Quasi-static stress calculations were shown to not be substantially affected by longitudinal stress waves. In a study of rabbit patellofemoral joint impact also employing a quasi-static plane strain formulation, a Young's modulus of 2 MPa and a Poisson's ratio of 0.49 were found to best match the FEM calculated stresses with contact pressures measured experimentally by pressure sensitive film.³¹⁸ Regions of elevated shear stress and tensile strain corresponded to areas of surface fissuring. Collectively, these investigations identified shear stress as a probable cause of experimentally observed damage.

A drawback of the above studies is that cartilage was assumed to be isotropic. Further work has demonstrated that cartilage should be considered transversely isotropic to effectively generate a stress field consistent with experimental findings.^{134,183} Because of the experimental discrepancy between a lack of damage at the cartilage-bone interface and FE data from isotropic models predicting peak stresses at the cartilage-bone interface, Garcia et al.¹⁸³ modeled articular cartilage as a transversely isotropic biphasic material. Using a spherical indenter ($r = 400$ mm) to apply the load, they found the highest shear and tensile stresses on the cartilage surface in the area in contact with the indenter. The shear and tensile stresses corresponded to the surface fissures observed experimentally post-impact. This work was then extended to investigate stress

during contact of two biphasic, transversely isotropic layers of cartilage.¹³⁴ This study also found peak stresses at the cartilage surface, and additionally showed that the highest tensile stresses occurred in the convex layer of two contacting surfaces. The results of these studies clearly demonstrate that carefully developed models can reasonably match experimental findings. Unfortunately, the FE studies described have either assumed material properties from the literature or performed parametric studies, a point we will return to below.

To provide theoretical backing to the observations that surface fissures develop in areas of increased shear and tensile stresses, Atkinson et al.^{33,34} attempted to predict articular cartilage failure. Using a quasi-static, finite deformation elastic model, peak force, impact energy, mean stress, maximum principal strain, minimum principal stress, cohesive strength (Coulomb-Mohr failure criterion), and maximum shear stress (Tresca failure criterion) were investigated as predictors of surface fissuring during impact. Logistic regression showed that maximum shear stress was the most significant predictor of surface fissuring.³⁴ When applied to a biphasic model, maximum shear stress in the solid matrix was again the best predictor of surface fissuring.³³

Finally, the proteoglycans of articular cartilage have been modeled from a microphysical perspective and incorporated into a fiber-reinforced poroelastic FEM to investigate injurious compression of osteochondral explants to 14 MPa at three strain rates.³⁴³ Stress calculated from the FEM reasonably matched experimentally measured stress at the lower two strain rates ($7 \times 10^{-3} \text{ s}^{-1}$ and $7 \times 10^{-5} \text{ s}^{-1}$), but not the high strain rate ($7 \times 10^{-1} \text{ s}^{-1}$). As strain rate increased, radial

strain in the superficial zone increased, which corresponded to the location at which surface cracks formed. Additionally, it was shown that pore pressure supported an increasing amount of the applied load as load rate increased, suggesting that cartilage's interstitial fluid protects the solid matrix at high loading rates.

It is well known that cartilage is a mechanically responsive tissue. Similar to predicting structural failure, injurious mechanical loading should also be modeled for the purpose of predicting the biological sequelae, such as cell death or molecular responses, especially considering the advent of multi-scale modeling techniques.²¹⁰ This knowledge could be useful, for example, as criteria for when treatment could be required following injury.

Contact and surface damage

In the case of a real joint injury, cartilage-to-cartilage contact is occurs. Further, the presence of material damage alters a material's mechanical response. For these reasons models of joint contact and surface fissuring are also relevant to mechanical injury of articular cartilage. To develop models of joint articulation, Eberhardt et al.^{138,139} have investigated the effects of varying geometrical and material properties of contacting layers of articular cartilage situated atop bone. In one model, an elastic sphere in an elastic cavity was studied;¹³⁸ in another, the contact of two elastic spheres was studied.¹³⁹ In both, it was determined that, given a particular Poisson's ratio and Young's modulus (linearly elastic properties), the stress distribution depended on the aspect ratio of contact to tissue thickness. Aspect ratios (a/h) from 0.0 to 5.0 were assessed,

showing tensile stress was observed for small a/h , while tensile strain existed for all values. Moreover, stresses in the cartilage were not significantly altered by a 10-fold decrease in subchondral bone stiffness. The stress distributions found were consistent with damage at the cartilage surface and cartilage-bone interface after mechanical injury. However, these elastic models do not account for the fluid component within the tissue.

Other authors have modeled contact within a joint including the cartilage layers as biphasic materials.²⁷ It was shown that the interstitial fluid pressure supports the majority of the load for the first 100 to 200 s following loading, once more suggesting a mechanical mechanism by which the solid matrix is protected from damaging stresses and strains. Failure of cartilage at the cartilage-bone interface was again predicted. Finally, a more complex version of this model showed that higher stress is found in the thicker of two contacting biphasic layers of articular cartilage. This finding may have implications in osteoarthritic joints, where cartilage is known to decrease in thickness.⁵¹³

While the FE and contact models have predicted stress distributions where damage or fracture of the cartilage surface occurs, none included the mechanics of fracture development. To address this limitation, Kuo and Keer²⁸⁹ modeled indentation of a cracked articular cartilage halfspace with underlying bone by applying a 50 N load to a spherical indenter ($r = 4$ cm). They concluded that crack propagation was affected by cartilage thickness and the cartilage to subchondral bone stiffness ratio. In a FE study, stress intensity factors were calculated for a layered half-space (i.e., cartilage-on-bone) under normal and

sliding Hertzian contact.¹⁴⁰ The results demonstrate that crack propagation is primarily due to in-plane shear and affected by contact friction. It was suggested that cartilage stiffening, as occurs during impact loading, reduces crack propagation due to in-plane shear. The effects of rapidly applied loads have also been modeled for cases of intact versus already cracked articular cartilage.^{271,272} For cartilage with an intact surface, fissures may be initiated by tensile stresses.²⁷² However, in contrast to the FE study just mentioned, except for cracks present along the cartilage-bone interface, tensile stress intensity factors were greater than shear stress intensity factors in already cracked cartilage.²⁷¹ Thus, in-plane shear may initiate surface cracking, which is then propagated by tensile stresses.

More recently, a three-phase (collagen, matrix, and synovial fluid), transversely isotropic, unconfined half-space model of articular cartilage was created for studying surface fissures.²⁶⁸ Interestingly, it was shown that collagen is in tension in the first 10 to 20 s of a rapidly applied compressive load, switching to compression thereafter if the load is held constant. The tensile stresses generated were within the range of reported tensile strength of collagen fibers, showing that failure of collagen could lead to surface fissuring. This was not the case for slowly applied loads. In another interesting study, Wilson et al.⁵⁰⁰ investigated mediators of collagen damage due to mechanical injury in a fibril-reinforced poroviscoelastic model of articular cartilage. Using differential immunohistochemistry, wherein distinct antibodies were used to separate staining of enzymatically cleaved collagen from other damaged collagen, it was

shown that shear and maximum strain in the collagen fibers corresponded to areas staining for mechanically damaged collagen. The results from investigations of surface fissuring implicate collagen as having a key role in keeping the surface intact when subjected to injurious mechanical loading.

Finally, in an experimental study, the fracture toughness of articular cartilage was assessed using the modified single edge notch and trouser tear tests.¹⁰¹ The fracture toughness of articular cartilage was measured to be 0.14 to 1.2 kN/m by the modified single edge notch test. These values were larger than, but correlated with, those obtained from the trouser tear test. It has also been experimentally shown that failure along the osteochondral junction is more likely to occur in skeletally immature tissue compared to skeletally mature,¹⁶⁹ perhaps due to maturation in the collagen network that occurs in the tissue over time.¹⁰⁵ Future FE studies should seek to incorporate fracture development and propagation as part of the model to obtain a more realistic description of the mechanics during injury.

Mechanical properties of articular cartilage measured during injurious loading

Dynamic mechanical properties and appropriate constitutive equations are necessary for successful modeling of articular cartilage mechanical injury. While extensive research on cartilage's biomechanical properties has been performed for quasi-static conditions in typical loading geometries (confined and unconfined compression and indentation), few studies performed to date have addressed cartilage behavior in dynamic situations. Theoretically, it has been shown that the $t = 0^+$ (i.e., immediate) mechanical response of a biphasic material is equivalent

to the response of a single-phase incompressible elastic material.^{18,28,138} Assuming isotropy, the Poisson's ratio is $\nu = 0.5$, and the equivalent Young's modulus is $E_Y = 3\mu_s$,¹⁸ where $3\mu_s$ is three times the shear modulus of the solid matrix measured assuming a biphasic material. Based on typical values of the solid matrix,³⁴⁹ $\mu_s = E_s/(2*(1+\nu_s))$ ranges from 0.11 to 0.75 MPa, such that Young's modulus of the equivalent incompressible elastic material would range from 0.33 to 2.25 MPa. However, these properties grossly underestimate the dynamic stiffness of articular cartilage. Garcia et al.¹⁸⁴ have noted that mechanical properties derived from infinitesimal strain experiments on articular cartilage result in large deformations in FE models of blunt impact. Though unpublished, we have also noted that mechanical properties calculated theoretically as above lead to unrealistically large compressive strains during impact loading. This suggests a need for accurate determination of cartilage material properties from dynamic loading experiments.

Because of the viscoelastic nature of articular cartilage, the effect of load rate on tissue stiffness has been examined. In an early study, Oloyede et al.³⁷⁶ showed that the compressive stiffness reached a limit as strain rate increased. Using a pendulum device for imparting impact loads, several strain rates ranging from $1 \times 10^{-5} \text{ s}^{-1}$ to $1 \times 10^3 \text{ s}^{-1}$ were studied. There was a linear increase in compressive stiffness measured at 0.5 MPa up to $5 \times 10^{-3} \text{ s}^{-1}$, after which stiffness reached a plateau at $\sim 20 \text{ MPa}$. Further, based on strain patterns observed in the tissue during loading, the authors suggested that cartilage behaves as a hyperelastic material in the high strain-rate regime. Work from another group

showed that, in a confined compression loading protocol, the dynamic modulus increased from 225 to 850 MPa as the load rate was increased from 25 to 1000 MPa/s.³³⁹

Other studies have investigated the effects of stress level on tissue stiffness. Using a drop tower that applied impacts ranging in energy from 0.5 to 0.9 J (note that, here and elsewhere, energy is calculated from the potential energy of the falling mass), the mean dynamic stiffness measured at 50 MPa ranged from 220 to 280 MPa.²⁵³ Later it was shown that the mean dynamic stiffness measured at 10 MPa during impact loads (0.12 to 0.37 J) depended upon tissue source and the loading geometry, such that the stiffness in an unconfined compression geometry was greater than if the tissue was radially confined by surrounding cartilage.²⁵⁵ The dynamic stiffness at 10 MPa ranged from 6.4 to 64 MPa. Together, these studies show that the dynamic stiffness of articular cartilage is much greater than predicted theoretically, is a function of the stress and stress rate levels, and depends on tissue source and loading geometry. However, none of the above mentioned studies reported cartilage stiffness with the underlying bone attached.

Recently, Burgin and Aspden⁸⁰ designed a system for impact testing of biological materials, such as articular cartilage. A study to measure the material properties of the cartilage-on-bone system using this apparatus demonstrated that the dynamic modulus of articular cartilage is two orders of magnitude greater than measured quasi-statically, varies non-linearly with the applied load, and is greater than the modulus of cartilage in isolation.⁸¹ For impact energies ranging

from 0.025 to 0.25 J, the mean dynamic stiffness at 10 MPa ranged from 71 to 95 MPa, while the maximum dynamic stiffness ranged from 86 to 237 MPa. Most interestingly, they showed that cartilage exhibits hysteresis in the loading curve during impact, and they calculated the coefficient of restitution (which has a value of 1 for elastic impacts and a value of 0 in a plastic collision where all the energy is dissipated). The coefficient of restitution was 0.636 for the 0.025 J impact, decreasing to 0.265 for the 0.25 J impact. These data suggest that, in contrast to previous thought, articular cartilage does not behave elastically during impact. Another group has also reported energy loss during impact.⁴⁶⁹

Perspectives on modeling the mechanical behavior of articular cartilage during injury

Given that impact loading occurs on very small time scales (order of ms and less) when fluid flow is limited, it is not likely that viscous drag of fluid flow during deformation is responsible for the energy dissipation. Alternatively, intrinsic viscoelasticity of the solid matrix or damage (i.e., plasticity) at the gross or microscopic levels are the likely mechanisms by which energy is dissipated, although, based on the stiffening and re-arrangement of collagen fibers at high strain rates,^{314,471} part of the lost energy may be diverted to those processes as well. Considering the studies presented in this section on the mechanical behavior of articular cartilage during injury, it seems that a transversely isotropic, hyperviscoelastic constitutive equation with a stiffness that depends on stress rate and the current stress level is required to accurately model articular cartilage impact. Surface fissure initiation and propagation should also be included if they

are observed experimentally. In addition to investigating tissue failure during the mechanical insult, this model should be used to predict the biological response following mechanical injury. However, such a model is recognizably difficult to implement.

Biological response of articular cartilage to mechanical injury

In addition to mechanically responding to the forces it experiences, tissue has a biological response. Mechanical loading of cartilage, such as during injury, generates streaming potentials, stress/strain fields, and hydrostatic pressure within the tissue. These effects are experienced at the cellular level by chondrocytes residing within the matrix. The biological response is started when the mechanical forces applied to the tissue activate intracellular signaling cascades, a process known as mechanotransduction. Chondrocytes are known to respond to mechanical load through integrin-cytoskeletal interactions, as well as ion and stretch activated channels located in the cell membrane.⁴⁹¹ For example, hydrostatic pressure has been shown to affect the activity of ion transporters^{73,215} and cause gene expression changes in chondrocytes.⁴⁵¹ Following mechanotransduction, the biological response evolves over time. Depending on the nature of the mechanical insult and the tissue's post-injury environment, cartilage may recover or degrade, the latter of which leads to post-traumatic OA (Fig. 1-1).

Both *in vivo* and *in vitro* models have been used to study mechanical injury of articular cartilage (Fig. 1-2). The *in vivo* studies have used guinea pigs,⁴⁴⁵ dogs,^{133,350,373,390,460,461} and rabbits,^{64,65,67,150,152-154,338,364-366,403,434}

providing us with the long term pathophysiological changes occurring in articular cartilage in response to mechanical overload. Compared to *in vitro* studies, *in vivo* investigations more closely match native physiology, but they have less environmental control.

In vivo investigations

- Proteoglycan loss, surface fibrillation, and inflammation

In vivo mechanical injury of articular cartilage can lead to proteoglycan loss, surface disruption, and inflammation. In one study, guinea pig hind limbs were subjected to injurious cyclical loading for 15 min per day over 3 weeks.⁴⁴⁵ The earliest identified change was stiffening of the subchondral bone. However, this stiffening returned to control values as the overlying cartilage degenerated, evident by loss of glycosaminoglycan (GAG) staining and fibrillation. In a study investigating the response of canine patellofemoral joint to a single impact load, surface fissures and fractures in the calcified cartilage zone were evident by 2 weeks.⁴⁶⁰ These lesions progressed to surface fibrillation and loss of proteoglycan staining at 6 months. Further study of this same system showed cell death and presence of the inflammatory molecules tumor necrosis factor- α (TNF- α), interleukin-1 β (IL1- β), and matrix metalloproteinase-3 (MMP-3) at 2 weeks.³⁷³ However, at 1 year there was evidence of a cartilage repair response, as some proteoglycan staining returned. Pickvance et al.³⁹⁰ further studied the inflammatory response, showing that TNF- α , IL-1 β , and MMP-3 are present at 2 weeks, but not at 3, 6, or 12 months, suggesting that the inflammatory response may be transient.

While surface damage is an obvious sign of cartilage injury, other processes can occur without surface damage. Borrelli et al.⁶⁷ used a pendulum device to deliver three levels of injurious loading (~14, 23, and 56 MPa) to the rabbit patellofemoral joint. Animals were sacrificed at 2, 6, and 12 weeks. The authors observed decreased proteoglycan staining in the injured specimens compared to control that was irrespective of stress level and time. Though the greatest stress was 46% of that needed to fracture the rabbit's medial femoral condyle, no cell cloning, surface damage, or enzymatic breakdown of aggrecan or collagen were evident. In another study, the rabbit femoral condyle was loaded (35 MPa at 420 MPa/s) in an open joint model of articular cartilage injury.³³⁸ Results showed surface damage immediately after injury, but not at 3 weeks. However, at 3 weeks cell death and proteoglycan loss were evident. These investigations show that visible signs of surface damage may be sufficient, but are not necessary, for the presence of underlying pathology.

- Changes in mechanical properties and subchondral bone thickening

While the above studies demonstrate that surface damage and proteoglycan loss are common features of articular cartilage damage following mechanical injury, none assessed the tissue's biomechanical properties. Using a load level below that which causes bone fracture (6.6 J), Newberry et al.³⁶⁴ showed that subchondral bone thickness increases and cartilage stiffness decreases by 12 months post-injury. The loss of tissue stiffness was accelerated using a daily exercise regimen.³⁶⁶ In the same system, to ascertain if there is a threshold of mechanical injury necessary to cause increased subchondral bone

thickness and decreased tissue stiffness, a 0.9 J impact (resulting in 16 MPa) was compared to the 6.6 J impact (26 MPa). The higher load replicated the findings of increased subchondral bone thickness and decreased tissue stiffness occurring by 6 months; the lower load showed no bone thickening or loss of tissue stiffness.³⁶⁵ In an attempt to ameliorate subchondral bone thickening and loss of tissue stiffness following the 6.6 J load, the mechanical insult was applied using a padded, as opposed to rigid, interface.¹⁵⁰ There was no increase in subchondral bone thickness, but cartilage stiffness was decreased at 4.5 and 12 months. Further, FE analysis showed the padded interface substantially decreased shear stress at the cartilage surface and cartilage-bone interface. More investigation of mechanically preventative modalities (e.g., the padded interface) should be investigated as ways to allow cartilage to tolerate greater loads without increased damage.

One advantage of *in vivo* models is that long term studies are feasible since the cartilage is maintained in a "natural" bioreactor. As an example, Ewers et al.¹⁵⁴ took the rabbit patellofemoral cartilage injury model out to 3 years, including measurement of transversely isotropic biphasic tissue properties and assessment of surface fissure length and depth. It was shown that, compared to baseline, the in-plane modulus of impacted tissue decreased while in-plane permeability increased. Compared to contralateral, unimpacted controls, the modulus and permeability in the direction perpendicular to the articular surface decreased and increased, respectively. Surface fissure length and depth were increased in impacted cartilage by 4.5 months and remained so thereafter.

Moreover, a high rate of impact (~7000 MPa/s) caused increased surface fissuring and subchondral bone thickening 1 year post-injury compared to a low rate of impact (~500 MPa/s); however, both caused decreases in tissue stiffness.¹⁵² Finally, in a clinical study, cartilage biopsies were examined for cell death 2.7 months following acute knee injury, showing increased apoptosis in injured tissue compared to control tissue.¹¹⁰ Together, these *in vivo* studies illustrate the long term detrimental effects mechanical injury can have on articular cartilage with respect to surface damage, cell death, inflammation, proteoglycan loss, and function. In contrast, *in vitro* investigations of cartilage injury have rarely looked beyond 2 weeks, providing a better picture of the early biological responses to injury.

In vitro investigations

- Cell death

With respect to *in vitro* articular cartilage mechanical injury, there are several different methods currently used based on type of loading, boundary conditions, and pre-injury tissue processing, all of which have been shown to differentially affect the experimental outcome. Types of loading include single sub-impact or injurious compression,^{137,293,342,400} single impact (as defined by Aspden et al.²⁶) applied via a drop tower,^{166,242,253,431} and cyclical loads.^{62,108,396,399} Furthermore, each of these loading types has been used with various energies, stresses and strains, and stress and strain rates. Boundary conditions refer to the presence or absence of underlying bone^{288,402} and test geometry,^{151,310,339,431,462} the latter of which ranges from confined or unconfined

compression to indentation and determines the degree to which the loaded tissue is radially constrained (Fig. 1-2). Pre-injury tissue processing refers to whether full thickness cartilage is used versus removal of the superficial zone²⁹³ and to whether the tissue is allowed to equilibrate for a certain amount of time before mechanical loading.⁴²¹ Additionally, tissue source²⁵⁵ and age^{294,309} have also been shown to affect cartilage's response to injurious mechanical loading. Hence, it is important to keep these many factors in mind when comparing articular cartilage mechanical injury studies.

Necrotic cell death can be an immediate consequence of mechanical injury. Torzilli et al.⁴⁶² indented the central region of chondral explants (Fig. 1-2C) at 35 MPa/s to peak stresses ranging from 0.5 to 65 MPa. The study showed that, immediately post-injury, cell death was initiated at 10 MPa and increased up to 35 MPa, after which there was no further increase. Cell death was isolated to cells below the indenter. In another study, cell death was investigated in confined chondral explants (Fig. 1-2B) immediately post-injury.³³⁹ Explants were loaded at stress rates varying from 25 to 1000 MPa/s, resulting in peak stresses between 10 and 40 MPa. It was found that the depth of cell death increased with increasing peak stress, but decreased with increasing stress rate. The authors suggest that cell death in the superficial region is due to water loss or tensile failure. The fact that cell death occurs immediately suggests it is necrotic in nature, as apoptotic cell death takes time.

It has also been shown that chondrocytes die by apoptosis post-injury. In a longer study, the effects of load rate (40 versus 900 MPa/s to a peak stress of

40 MPa) were investigated during unconfined compression of chondral explants (Fig. 1-2A).¹⁵¹ At 4 days, the higher load rate resulted in less cell death, but increased surface fissure length and depth. Further, both load rates caused a transient increase in nitric oxide release from injured tissue. Following injurious compression of chondral explants (50% strain at 1 s^{-1}), increased cell death via apoptosis was measured at 3 days.³⁸⁶ Huser and Davies²⁴² loaded chondral explants with ~ 0.125 , 0.25 , and 0.5 J impacts. At 48 hrs, there was increased apoptosis for each impact level, with the 0.25 and 0.5 J impacts having the most cell death. The 0.125 J impact was followed for 20 days in culture, demonstrating increased percent cell death at 1, 2, 5, and 10 days. The authors have gone on to show that the mechanism of cell death they observed is calcium mediated²⁴⁴ and involves caspases 3 and 9.²⁴³ Collectively, these chondral explant studies suggest a threshold for the initiation of cell death of at least 10 MPa , demonstrate cell death via both necrosis and apoptosis, and show that increased loading rates cause less cell death. However, since all these studies were performed without underlying bone, cartilage was not restrained as it is physiologically.

The presence of bone beneath cartilage alters the boundary conditions during mechanical injury, which can ultimately change the tissue's biological response. Indeed, it has been demonstrated that underlying bone spares cartilage during impact by decreasing peak force.⁴⁰² In a study directly investigating the presence of underlying bone during mechanical injury, it was demonstrated that less surface fissuring and cell death occur in osteochondral explants compared to chondral explants when loaded in unconfined compression

(Fig. 1-2 D vs A) to 30 MPa at both 30 and 600 MPa/s.²⁸⁸ With respect to human tissue, Repo and Finlay⁴⁰⁸ impacted osteochondral explants at strain rates of 500 and 1000 s⁻¹. Cell death initiated at ~25 MPa, and fissuring oriented parallel with split-lines was observed. In another study, bovine osteochondral explants were injuriously compressed in unconfined compression (Fig. 1-2E) to 3.5, 7, and 14 MPa at strain rates ranging from 7×10^{-5} to 7×10^{-1} s⁻¹, based on 7×10^{-4} s⁻¹ being the calculated “gel diffusion” rate in this system.³⁴² For strain rates of 7×10^{-3} s⁻¹ and above, cell death occurred in the superficial zone for all three stress levels. There was no change in cell viability at the “gel diffusion” rate; however, substantial cell death was observed throughout the specimen at the lowest strain rate for all stress levels. The authors concluded that the “gel diffusion” rate represents a threshold for change in the cell death response of cartilage to injurious loading. Comparing the human to the bovine osteochondral studies, it appears that the threshold for cartilage damage may be species dependent. This is supported by an observation that less damage occurred in human cartilage compared to bovine cartilage when subject to the same impact loads.²⁵⁵

Finally, in another step towards the *in vivo* situation, several investigations have used an *ex vivo* approach, or one in which the cartilage is left in its *in situ* position during mechanical injury. This setup includes underlying bone and radially confines the tissue by adjacent tissue (Fig. 1-2 F&G), which again changes the boundary conditions of the mechanical insult. Bovine patellae (Fig. 1-2F) were impacted to 53 MPa at ~200 MPa/s, followed by removal of cartilage explants corresponding to the injured area. Cell death was observed only around

cracks that formed in the tissue.³¹⁰ Another study examined 0.06, 0.1, and 0.2 J impacts to Yucatan minipig patellae.¹³⁷ Under these low loads, no structural damage was observed via India ink staining or scanning electron microscopy. However, cell death occurred immediately and increased with increasing energy, suggesting that chondrocyte death can precede identifiable structural damage. The 0.2 J impact corresponded to a surface stress level of 3 MPa. In an interesting study, Green et al.¹⁹⁹ delivered three successive impacts (20-25 MPa) to canine femoral condyles. At 7 days, cell death was increased in the impact site and at distances greater than 10 mm from the impact site. Further, culture of the condyles in the presence of mononuclear lymphocytes increased cell death within and up to 9 mm from the impact site. This finding suggests that *in vivo* chondrocyte death following injury may be enhanced by an inflammatory response.

To better understand the spatio-temporal profile of cell death in injured cartilage, Natoli et al.³⁵⁹ examined impacted bovine proximal ulnas (Fig. 1-2G). Following either a 1.1 J (resulting in 3.1 MPa) or 2.8 J (9.1 MPa) impact, cartilage explants were removed from the subchondral bone and cultured for 4 weeks. Following the 1.1 J impact, cell death was increased at 24 hrs and 4 weeks; following the 2.8 J impact, cell death was increased at 24 hrs, 1 week, and 4 weeks, reaching 50%. Cell death began in the superficial zone. Over time, cell death spread through the depth of the explant, but did not spread radially. The lack of radial spread is in contrast to the above mentioned study,¹⁹⁹ and to a model of mechanical injury involving cyclical indentation loading of canine

chondral explants.³⁰⁸ The discrepancy between these studies may be due to different loading regimens, maximum loads reached, or to tissue source. Further work is necessary to tease out the specifics of chondrocyte death in response to mechanical injury.

- Proteoglycan release and synthesis

Studies investigating the biochemical content of the ECM have found that mechanical injury causes sulfated GAG (sGAG) to be released into the culture medium and chondrocyte proteoglycan synthesis to decrease. Injurious compression of chondral explants, radially confined by surrounding tissue, from 5 to 65 MPa at 35 MPa/s showed decreased proteoglycan synthesis at 24 hrs.⁴⁶² In another study, a drop tower was used to apply several levels of impact to bovine articular cartilage explants to assess matrix loss and synthesis during 2 weeks of culture.²⁵⁴ Results indicated that both collagen and sGAG were lost to the culture medium and that an initial decrease in ECM synthesis normalized to the number of viable cells recovered in a manner dependent upon applied load; for a 1 J load, it took 12 days for recovery to control values. A different study looked at sub-impact loading (3.5 to 14 MPa at 3×10^{-5} to 0.7 s^{-1}) of bovine osteochondral explants, and found that sGAG was released into the medium during 4 days of culture and that proteoglycan synthesis decreased with increasing peak stress.⁴⁰⁰ However, since the culture time was not longer, one can not assess if the decrease recovered.

Furthermore, injuriously compressed bovine cartilage explants (50% strain at 0.01, 0.1, or 1 s^{-1}) had decreased proteoglycan and total protein synthesis at 3

days when normalized to viable cells for the 0.1 and 1 s⁻¹ strain rates.²⁹³ DiMicco et al.¹³⁰ subjected bovine cartilage explants to injurious compression (50% strain, 1 s⁻¹) and found that sGAG release was highest during the first 4 hrs post-injury. However, between 24 and 72 hrs the amount of sGAG released became similar to control. Additionally, using the same loading protocol, it was found that the cytokines TNF- α and IL-1 α act synergistically with injury, causing the tissue to lose up to 54% of its proteoglycan content.³⁸⁵ When one considers that, due to cell death, fewer cells are available for proteoglycan synthesis, and that proteoglycan synthesis decreases even when normalized to cell number, the two most likely causes of sGAG release following injury are collagen damage and enzymatic degradation of the proteoglycan species themselves. This notion is corroborated by the decrease in sGAG release seen in experiments using MMP inhibitors post-injury (see below).^{55,130}

- Decreased tissue stiffness

Despite the important mechanical functions fulfilled by articular cartilage, relatively few studies have assessed changes in the tissue's biomechanical properties in response to mechanical injury. Following injurious compression of immature bovine chondral explants to 50% strain at 0.1 s⁻¹ and 1 s⁻¹, the dynamic compressive stiffness was decreased by 6 hrs and remained so at 3 days.²⁹³ The dynamic shear stiffness was decreased only for the 1 s⁻¹ rate. Unconfined impact loading (0.491 to 1.962 J) of osteochondral explants was examined for its ability to alter the storage and loss dynamic viscoelastic moduli under compression regimens simulating walking and running.⁴⁷² The storage modulus decreased

significantly following the 1.962 J impact under both walking and running simulations, while it decreased only under running conditions for a 1.472 J load. In contrast, the loss modulus increased for both walking and running conditions at all impact levels. The authors suggest that a threshold of 25 MPa at strain rates above 1500 s^{-1} is required for initiation of changes in cartilage mechanical properties post-injury.

In contrast, another impact study showed that the aggregate modulus of injured tissue decreased immediately following only a 2.8 J impact (with corresponding 9.1 MPa peak stress).⁴³¹ The difference in threshold could be due to the very high stress rate used in the latter study ($> 13,000 \text{ MPa/s}$) or the experimental conditions (e.g., bovine proximal ulna as opposed to femoral condyle or presence of radially confining tissue). Natoli et al.³⁵⁹ demonstrated that the 2.8 J impact used in the previous study continued to have decreased stiffness at 24 hrs, 1 week, and 4 weeks. Further, a 1.1 J also decreased the tissue's aggregate modulus at 4 weeks, though not at earlier time points. Further, the loss of tissue stiffness correlated with sGAG release and cell death. These observations suggest that, given enough time, lower levels of injury can accumulate enough degradative changes to cause changes in mechanical properties similar to higher levels of injury. More study of changes in cartilage function due to injurious loading are needed to ascertain the parameters that govern cartilage's injury threshold from system to system.

Perspectives on the biological response of articular cartilage from different models of mechanical injury

Mechanical injury of cartilage has been examined in the context of chondral, osteochondral, *ex vivo*, and *in vivo* systems. There are merits and disadvantages for each. The study of chondral explants isolates cartilage specific responses, but the nature of the mechanical injury is altered without underlying bone. This system may be best suited for isolating cartilage specific mechanics. Osteochondral explants restrain cartilage at the cartilage-bone junction, but still lack natural radial confinement. However, culture of osteochondral explants may better reflect the *in vivo* case, wherein the two tissues are together. The *ex vivo* model is an attractive alternative, but specimen geometry makes experimental set-up more involved. On the other hand, cartilage can be loaded in its *in situ* position and then be explanted for culture to determine the cartilage-specific biological response, or it can be cultured *in situ* with the attached underlying bone.

Unfortunately, all *in vitro* cartilage explant culture systems have the inherent limitation that tissue quality diminishes over time due to disuse.^{359,423} While *in vivo* models overcome this last limitation, costs of performing the long-term studies can be prohibitive. However, they are the only system that retains native physiology and allows the joint to be injured with all of its supporting tissues (muscles, ligaments, tendons, etc.) in place. Thinking towards treatment studies, the *in vitro* model systems may be useful for screening potential therapeutics, but the *in vivo* models will be necessary for proving their efficacy and determining potential side effects. Until an appropriate system for

mechanical injury of articular cartilage is defined, comparison among present and future studies will remain a challenge.

Interventions following mechanically-induced cartilage injury

Understanding the mechanical and biological responses of articular cartilage to mechanically-induced injury provides insight into methods for preventing tissue degradation. While investigations into treatment strategies for established OA have been occurring for some time, treatment studies following mechanical injury are just beginning. Based on the pathways of cartilage degeneration, treatment agents have been chosen that specifically target cell death, matrix breakdown, and/or inflammation, which constitute the main biological responses uncovered thus far. In general, these agents have been used in both injurious compression and impact loading protocols, achieving some success at reducing cell death and sGAG loss post-injury. Tables 1-I and 1-II summarize the results of these efforts.

Interventions targeting cell death

As discussed above and in other work,^{66,386,475} cell death may be necrotic or apoptotic, and agents directed towards both have been investigated. Specifically, the pan-caspase inhibitor z-vad.fmk, dexamethasone, insulin-like growth factor-I (IGF-I), inhibitors of caspases 3, 8, and 9, glucosamine and some of its derivatives (Glu5 and Glu11), inhibitors of the calcium dependent enzymes calpain and calcium/calmodulin-regulated kinase II (CaMKII), antioxidants and nitric oxide synthase inhibitors, and the poloxamer 188 (P188) have been studied

(Table 1-I). Based on the premise that increased chondrocyte survival is beneficial following mechanical injury, inhibition of caspases, known inducers of apoptosis, has been a prime target to prevent chondrocyte death. Following an unconfined injurious compression of 23 MPa for 0.5 s, D'Lima et al.¹¹⁸ cultured cartilage explants in the presence of 100 mM z-vad.fmk (a pan-caspase inhibitor). They showed a significant decrease in apoptosis 48 hrs post-injury. The same study also showed that IGF-I (50 ng/mL) and dexamethasone (0.1 mM) decreased apoptosis at 48 hrs. Following a lower level of loading (14 MPa for 0.5 s), z-vzd.fmk reduced apoptosis by 50% at 96 hrs post-injury.¹¹⁶ Further, z-vad.fmk also reduces sGAG release from injured explants.^{117,118}

Though pan-caspase inhibition was successful, more specific targets could be desirable. In this respect, inhibition of the specific caspases 3, 8, and 9 was studied after a single 0.245 J impact load.²⁴³ Mature horse explants were pre-cultured for 3 hrs in the presence of 200 μ M of these specific caspase inhibitors, impacted by a 500 g mass dropped from 5 cm, and returned to culture for an additional 48 hrs. Both caspase 3 and 9 inhibition decreased impact-induced apoptosis by more than 50%; inhibition of caspase 8 had no effect. Additionally, caspase 9 inhibition decreased sGAG release from explants post-injury. Based on the differential effects of caspase inhibition, it appears that mechanical injury activates the intrinsic apoptotic pathway, not the extrinsic.²⁴³ Longer time points in the presence of caspase inhibition and mechanistic dissection of the particulars of the caspase pathway post-injury could be future areas of fruitful research.

Other, non-caspase inhibiting, agents have also been studied for decreasing cell death after mechanical injury of articular cartilage. In a preliminary report, Huser and Davies²⁴⁵ treated impacted cartilage explants with 3 mM N-acetyl-glucosamine or the more lipophilic derivatives Glu5 and Glu11 (also 3 mM). At 48 hrs post-impact, treatment with Glu5 decreased cell death, while treatment with Glu11 increased cell death. N-acetyl-glucosamine had no effect. The authors speculated that the increased cell death with Glu11 was due to toxic accumulation within the cells because of Glu11's more lipophilic design. Further, it is suggested that Glu5 may be working through a mechanism involving decreased mitochondrial depolarization post-impact, potentially linking the process back to diminished caspase activity. Inhibitors of calpain (10 μ M) and CaMKII (10 μ M), two enzymes upstream in the caspase induced apoptosis pathway, also decreased the amount of cell death 48 hrs following a 0.245 J impact.²⁴⁴ Moreover, the calpain inhibitor decreased sGAG loss and mitochondrial depolarization. Inhibition of the lysosomal protease cathepsin B did not decrease cell death.

Inhibitors of inflammation and immune responses have been investigated post-mechanical injury. In a study employing a custom designed triaxial mechanical stimulator for applying variable shear stress as the mechanical insult, it was demonstrated that 2.5 mM *n*-acetylcysteine, 100 μ M vitamin E, and 1 mM *N*-nitro-L-arginine methyl ester (an inhibitor of nitric oxide (NO) synthase) decreased cell death 24 hrs post-injury, most evident in the group subjected to 900 cycles of 5 MPa axial compression at 1 Hz.³³⁰ Green et al.¹⁹⁹ showed that

inhibition of NO synthase with 1 mM N^G -methyl-L-arginine decreased cell death at 7 days following three successive impacts of 20-25 MPa applied to canine femoral condyles. Creatively, they also showed that culture of impacted cartilage with autologous mononuclear leukocytes increased cell death, and that this increase could be mitigated by 0.1 mM desfuroxamine (an iron chelator) and antibodies against CD18 (50 μ g/mL). Blocking CD18 prevents leukocytes from attaching to chondrocytes. Inflammatory and immune responses following articular cartilage mechanical injury has not been studied in great detail. The promising results from these experiments support further research in this area.

The poloxamer P188 has also been used to decrease cell death. P188 is an 8.4 kDa non-ionic surfactant tri-block copolymer of poly(oxyethylene) and poly(oxypropylene) which selectively inserts into damaged membranes, such as cells undergoing necrosis, and is squeezed out once the membranes are reconstituted.³³¹ With respect to articular cartilage injury, Haut's group has shown promising results with P188 following injurious compression of explants^{37,389} and in an *in vivo* study of rabbit patellofemoral joint trauma.⁴²⁰ In one study, they delivered P188 (8 mg/mL) in the culture medium following a 25 MPa load and examined cell viability at 1 and 24 hrs post-trauma. An increased percentage of viable cells in the superficial zone at 1 hr, and an increased percentage in all zones at 24 hrs, were found.³⁸⁹ In another study, they showed that P188 treatment for the first 24 hrs reduces the percentage of apoptotic cells at both 4 and 7 days after injury.³⁷ Furthermore, in a 4 day *in vivo* study, a one-time intra-articular injection of P188 was effective at reducing cell death in impacted

retropatellar cartilage.⁴²⁰ Natoli and Athanasiou³⁵⁷ have investigated P188 (8 mg/mL also) following two levels of impact loading (1.1 and 2.8 J) applied to radially confined tissue with attached underlying bone. Using continuous treatment, a 75% decrease in cell death was found at 1 week following the 1.1 J impact. In contrast to previous P188 work, no compression protocol was needed to achieve this beneficial effect. Future experiments combining treatments for apoptotic and necrotic cell death could lead to further chondrocyte preservation post-injury.

Interventions targeting sGAG release and others

In addition to cell death, another important pathway of cartilage degeneration is sGAG loss from the tissue. Several matrix metalloproteinase (MMP) inhibitors, two cyclooxygenase (COX) inhibitors, and IGF-I have been investigated for their ability to decrease sGAG loss post-injury (Table 1-II). To ascertain the mechanism of sGAG release from injuriously compressed immature articular cartilage explants, inhibitors of biosynthesis, MMPs, and aggrecanase were studied.¹³⁰ At 3, 5, and 7 days following a 50% compression at 100% s⁻¹, the MMP inhibitor CGS 27023A decreased cumulative sGAG release compared to loaded, untreated controls. Another MMP inhibitor (GM 6001) and an aggrecanase inhibitor (SB 703704) had no effect. Blumberg et al.⁵⁵ showed that continuous treatment with the MMP inhibitor doxycycline (100 µM) decreased cumulative sGAG loss at 1 and 2 weeks following 2.8 J impact loading of tissue with underlying bone attached. Moreover, they demonstrated that treating for only the first of 2 weeks yielded similar results to treating continuously for 2

weeks, suggesting treatment post-injury may only be necessary for a brief amount of time. Future studies should investigate different time courses of treatment, as doing so may be able to identify the appropriate “therapeutic window” for treatment of articular cartilage mechanical injuries.

Non-MMP inhibitors have also been used to decrease sGAG release post-injury. To determine whether COX inhibition could prevent matrix degradation, Jeffrey and Aspden²⁵⁶ treated 0.13 J impacted human articular cartilage explants with several concentrations of indomethacin (non-selective COX inhibitor) and celecoxib (a COX-2 inhibitor). They found a dose dependent decrease in prostaglandin E₂ using these agents, but no effect on sGAG release. However, 0.1 μ M celecoxib and 10 μ M indomethacin significantly decreased impact-induced apoptosis. Furthermore, IGF-I was investigated following injury of radially confined tissue with attached underlying bone, showing a 49% decrease in sGAG loss following a 1.1 J impact.³⁵⁷ Unfortunately, the only studies to ascertain the effects of preventing sGAG loss on tissue function did not observe beneficial effects on the compressive stiffness.^{55,357} A myriad of enzymes could be responsible for matrix breakdown following mechanical overload. More research is needed into the different enzymes responsible and whether inhibition of these enzymes can prevent matrix loss post-injury.

Finally, there are two intervention studies worth noting that did not target cell death or sGAG release. Following impact (0.175 J) of horse articular cartilage explants, several concentrations of fibroblastic growth factor-2 (FGF-2) were assessed for their ability to promote intrinsic repair of articular cartilage.²²⁴ It

was found that 50 and 100 ng/mL FGF-2 increased the number of new cells on the articular cartilage surface at 7, 10, 20, and 28 days post-impact. These cells, termed putative chondrocyte progenitor cells, stained for collagen types II, IX, and XI, but not collagen type I. The results indicate that mechanically damaged cartilage may be able to mount an intrinsic cellular repair response. Secondly, in an *in vivo* study of rabbit patellofemoral joint impact, animals were treated with intramuscular injection (2 mg/kg) of a semisynthetic GAG (Adequan) every 4 days for 6 weeks. The results at 30 weeks post-injury showed that the treatment group did not experience the decrease in tissue compressive stiffness seen in the injured, untreated control group.

Collectively, the intervention studies have shown some success towards ameliorating degradative changes in articular cartilage following mechanical injury. However, few have looked at time points longer than 1 week, and even fewer have been tested *in vivo*. There is great need for continued study of potential interventions, as well as translation of these findings to *in vivo* models and, ultimately, the clinical setting.

Conclusions

Mechanical injury of living tissues can be thought of in terms of a mechanical response followed by a biological response. Further, the mechanical injury problem consists of two systems, internal (i.e., tissue) and external (i.e., device used to impart the mechanical insult). The response of the internal system to the external insult determines the tissue's mechanical response, which then sets in motion the biological sequelae.

Mechanical injury of articular cartilage has been extensively studied, providing much insight into cartilage mechanobiology. To understand the mechanical response of cartilage to injury, investigators have employed both analytical and computational models. However, since most tissues exhibit rate-dependent mechanical behavior, the appropriateness of models for dynamic processes that use quasi-static tissue properties should be verified. With respect to the biological response, cell death has received much attention following mechanical injury due to its early occurrence and contribution to articular cartilage degeneration, but proteoglycan loss and surface fissuring are two other prominent degradative changes post-injury. Because cartilage's primary function is mechanical, more studies should include measurements of tissue biomechanical properties as part of their outcomes. Particularly, tensile properties following injury have not been assessed.

Though much is known about how cartilage degenerates, no proven disease-modifying interventions exist. However, in the past few years, studies investigating treatments after mechanical injury to articular cartilage have begun. Based on knowledge gained from the biological response of cartilage to injury, prime targets have been cell death and sGAG release. Generally speaking, more treatments need to be studied and for longer time points. Successful treatments need to be carried into animal models, where unwanted side effects can also be uncovered. Additionally, as mentioned above, testing of biomechanical properties must be included in assessing the interventions.

In addition to articular cartilage, many other tissues in the body experience mechanical injury (e.g., brain, bone, and knee menisci). We believe that the lessons learned from studying mechanical injury of articular cartilage can be applied to these tissues as well. In all cases, the framework of a mechanical and biological response is appropriate. Characterizing the mechanical response and causes/modes of failure can enable better design of protective modalities for preventing injury. Understanding tissue specific biological responses to various levels of mechanical overload can identify the appropriate targets for biological intervention. Cell death, one biological response, is ubiquitous following mechanical injury to any tissue. Some of the agents used to treat cell death in cartilage post-mechanical injury may find use in these other tissues as well.

Table 1-I: Post-injury interventions affecting cell death

Agent	Main outcome	Experimental system			Reference
		Boundary conditions	Pre-injury processing	Species ^h	
Poloxamer 188 [†]	Decreased at 1 hr, 24 hrs, 4 days, and 1 week	Inj. comp. ^f	48 hr pre-equilibration	Cow	37,389
	Decreased at 1 week	Impact	None	Cow	357
	Decreased at 4 days	Impact	<i>In vivo</i>	Rabbit	420
Pan-caspase inhibitor (z-vad.fmk)	Decreased at 48 hrs	Inj. comp.	48 hr pre-equilibration	Cow, Human	117,118
Inhibitors of caspases 3 and 9 [*]	Decreased at 96 hrs	Inj. comp.	48 hr pre-equilibration	Human	116
	Decreased at 48 hrs	Impact	4 hr pre-equilibration	Horse	243
Glucosamine derivative (Glu5) [*]	Decreased at 48 hrs	Impact	- Bone	Horse	245
Inhibitors of calcium activated enzymes ^{a,*}	Decreased at 48 hrs	Impact	- Bone	Horse	244
Antioxidants ^{b,**}	Decreased at 24 hrs	Cyclical shear	- Bone	Human	330
L-NMA ^c	Decreased at 7 days	Impact (x3)	+ Bone, + RC	Dog	199
COX inhibitors ^d	Decreased at 6 days	Impact	- Bone	Human	256
IGF-I ^e	Decreased at 48 hrs	Inj. comp.	72 hr pre-equilibration	Human	118
Dexamethasone	Decreased at 48 hrs	Inj. comp.	48 hr pre-equilibration	Cow, Human	118

[†], a post-treatment compression protocol was sometimes necessary for the effect

^{*}, tissue was incubated for 3 hrs pre-injury in the presence of these agents

^{**}, tissue was incubated for 2 hrs pre-injury in the presence of these agents

^a, calpain and calcium/calmodulin-regulated kinase II (CaMKII)

^b, *n*-acetylcysteine, vitamin E, and N-nitro-L-arginine methyl ester (L-NAME)

^c, L-NMA = N⁶-methyl-L-arginine

^d, indomethacin and celecoxib

^e, IGF-I = insulin-like growth factor-1

^f, Inj. comp. = Injurious compression

^g, RC = radially confined by surrounding tissue

^h, all animals for the studies in this table were mature

Table 1-II: Post-injury interventions affecting glycosaminoglycan release, tissue stiffness, and progenitor cells

Agent	Main outcome	Experimental system			Reference
		Loading	Boundary conditions	Pre-injury processing	
MMP inhibitor (CGS 27023A)*	Decreased GAG ^c release at 3, 5, and 7 days	Inj. comp. ^d	- Bone, Unconfined	72 hr pre-equilibration, Superficial zone removed	Cow 130
MMP inhibitor (doxycycline)	Decreased GAG release at 1 and 2 weeks	Impact	+ Bone, + RC ^e	None	Bovine 55
IGF-I ^a	Decreased GAG release at 1 week	Impact	+ Bone, + RC	None	Bovine 357
z-vad.fmk	Decreased GAG release at 48 hrs	Inj. comp.	- Bone, Unconfined	48 hr pre-equilibration	Cow, Human 117,118
Inhibitor of caspase 9	Decreased GAG release at 48 hrs	Impact	- Bone	4 hr pre-equilibration	Horse 243
Inhibitor of calpain	Decreased GAG release at 48 hrs	Impact	- Bone	4 hr pre-equilibration	Horse 244
Polysulphated GAG (Adequan)	Mitigated loss of tissue stiffness at 30 weeks	Impact	<i>In vivo</i>	<i>In vivo</i>	Rabbit 149
FGF-2 ^b	Increased number of chondrocyte progenitor cells	Impact	- Bone	None	Horse 224

* tissue was incubated for 6 hrs pre-injury in the presence of CGS 27023A

^a IGF-I = insulin-like growth factor-1

^b FGF-2 = fibroblastic growth factor-2

^c GAG = glycosaminoglycan

^d Inj. comp. = Injurious compression

^e RC = radially confined by surrounding tissue

^f all animals for the studies in this table were mature, except for reference ¹³⁰

Figure 1-1: Framework for mechanical injury of living tissues

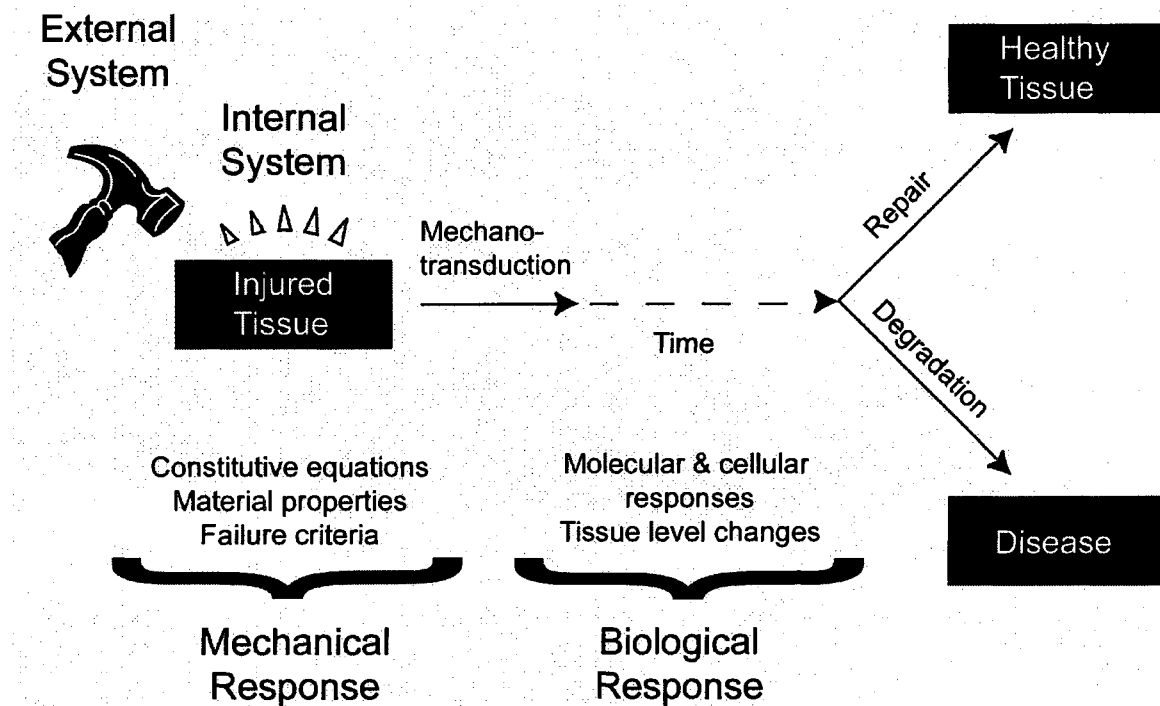


Figure 1-1. A framework for mechanical injury of living tissues. The framework consists of two dichotomies. The first separates the external and internal mechanical systems; the second separates the mechanical and biological responses. The external system is the method by which the mechanical insult is delivered. The tissue (internal system) then responds mechanically to the insult in a way dependent upon the tissue's properties, failure criteria, etc. This mechanical response activates mechanotransductive cascades that initiate the tissue's biological response at both molecular and cellular levels. After some time, tissue level changes occur that determine whether the tissue has repaired itself from the mechanical injury (healthy tissue), or whether the tissue will degrade in a process leading to disease.

Figure 1-2: Different models used for mechanical injury of articular cartilage

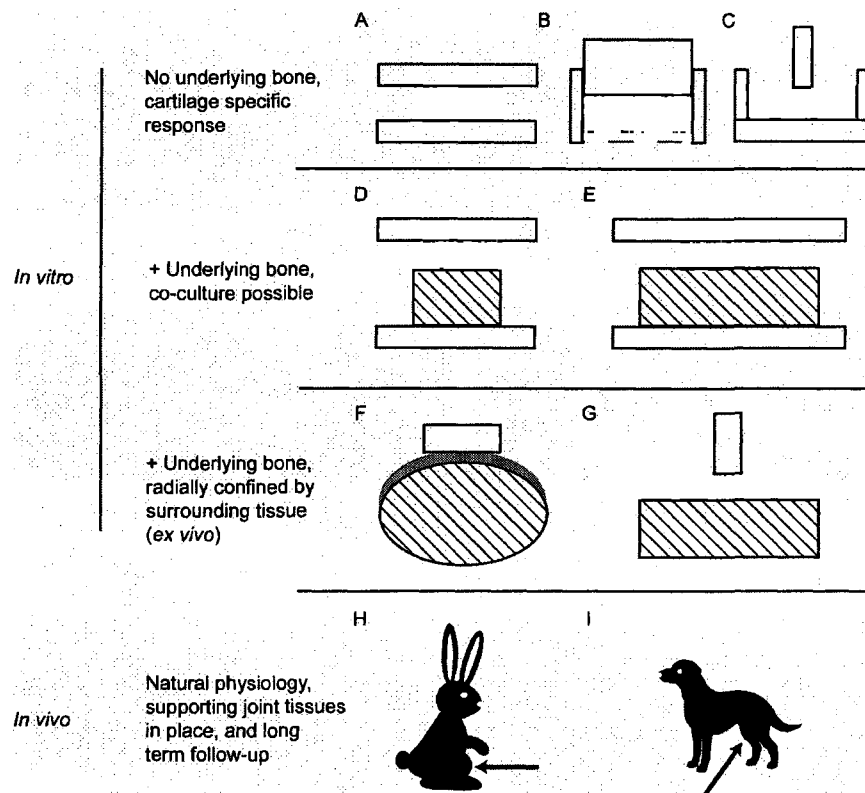


Figure 1-2. Pictorial representation of the many experimental systems used to create mechanical injuries of articular cartilage. Both *in vitro* and *in vivo* models have been used. An important feature of each model is the loading geometry, since this determines the boundary conditions for the mechanical problem. In this figure, articular cartilage is grey, underlying bone is hatched white, and the loading chamber and platens are white. A-C) Different geometries used to mechanically injure cartilage without underlying bone, D & E) the two loading geometries that have been used for osteochondral explants, F & G) *ex vivo* loading in which cartilage is left in its *in situ* position during injury (e.g., F represents an intact patella, G represents the proximal ulna), and H & I) *in vivo* models of rabbit and canine patellofemoral (PF) injury. In A-G, the load is applied perpendicular to the cartilage surface through the uppermost platen. In H & I, the animal's PF joint is positioned perpendicular to the mass delivering the mechanical insult (mass's path represented by black arrows). See text for specific references that have employed each model.

Chapter 2: Temporal effects of impact on articular cartilage cell death, gene expression, matrix biochemistry, and biomechanics*

Abstract

Articular cartilage injury can cause post-traumatic osteoarthritis, but early processes leading to the disease are not well understood. The objective of this study was to characterize two levels of impact loading at 24 hrs, 1 week, and 4 weeks in terms of cell death, gene expression, extracellular matrix biochemistry, and tissue biomechanical properties. The data show cell death increased and tissue stiffness decreased by 24 hrs following High impact (2.8 J). These degradative changes persisted at 1 and 4 weeks, and were further accompanied by measurable changes in ECM biochemistry. Moreover, following High impact at 24 hrs there were specific changes in gene expression that distinguished injured tissue from adjacent tissue that was not loaded. In contrast, Low impact (1.1 J) showed little change from control specimens at 24 hrs or 1 week. However, at 4 weeks, a significant increase in cell death and significant decrease in tissue stiffness were present. The constellation of findings indicates Low impacted tissue exhibited a delayed biological response. The study characterizes a model system for examining the biology of articular cartilage post-impact, as well as identifies possible time points and success criteria to be used in future studies employing intervention agents.

*Chapter published as Natoli RM, Scott CC, and Athanasiou KA, "Temporal effects of impact on articular cartilage cell death, gene expression, matrix biochemistry, and biomechanics," *Ann Biomed Eng* 36(5):780-92, 2008.

Introduction

Impact loading of articular cartilage leads to post-traumatic OA through effects on the cells and extracellular matrix (ECM) of the tissue. In such cases, cartilage function is believed to deteriorate as a result of chondrocyte death,⁵² changes in the biochemical characteristics of the ECM,³²⁵ and weakening of the tissue's biomechanical properties.²¹⁶ Several studies have identified similar characteristic responses of articular cartilage to mechanical injury, showing the level of impact or injurious compression correlates with increasing cell death and degradative changes in the ECM,^{253,339} which ultimately manifest as detrimental changes in tissue biomechanical properties.^{150,154,293} The present study employs an *ex vivo* system of impact loading applied to full thickness, mature bovine articular cartilage, radially confined by surrounding tissue with underlying bone attached.

Several *in vitro* explant studies have investigated the nature and degree of cell death following mechanical injury, though the majority has looked only at early times, typically less than seven days. Studies employing impact loading to chondral explants have demonstrated that cell death increases with increasing impact energy.^{242,253} Onset of cell death has been shown at stresses as low as ~3-6 MPa.^{137,162} In contrast, other studies suggest a threshold of 15-20 MPa for the initiation of cell death, with further increase in peak stress causing both increased amount and depth of cell death from the surface.^{339,462} In a relatively long *in vitro* study, canine cartilage explants were cyclically loaded at 0.3 Hz to 5 MPa at a rate of 60 MPa s⁻¹ and subsequently cultured for 3 weeks.³⁰⁸ Cell death

was found to increase with time in culture, be highest inside the impact area, and spread to adjacent tissue, demonstrating that damaged tissue can affect adjacent tissue. However, to our knowledge, no *in vitro* study of mechanical injury to articular cartilage has investigated cell death beyond 3 weeks.

Studies measuring the biochemical content of the ECM post-injury have found impact causes glycosaminoglycan (GAG) release and proteoglycan synthesis to decrease. In one study, a drop tower was used to apply several levels of impact to bovine articular cartilage explants to assess matrix loss and synthesis over 2 weeks of culture.²⁵⁴ Results indicated both GAG and collagen were lost to the culture media, and an initial decrease in ECM synthesis recovered, with recovery time depending on intensity of the impact load. Sub-impact loading of bovine osteochondral explants also resulted in GAG release to the media over 4 days, with proteoglycan synthesis decreasing with increased loading.⁴⁰⁰ GAG release has been shown to consist of both aggregating proteoglycans and degradation fragments.³⁹⁹ Finally, a differential response of injured tissue compared to adjacent tissue has been observed for the ECM in terms of damage²⁵⁵ and proteoglycan synthesis.⁴⁰⁰

To begin to understand chondrocyte molecular biological responses to mechanical trauma, gene expression patterns have been examined up to 24 hrs post-injury. One study used gene chip technology to investigate expression changes following cyclical loading, and found 172 genes showed significantly different expression compared to controls.⁸³ Using a custom-made bovine cDNA array and qRT-PCR, Chan et. al.⁹⁴ identified several genes with significantly

altered expression 3 hrs post injurious compression to a peak stress of 30 MPa, some of which were matrix metalloproteinases. Another study used qRT-PCR, demonstrating increased expression of aggrecan, matrix metalloproteinase-1, tissue inhibitor of matrix metalloproteinase-1, and collagen type I after injurious compression.³⁰³ However, no data on gene expression following injurious loading are available past 24 hrs.

Collectively, the studies described above underscore the detrimental effects mechanical injury can produce. Though cell death and matrix damage have been widely studied, only one *in vitro* study has looked at changes in mechanical properties, showing decreased stiffness following injurious loading. However, that study was only taken out to 3 days.²⁹³ To further understand post-traumatic OA, better characterization of the biomechanical behavior of articular cartilage post-impact loading is needed to see if there is continued loss of tissue stiffness. Moreover, spatio-temporal characterization of gene expression profiles may aid in understanding early stages of the disease process. In this study we investigated, simultaneously, changes taking place in articular cartilage cell viability, gene expression, matrix biochemistry, and biomechanical properties at 24 hrs, 1 week, and 4 weeks following impact loading at two levels. Our goals were to 1) characterize established responses of articular cartilage to mechanical injury, as occurring in our system, and 2) investigate differential gene expression and matrix biochemical content in injured, compared to surrounding, tissue. We hypothesized that tissue stiffness would continue to decrease over time in culture following impact injury, which would be paralleled by increased cell death and

GAG loss. Further, based on the differential response of the ECM from injured compared to adjacent tissue reported in the literature, we expected spatial variation in gene expression. The comprehensive approach of this study enables multiple correlations between different assays to be drawn, and a description of events taking place post-impact from the molecular level to the tissue level to be made.

Materials and methods

Tissue harvest and articular cartilage impact

Tissue harvest and impact were performed as previously described.⁴³¹ Briefly, bovine elbow joints from 24 skeletally mature heifers were acquired from a local abattoir within 4 hrs of slaughter and harvested within 18 hrs. The distal portion of the proximal ulna was cut from the specimen parallel to the articular surface using a reciprocating saw (Ryobi, Hiroshima, Japan) leaving ~1 cm of attached underlying bone. Specimens were washed with sterile PBS and transferred *in situ* onto a sterile specimen clamp. The specimen clamp was then positioned in the impact instrument. The impact instrument consists of linear bearings with an attached sliding plate to which variable weight can be added. The plate slides down the bearings until striking an impact interface attached to an impact tip that is contact with the tissue surface. The tissue surface is rendered immobile by its positioning in the specimen clamp. The accelerometer is attached to the underside of the impact interface.⁴³¹ For this study two levels of impact were employed, which will hereon be designated as 'Low' (6 cm drop for an 18.4 N tup weight, 1.1 J) and 'High' (10 cm drop for a 27.8 N tup weight, 2.8

J). These levels were chosen such that the Low level does not visibly damage the cartilage, whereas the High level causes immediate grossly identifiable damage.⁴³¹ For this study, the impact area was defined as the cartilage tissue immediately below the 5 mm diameter impact tip. Impact was performed in the middle of the medial compartment with underlying bone still attached and 2-3 radii of separation between each impact area. For each joint, tissue was randomly assigned to the control, Low, or High impact levels.

Explant culture and processing

After impact, 8 mm diameter explants centered about the 5 mm impact area (described above) were removed using a dermatological punch and a #10 scalpel blade. Baseline explants (tissue without impact or time spent in culture) were randomly taken from six animals and processed on the same day as tissue harvest. For each animal the control, Low, and High impact explants were placed into individual wells of a 6-well tissue culture plate with 3 mL of media containing Dulbecco's modified eagle medium (DMEM) with GlutamaxTM (Invitrogen, New York), supplemented with 100 units/mL Penicillin (Biowhittaker, Maryland), 100 µg/mL Streptomycin (Biowhittaker), 50 µg/mL Gentamycin (Invitrogen), 50 µg/mL Kanamycin (Sigma, Missouri), 2.5 µg /mL Fungizone (Biowhittaker), 0.1 mM non-essential amino acids (Invitrogen), 50 µg/mL ascorbic acid, and 10% Fetal Bovine Serum (FBS) (Gemini Bioproducts, California). The explants were cultured for 24 hrs, 1 week, or 4 weeks with media changes at 24 hrs and every 2-3 days thereafter. Spent media were combined to yield collections

corresponding to 0-24 hrs, 0-7 days, 8-14 days, 15-21 days, and 22-28 days and stored at -20°C for later analysis.

After 24 hrs, 1 week, or 4 weeks in culture, explants were processed for qRT-PCR, matrix biochemistry, and biomechanics assays. First, from the center of the 8 mm explant, a 5 mm diameter punch was taken yielding the tissue area that was subjected to the impact load plus an outer ring (designated outside the impact area). Half of the outer ring was stored in RNA/later[®] (Ambion, Austin, TX) at -20°C until RNA isolation. The rest was weighed and lyophilized for at least 48 hrs. Second, from the center of the 5 mm punch corresponding to the impact area, a 3 mm diameter punch was taken yielding biomechanics specimens plus an inner ring (designated inside the impact area). The 3 mm diameter portion of tissue was wrapped in gauze soaked with normal saline plus protease inhibitors (10 mM N-ethylmaleimide, 5 mM benzamidine, 2 mM EDTA, and 1 mM phenylmethylsulfonyl fluoride) and stored at -20°C until creep indentation biomechanical testing. The remaining inner ring was cut in half and processed in the same manner as the outer ring.

Viability staining

Cell viability was assessed on a separate set of explants. Staining (Live/Dead[®] assay; Molecular Probes, Eugene, Oregon) was performed on 0.5 mm thick sections of 8 mm diameter baseline tissue or explants taken directly from culture at each time point, allowing assessment of impacted and adjacent tissue areas. Sections were incubated in 0.5 µL calcein-AM and 2 µL ethidium homodimer-1 per mL of complete media for 20 min at 37°C. Viability pictures

were taken with an epi-fluorescence microscope (Zeiss, New York), and images were analyzed using ImageJ (National Institutes of Health, Maryland). Percent viability was measured over a square area defined by the full thickness of the explant.

RNA isolation and qRT-PCR

RNA isolation was performed simultaneously for all 16 groups: 1) baseline, 2-4) 24 hr, 1 week, and 4 week culture controls (CCs), 5-7) 24 hr, 1 week, and 4 week Low impact inside the impact area (LI), 8-10) 24 hr, 1 week, and 4 week Low impact outside the impact area (LO), 11-13) 24 hr, 1 week, and 4 week High impact inside the impact area (HI), 14-16) and 24 hr, 1 week, and 4 week High impact outside the impact area (HO). Tissue was homogenized in TriZol (Invitrogen, Carlsbad, CA) using a Polytron homogenizer (Kinematica, Switzerland), and RNA was isolated following the manufacturer's protocol. The RNA concentration of each sample was determined using a spectrophotometer (Nanodrop, Wilmington, DE), and 300 ng of RNA was used in the reverse transcriptase (RT) reaction. The RT reaction consisted of incubating 1mM dNTPs, 1mM random hexamers, RNase Block, and Stratascript RT enzyme (Stratagene, Inc. LaJolla, CA) at 42°C for 60 min, followed by termination at 90°C for 5 min. All samples were RT'd simultaneously.

qRT-PCR was performed for the following genes: glyceraldehyde-3-phosphate dehydrogenase (GAPDH), collagen type I (Col1), collagen type II (Col2), aggrecan (AGC), superficial zone protein (SZP), matrix metalloproteinase-1 (MMP-1), and tissue inhibitor of MMP-1 (TIMP-1). The

sequences for the primers and probes (Table 2-I) have been previously developed in our lab and were used with the Multiplex Master Mix kit (Qiagen, Valencia, CA).^{123,219} Briefly, the qRT-PCR consisted of 25 μ L containing 1 μ L cDNA from the RT reaction, 0.025 U/ μ L HotStar-Taq polymerase, 3.5 mM MgCl₂, 0.2 mM dNTPs, buffer, and primer (synthesized by Sigma-Genosys, Woodlands, TX) and probe (synthesized by Biosearch Technologies, Novato, CA) concentrations ranging from 50 to 125 nM depending on the triplex. The reaction conditions were optimized to yield efficiencies in the range 0.9 to 1. qRT-PCR was performed using a Rotor-Gene™ (Corbett Research, Sydney, AU) with a 15 min denaturing step followed by 45 temperature cycles (15 sec at 90°C, 30 sec at 60°C). Since the amount of RNA used for each RT reaction was equal, it was possible to calculate abundance values and thereby compare gene expression quantitatively. The abundance level for the gene of interest (A_{GOI}) was calculated using the take-off cycles for the gene of interest (C_t) according to the following equation:

$$A_{GOI} = \frac{1}{(1 + E_{GOI})^{C_t}}$$

where E_{GOI} is the reaction efficiency for the gene of interest.⁸

Biochemical characterization

Biochemical assays were performed for sGAG, total collagen, and DNA content. For all assays, samples were digested in 2 mL papain solution¹¹ for 18 hrs, or until no tissue remained. sGAG content was tested using a 1,9-dimethyl-

methylene blue colorimetric assay (Blyscan™ Sulfated GAG Assay kit, Accurate Chemical and Scientific Corp., Westbury, NY). sGAG released to the media was normalized to tissue volume, with volume calculated knowing the explant area (8 mm Ø) and thickness. Collagen content was measured using a modified chloramine T and dimethylaminobenzaldehyde colorimetric assay⁴⁰⁵ using SIRCOL Collagen Assay (Accurate Chemical, Westbury, NY) as the standard. Total DNA content of each sample was also assayed (Quant-iT™ PicoGreen® dsDNA Assay Kit, Molecular Probes, Eugene, Oregon). Cell number for a sample was calculated assuming 7.8 pg of DNA per chondrocyte.²⁷⁹

Creep indentation biomechanical properties

Prior to mechanical testing, the 3 mm diameter samples (see explant processing above) were thawed for 1 hr at room temperature in normal saline with protease inhibitors. A creep indentation apparatus was used to determine the compressive creep and recovery behavior of the cartilage explants.³⁰ Each sample was attached to a flat stainless steel surface with a thin layer of cyanoacrylate glue and equilibrated for 20 min in normal saline with protease inhibitors. The sample was then placed into the creep indentation apparatus, which automatically loaded and unloaded the specimen while recording the tissue's creep and recovery behavior. A tare load of 0.005 N (0.5 g), followed by a test load of 0.02 N (2 g), was applied to the sample with a 0.8 mm diameter, flat-ended, rigid tip (50% porosity, 50 µm pore diameter). Specimen thickness was measured using a needle probe, force transducer, and linear variable

differential transformer.⁴⁵⁸ To calculate the specimen's material properties, a semi-analytical, semi-numeric, linear biphasic model was used.³⁴⁸

Statistical analysis

A sample size of $n = 4-6$ was used for gene expression. For cell viability, sGAG release and tissue content, total collagen content, DNA content, and creep indentation measurements, a sample size of $n = 5-6$ was used. Sample size was based on a power analysis ($\alpha = 0.05$ and $\beta = 0.2$) of pilot gene expression and creep indentation data allowing detection of a 40% change. Standard deviations associated with the other analyses (cell death and matrix biochemistry) were substantially less than those of gene expression or tissue stiffness, so the magnitude of change detected was less than 40%. We chose an $n = 6$ for each assay based on the power analysis, though some gene expression groups had $n = 4$ and some biomechanics groups had $n = 5$. The decreased sample number in these groups was due to the samples not being of sufficient quality to test, for example, samples with RNA isolations not meeting the recommended A260/A280 ratio. For gene expression data, each group (combination of time and impact/tissue area) was first normalized to the baseline abundance value of that gene to yield fold change from native expression. Subsequently, a 2-way ANOVA was performed. For all other assays, a 1-way ANOVA was performed on all data, including baseline values (StatView, Abaqus Concepts, Berkeley, CA). If significance ($p < 0.05$) was found, a Student-Newman-Keuls post-hoc test was performed.

Results

Impact measurements

The impact instrument consistently reproduced two distinct levels of loading. Table 2-II characterizes the Low and High impact levels in terms of the following metrics: peak stress, time to peak stress, and duration of impact. Comparing the two impact levels, peak stress and duration of impact were significantly different as seen previously.⁴³¹ Of note, these impacts satisfy the definition put forth by Aspden et al.²⁶ in that they occur in on the order of ms at stress rates greater than 1000 MPa s^{-1} .

Gross morphology and cell viability

As previously shown,⁴³¹ High impact caused immediate grossly identifiable damage that persisted over 4 weeks in culture. Low impact did not cause immediate damage, nor did any noticeable damage develop in culture. As expected, non-impacted CCs also showed no gross damage throughout the experiment. Figure 2-1 shows 100X magnification pictures of specimens stained for viability. Dead cells fluoresce red and living cells fluoresce green. Inside the impact area, cell death increased both with time in culture and level of impact. At baseline, almost all of the chondrocytes were alive (Fig. 2-1a), similar to what was seen in the non-impacted CC specimens at 24 hrs and 1 week (Figs. 2- 1b and 1e). However, the 4 week non-impacted CCs began to show cell death in the superficial zone (Fig. 2-1h). An increased amount of cell death due to time in culture was also seen following Low (Fig. 2- 1c, 1f, and 1i) and High impact (Fig. 2- 1d, 1g, and 1j). Further, increasing impact level also caused increased cell

death. At 24 hrs following Low or High impact cell death was limited to the superficial zone. At 1 and 4 weeks cell death in the Low and High impact groups increased in the deeper zones of the tissue (Figs. 2- 1f, 1g and 1i, 1j). Note the surface damage characteristic of High impact. There was little to no cell death noted outside the impact area at 24 hrs or 1 week for control, Low, or High impact. At 4 weeks, some cell death appeared in the superficial zone of adjacent tissue for Low and High impact, similar to the 4 week non-impacted CC described above.

The qualitative amount of cell death observed due to impact or time in culture was reflected quantitatively. Figure 2-2 shows a graph of percent cell death inside the impact area. Percent cell death in baseline specimens (2.6 ± 0.9) and the 24 hr (1.8 ± 0.8) and 1 week (4.9 ± 3.1) CCs was not significantly different. However, at 4 weeks cell death in the non-impacted CC (10.5 ± 4.0) was significantly increased over baseline and 24 hr CCs, though similar to the 1 week CC. At 24 hrs, both Low (9.9 ± 1.1) and High impact (18.8 ± 3.7) resulted in significantly increased cell death compared to baseline and the 24 hr CC. Further, cell death following High impact was significantly increased compared to Low impact at 24 hrs. This trend was also seen at 1 and 4 weeks. Following Low impact, cell death did not significantly increase between 24 hrs and 1 week (11.4 ± 2.1), but, at 4 weeks (35.6 ± 5.1), Low impacted specimens showed significantly more cell death than was present at 1 week. In contrast, High impact resulted in significantly increasing cell death at each time point (27.8 ± 6.1 and 47.3 ± 7.7 for 1 and 4 weeks, respectively). Though cell death in controls did

increase 9 percentage points from 24 hrs to 4 weeks, both Low and High impact boasted increases of 30 percentage points. Thus, the vast majority of cell death following impact was due to the injury and not time in culture.

qRT-PCR

GAPDH abundance showed no significant change for any group in this study ($p = 0.18$). Though quantitative, abundance does not have any physical meaning. Because of this, abundance values for each gene assayed were normalized to the gene's native expression (measured from baseline explants) to reflect fold change. This also enabled a 2-way ANOVA to be performed on time in culture and tissue area/impact level. Mean native abundance values were 2.1×10^{-4} , 2.2×10^{-6} , 1.9×10^{-6} , 3.9×10^{-7} , 3.0×10^{-9} , and 5.2×10^{-12} for Col2, SZP, AGC, TIMP-1, Col1, and MMP-1, respectively. This order for abundance agrees reasonably with prior work,³⁰³ for which any differences may be due to the age of the animals used.

For each gene investigated, time was a significant factor, while only for SZP was tissue area/impact level a significant factor. Several additional differences were found at 24 hrs following High impact. Figure 2-3 shows the temporal expression patterns inside the impact area for AGC, Col2, and SZP (Fig. 2-3a) and Col1, MMP-1, and TIMP-1 (Fig. 2-3b). At 24 hrs AGC expression had increased 2.4 fold from its native value. Further, 24 hr AGC expression in HO tissue was significantly increased over the 24 hr CC, LI, and LO groups (Fig. 2-4a). AGC expression remained increased at 1 week, but significantly decreased expression at 4 weeks. Col2 expression at 24 hrs was 75% of its

native expression level and then significantly decreased at 1 and 4 weeks. Similar to AGC, SZP expression was increased 2.8 fold at 24 hrs and expression in HO tissue was significantly increased over CC, LI, LO, and HI groups (Fig 2-4b). However, between 24 hrs and 1 week SZP expression decreased significantly to an expression level only 4% of its native value. This decrease recovered to 40% at 4 weeks, though not significantly.

Col1 expression changed most dramatically in this study compared to the other genes, so much so that the Col1 data in figure 2-3b have been scaled down by a factor of 10 (i.e., the ~37 fold increase at 4 weeks is really a 370 fold increase) to fit on the same graph as MMP-1 and TIMP-1. Col1 expression at 24 hrs dropped to 4% of its native expression. At 1 week, this drop recovered to exceed native expression 35 fold, though not significantly. Notably, while expression at 1 week in the non-impacted CC, LI, and LO averaged only a 1.8 fold increase, the average increase for HI and HO was 78 fold. Finally, all tissue area/impact groups at 4 weeks demonstrated a minimum 323 fold increase, with the average being 378 fold. MMP-1 expression at 24 hrs was 19 times its native expression level. Further, 24 hr MMP-1 expression in HI tissue was significantly increased over the 24 hr non-impacted CC (Fig. 2-4c). MMP-1 expression significantly decreased at 1 and 4 weeks. TIMP-1 expression paralleled MMP-1 expression with 24 hr expression being significantly increased compared to both 1 and 4 weeks. Also, at 24 hrs, TIMP-1 expression in HO tissue was significantly increased over the 24 hr CC, LO, and HI groups (Fig. 2-4d). There were no significant changes observed for the MMP-1/TIMP-1 ratio.

Biochemistry

Table 2-III shows the results from characterization of matrix biochemical content at 1 and 4 weeks. Specifically, sGAG, collagen, and DNA content as percentage of wet weight, as well as %H₂O of the explants are presented. In terms of sGAG content, no significant changes were noted at 1 week. However, by 4 weeks LI and both HI and HO experienced significant decreases in sGAG content from baseline. Collagen content trended down at 1 week compared to baseline for all groups. At 4 weeks, the downward trend was reversed with all groups showing slightly increased total collagen content compared to baseline. Notably, collagen content for HI was significantly increased from its respective 1 week value. The DNA content inside the impact area was significantly decreased for both impact levels compared to outside the impact area and the non-impacted CC at 1 week. There was a decrease in the number of cells present as time in culture increased. This was significant for the 4 week CC, and both LO and HO, but not for LI and HI. Percent water, reflecting tissue hydration and swelling, was not significantly different for any group.

Figure 2-5 shows cumulative sGAG release from the explants. Increased culture duration caused an increase in sGAG release. With respect to impact level, at 24 hrs there were no significant differences (1.8 ± 0.5 , 3.7 ± 1.1 , and $3.5 \pm 1.2 \mu\text{g mm}^{-3}$, for CC, Low, and High respectively). However, at both 1 and 4 weeks High impact (23.9 ± 12.7 and $55.7 \pm 11.6 \mu\text{g mm}^{-3}$, respectively) resulted in a significant increase in sGAG release compared to non-impacted CCs (11.6 ± 4.2 and $32.5 \pm 7.2 \mu\text{g mm}^{-3}$, respectively) and Low impact (14.4 ± 5.1 and $38.2 \pm$

4.4 $\mu\text{g mm}^{-3}$, respectively). Finally, sGAG release showed a significant linear correlation with cell death ($R^2 = 0.68$, $p = 0.006$).

Biomechanics

Tissue stiffness (Fig. 2-6), as measured by aggregate modulus, was significantly affected by impact level and time spent in culture. The aggregate moduli of baseline specimens (687 ± 65 kPa) and the 24 hr (654 ± 128 kPa) and 1 week (696 ± 202 kPa) non-impacted CCs were not significantly different, but, at 4 weeks tissue stiffness in the CC (392 ± 83 kPa), was significantly decreased compared to baseline and the 24 hr and 1 week CCs. In terms of impact level, at 24 hrs High impact (402 ± 32 kPa) resulted in a significant decrease in aggregate modulus compared to the CC and Low impact (560 ± 156 kPa) specimens. This was also observed at 1 week (266 ± 68 and 503 ± 192 kPa for High and Low impact, respectively). It is notable, however, that at 4 weeks both Low (183 ± 37 kPa) and High (156 ± 59 kPa) impact explants experienced a significant decrease in aggregate modulus compared to the 4 week non-impacted CC, and were not different from each other. To help understand the causes for the loss of tissue stiffness observed, the aggregate modulus was correlated with cumulative sGAG loss and percent cell death. Significant linear correlations were found with $R^2 = 0.67$ ($p = 0.007$) and $R^2 = 0.87$ ($p = 0.0002$), respectively. There were no significant differences in tissue permeability (range 0.32 - $11.32 \times 10^{-15} \text{ m}^4\text{N}^{-1}\text{s}^{-1}$). Analysis of Poisson's ratio (range 0.0 - 0.32) showed that 1 week Low impact was significantly decreased from baseline but recovered by 4 weeks.

Discussion

In this study we characterized the response of articular cartilage following two levels of impact loading at 24 hrs, 1 week, and 4 weeks post-impact. While High impact resulted in early degenerative changes, Low impact exhibited a delayed biological response. Further, to the authors' knowledge, this study is the first to examine gene expression following mechanical injury at time points greater than 24 hrs (including injured and adjacent tissue sites) and to simultaneously assess gene expression and protein levels. The data demonstrate that a High impact load of 2.8 J resulted in cell death and decreased tissue stiffness at 24 hrs. At 1 and 4 weeks, these degenerative changes remained, and further tissue degradation was manifested by increased GAG release from, and an accompanying decrease in GAG content measured in, the tissue. In contrast, a Low impact of 1.1 J caused little change from the non-impacted culture controls at either 24 hrs or 1 week, but, at 4 weeks, Low impact showed similar detrimental changes as seen following High impact. This was most noteworthy for a measurement of tissue functionality, where the aggregate moduli following Low and High impact declined 73% and 77% from baseline, respectively. Moreover, there were specific changes in gene expression resulting from High impact that manifested at the early time points. Finally, results from cell viability, matrix biochemical content, and gene expression indicated differences between tissue subjected to the mechanical load compared to adjacent tissue.

The impact levels in this study meet the definition set forth by Aspden et al.²⁶ in that they occur in less than 30 ms and are greater than a stress rate of 1000 MPa s⁻¹. Other studies have used higher peak stresses but report the impact measurements in various ways. Repo and Finley⁴⁰⁸ found the peak stress threshold for gross damage of articular damage in the presence of underlying bone to be 25 MPa at strain rates of 500 and 1000 s⁻¹, whereas Haut²¹⁸ found 25 MPa to cause subchondral bone fracture. Further, Duda et al.¹³⁷ found cell death at peak stresses as low as 3 MPa, though others have suggested 15-25 MPa as a threshold for the initiation of cell death.^{408,462} Thus, while the peak stresses (3.1 MPa and 9.1 MPa) measured in this study were not as high as some studies, the differences with respect to gross damage and cell death are likely due to the very high stress rates (~4,420 and 18,200 MPa s⁻¹ for Low and High, respectively). In a similar drop tower experiment to cartilage without underlying bone²⁵⁵, stress rates of ~15,000 MPa s⁻¹ were found, but with a peak stress of 22 MPa. The difference between peak stresses between the experiment just described and ours is indirect evidence that underlying bone attenuates the peak loads experienced by cartilage, thus protecting it from injury, a function supported by previous work.^{253,288,402}

In this experiment, the amount of cell death increased with time and impact level, as well as exhibited a spatio-temporal pattern. It has been previously shown that loading rate affects cell death such that increased rate causes less cell death,^{151,339,342} though these studies explored rates less than or equal to 1000 MPa s⁻¹. The present study found increased death with increased

impact energy. In support of this, other very high stress rate experiments have also shown increased cell death with increasing energy of impact.^{242,253} At 24 hrs, cell death was limited to the superficial zone inside the impact area. Cell death then spread to deeper regions of the cartilage over time in culture, but there was no noticeable radial spread. These findings are similar to previous work that loaded cartilage from 0-65 MPa at 35 MPa s⁻¹ without underlying bone.⁴⁶² In that study, cell death immediately following a 10 MPa injury was limited the superficial zone. At 24 hrs, cell death did not extend into the unloaded region, but appeared to extend throughout the depth of the explant. This is in contrast to work by Levin et al.³⁰⁸ who cyclically loaded canine articular cartilage and observed direct evidence for the spread of cell death from injured to non-injured tissue, suggesting that loading regiment may alter the spatio-temporal pattern of cell death. This possibility is supported by another single impact loading study that showed little cell death in tissue adjacent to the impact site and no spread over five days in culture.³¹⁰ Lastly, similar to cell viability staining, in the present study DNA content measured in the tissue showed injured tissue contained significantly fewer cells than control or adjacent tissue at 1 week, and, at 4 weeks, changes in the adjacent tissue were comparable to changes in controls.

The gene expression data show that High impact (2.8 J) resulted in significantly different expression from non-impacted culture controls and there is a temporal profile of gene expression changes resulting from explanting the tissue. Compared to native expression levels, AGC, SZP, and TIMP-1 all showed increased expression in the tissue adjacent to the impact site at 24 hrs following

High impact. This observation may represent a decreased ability of the impact area to attempt repair, or the surrounding area attempting to heal itself. Additionally, MMP-1 expression increased in the injured tissue at 24 hrs. This finding is similar to work by Lee et al.³⁰³ who showed that AGC, TIMP-1, and MMP-1 were increased in loaded tissue 24 hrs post injurious compression to 50% strain at 1 s^{-1} (resulting in a $\sim 20 \text{ MPa}$ load). Further, increased MMP-3 expression has been observed for the same loading protocol just described, as well as following injury at 30 MPa at a rate of 600 MPa s^{-1} .^{94,385} Interestingly, in the present study SZP expression was significantly decreased in HI tissue compared to HO and Col1 had dramatically increased expression in both HI and HO tissue at 1 week. Both of these changes are signs of chondrocyte de-differentiation.¹²³ The constellation of de-differentiation, decreased expression of normally expressed matrix molecules, and increased expression of several MMPs suggests, at least in these *in vitro* studies, that a degenerative process is initiated early post-injury. Moreover, these results are similar to *in vivo* work that has looked at osteoarthritis (OA) and cartilage injury in humans,^{427,459,517} such as Col1A1 and Col1A2 having increased expression in damaged cartilage taken from OA joints.⁴²⁷ It is briefly worth speculating on molecular mechanisms that may transduce the impact load and lead to changes in gene expression. Impact loading of cartilage generates streaming potentials, stress/strain fields, and hydrostatic pressure fields within the tissue, all of which are experienced at the cellular level. It has been shown that chondrocytes respond to mechanical load through integrin-cytoskeletal interactions, as well as ion and stretch activated

channels located in the cell membrane.⁴⁹¹ Indeed, hydrostatic pressure applied to chondrocytes has been shown to affect ion transporters^{73,215} and cause changes in collagen type II and aggrecan gene expression.⁴⁵¹ Further characterization of temporal gene expression profiles may aid in discovery of clinical tools to diagnose or monitor treatment of post-traumatic OA.

Turning to matrix biochemistry, at 4 weeks GAG concentration significantly decreased and total collagen concentration trended upwards. GAG concentration decreased in injured tissue following Low and High impact as well as in tissue adjacent to High impact. Notably, changes in tissue GAG took 4 weeks to become significant, while GAG release to the media was significant at 1 week (Table 2-III and Fig. 2-5). Thus, it appears GAG release into culture media is more sensitive than GAG in the tissue to detect ECM degradation. While the amount of GAG in the tissue is due to a balance of loss and production, decreased synthesis in response to injurious loads has been reported.^{254,293,400} Though we observed increased AGC expression, increased mRNA levels may not translate to increased protein production. An alternative explanation for the increased GAG release to the media is that increased enzymatic activity caused more collagen matrix breakdown, freeing GAG, either whole or degradation fragments, from the tissue. Such a mechanism is supported by DiMicco et al.¹³⁰ who showed MMP inhibition reduced cumulative sGAG loss from injured tissue while inhibitors of biosynthesis had no significant effect. Though total collagen concentration for any group at 4 weeks was not significantly different from baseline, collagen concentration trended upwards from 1 week to 4 weeks,

significantly so for HI tissue. This trend may reflect the increase in Col1 gene expression and/or the decrease in tissue stiffness seen for control, Low, and High impact.

Tissue stiffness of cartilage post-injury was observed to decrease with time. Compared to non-impacted culture controls, High impact resulted in a significant decrease in tissue stiffness by 24 hrs that increased with subsequent culture. In contrast, tissue stiffness following Low impact was similar to culture controls at 24 hrs and 1 week, but by 4 weeks, became similar to High impacted tissue. The drop in tissue stiffness between 1 and 4 weeks following High impact paralleled culture controls (44% and 41% decreases for control and High, respectively), reflecting the fact that the majority of change in tissue stiffness following High impact occurred during the 1st week of culture. However, during the same time, stiffness of Low impacted tissue significantly decreased 64%, a full 20% points more than culture controls. Moreover, tissue stiffness correlated well with GAG release and percent cell death, and the gene expression data showing a decrease in Col2 and an increase in Col1 indicate a more fibrocartilaginous collagen matrix in all groups at 4 weeks,^{187,188} possibly contributing to the decreases in tissue stiffness observed. Changes in mechanical properties of cartilage are well documented in OA,²¹⁶ but not extensively studied for acute injury. In a 3 day *in vitro* study of injurious compression (loaded to 50% strain at a rate 0.01, 0.1, or 1 s⁻¹ with resulting peak stresses of 12, 18, and 24 MPa, respectively), the dynamic compressive stiffness of injured tissue was shown to decrease with increasing strain rate. Additionally,

two *in vivo* studies have shown decreased stiffness in rabbit patellofemoral cartilage beginning 4.5 months post-injury.^{150,154} Though *in vivo* studies may be a better representation of the human condition, an advantage of *in vitro* models is the ability to create the same observation in a shorter time period, a fact that may become important in screening potential therapeutic interventions.

We have previously shown in the same system that High impact results in an immediate decrease in tissue stiffness resulting from purely mechanical phenomena and correlating to the presence of surface damage.⁴³¹ Considering this fact, the present results suggest that mechanical insult initiates a detrimental biological response that causes continued loss of tissue stiffness, cell death, and ECM degradation. As a corollary, the delayed loss of tissue stiffness and cell death in Low impacted tissue is potentially explained by a delayed biological response occurring some time between 1 and 4 weeks, perhaps with similar changes in gene expression that were seen following High impact at 24 hrs.

In summary, the results of this explant study characterize the temporal effects of two levels of impact injury to articular cartilage in terms of cell death, gene expression of pertinent cartilage markers, ECM biochemistry, and tissue biomechanical properties. Our results parallel established changes from other cartilage injury studies, as well as provide new data in the form of spatial and temporal gene expression patterns and show tissue subjected to a Low level of impact exhibits a delayed biological response. It has been suggested that some cases of joint injury with normal arthroscopic, radiologic, and laboratory findings go undiagnosed at early time points³²⁰ and said that cartilage without visible

damage is considered intact, thus neglecting initial damage occurring at the cellular level.¹³⁷ Though both Low impact and baseline tissue were not different in terms of gross morphology or aggregate modulus at 24 hrs, Low impact explants at 4 weeks exhibited a tableau in terms of cell death and loss of tissue stiffness comparable to that of High impact, supporting the notion of clinically silent injuries developing into identifiable disease. Ultimately, understanding the temporal effects of impact loading will help to elucidate the processes that occur in post-traumatic OA and point to future avenues of inquiry to prevent or reverse this disease.

Table 2-I: qRT-PCR target gene primers and probes and dyes and quenchers

Gene (accession number, product size)	Forward Primer (5' – 3') Reverse Primer (5' – 3') Probe (5' – 3')	Dye Quencher
Glyceraldehyde-3-phosphate dehydrogenase (U85042, 86bp)	ACCCTCAAGATTGTCAGCAA ACGATGCCAAAGTGGTCA CCTCCTGCACCACCAACTGCTT	FAM BHQ-1
Aggrecan (U76615, 76bp)	GCTACCCTGACCCTTCATC AAGCTTTCTGGGATGTCCAC TGACGCCATCTGCTACACAGGTGA	Quasar 670 BHQ-2
Collagen type II (NM_174520, 69bp)	AACGGTGGCTTCCACTTC GCAGGAAGGTCATCTGGA ATGACAACCTGGCTCCCAACACC	ROX BHQ-2
Superficial Zone Protein (AF056218, 77bp)	CACCATCAGGATTCCTACTACACA TCACTTTAACTTCATTATGGAGGA CCCGTCAGAGTCCCTTATCAAGACA	ROX BHQ-2
Collagen type I (X02420, 97bp)	CATTAGGGGTCACAATGGTC TGGAGTTCCATTTTCACCAG ATGGATTTGAAGGGACAGCCTTGGT	Quasar 670 BHQ-2
Matrix Metalloproteinase I (X74326, 82bp)	CAAATGCTGGAGGTATGATGA AATTCGCGGAAAGTCTTCTG TCCATGGATGCAGGTTATCCCAA	Quasar 670 BHQ-2
Tissue Inhibitor of Matrix Metalloproteinase I (NM174471, unknown)	GAGATCAAGATGACTAAGATGTTCAA GGTGTAGATGAACCGGATG AGGGTTCAGTGCCTTGAGGGATG	ROX BHQ-2

Table 2-I. Primers, probes, dyes, and quenchers used for qRT-PCR.

Table 2-II: Impact measurements for the Low and High levels

Impact Level	Tup weight (N)	Drop height (cm)	Energy (J)	Peak stress (MPa)	Time to peak stress (ms)	Duration (ms)
Low	18.4	6	1.1	3.1 ± 0.7^A	0.7 ± 0.3	1.6 ± 0.4^A
High	27.8	10	2.8	9.1 ± 4.1^B	0.5 ± 0.3	1.0 ± 0.3^B

Table 2-II. Impact measurements for the Low and High impact levels. Data given as mean \pm S.D. (n = 10 per impact level). Within a column, numbers with different superscripted letters ('A' and 'B') are significantly different ($p < 0.05$).

Table 2-III: Data for tissue matrix biochemical content

Group	GAG content (% WW)	Collagen content (% WW)	DNA Content (Cells $\times 10^6$ per g WW)	% H ₂ O
Baseline	5.5 ± 0.5^A	13.6 ± 1.6	$55.7 \pm 7.2^{A,B,C}$	75.0 ± 1.1
1 week	CC	4.7 ± 1.4	61.8 ± 15.8^A	77.5 ± 3.1
	LI	4.7 ± 0.5	38.4 ± 6.4^D	77.6 ± 1.5
	LO	5.0 ± 0.6	$59.6 \pm 10.0^{A,B}$	76.9 ± 2.6
	HI	4.1 ± 0.6	37.2 ± 5.5^D	76.3 ± 2.4
	HO	4.8 ± 0.8	$58.7 \pm 5.7^{A,B}$	76.3 ± 2.6
4 weeks	CC	4.5 ± 0.6	$46.2 \pm 4.9^{B,C,D}$	74.9 ± 1.8
	LI	3.7 ± 0.9^B	38.4 ± 12.5^D	72.3 ± 6.3
	LO	4.0 ± 0.8	$44.0 \pm 10.5^{C,D}$	75.0 ± 2.0
	HI	3.7 ± 1.6^B	31.9 ± 10.6^D	73.4 ± 5.1
	HO	3.5 ± 1.3^B	$42.7 \pm 5.4^{C,D}$	73.9 ± 3.0

Table 2-III. Data for tissue extracellular matrix biochemical content. Values in table are mean \pm S.D. (n = 6). WW = wet weight. CC = Culture Control, L = Low impact, H = High impact, I = Inside impact area, O = Outside impact area. Within a column, groups not sharing a similar letter are significantly different from one another ($p < 0.05$). GAG content significantly decreased from baseline in the 4 week LI, HI, and HO groups. Collagen content significantly increased from 1 to 4 weeks in HI tissue.

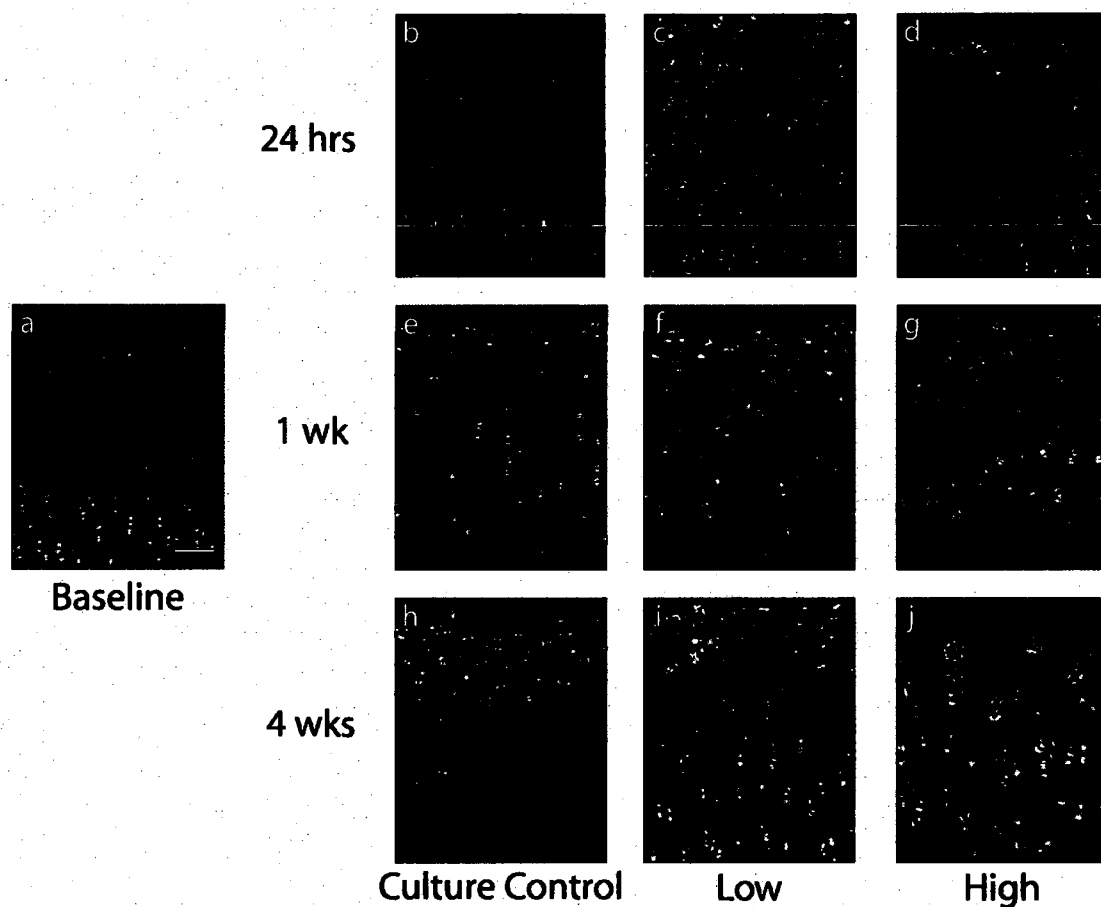
Figure 2-1: Cell viability staining

Figure 2-1. Viability staining. a) Baseline, b) 24 hr culture control, c) 24 hr Low impact, d) 24 hr High impact, e) 1 week culture control, f) 1 week Low impact, g) 1-week High impact, h) 4 week culture control, i) 4 week Low impact, j) 4 week High impact. All images are from inside the impact area. Red stain indicates dead cells and green indicates living cells; scale bar 100 μ m. Baseline explants were neither impacted nor cultured. Culture controls were not impacted. At 24 hrs cell death was limited to the superficial zone following Low and High impact. Cell death increased and spread to deeper regions of the cartilage over time.

Figure 2-2: Quantification of cell viability

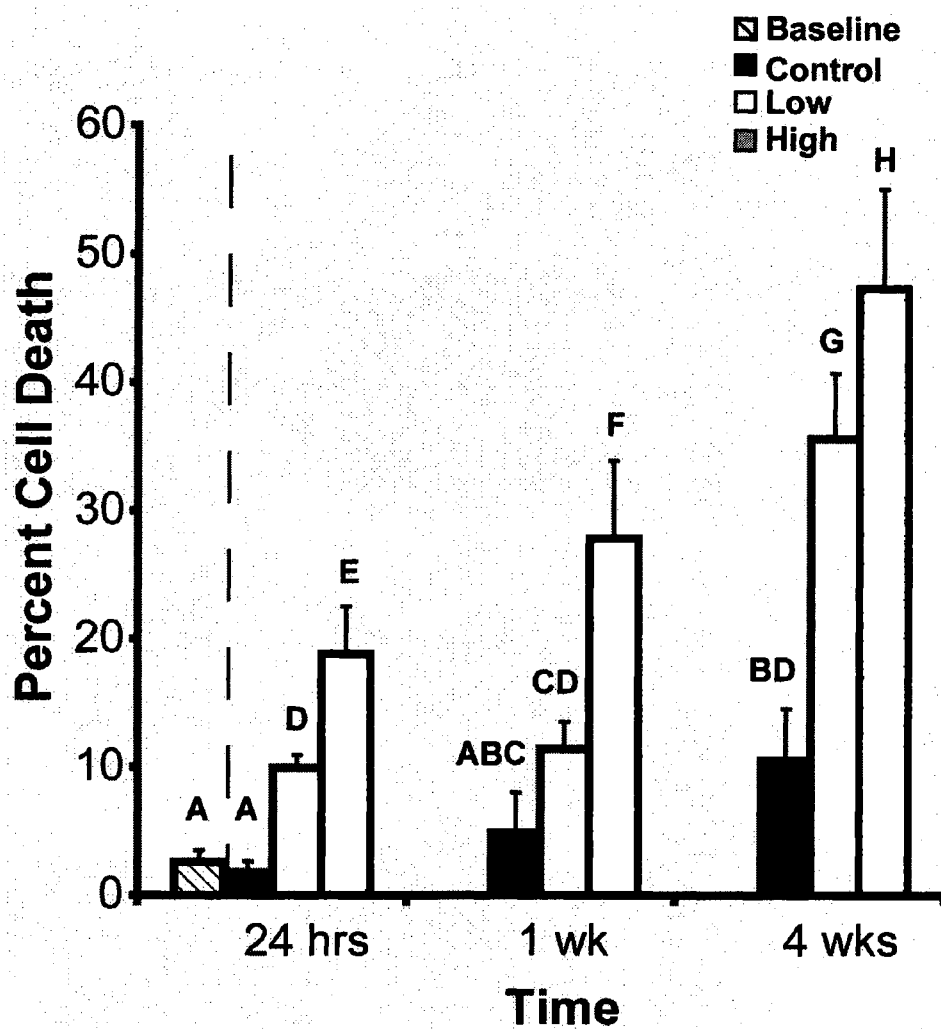


Figure 2-2. Percent cell death quantified from viability staining expressed as mean \pm S.D. Groups not connected by the same letter are significantly different from one another ($p < 0.05$). To the left of the vertical dotted line is the baseline group, representing immediate characterization of native tissue. Cell death significantly increased at 24hrs following Low and High impact. Further, there was a temporal increase in cell death which, following Low impact, was magnified between 1 and 4weeks.

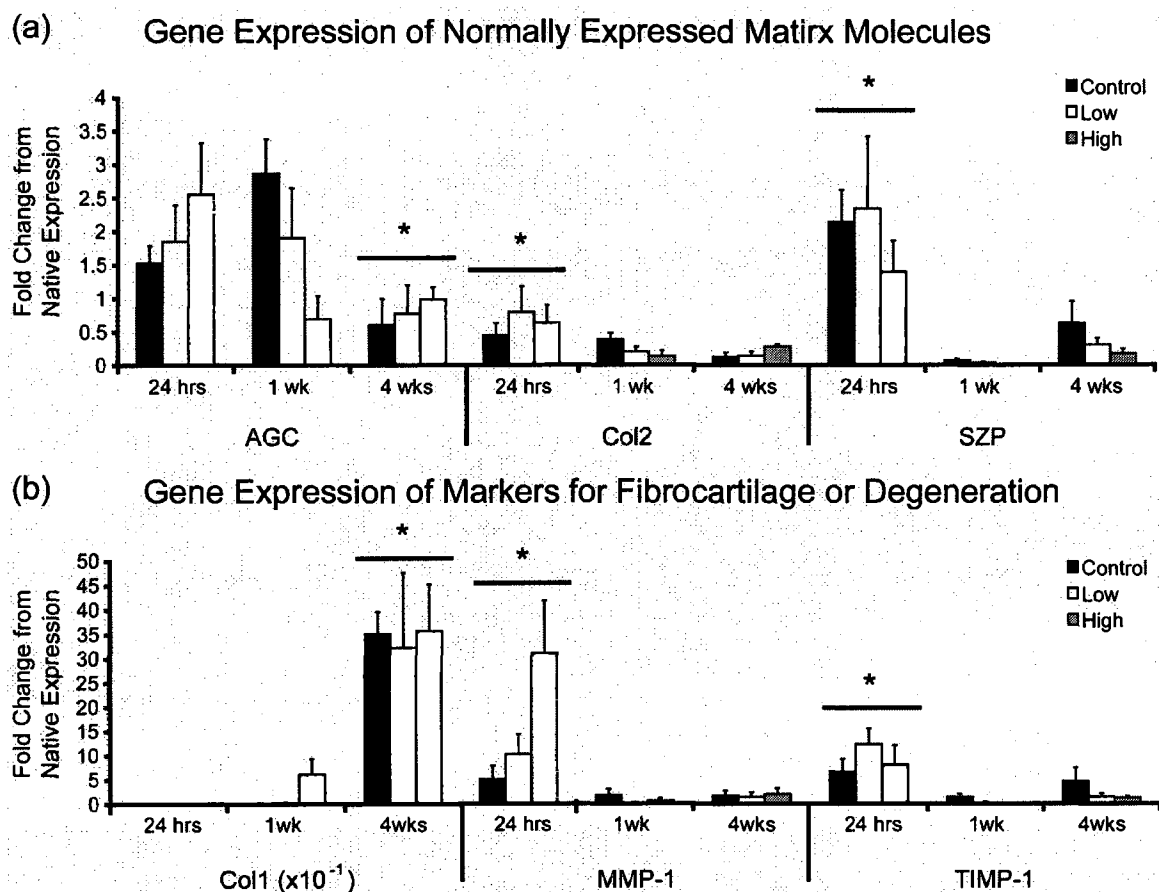
Figure 2-3: Temporal profile of gene expression

Figure 2-3. Fold change in expression from native values with respect to time for the various genes examined in this study. Data for Low and High impact are from tissue inside the impact area. A value of one implies no change from native expression. AGC = aggrecan, Col2 = collagen type II, SZP = superficial zone protein, Col1 = collagen type I, MMP-1 = matrix metalloproteinase-1, and TIMP-1 = tissue inhibitor of MMP-1. Values are mean \pm S.E.M. * indicates significantly different from other time points for the gene of interest ($p < 0.05$). Note, to accommodate scale, the actual values for Col1 presented in the figure are one tenth of what was actually measured. Col2, SZP, MMP-1, and TIMP-1 all experienced significantly decreased expression at 1 and 4 weeks compared to 24 hrs. AGC expression significantly decreased between 1 and 4 weeks whereas Col1 expression significantly increased.

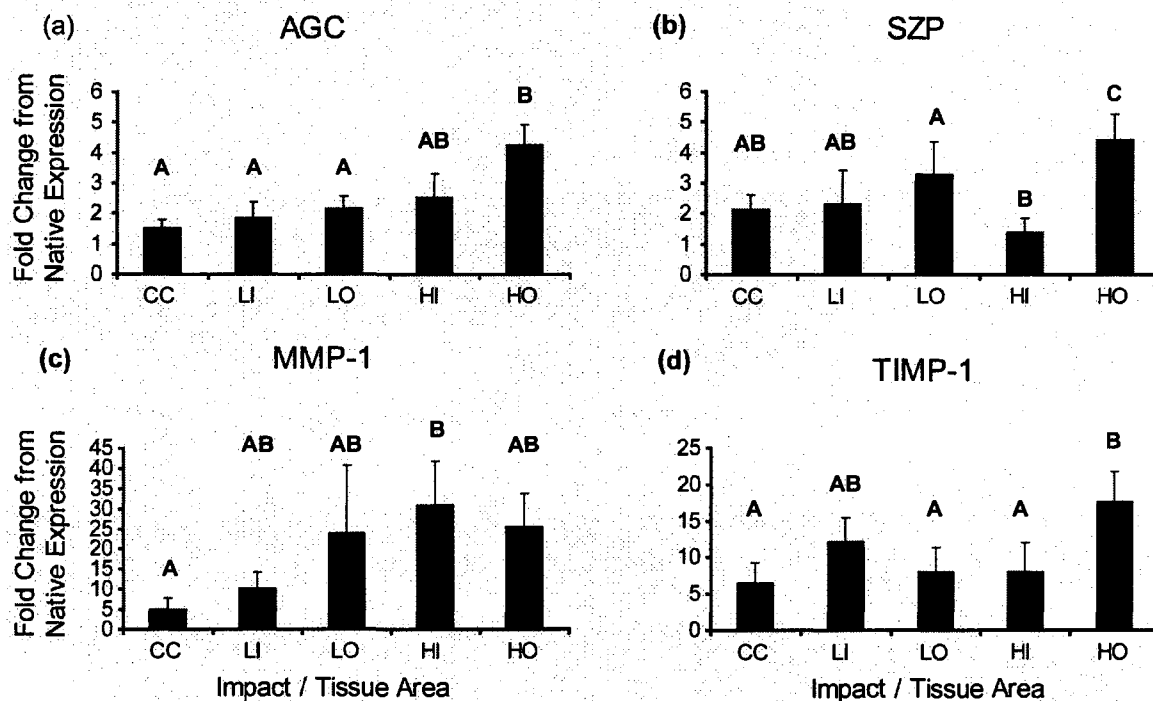
Figure 2-4: 24 hr gene expression

Figure 2-4. Fold change in expression from native values at 24 hrs for AGC (a), SZP (b), MMP-1 (c), and TIMP-1 (d) for all impact levels and tissue areas. CC = Culture Control, L = Low impact, H = High impact, I = Inside impact area, O = Outside impact area. Values are mean \pm S.E.M. Within a panel, groups not sharing a similar letter are significantly different from one another ($p < 0.05$). AGC, SZP, and TIMP-1 expressions in tissue adjacent to High impact were significantly increased compared to the culture control. Also, SZP expression for High impact inside the impact area was decreased compared to outside the impact area. Finally, MMP-1 expression was significantly increased over culture control in tissue subjected to High impact. There were no significant differences among the groups for Col1 or Col2 at 24 hrs.

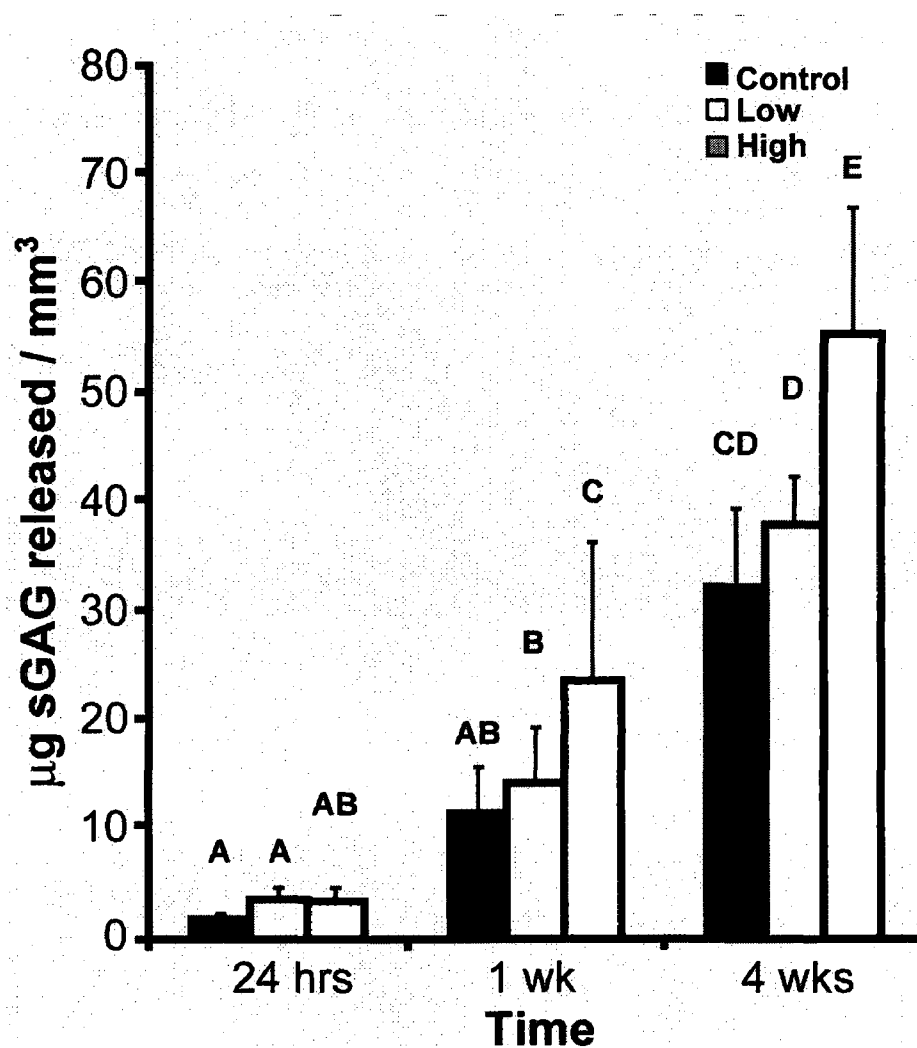
Figure 2-5: Cumulative sGAG release

Figure 2-5. Comparison of cumulative GAG released to the media for the impact levels and time points examined in this study. Values are mean \pm S.D. Groups not connected by the same letter are significantly different from each other ($p < 0.05$). GAG release significantly increased with time in culture. Further, GAG release following High impact was increased over non-impacted controls at the 1 and 4 week time points.

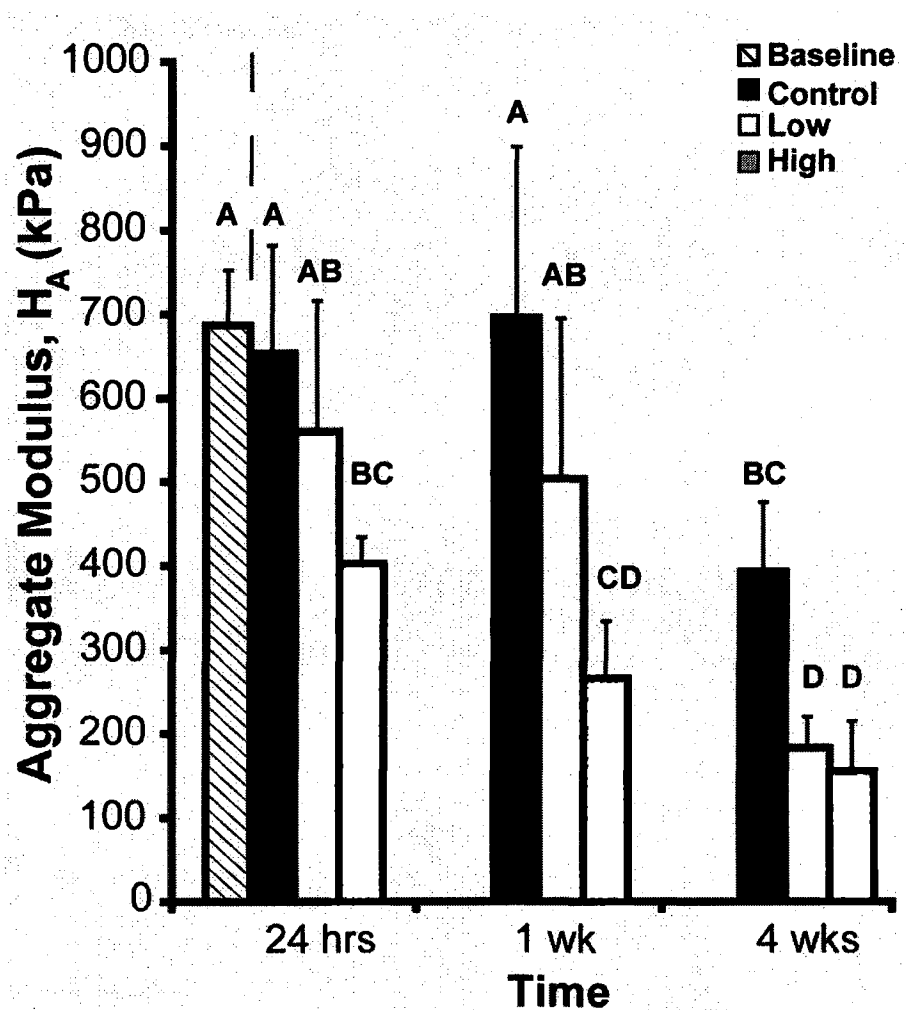
Figure 2-6: Tissue compressive stiffness

Figure 2-6. Comparison of aggregate moduli for the impact levels and time points examined in this study. Values are mean \pm S.D. Groups not connected by the same letter are significantly different from each other ($p < 0.05$). To the left of the vertical dotted line is the baseline group, representing immediate characterization of native tissue. At 24 hrs, the stiffness of High impacted tissue was significantly decreased compared to the non-impacted culture control. This trend remained at 1 and 4 weeks. Though similar to controls at 24 hrs and 1 week, Low impacted tissue at 4 weeks had significantly decreased stiffness compared to controls and was similar to High impacted tissue.

Chapter 3: P188 reduces cell death and IGF-I reduces GAG release following single-impact loading of articular cartilage

Abstract

Prior joint injury predisposes an individual to developing post-traumatic osteoarthritis, for which there is presently no disease modifying treatment. In this condition, articular cartilage degenerates due to cell death and matrix breakdown, resulting in tissue with diminished biomechanical function. P188, a non-ionic surfactant, and the growth factor IGF-I have been shown to decrease cell death. Additionally, IGF-I is known to have beneficial effects on cartilage matrix. The objective of this study was to determine the efficacy of P188, IGF-I, and their combination following articular cartilage impact injury with two energy levels, 1.1 J ('Low') and 2.8 J ('High'), at 24 hrs and 1 week. Bovine articular cartilage with attached underlying bone was impacted at the Low or High level. Impact sites were explanted and examined immediately or cultured for 24 hrs or 1 week in serum-free media supplemented with P188 (8 mg/mL), IGF-I (100 ng/mL), or their combination. Gross morphology, cell viability, GAG release to the media, and tissue mechanical properties were assessed. Immediately post-impact, High level impacted tissue had significantly increased gross morphology scores, indicating tissue damage, which were maintained over 1 week. Gross scores following Low impact were initially similar to non-impacted controls, but, at 24 hrs and 1 week, Low impact gross scores significantly increased compared to

*Chapter published as Natoli RM and Athanasiou KA, "P188 Reduces Cell Death and IGF-I Reduces GAG Release Following Single-Impact Loading of Articular Cartilage," *J Biomech Eng* 130(4):041012, 2008.

non-impacted controls. Additionally, at 24 hrs High impact resulted in increased cell death, and both Low and High impact had increased GAG release compared to non-impacted controls. Furthermore, High impact caused decreased tissue stiffness at 24 hrs that appeared to worsen over 1 week, evident by the percent decrease from non-impacted controls increasing from 16% to 26%. No treatment type studied mitigated this loss. The combination did not perform better than either individual treatment; however, following Low impact at 1 week, P188 reduced cell death by 75% compared to no treatment and IGF-I decreased GAG release from the tissue by 49%. In conclusion, High impact resulted in immediate tissue changes that worsened over 1 week. Though not causing immediate changes, Low impact also resulted in tissue degeneration evident by 24 hrs. No treatment studied was effective at 24 hrs, but by 1 week P188 and IGF-I ameliorated established detrimental changes occurring in articular cartilage post-impact. However, further work is needed to optimize treatment strategies to prevent and/or reverse cell death and matrix destruction in a way that maintains tissue mechanical properties, and hence its functionality.

Introduction

Osteoarthritis (OA) is the most common form of arthritis, affecting more than 20 million Americans.^{77,163} As the population ages, the incidence and economic burden of this disease will increase; however, there is currently no disease modifying treatment. There are several risk factors for OA, with prior joint injury resulting in an increased risk of developing post-traumatic OA.⁷⁶ With respect to the articular cartilage in a joint, characteristic features of OA include

cell death,³ loss of proteoglycans,⁴⁴² and softening of the tissue.²¹⁶ These three characteristics, in addition to others, have been reproduced in both *in vivo* and *in vitro* models of cartilage impact.^{66,430,475}

There has been a wide range of *in vivo* and *in vitro* studies of articular cartilage impact correlating increased cell death with increasing impact energy,^{242,253} increasing stress or strain,^{167,338,462} and the rate of load application.^{151,293,339,342} Moreover, the various models of cartilage mechanical injury employed in these studies have demonstrated GAG loss from the tissue and decreased proteoglycan synthesis.^{151,242,254,462} While the majority of explant models use unconfined compression of chondral explants (without underlying bone) following pre-equilibration, it has been shown that matrix damage and chondrocyte death are increased by these methods compared to injury in the presence of underlying bone without an equilibration period.^{253,288,402,421} Finally, these degenerative changes result in a loss of tissue integrity represented by decreased stiffness and increased permeability.^{150,154,293}

While investigations into treatments for established OA have been occurring, treatment of impact injuries is just beginning. One such treatment possibility is Poloxamer 188 (P188). P188 is an ~8.4 kDa tri-block copolymer containing both hydrophobic and hydrophilic regions. It has been used to protect neurons and skeletal myocytes from necrosis following various types of insult.^{200,328} The accepted mechanism of action is selective insertion into damaged cell membranes,^{328,331} thereby preventing ionic imbalance and loss of important cellular content. Haut et al.^{37,389,420} have shown promising results with

P188 following injurious unconfined compression of cartilage explants and in an *in vivo* study of rabbit patellofemoral joint trauma. In one study,³⁸⁹ P188 was delivered at 8 mg/mL following a peak load of 25 MPa, and cell viability was examined at 1 and 24 hrs. Compared to injured untreated controls, an increased percentage of viable cells in the superficial zone at 1 hr, and an increased percentage in all zones at 24 hrs, was found. In another study,³⁷ though only treating for the first 24 hrs, percent cell death remained decreased at 4 and 7 days post-injury compared to no treatment. These studies underscore the utility of P188 in mitigating cell death following articular cartilage injury.

Another potential intervention is insulin-like growth factor-I (IGF-I). Exogenous IGF-I has been shown to enhance chondrogenesis in cartilage defects and promote further IGF-I transcription.^{173,371} In cartilage explants, it has been shown that IGF-I increases matrix synthesis, an action further enhanced when combined with dynamic compression. Dynamic compression also resulted in faster IGF-I transport into the tissue.^{60,61} Further, it has been shown that IGF-I maintains the physical properties of cartilage explants over 3 weeks in culture.⁴²³ In terms of mechanical injury, D'Lima et al.¹¹⁸ applied a 500 ms static load of 23 MPa to bovine cartilage explants followed by treatment with 50 ng/mL of IGF-I. A significant decrease in apoptosis was observed in the loaded plus treatment group compared to the loaded untreated group.

Based on work mentioned above, the use of P188 and IGF-I to prevent cell death and of IGF-I to increase matrix synthesis and preserve tissue mechanical properties warrants further examination. Moreover, there are

presently no data for the effects of these treatments on GAG loss from the tissue, the tissue's biomechanical properties, or the two agents' effects in combination following impact loading. In this study, we hypothesized that the combination of P188 and IGF-I would reduce cell death post-impact in a synergistic or additive manner. In addition, the combination was expected to maintain matrix integrity, thereby preventing and/or reversing loss of mechanical properties and allowing cartilage to maintain normal function. Hence, the effects of P188, IGF-I, and their combination were examined following articular cartilage injury with two levels of impact loading at 24 hrs and 1 week.

Materials and methods

Articular cartilage tissue harvest

A total of 51 proximal bovine ulnas were obtained from the elbow joints of skeletally mature animals (Animal Technologies, Tyler, TX) within 48 hrs of slaughter. Under sterile conditions, the proximal ulna was cut parallel to the articular surface using a reciprocating saw (Ryobi, Hiroshima, Japan) with a sterile blade. Beneath the articular cartilage surface approximately 1.5 cm of bone was left in place to more realistically capture the in vivo situation compared to a thin layer of bone. The articular surface was then covered with sterile gauze and hydrated with sterile phosphate-buffered saline (PBS). Following tissue harvest, the articular surface, including underlying bone, was placed into a custom designed stainless-steel autoclaved specimen clamp and prepared for impact.

Impact of articular cartilage

Cartilage impact was carried out as described previously.⁴³¹ Briefly, the impact mass was raised to the specified height and dropped onto the impact interface, which connects to a 5 mm diameter, non-porous, flat-ended, rigid, cylindrical impact tip. Two levels of impact were employed. A 'Low' impact (6 cm drop height with an 18.4 N tup) and a 'High' impact (10 cm, 27.8 N tup), delivering 1.1 J and 2.8 J of energy, respectively. Each articular surface, still with subchondral bone attached, was impacted four times – twice at the Low level and twice at the High level – in distinct locations that were separated by at least 5 mm. Impact locations were randomized across all groups studied. These levels were chosen based on previous work in our laboratory⁴³¹ such that the Low level of impact does not cause immediate grossly identifiable surface damage, whereas the High level repeatedly does. Of note, injury to underlying bone resulting from impact was not assessed due to this study's objective of analyzing the effects of the interventions on cartilage tissue alone.

Explant and culture of articular cartilage

Following impact, 5 mm diameter full thickness articular cartilage explants were removed from the subchondral bone using a sterile dermal biopsy punch and a #10 scalpel blade. Explants were placed directly into 6-well, non-TCP plates for culture. In addition to the four impacted explants, two 5 mm non-impacted explants were removed from each joint and used as controls. All cartilage explants (control, Low impact, and High impact) were randomly assigned into one of eight treatment groups. Groups one through four were the

following: 1) culture media alone, 2) culture media supplemented with 8 mg/mL P188 (Sigma, MO), 3) culture media supplemented with 100 ng/mL IGF-I (Peprotech, NJ), or 4) culture media plus combination of P188 (8 mg/mL) and IGF-I (100 ng/mL). Groups five through eight were identical to the aforementioned, except they were subjected to 10 manual compressions of ~1 MPa at 0.1 Hz (cycle = 2 sec of load followed by 8 sec of recovery) using a custom made stainless steel non-porous platen every time the culture medium was changed. The motivation for compression was that all prior in vitro work with P188 on cartilage explants suggests this compression protocol would be required to see effects of P188.^{37,389} Of note, this protocol is not intended to reflect, or to have the effects, of dynamic compression protocols used to study compression aided delivery of nutrients, growth factors, etc. into articular cartilage.

Explants were cultured in 3 mL of the above formulations, with the culture media defined as serum-free Dulbecco's Modified Eagle Medium (DMEM) with GlutamaxTM (Invitrogen, NY) containing 100 units/mL Penicillin (Biowhittaker, MD), 100 µg/mL Streptomycin (Biowhittaker), 2.5 mcg/mL Fungizone (Biowhittaker), 0.1 mM non-essential amino acids (Invitrogen), and 50 mg/L ascorbic acid. Explants were cultured for either 24 hrs or 1 week. For those explants cultured 1 week, culture medium was replaced every 48 hrs. Treatment groups had P188, IGF-I, or the combination added fresh with each media change. All culture medium used in this study was collected and stored at -20°C for later use in GAG release quantification. In addition to explants cultured for 24 hrs and 1 week, another group of explants consisting of non-impacted controls,

Low impact, and High impact specimens were examined immediately following injury for gross morphology, cell viability, and biomechanical properties.

Explant processing

After either 24 hrs or 1 week, explants were removed from culture and processed for gross morphology, cell viability, and biomechanics testing. Briefly, a 3 mm diameter punch was removed from the center of the 5 mm explant using a dermal biopsy punch. This piece of tissue was placed directly into a 2% solution of India ink (Higgins Violet; Eberhard Faber, Inc., Lewisburg, Tennessee) in PBS and allowed to sit for at least 5 min, after which time no increased staining was observed. The remaining ring of the explant was cut perpendicular to the articular surface to generate several surfaces for confocal viability imaging. These tissue pieces were placed into PBS containing 0.5 μ l calcein-AM and 2 μ l ethidium homodimer-1 (Live/Dead[®] assay; Molecular Probes, Eugene, Oregon) per mL of PBS.

Gross morphology and cell viability

Following India ink staining, images of all explants were collected and randomized before being rated by seven blinded, independent observers. The gross morphology rating scale is shown in Table 3-I, which is modified from a previously used version.⁴³¹ Each category was summed to obtain a total score, which was then averaged over the seven raters. Viability images were obtained at 10X magnification using a Zeiss LSM 510 confocal microscope (Carl Zeiss Microscopes, Jena, Germany). Since the sectioning process resulted in some cell death on the sectioned surface, care was taken to image at a tissue depth of

~50 μm . Finally, percent viability was measured over a square area defined by the full thickness of the explant using the 'threshold' and 'analyze particle' functions of ImageJ (National Institutes of Health, Maryland). Dead cells were able to be distinguished by number of pixels based on the color the cell stained. Red (indicating a dead cell) was associated with fewer pixels due to ethidium homodimer-1 staining only the nucleus. Conversely, green (indicating a live cell) was associated with more pixels since calcein-AM stains the entire cytoplasm. For calibration, all dead controls, made by incubating cartilage in EtOH for 20 min, were used to determine the upper limit of dead cell size. Particles above this size were counted as alive. Some out-of-plane live cells, having a lower pixel count, were counted as dead. This was corrected by scaling the counted live cells by 1.16, with the scale factor being determined through analysis of images displaying only live cells. Percent cell death was then calculated as $100 \times [1 - (\text{live cells} / \text{total cells})]$.

GAG release to media

A 1,9-dimethyl-methylene blue (DMMB) colorimetric assay was used to determine the amount of GAG released to the media (Blyscan Sulfated GAG Assay, Accurate Chemical and Scientific Corp., New York). Chondroitin 4-sulfate was used for the standard. Total quantity of GAG released was normalized to tissue volume, which, if in the presence of tissue swelling, represents a lower limit. Tissue volume was calculated knowing the tissue surface area (5 mm diameter) and thickness, as measured upon biomechanical testing (*vida infra*).

Creep indentation biomechanical testing

Following photography for gross morphology, the 3 mm diameter, India ink stained tissue specimens were wrapped in gauze soaked in PBS containing protease inhibitors (10 mM N-ethylmaleimide, 5 mM benzamidine, 2 mM EDTA, and 1 mM phenylmethylsulfonyl fluoride) and frozen at -20°C until mechanical testing. Prior to testing, samples were thawed for at least one hr at room temperature in PBS with protease inhibitor solution and then affixed to a flat stainless steel surface with a thin layer of cyanoacrylate glue. A creep indentation apparatus was used to determine the compressive creep and recovery behavior of the cartilage explants.³⁰ Testing conditions consisted of a tare load of 0.005 N followed by a test load of 0.02 N applied to the sample through a 0.8 mm diameter, flat-ended, rigid, porous tip. Creep and recovery behavior was recorded using LabView software (National Instruments, Austin, TX). A semi-analytic, semi-numeric model,³⁴⁸ which needs only the last 30% of the deformation history and no recovery data, was used to determine the linear biphasic properties (aggregate modulus, permeability, and Poisson's ratio), of the tissue from the time-displacement curves. Tissue thickness was measured across the entire 3 mm specimen using digital calipers.

Statistical analysis

The study consisted of a balanced, full-factorial experimental design. Each time point was conducted and analyzed as an independent experiment because separate controls from distinct pools of animals were used to decrease the affect of inter-animal variability. Immediately post-impact, a 1-way ANOVA was

performed with impact level as the predictor variable on gross morphology, cell viability, and biomechanical properties. At both 24 hrs and 1 week, a 3-factor ANOVA (impact level, treatment type, and delivery method) was performed on the gross morphology, GAG release, cell viability, and biomechanical properties data. If a factor was found to be significant ($p < 0.05$), a Tukey HSD post-hoc test was performed to compare amongst factor levels. Predominantly, $n = 6$ was used for all groups and assays in this study, where group is a combination of impact, treatment, and delivery method. However, some groups resulted in an $n = 5$ due to the sample being of too poor quality for the assay or being identified as an outlier via the method of Studentized Deleted Residuals.²⁹⁵

Results

Compression protocol

The compression protocol used was only a significant factor for Poisson's ratios measured at 1 week ($p = 0.003$) and 24 hr gross morphology scores ($p = 0.003$). Compression resulted in increased Poisson's ratios and decreased total gross scores. The compression protocol did not significantly affect GAG loss to the media, the tissue's aggregate modulus or permeability, and, contrary to our expectation, cell viability. Since compression was principally not a significant factor, the remainder of the results is presented in terms of impact level and treatment type.

Gross morphology

Figures 3- 1A, 2A, and 3A show the results for gross morphology scoring immediately following impact, 24 hrs after impact, and 1 week after impact, respectively. Immediately following impact gross morphology showed that High impact resulted in significantly increased scoring, indicative of greater damage, compared to Low impact and non-impacted controls. Low impact and controls had similar gross scores (Fig. 3-1A). Figure 3-1D shows representative gross morphology pictures. Note the appearance of tissue damage, staining heterogeneity, and surface irregularity resulting from High impact, while Low impact specimens appear grossly identical to control specimens.

In contrast, 24 hrs after impact, gross morphology scoring showed that Low impact now had significantly increased scores compared to non-impacted controls. High impact scoring continued to remain significantly increased over both non-impacted controls and Low impact (Fig. 3-2A). This same relationship was also observed at 1 week (Fig. 3-3A). Gross scores for non-impacted controls and High impact remained relatively constant over the course of the study, whereas the scores for Low impact increased. Treatment type was not a significant factor in gross morphology scoring.

GAG release to media

GAG release from explants was significantly affected at 24 hrs and 1 week by both impact level ($p = 0.0004$, 24 hrs; $p < 0.0001$, 1 week) and treatment type ($p = 0.02$, 24 hrs; $p = 0.0002$, 1 week). At 24 hrs, both Low and High impact demonstrated increased GAG release compared to non-impacted controls. Also,

P188 treatment resulted in significantly increased GAG loss to the media compared to IGF-I treatment, though neither was significantly different from no treatment or the combination (Fig. 3-2D).

Similar to 24 hrs, at 1 week both Low and High impacted specimens had increased GAG loss compared to non-impacted controls. Further, IGF-I treatment significantly decreased GAG loss compared to all other treatment types. Comparing the Low impact, IGF-I treatment group to Low impact, no treatment revealed a 49% reduction in GAG release. For both non-impact controls and High impact, comparing no treatment to IGF-I treatment showed an 18% reduction. In addition, for the groups shown in figures 3- 2D and 3D, the average GAG released in the first 24 hrs was 34% of the total released over 1 week, with a range from 26% (Low impact, no treatment) to 47% (Low impact, IGF-I treatment).

Cell viability

Figure 3-1D shows representative confocal images. Immediately after impact, there was little to no cell death in non-impacted controls, whereas cell death was evident in the superficial zone of Low and High impacted specimens. Though not significant, cell death following High impact was over 1.6 times greater than either Low impact or non-impacted controls (Fig. 3-1B).

However, by 24 hrs post-injury, impact level significantly affected percent cell death ($p < 0.0001$). Post-hoc analysis showed High impact had significantly more cell death compared to Low impact and non-impacted controls. Treatment type was not significant (Fig. 3-2B).

At 1 week, both impact level and treatment type significantly affected cell viability ($p = 0.0009$ and 0.03 , respectively; Fig. 3-3B). Different from 24 hrs post-impact, post-hoc analysis showed that both Low and High impacted specimens had increased cell death compared to non-impacted controls. Moreover, P188 treatment significantly reduced percent cell death compared to no treatment. This was most evident in the 75% reduction in cell death for Low impact, P188 treatment compared to Low impact, no treatment. Reductions compared to no treatment were not as dramatic for non-impacted controls and High impact specimens treated with P188, measuring 66% and 36%, respectively. Treatment with IGF-I or the combination was similar to both the P188 and no treatment groups.

Biomechanical properties

Figures 3- 1C, 2C, and 3C show the data for the tissue's aggregate modulus measured by creep indentation immediately post-impact, 24 hrs after impact, and 1 week after impact, respectively. Immediately following impact, there was a 22% loss of aggregate modulus in High impact specimens from non-impacted controls, but this change was not significant. However, by 24 hrs, impact level significantly affected the aggregate modulus ($p = 0.02$), with High impacted tissue being significantly softer in compression compared to Low impact and non-impacted controls. Impact level remained significant at 1 week ($p = 0.003$); however, while High impact remained significantly different from non-impacted controls, the aggregate moduli of Low impact samples were now

indistinguishable from High impact. Treatment type was not a significant factor at 24 hrs or 1 week.

Tissue permeability and Poisson's ratios are reported in Table 3-II. Tissue permeability was not significantly affected by impact level or treatment type immediately following impact or at 1 week post-impact. However, at the 24 hr time point, treatment type was a significant factor ($p = 0.02$), with IGF-I treatment resulting in an increased permeability compared to all other treatment types. Impact level was not a significant factor at 24 hrs. Poisson's ratios were unaffected by impact level or treatment type at any time point. Finally, it should be noted that the results reported here assume ideal test geometry. While non-impacted controls and Low impact explants fit this geometry well, High impact specimens do not due to the presence of surface cracks. Thus, the reported values for High impact represent an upper limit for tissue stiffness and lower limit for permeability.

Discussion

The objective of this study was to determine the effects of P188 and IGF-I on gross morphology, cell viability, GAG release, and tissue biphasic material properties following mechanical impact of articular cartilage. At 1 week post-injury, 8 mg/mL P188 treatment reduced percent cell death by 75% and 36% following Low (1.1 J) and High (2.8 J) impact, while 100 ng/mL IGF-I treatment reduced GAG release from the explant by 49% and 18%, respectively. Despite the individual usefulness of P188 and IGF-I, synergy was not observed. The use of these agents in combination resulted in them losing their effects and becoming

similar to no treatment. Several possible explanations for this observation are that the concentrations and dosing times used in this study are not yet optimized for use together, simultaneous presence of the two species reduces each other's activities, and P188 may interfere with IGF-I signaling, rendering it ineffective in the presence of P188. Nevertheless, the results of this study show that detrimental changes in cell viability and GAG release occurring after impact can be lessened with targeted bioactive agents.

The gross morphology scale used in this study is a good indicator of articular cartilage damage and captured the effects of impact level and time post-injury. Supporting this claim, the scale correlated with most parameters assayed at both time points; however, low R^2 values (range 0.04-0.20) suggest there are other important factors. Though the scale was modified, the results of the present study agree with previous work done in our laboratory in that High impact resulted in immediately increased gross scores compared to non-impacted controls and Low impact specimens.⁴³¹ Gross morphology has been assessed in other studies of cartilage mechanical injury. Prior work using injurious compression found that increasing load rate from 40 MPa/s to ~900 MPa/s was associated with greater surface fissuring,¹⁵¹ which was reduced when underlying bone was present.²⁸⁸ In this study, fissuring observed following High impact (2.8 J) was qualitatively less than images published in the aforementioned studies, consistent with the presence of underlying bone. Other studies have also shown that impact of cartilage removed from subchondral bone results in surface fissuring,⁴⁰⁸ and Borrelli et al.⁶⁷ have shown that cartilage can tolerate injurious

loads up to half the joint fracture threshold when underlying bone is present. Further, following injurious compression, increased cell death was noted in the superficial zone,⁴²¹ as was also found in this study. Another articular cartilage surface damage score has captured the effect of impact, but that score was based on histological evaluation.²⁴² The scoring method of the current study presents an improvement, if nothing more than in ease of tissue processing, over the histology-based scale. Further, the scale used in this study was able to capture temporal changes in gross morphology, evident by the increasing scores for Low impact (1.1 J), and correlated with a quantitative measure of tissue stiffness.

P188 reduced cell death at 1 week compared to no treatment, but it did not do so at the 24 hr time point. This result is not consistent with previous work, which showed that P188 reduced cell death in all zones at 24 hrs.³⁸⁹ A possible explanation for the discrepancy is the different loading protocols used, such that the presence of surrounding tissue and underlying bone in the present study provided constraint of the impacted region that protected cells from death more so than in an unconfined compression protocol. Bone likely protects cells from overt necrosis at the moment of injury,⁶⁷ but the stresses, strains, fluid shear, pore pressure etc. generated in the tissue during impact may still initiate mechanotransductive pathways leading to apoptosis, perhaps explaining the continued death during culture. Indeed, bone has been shown to spare chondrocytes from death after mechanical loading,^{288,402} such that 10 times the amount of energy is needed to produce similar changes in cartilage when bone is

present.²⁵³ In this respect, our results are in good agreement with studies reporting energy as the impact metric.^{242,253} For example, a 0.28 J impact would yield 12.24% cell death according to the linear regression in Jeffrey et. al.²⁵³ compared to the 14.84% for the 2.8 J impact seen in the present study immediately post-injury. Notably, compression was not necessary in this study for P188 to be effective, in contrast with two previous studies suggesting it was.^{37,389} It is possible that the compression protocol used in this study was different, as the compression frequency was not described in the prior studies. Using that protocol may have furthered the beneficial effects we observed with P188.

Though the current accepted view is that P188 prevents necrosis by repairing damaged cell membranes, data from this study, along with the observation that apoptosis may be occurring at later time points, suggest that P188 may have additional mechanisms of action in chondrocytes. Indeed, work on mechanical trauma to neurons has established P188 reduces apoptosis in that cell type.⁴³³ It has been suggested that cell death by necrosis following impact does not occur past one day,^{37,151,310} but apoptosis post-injury has been observed to increase with time over seven days in culture.^{37,116} In fact, several studies using very different loading protocols have shown that treatment with caspase inhibitors following mechanical injury effectively reduces apoptotic cell death.^{116-118,243} In contrast to our results, these studies also found a decrease in GAG release associated with increased cell viability. Moreover, P188 has been previously shown to maintain its efficacy for 1 week, yielding a 46% reduction in DNA fragmentation compared to no treatment when treatment was applied for

only the first 24 hrs.³⁷ In the current study, there were 75% and 36% reductions in percent cell death at 1 week for Low and High impact, respectively. Compared to the 46% reduction seen in prior work, an explanation for the increased efficacy seen in this study following Low impact is that treatment was continuous over the culture period; however, formal proof of this would require comparison of treatment duration following identical injurious loading protocols. On the other hand, less necrosis may lead to decreased apoptosis by preventing the release of apoptosis initiators from necrotic cells, thereby preventing further cell death at later time points and explaining the observed efficacy of P188 at 1 week in this model system. Further experimentation is necessary to delineate between these two possibilities.

While a prior study with IGF-I showed it decreased apoptosis post-injury,¹¹⁸ we did not find it effective at preventing cell death, perhaps due to differences in the loading metrics used in our study. Loading regimens in the literature vary with respect to peak stress, time to peak stress, stress rate, and duration.⁴³⁰ The present study employed impact loading to cartilage with underlying bone attached on a sub-millisecond time scale,⁴³¹ while the previous work statically loaded chondral explants to 23 MPa over 500 ms. During impact loading, a higher proportion of the stress is borne by interstitial fluid pressurization,^{296,339} which may protect chondrocytes when compared to lower loading rates, wherein the solid matrix begins to share the load. With lower loading rates, interaction of cells with the ECM may cause them to respond to the load borne by the solid matrix, triggering cellular death pathways that create a

larger pool of dying chondrocytes susceptible to the actions of IGF-I. Work done by Morel et al.^{343,344} has shown cell death following injurious compression is related to macroscopic cracks due to radial strain generated in the superficial zone during loading, and increasing pre-strain before loading can alleviate a portion of the cell death. Thus, radial strain is one biomechanical mechanism that may describe the presence of surface fissures and increased cell death immediately following High impact in this study. Additionally, the peak stresses associated with the current study's impact levels are below 8 MPa.⁴³¹ It has been suggested that there is a threshold level of peak stress (15-20 MPa) at which cell death begins for low loading rates, 35 MPa/s.⁴⁶² Our results demonstrate that this threshold is decreased at higher loading rates, consistent with a previous proposition that peak power delivered during impact may be the important factor.²⁹³ Determining which metrics defining mechanical impact are responsible for the initiation of cell death is an area needing continued research.

Though not effective at preventing cell death, IGF-I reduced GAG release following injury in this model system at 1 week. While IGF-I has been shown to increase GAG synthesis,⁶⁰ and one would then expect GAG release to increase from the explant, we observed IGF-I to decrease GAG release. Consistent with this observation would be a mechanism by which IGF-I decreases matrix breakdown by inhibiting degradative enzymes, perhaps MMPs. DiMicco et al.¹³⁰ found that a specific MMP inhibitor (CGS 27023A) was able to decrease GAG loss from articular cartilage following mechanical insult. Furthermore, IGF-I caused an increase in the tissue's permeability at 24 hrs compared to no

treatment, which then recovered by 1 week, a finding consistent GAG release being decreased at 1 week due to this intervention. This observation exemplifies the importance of evaluating treatment strategies over sufficient time courses in *in vitro* models. Such time course experiments have suggested that there may be optimal "therapeutic windows."^{116,130}

While P188 reduced cell death and IGF-I reduced GAG release at 1 week, no treatment in this study was able to prevent and/or reverse the loss of tissue stiffness post-impact. A possible explanation of this observation is that early GAG loss following injury, which is presumably due to mechanical disruption of the collagen matrix,^{130,151,462} is enough to cause a decrease in tissue stiffness. One would not then expect tissue stiffness to recover until a repair response has occurred. Decreased tissue stiffness immediately following impact has previously been shown in our system,⁴³¹ though results of the present study did not reach significance. At 24 hrs, tissue impacted at the High level (2.8 J) had an average 16% loss in the aggregate modulus, which increased to 26% at 1 week. Due to its avascular, aneural, post-mitotic nature, damaged cartilage has a notoriously deficient healing response, with the fibrocartilaginous repair tissue demonstrating inferior mechanical properties.²¹⁶ Several *in vivo* studies^{150,152,154} impacting the rabbit patellofemoral joint and two *in vivo* studies^{293,431} have documented decreased tissue stiffness using various material models at various times post-injury. The requirement of cartilage to function in a demanding mechanical environment necessitates evaluation of the effects of a treatment on its mechanical properties. One *in vivo* study of joint impact showed that treatment

with polysulphated GAG was able to prevent the loss tissue stiffness that occurred.¹⁴⁹ Ultimately, it is desirable to have a treatment strategy that prevents tissue degeneration via cell death and matrix breakdown which also maintains tissue functionality.

In conclusion, the results of this study support the ability of two treatments to mitigate well-known degenerative changes in cartilage following single-impact loading. Based on the time course evaluation, changes occurring following impact injuries at or less than 24 hrs may not be able to be ameliorated with these interventions, suggesting initial changes are due solely to mechanical trauma and uncoupled from the tissue's biological response. Additional studies must be performed to delineate the magnitude of cell death and matrix damage due to the mechanical insult alone from the subsequent amount resulting from biological responses. Where treatments employed in this experiment only affected the latter, it is desirable to identify agents that can promote a healing response in order to reverse the former changes. Further study with other concentrations and combinations of bioactive agents capable of preventing and/or reversing cell death and matrix breakdown is justified. Additionally, more detailed examination of the mechanisms of action of these agents would be helpful information in the campaign to understand and prevent the development of post-traumatic OA.

Table 3-I: Gross morphology grading scale

A. Tissue Morphology	
Healthy, no damage	0
Some tissue damage	1
Extensive tissue damage	2
Complete tissue destruction	3
B. India ink staining	
Homogeneous	0
Some staining heterogeneity	1
Moderate staining heterogeneity	2
Vast staining heterogeneity	3
C. Surface regularity	
Smooth	0
Small area of surface irregular	1
Moderate area of surface irregular	2
Most of surface irregular	3
Total	9 (max)

Table 3-I. Gross morphology grading scale. Each of the three categories can be rated 0-3, making the scale range from a minimum of 0 to a maximum of 9.

Table 3-II: Tissue permeability and Poisson's ratio as measured by creep indentation

Time Point	Treatment Type	Impact Level	Permeability ($\text{m}^4/\text{N}\cdot\text{s} \times 10^{-15}$)	Poisson's Ratio
Immediate		Control	4.4 ± 1.3	0.035 ± 0.086
		Low	6.0 ± 3.1	0.032 ± 0.070
		High	3.7 ± 2.0	0.074 ± 0.089
24 hrs after Impact	None	Control	2.9 ± 1.8	0.024 ± 0.048
		Low	3.1 ± 2.9	0.055 ± 0.080
		High	3.1 ± 2.1	0.050 ± 0.077
	P188	Control	3.4 ± 1.9	0.026 ± 0.051
		Low	3.5 ± 2.1	0.092 ± 0.095
		High	3.7 ± 2.1	0.092 ± 0.079
	IGF-I*	Control	4.6 ± 3.3	0.096 ± 0.095
		Low	4.0 ± 2.3	0.059 ± 0.092
		High	4.8 ± 3.6	0.091 ± 0.091
	Combo	Control	2.4 ± 1.3	0.090 ± 0.115
		Low	4.0 ± 2.3	0.037 ± 0.069
		High	3.6 ± 2.1	0.083 ± 0.094
1 week after Impact	None	Control	3.5 ± 2.3	0.046 ± 0.070
		Low	6.3 ± 3.9	0.105 ± 0.081
		High	3.8 ± 2.6	0.120 ± 0.083
	P188	Control	3.0 ± 1.6	0.042 ± 0.057
		Low	4.6 ± 2.6	0.057 ± 0.066
		High	3.7 ± 2.5	0.085 ± 0.074
	IGF-I	Control	3.3 ± 1.9	0.109 ± 0.092
		Low	2.7 ± 2.7	0.066 ± 0.076
		High	4.6 ± 3.3	0.063 ± 0.072
	Combo	Control	3.4 ± 3.5	0.053 ± 0.071
		Low	3.4 ± 2.3	0.090 ± 0.087
		High	3.5 ± 2.7	0.068 ± 0.076

Table 3-II. Tissue permeability and Poisson's ratio as measured by creep indentation. For the immediate time point, values are mean \pm S.D for $n = 5-6$. At 24 hrs and 1 week, values are mean \pm S.D for $n = 10-12$. Separate statistical analyses were performed at each time point. * Denotes significant effect ($p = 0.02$) of treatment type on permeability at the 24 hr time point. Treatment with IGF-I caused a significant increase in permeability compared to no treatment controls and the combination treatment, but was not significantly different than P188 treatment.

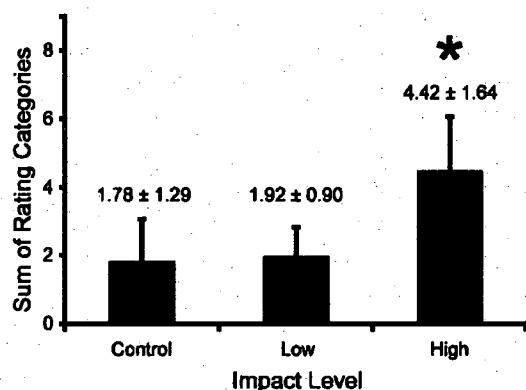
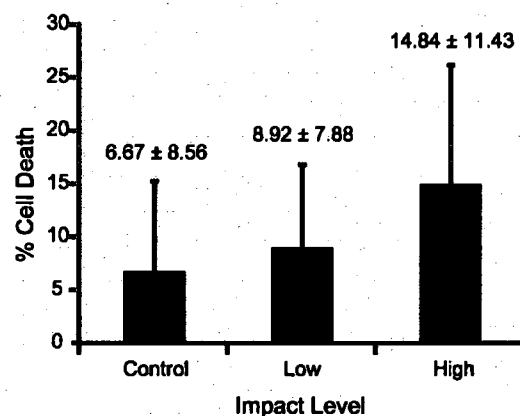
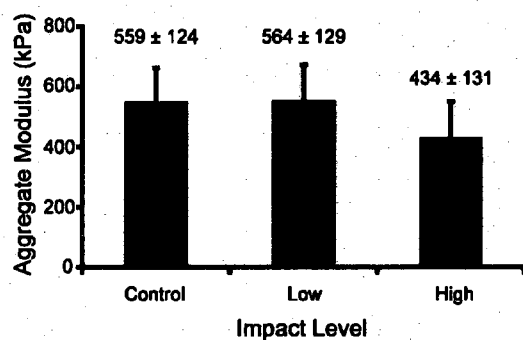
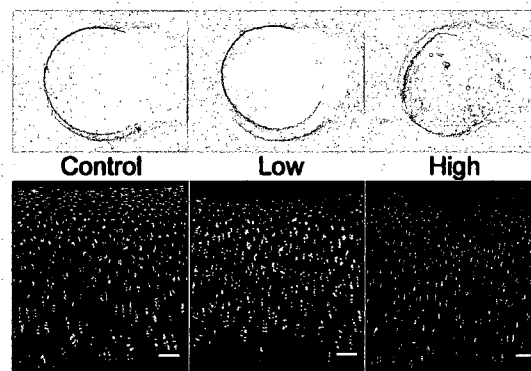
Figure 3-1: Tissue response immediately post-injury**A. Average Gross Morphology Score Immediately after Impact****B. Cell Viability Immediately after Impact****C. Tissue Stiffness Immediately after Impact****D. Gross Morphology and Cell Viability Images**

Figure 3-1. Response of articular cartilage immediately post-injury. A) Gross morphology scores.

* denotes High impact significantly different from non-impacted control and Low impact groups ($p < 0.05$).

B) Cell viability. C) Tissue stiffness (aggregate modulus). D) Representative gross morphology and cell viability images obtained in this study. Each bar represents mean \pm S.D for $n = 5-6$. Scale bar = 100 μm .

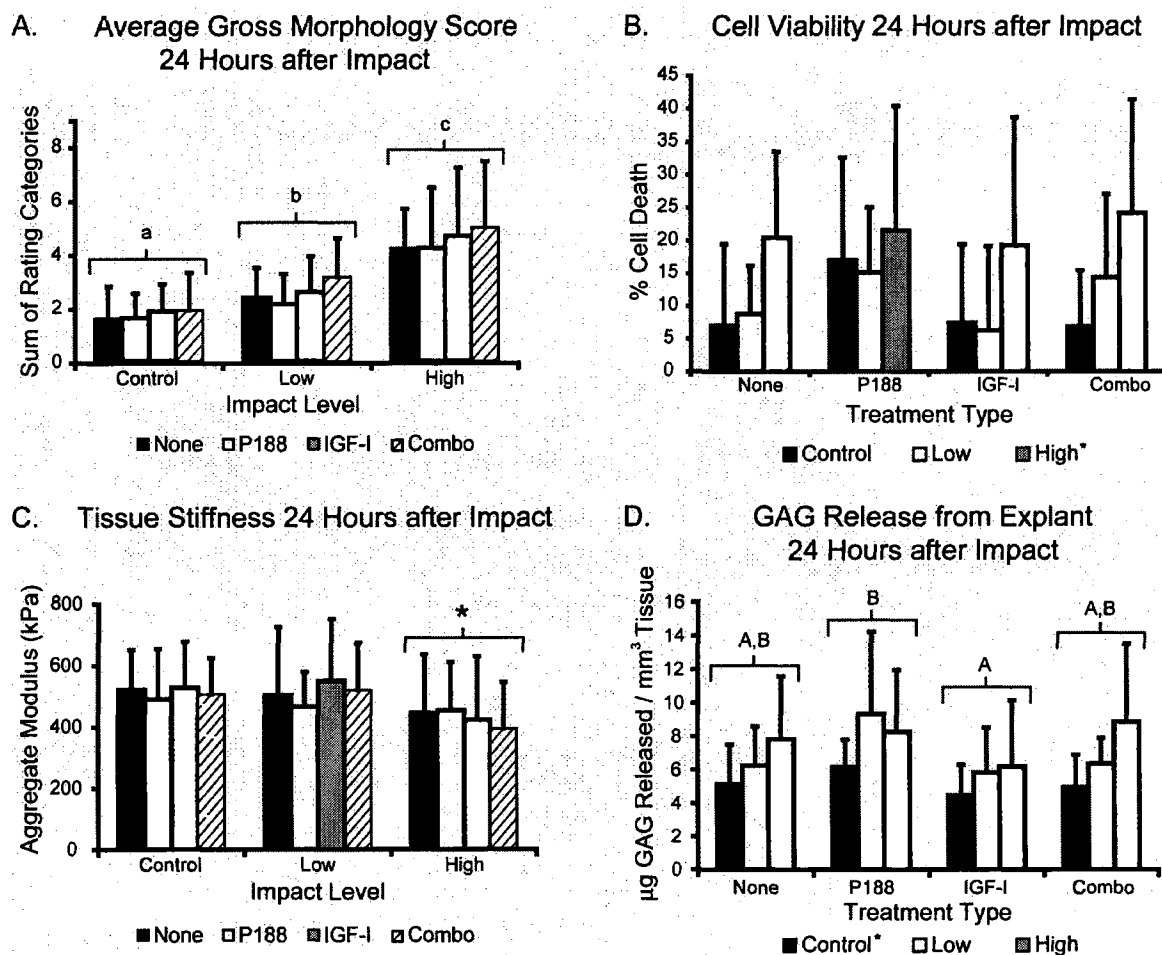
Figure 3-2: Tissue response 24 hrs post-injury

Figure 3-2. Response of articular cartilage 24 hrs post- injury. A) Gross morphology scores. B) Cell viability. C) Tissue stiffness (aggregate modulus). D) GAG release. Within a panel, groups not connected by the same letter are significantly different from one another (lower case reserved for impact level and upper case for treatment type); * denotes significant difference from all other levels of the same factor ($p < 0.05$). Each bar represents mean \pm S.D for $n = 10-12$.

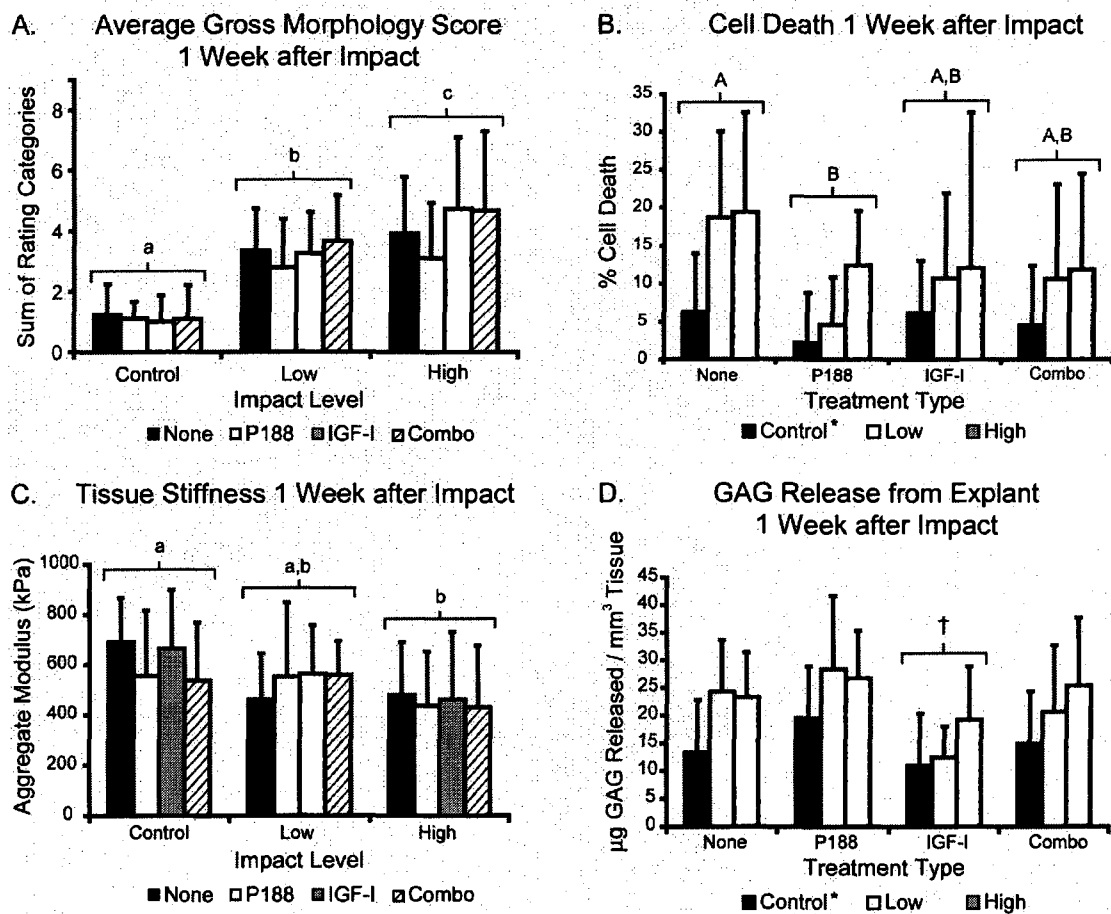
Figure 3-3: Tissue response 1 week post-injury

Figure 3-3. Response of articular cartilage 1 week post-injury. A) Gross morphology scores. B) Cell viability. C) Tissue stiffness (aggregate modulus). D) GAG release. Within a panel, groups not connected by the same letter are significantly different from one another (lower case reserved for impact level and upper case for treatment type); *, † denote significant difference from all other levels of the same factor ($p < 0.05$). Each bar represents mean \pm S.D for $n = 10-12$.

Chapter 4: Effects of doxycycline on articular cartilage GAG release and mechanical properties following impact*

Abstract

The effects of doxycycline were examined on articular cartilage glycosaminoglycan (GAG) release and biphasic mechanical properties following two levels of impact loading at 1 and 2 weeks post-injury. Further, treatment for two continuous weeks was compared to treatment for only the 1st week of a 2 week culture period. Following impact at two levels, articular cartilage explants were cultured for 1 or 2 weeks with 0, 50, or 100 μ M doxycycline. Histology, GAG release to the media, and creep indentation biomechanical properties were examined. The 'High' (2.8 J) impact level had gross surface damage, whereas 'Low' (1.1 J) impact was indiscernible from non-impacted controls. GAG staining decreased after High impact, but doxycycline did not visibly affect staining. High impact resulted in decreased aggregate moduli at both 1 and 2 weeks and increased permeability at 2 weeks, but tissue mechanical properties were not affected by doxycycline treatment. At 1 week, High impact resulted in more GAG release compared to non-impacted controls. However, following High impact, 100 μ M doxycycline reduced cumulative GAG release at 1 and 2 weeks by 30% and 38%, respectively, compared to no treatment. Interestingly, there was no difference in GAG release comparing 2 weeks continuous treatment with 1 week on, 1 week off. These results support the hypothesis that doxycycline can

*Chapter published as Blumberg TJ, Natoli RM, and Athanasiou KA, "Effects of doxycycline on articular cartilage GAG release and mechanical properties following impact," *Biotechnol Bioeng* 100(3):506-15, 2008.

mitigate GAG release from articular cartilage following impact loads. However, doxycycline was unable to prevent the loss of tissue stiffness observed post-impact, presumably due to initial matrix damage resulting solely from mechanical trauma.

Introduction

Post-traumatic osteoarthritis (PTOA) is a disease state characterized by progressive articular cartilage degeneration, joint pain and dysfunction, and altered cartilage biomechanics.²¹² While a combination of mechanical, inflammatory, and enzymatic factors are thought to contribute to the sequelae of PTOA,^{63,66,212,373} little is known of the etiology or pathogenesis of PTOA as a clinical disease.³⁷⁷ Numerous degenerative changes in articular cartilage occur following traumatic mechanical injury,^{66,154,373} including collagen breakdown, reduced proteoglycan synthesis, loss of extracellular matrix (ECM) components, and a decrease in tissue biomechanical integrity, which are also hallmarks of PTOA development.^{99,116,242,321,442}

Though difficult to assess articular cartilage injury *in vivo*, it is possible to observe the effects of articular cartilage damage following impact-induced injuries using *ex vivo* animal models and explant studies. Such studies have connected mechanical impact to PTOA by a variety of mechanisms that damage both the ECM and chondrocytes.^{242,385,462} Traumatic mechanical injury induces chondrocyte death, disrupts the collagen network, and causes glycosaminoglycan (GAG) release from articular cartilage. One study found that human cartilage subjected to a 14 MPa load released GAGs— over two times as

much as unloaded samples – during the first four days following impact.¹¹⁶ An *in vitro* study of the kinetics of GAG release found that a third of the GAG released during the first 24 hrs occurred during the first 4 hrs of culture, and remained significantly higher than controls at 24 hrs.¹³⁰ The same study also found a 50-60% reduction in the incorporation of ³⁵S-sulfate and ³H-proline, indicative of decreased GAG and collagen synthesis, in articular cartilage specimens subjected to injurious compression at a strain rate of 1/sec. Furthermore, impact level has been found to correlate with tissue damage, demonstrating that there is a direct relationship between the degree of articular cartilage breakdown and the peak stress, stress rate, and energy delivered by the impact.^{151,254,339,462} One study found progressively greater levels of cell death at 15, 25, and 35 MPa; however, below the threshold stress level of 15 MPa, cells remained viable and the tissue matrix was not damaged. The threshold stress also correlated with proteoglycan biosynthesis, which was found to decrease significantly once the threshold was reached. In addition, Jeffrey et al.²⁵⁴ found that greater impact energy, ranging from 0.1 to 1.0 J, corresponded to greater levels of matrix loss over a 2 week culture period. Ultimately, the collective tissue damage leads to detrimental changes in tissue mechanical properties.²⁹³

With better understanding of the mechanisms of osteoarthritis (OA) development, the search to identify and develop successful disease modifying OA drugs to aid in tissue repair and prevent further degeneration in diseased tissue has begun. Much effort has focused on matrix metalloproteinases (MMPs) as potential targets in OA prevention and treatment,³³⁷ though other matrix

degrading enzymes, such as aggrecanases and hyaluronidase, may have important roles as well.^{193,426,457} A study by DiMicco et al.¹³⁰ found that GAG release between 1 and 7 days post-injury was markedly reduced using an MMP inhibitor compared to no treatment. Tetracycline analogs and derivatives have also exhibited success in the inhibition of MMPs by multiple mechanisms in both *in vivo* and *in vitro* studies.^{20,194,195,201,202} Furthermore, doxycycline, a member of the tetracycline family and an MMP inhibitor, has been found to reduce collagenolytic activity^{448,521} and levels of MMP-1 and MMP-13 mRNA and protein.⁴³⁹ Because the development of PTOA typically occurs several years after injury,²⁸⁸ it is difficult to measure the effects of an early intervention. However, a clinical trial by Brandt et al.⁷⁰ found that doxycycline treatment given to patients with unilateral OA for 30 months significantly decreased the rate of joint space narrowing. Also, prophylactic doxycycline has also been shown to effectively reduce the severity of OA in dogs following ACL transection.⁵²² These studies underscore the potential for using doxycycline to prevent GAG loss after injury to articular cartilage.

Ameliorating the immediate damage and ensuing degenerative cascade following articular cartilage injury could improve the daily activity of individuals suffering from PTOA. While results from studies involving doxycycline are certainly promising, further examination is needed. Current literature has not established the effects of doxycycline on GAG release or tissue mechanical properties following impact loads, nor has any MMP inhibitor been studied following mechanical trauma for more than 1 week post-injury. In the present

study, an experimental system of mechanical injury was utilized to invoke two levels of impact, two concentrations of doxycycline, and two doxycycline treatment regimens in order to investigate its use following impact at 24 hrs, 1 week, and 2 week time points. It was hypothesized that doxycycline treatment would decrease GAG release by 1 week in a dose-dependent manner. Additionally, the 2 week continuous doxycycline treatment was hypothesized to result in less GAG release and yield greater aggregate moduli in explants compared to treatment for only the 1st week of a 2 week culture period.

Materials and methods

Articular cartilage tissue harvest

A total of 27 proximal bovine ulnas were obtained from the elbow joints of skeletally mature animals (Animal Technologies, Tyler, TX) within 48 hrs of slaughter. Under sterile conditions, the proximal ulna was cut parallel to the articular surface using a reciprocating saw (Ryobi, Hiroshima, Japan) with a sterile blade. Approximately 1.5 cm of bone was left in place beneath the articular cartilage surface. The articular surface was then covered with sterile gauze and hydrated with sterile phosphate-buffered saline (PBS). Following tissue harvest, the articular surface, including underlying bone, was placed into a custom designed stainless-steel autoclaved specimen clamp and prepared for impact.

Impact of articular cartilage

Cartilage impact was carried out as described previously.⁴³¹ Briefly, the impact mass was raised to the specified height and dropped onto the impact

interface, which connects to a 5 mm, non-porous, cylindrical impact tip. Two levels of impact were employed: a 'Low' impact (6 cm drop height with a 1.88 kg mass) and a 'High' impact (10 cm, 3.43 kg mass), delivering 1.1 J and 2.8 J of energy, respectively. Each proximal ulna was impacted four times (two at the High level and two at the Low level) in distinct locations that were separated by at least 5 mm. Impact location was randomized across all groups studied.

Explant and culture of articular cartilage

Following impact, 5 mm diameter full thickness articular cartilage explants were removed from each ulna using a sterile dermal biopsy punch and a #10 scalpel blade. Explants were placed directly into 6-well plates for culture. In addition to the four impacted areas, two 5 mm non-impacted explants were removed from each joint and used as controls. All cartilage explants (control, Low impact, and High impact) were randomly assigned into one of three treatment groups consisting of either 0, 50, or 100 μ M doxycycline supplemented in the media (Sigma, St. Louis, MO). Explants were cultured in 3 mL of serum-free Dulbecco's Modified Eagle Medium (DMEM) with GlutamaxTM (Invitrogen, NY) containing 100 units/mL Penicillin (Biowhittaker, MD), 100 μ g/mL Streptomycin (Biowhittaker), 2.5 mcg/mL Fungizone (Biowhittaker), 0.1 mM non-essential amino acids (Invitrogen), and 50 μ g/mL ascorbic acid. Medium was replaced at 24 hrs, and then every 2-3 days for the remaining time in culture. Collected medium was stored at -20°C for GAG release quantification. Groups assigned to receive treatment had freshly dissolved doxycycline delivered during each media change. As shown in figure 4-1, culture duration was either 1 week with

continuous treatment, 2 weeks with continuous treatment, or 2 weeks of culture with treatment for the 1st week but not the 2nd. Pilot studies showed 100 μ M doxycycline did not cause significant cell death (data not shown).

Histology

Tissue samples were cryoembedded and sectioned at 14 μ m. Samples were fixed in 10% phosphate buffered formalin and stained with Safranin O/fast green to examine GAG distribution. Slides were then dehydrated through ascending alcohols before being coverslipped with Permount™ and examined under 10X magnification with a light microscope.

GAG release to media

Each sample of collected culture media was removed from -20° C, thawed, and vortexed thoroughly before assaying 50 μ L with a 1,9-dimethyl-methylene blue colorimetric assay to detect GAG released to the media (Blyscan Sulfated GAG Assay, Accurate Chemical and Scientific Corp., New York). Chondroitin 4-sulfate was used as the standard. Total GAG released into the media was then back calculated and normalized to tissue volume. Tissue volume was calculated knowing the tissue surface area (5 mm diameter circle) and thickness, as measured immediately following biomechanical testing (see below).

Creep indentation biomechanical testing

Following culture, a dermal biopsy punch was used to remove the inner 3 mm diameter portion of the 5 mm diameter explant. These specimens were wrapped in gauze soaked in PBS containing protease inhibitors (10 mM N-ethylmaleimide, 5 mM benzamidine, 2 mM EDTA, and 1 mM

phenylmethanesulfonyl fluoride) and frozen at -20°C until testing. Prior to testing, samples were thawed for at least 1 hr at room temperature in the same PBS with protease inhibitor solution and affixed to a flat stainless steel surface with a thin layer of cyanoacrylate glue. A creep indentation apparatus was used to determine the compressive creep and recovery behavior of the cartilage explants.³⁰ Testing conditions consisted of a tare load of 0.005 N followed by a test load of 0.02 N applied to the sample through a 0.8 mm diameter, flat-ended, rigid, porous tip. Creep and recovery behavior was recorded using LabView software (National Instruments, Austin, TX). A semi-analytical, semi-numerical model was used to determine the tissue's linear biphasic properties of aggregate modulus, permeability, and Poisson's ratio from the time-displacement curves.³⁴⁸ Tissue thickness was measured across the entire 3 mm specimen using digital calipers.

Statistical analysis

The study was based on a full-factorial experimental design. The JMP IN 5.1 statistical software package (SAS Institute, Cary, NC) was used to perform a two-factor ANOVA (impact level and doxycycline concentration) on the biomechanical properties and amount of GAG released from each explant for the 1 and 2 week continuous treatment groups. This model was also used on media samples collected at 24 hrs. Another two-factor ANOVA (impact level and treatment regimen) was used to compare the effects of 2 week continuous treatment to 1 week on followed by 1 week off treatment with 50 or 100 μM doxycycline. If significance ($p < 0.05$) was found, a Tukey HSD post-hoc test was

performed to compare amongst factor levels. For the GAG release and biomechanics assays, an $n = 6$ was used for each group. For histology, an $n = 2$ was examined for each group. Data are displayed in the figures as mean \pm S.D.

Results

Histology

Histological staining for GAG with Safranin O/fast green revealed no gross staining differences among the 0, 50, or 100 μ M doxycycline concentrations at 1 or 2 weeks following injury for all impact levels. Figure 4-2 shows representative images from the 1 week time point for 0 and 100 μ M doxycycline treated control, Low, and High impact specimens. In addition, 2 week samples treated with doxycycline for only 1 week of a 2 week culture period were found to have no identifiable differences compared to samples treated continuously for 2 weeks. Non-impacted controls showed no surface damage, whereas those impacted at the High level had considerable surface damage, including delamination, surface fissures, and gross injury that progressed beyond the superficial layer into the middle-deep zone. Specimens impacted at the Low level showed no gross surface damage. Furthermore, GAG staining appeared noticeably reduced in samples impacted at the High level compared to non-impacted controls, while staining for Low impact appeared similar to controls.

GAG release

Figure 4-3A shows GAG release data for 24 hrs and days 2-7. Impact level was a significant factor 24 hrs following injury ($p < 0.001$), with High impact

resulting in a greater amount of GAG release to media than both Low impact and non-impacted control groups. At 24 hrs no significant differences were found for GAG release due to doxycycline treatment. For days 2-7, impact level did not significantly affect GAG release ($p = 0.11$); however, doxycycline treatment was a significant factor ($p < 0.001$), with 100 μM doxycycline resulting in decreased GAG release compared to both 0 and 50 μM doxycycline. Cumulative 1 week GAG loss was calculated by adding the 24 hr and 2-7 day collections. Both impact level and doxycycline concentration were significant factors ($p = 0.015$ and 0.022 , respectively). Post-hoc analysis of factor levels showed High impact caused significantly more GAG to be released to the media compared to non-impacted controls and treatment with 100 μM doxycycline significantly decreased GAG release compared to no treatment. For the control, Low, and High impact levels, treatment with 100 μM doxycycline resulted in 29%, 14%, and 30% reductions in GAG loss, respectively. Notably, of the total GAG released in 1 week, at least 33% was released in the first 24 hrs for all groups studied.

The amount of GAG released during days 8-14 of culture was not significantly affected by either impact level or doxycycline treatment. However, for 2 week cumulative GAG release, calculated by adding the 1 week cumulative GAG release with the 8-14 day collection, impact level was not a significant factor ($p = 0.32$), but doxycycline concentration was ($p < 0.001$). Post-hoc analysis showed 100 μM doxycycline significantly decreased 2 week cumulative GAG release compared to 0 or 50 μM doxycycline (Fig. 4-3B). Compared to no treatment, treatment with 100 μM doxycycline of specimens impacted at the

control, Low, and High levels resulted in 50%, 49%, and 38% respective decreases in cumulative GAG released over 2 weeks.

To test whether doxycycline's effects are specific to a particular window of time, cartilage explants were treated for only the 1st week of a 2 week culture period and compared to explants treated continuously for 2 weeks. For both 50 and 100 μ M doxycycline, there was no significant difference in GAG release between the two treatment regimens (Fig. 4-3C).

Biomechanical properties

Biomechanical properties provide indices for the ability of the tissue to function as needed in its mechanical environment. The approach employed in this study, based on the linear biphasic theory,³⁴⁶ allows determination of tissue aggregate modulus, permeability, and Poisson's ratio. Figures 4- 4A and 4B show the aggregate moduli of all explants that received continuous doxycycline treatment in this study. Data at 1 week and 2 weeks were analyzed separately. Both analyses revealed that impact level was a significant factor ($p = 0.039$ and $p = 0.047$ for 1 and 2 weeks, respectively). Post-hoc analyses showed that High impact resulted in a significant decrease in aggregate modulus at both 1 and 2 weeks compared to non-impacted controls, while the aggregate moduli measured from articular cartilage that was impacted at the Low level were not significantly different from either non-impact control or High impact levels at both 1 and 2 weeks post-injury. At 1 week, the aggregate modulus of the High impact 0, 50, and 100 μ M doxycycline treated explants had decreased 32%, 41% and 36% compared to their respective treated, non-impacted, controls. For the 2

week time point, the same values were 32%, 9%, and 28%. Notably, treatment of Low impact specimens with 100 μ M doxycycline resulted in only a 3% decrease in aggregate modulus at 1 week.

In terms of tissue permeability, at 2 weeks post-injury impact level was a significant factor ($p = 0.007$). Post-hoc analysis showed the permeability of articular cartilage following High impact loading was significantly increased (1.5-1.8 fold) compared to non-impacted controls (Table 4-I). The permeability of explants subjected to Low impact was similar to both non-impacted controls and the High impact level. Poisson's ratio was not significantly affected by impact level at any time point.

Furthermore, continuous doxycycline treatment had no significant effect on any of the tissue's material properties across all impact levels and time points. Also, looking within the individual impact levels, treatment with doxycycline for the 1st week but not the 2nd did not significantly affect mechanical properties measured at 2 weeks compared to groups that were given 2 week continuous doxycycline treatment.

Discussion

The objective of this study was to determine the effects of doxycycline on GAG release from and mechanical properties of articular cartilage following mechanical impact. Our results indicate that doxycycline mitigates GAG loss from articular cartilage following a single impact injury. In particular, it was demonstrated that treatment with 100 μ M doxycycline significantly reduced GAG

release from the tissue at both 1 and 2 weeks post-injury. Additionally, doxycycline treatment for only the 1st week of a 2 week culture period was found to provide the same chondroprotective properties as doxycycline delivered continuously for 2 weeks. These results suggest doxycycline merits further study in already established animal models of mechanical injury to articular cartilage.^{64,154,338,373}

The temporal GAG release profile observed in this study supports a model in which mechanical trauma is responsible for initial GAG loss, while subsequent GAG loss results from enzymatic degradation. In this study, impact loading resulted in GAG release from injured tissue that was significantly greater for the High level of impact (2.8 J) at 24 hrs compared to both Low impact (1.1 J) and non-impacted controls. These results agree with findings from other groups that show increasing impact energies (0.1-1 J) result in higher levels of GAG release.^{242,254} Further, studies show that the majority of GAG loss occurs at early time points, typically less than 72 hrs post-injury.^{130,151,242,254} Similarly, in the present study, 33% of the total GAG released over 1 week occurred in the first 24 hrs. However, doxycycline treatment did not significantly affect immediate GAG release following injury, suggesting that the mechanisms behind initial GAG loss cannot be stopped with an MMP inhibitor alone. Therefore, one possibility is that mechanical damage and loosening of the collagen network is responsible for immediate GAG release following impact injury. DiMicco et al.¹³⁰ demonstrated similar findings, showing that GAG loss during the first 24 hrs following injury was due to mechanical damage, while GAG loss that occurred in subsequent days

could be attributed to MMP activity. Alternatively, GAG release in the first 24 hrs may also be mediated by other enzymes unaffected by doxycycline, such as hyaluronidases or aggrecanases.^{193,426,457}

Further, our data suggest that long term doxycycline treatment following impact injury may not be necessary to result in decreased GAG loss from the tissue, though further *in vitro* work to identify the minimal treatment time and subsequent *in vivo* validation are needed. Jeffrey et al.²⁵⁴ observed evidence of a repair response through a mechanism in which GAG was synthesized at higher rates by injured tissue compared to control. A higher rate of GAG synthesis is beneficial in a repair response, though it may be hindered by the increase in MMP activity that occurs following injury.^{59,130,439} Therefore, use of an MMP inhibitor such as doxycycline, coupled with the physiological response of increased GAG synthesis post-injury, may provide an opportunity for tissue recovery, such that the benefits may continue to be seen after treatment is stopped. This is one possible explanation for the results that indicated 2 weeks of continuous doxycycline treatment is equivalent to treatment for only the 1st week of a 2 week culture period. If latent MMP activity and MMP synthesis is only up-regulated following injury for a short period of time, and these enzymes are responsible for a considerable amount of the matrix catabolism, then early treatment with doxycycline may have beneficial outcomes in the long-term. Further supporting this argument, doxycycline treatment has been shown to decrease mRNA and protein levels of MMP-1 and MMP-13 in normal and OA chondrocytes.⁴³⁹

While the present study does not specifically address whether the GAG released is due to *de novo* synthesis or degradation of existing matrix, both literature and our data support a mechanism whereby doxycycline reduces GAG release through inhibition of matrix catabolism post-impact. Following impact there is a decrease in GAG synthesis,^{254,293} which Jeffery et al.²⁵⁴ have shown takes 12 days to recover and increase in impacted cartilage (~1 J) over uninjured controls. However, increased synthesis is not likely in our system, since, from 8-14 days, we observed no differences in GAG release among all groups studied. Further, increased cell death with increasing impact level has been observed both in our system (data not shown) and in previously published work.^{243,253} The model that doxycycline prevents tissue degradation is further substantiated by the fact that higher levels of GAG release were still observed despite a greater level of cell death resulting from High impact. With fewer cells to synthesize GAG, decreased GAG release with doxycycline treatment must result from inhibition of matrix degradation, a model supported by literature.¹³⁰

Increased GAG release from the tissue caused by impact was supported histologically. Results showed decreased GAG staining for High impact, especially in areas of surface delamination and fissuring. Though doxycycline was seen to reduce the amount of GAG loss when assayed quantitatively, this was not identifiable by the qualitative nature of histology. Indeed, one study has shown that a histological proteoglycan loss score could not distinguish impacted specimens from controls.²⁴² Considering that the effects of impact are likely greater than the effects of doxycycline treatment, it is not surprising that a

reduction in GAG release due to doxycycline is not observed histologically. However, this contrasts with work done in a rat model of OA that found increased GAG staining in the doxycycline treated group following chemical insult with iodoacetate.¹¹⁵ The discrepancy is likely due to use of mechanical impact in our study and a different animal model.

Similar to the current study, other investigators have tested the effects of MMP inhibitors on GAG release from articular cartilage. One study utilized iodoacetate to stimulate cartilage damage in rats, and found MMP inhibitors effectively reduced cartilage damage.²⁵² Another study initiated cartilage degeneration by activating latent MMPs with 4-aminophenylmercuric acetate.⁵⁹ In that study, two MMP inhibitors were found to inhibit proteoglycan loss, one of them up to 95%. The study also found maintenance of the tissue's streaming potential, electrokinetic coupling coefficient, dynamic stiffness, and equilibrium modulus. In contrast with the present study, though tissue stiffness decreased significantly following impact, we did not observe recovery of tissue biomechanical properties with doxycycline treatment. An explanation for this observation is that the early GAG loss following injury, presumably due to immediate mechanical disruption of the tissue's collagen matrix and, therefore, not preventable by doxycycline, is enough to cause a decrease in tissue stiffness. Though GAG is considered the prominent determinant of tissue stiffness, organization of the collagen matrix has been shown to play a prominent role as well.²⁸⁷ Decreased tissue stiffness immediately following impact has previously been shown in our system,⁴³¹ and tissue stiffness would not be

expected to recover until a repair response has occurred. Further, at 2 weeks a significant increase in tissue permeability in High impacted explants was found. Increased tissue permeability is a hallmark of OA,²¹⁶ and a 1.3 fold increase has also been reported in a rabbit model of traumatic cartilage injury beginning 7.5 months post-injury, increasing to 2.1 fold by 36 months.¹⁵⁴

While neither 50 nor 100 μ M doxycycline may be the optimal concentration, it is noteworthy that 100 μ M doxycycline effectively decreased GAG release, while the 50 μ M concentration did not. Concentrations used in this study were carefully chosen from values reported previously in literature and pilot studies, though choosing doxycycline concentrations was complicated by using tissue explants, since previous studies used cells or animal models. Shlopov et al.^{439,440} utilized concentrations of \sim 2 μ M, 4 μ M, and 100 μ M when working with OA cells in one study, as well as concentrations of \sim 20 and 50 μ M in another study with healthy chondrocytes. In work to determine the kinetics of doxycycline inhibition of various MMPs, concentrations up to 90 μ M were utilized.⁴⁴⁸ Though 100 μ M is higher than what is achieved in the tissue following intravenous administration (measured as \sim 10.5 μ g doxycycline per g of cartilage³⁰⁵), 100 μ M doxycycline could be delivered via intra-articular injection. Choosing an ideal doxycycline concentration and treatment regimen are just some components of any future clinical application, but we acknowledge that this study has constraints that limit extrapolation to the clinical setting. First, and perhaps most important, is the fact that this study utilized a bovine model. Doxycycline could have other effects in human tissue. Additionally, there are other components of cartilage

breakdown that need to be further assessed, such as the effects of doxycycline on collagen release and non-MMP matrix degrading enzymes. Nonetheless, the positive results of this study, namely 100 μ M doxycycline decreasing GAG release, indicate future study would be productive.

In conclusion, we found that the mechanical damage of impact loading causes significant tissue disruption, loss of GAG from the ECM, and decreased tissue stiffness. While Low impact did not cause gross surface damage or release as much GAG initially, it became equivalent to the High level of impact at 1 week in terms of tissue stiffness and GAG release. This result indicates that an impact not causing immediate grossly observable damage can result in enough damage at the molecular level to be similar to a High level of impact after 1 week. Though tissue stiffness was not preserved, the data in this study support the hypothesis that doxycycline can mitigate GAG loss following cartilage impact injury. Further, it was interesting that 1 week of doxycycline treatment in a 2 week culture was equivalent to 2 weeks of continuous treatment, suggesting a post-injury treatment regimen may not need to be long. However, further exploration must be undertaken to fully elucidate doxycycline's beneficial effects, and efforts should be made to optimize doxycycline delivery and dosage. Additional study into the use of doxycycline combined with other chondroprotective treatments, such as those that initiate growth and repair mechanisms or specifically target other matrix degrading enzymes, would also be of interest.

Table 4-I: Tissue permeability and Poisson's ratio as measured by creep indentation

Time Point	Impact Level	Doxycycline Concentration (μM)	Permeability ($\text{m}^4/\text{N}\cdot\text{s} \times 10^{-15}$)	Poisson's Ratio
1 week	Control	0	2.08 ± 1.09	0.123 ± 0.102
		50	4.38 ± 3.82	0.222 ± 0.217
		100	3.85 ± 0.65	0.096 ± 0.108
	Low	0	6.16 ± 3.33	0.070 ± 0.081
		50	4.45 ± 1.75	0.123 ± 0.144
		100	6.21 ± 4.27	0.048 ± 0.065
	High	0	2.52 ± 2.04	0.123 ± 0.107
		50	5.03 ± 2.97	0.057 ± 0.092
		100	4.99 ± 2.49	0.048 ± 0.085
2 week Continuous	Control	0	2.71 ± 0.90	0.048 ± 0.061
		50	3.70 ± 1.29	0.101 ± 0.118
		100	3.95 ± 1.23	0.070 ± 0.115
	Low	0	4.74 ± 2.01	0.039 ± 0.074
		50	3.44 ± 1.84	0.048 ± 0.085
		100	4.41 ± 0.95	0.066 ± 0.077
	High*	0	4.85 ± 1.20	0.131 ± 0.078
		50	5.61 ± 1.88	0.022 ± 0.054
		100	7.26 ± 5.05	0.057 ± 0.073
1 week On, 1 week Off	Control	50	4.57 ± 1.50	0.022 ± 0.020
		100	4.77 ± 1.74	0.079 ± 0.113
	Low	50	5.31 ± 2.90	0.018 ± 0.032
		100	4.86 ± 1.20	0.005 ± 0.012
	High	50	5.21 ± 1.26	0.066 ± 0.102
		100	7.12 ± 4.48	0.053 ± 0.072

Table 4-I. Tissue permeability and Poisson's ratio as measured by creep indentation. Values given as mean \pm 1 S.D of $n = 6$ samples. * Denotes significant effect ($p = 0.007$) of impact level on permeability at the 2 week time point. The 'High' level of impact resulted in a significant increase in permeability compared to non-impacted controls.

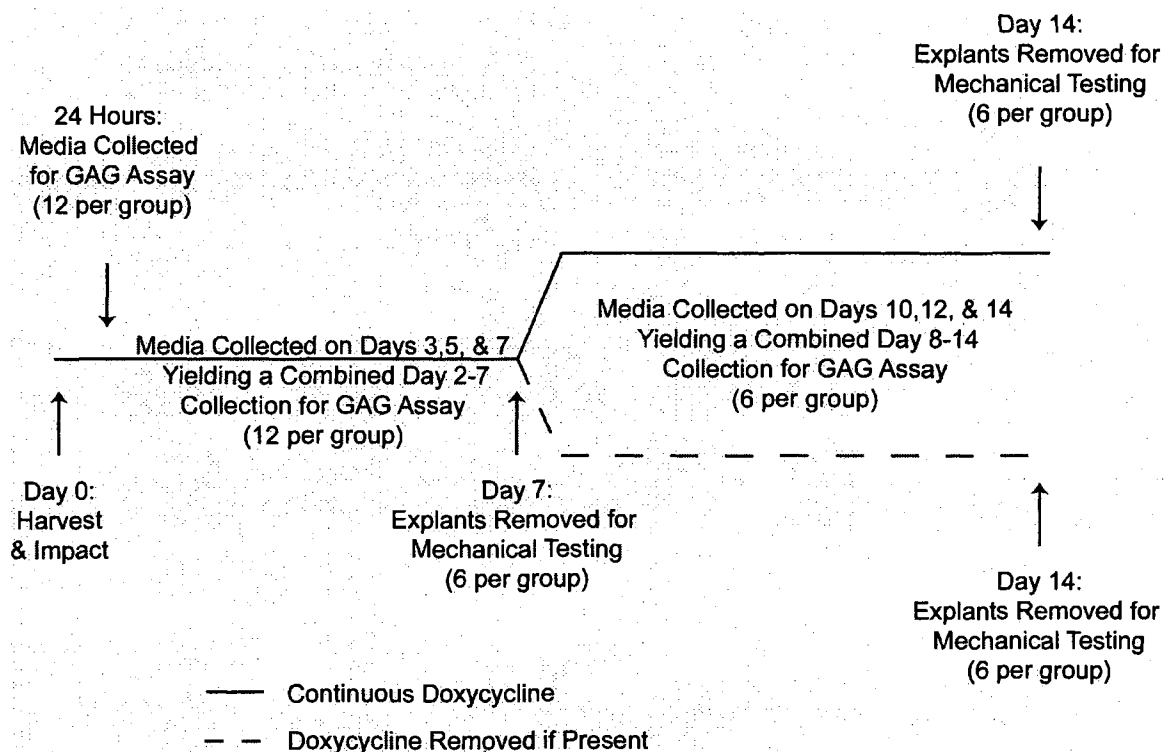
Figure 4-1: Experimental timeline

Figure 4-1. Time line description of experiments. Cartilage was harvested and impacted on day 0 and cultured with 0, 50, or 100 μ M doxycycline. Medium was collected and stored separately at 24 hrs. Medium was also obtained to yield collections corresponding to days 2-7 and days 8-14. At 1 week, six explants per group were removed for mechanical testing while the rest continued to be cultured in the presence (solid line) or absence (dashed line) of doxycycline. After 2 weeks of culture, the remaining explants were removed for mechanical testing.

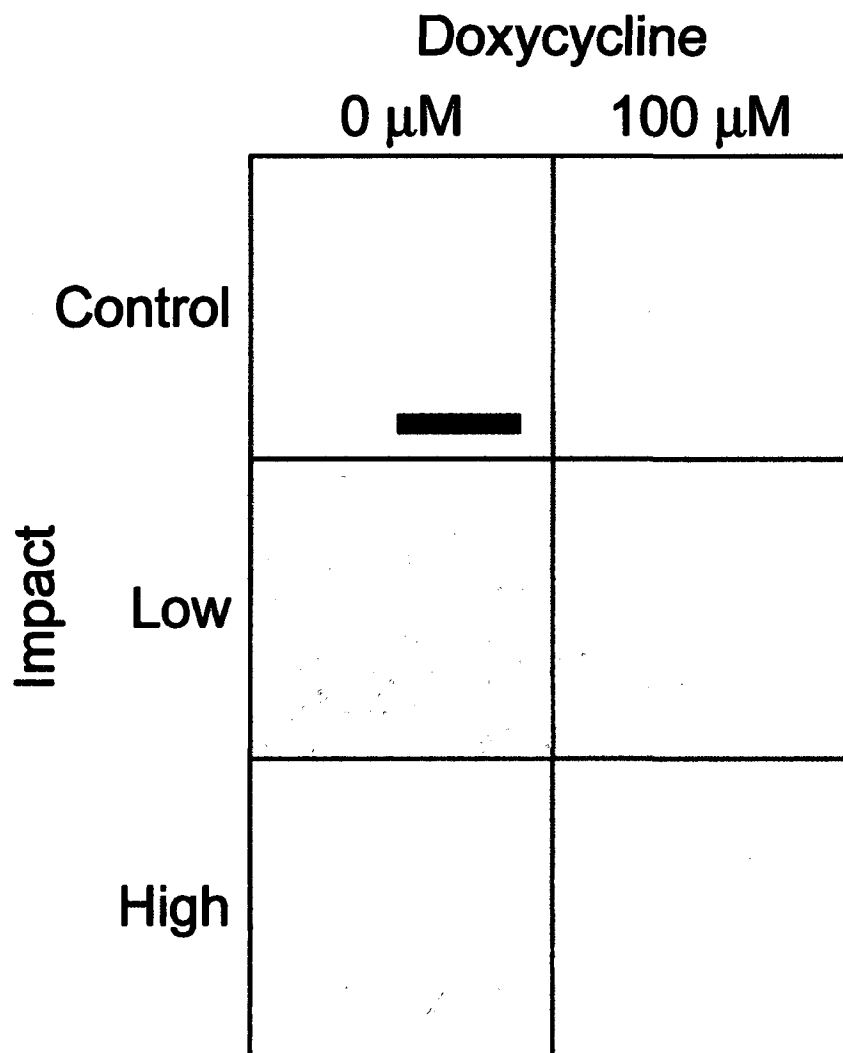
Figure 4-2: Histology

Figure 4-2. Representative histological images of tissue samples stained for proteoglycans after 1 week of culture in 0 and 100 μM doxycycline treated explants at each impact level. Scale bar = 500 μm . Note the extensive damage caused by High impact and resulting decreased staining. No differences in staining were apparent due to doxycycline treatment.

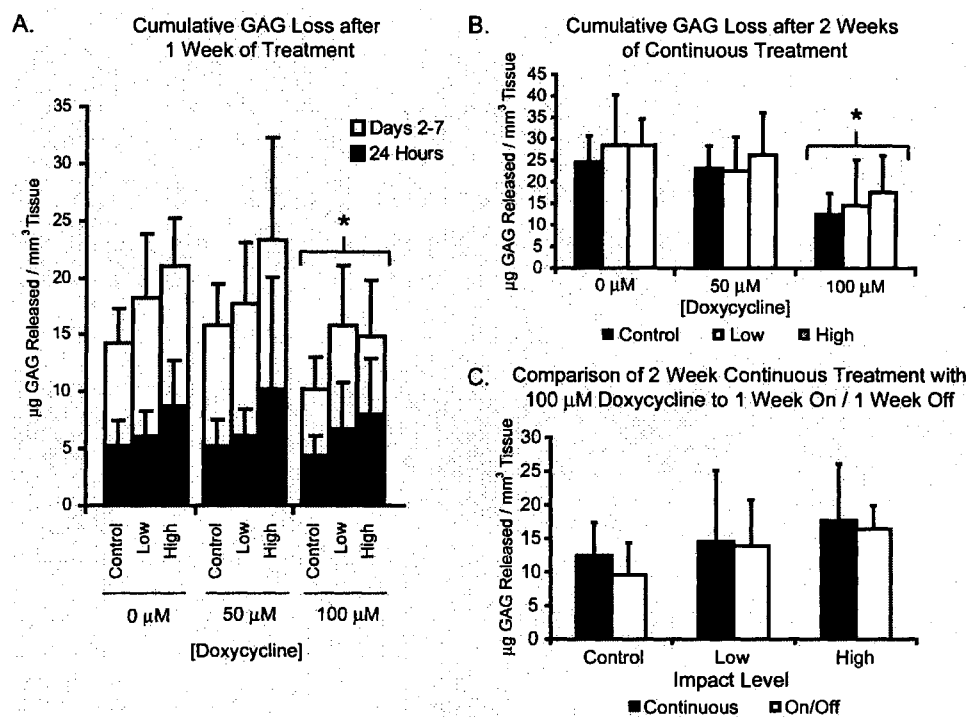
Figure 4-3: Cumulative sGAG release data

Figure 4-3. Data from GAG release assay. A) Comparison of GAG release for all impact and doxycycline levels at 24 hrs and 1 week. The top of the white bar represents cumulative 1 week GAG release. While only impact was a significant factor at 24 hrs ($p < 0.001$), both impact level and doxycycline concentration were significant factors ($p = 0.015$ and 0.022 , respectively) for 1 week cumulative GAG release, with High impact resulting in more GAG release compared to non-impacted controls and 100 μM doxycycline resulting in decreased GAG release compared to no treatment (* = $p < 0.05$ with Tukey HSD *post-hoc*). B) Cumulative GAG release after 2 weeks of continuous doxycycline treatment. Treatment with 100 μM doxycycline significantly decreased GAG release compared to 0 and 50 μM groups (* = $p < 0.05$ with Tukey HSD *post-hoc*). C) Comparison of 2 weeks continuous treatment with 1 week of treatment followed by 1 week without at the 100 μM concentration. Treatment regimen did not significantly affect GAG release. The same was seen with 50 μM doxycycline. Each bar represents the mean plus 1 S.D. of $n = 6$ samples.

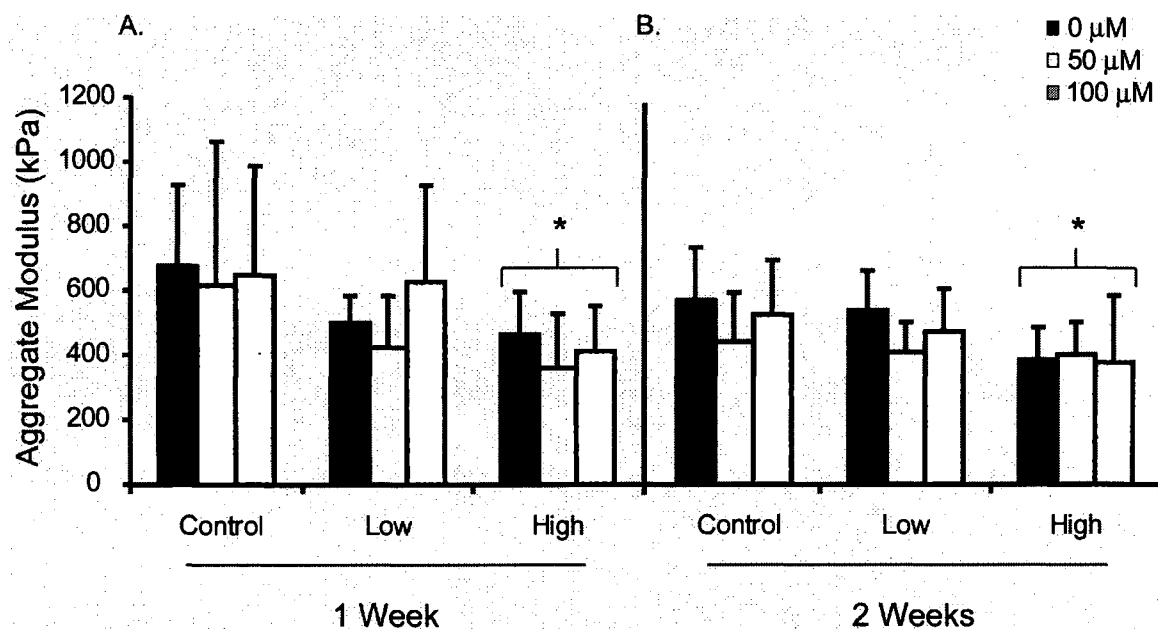
Figure 4-4: Compressive stiffness

Figure 4-4. Aggregate modulus of explants treated continuously with doxycycline for either 1 or 2 weeks of culture. Impact level significantly affected the aggregate moduli, with High impact causing a decrease in tissue stiffness at both the 1 and 2 week time points compared to non-impacted controls (* = $p < 0.05$ with Tukey HSD *post-hoc*). Aggregate moduli following Low impact were similar to both non-impacted controls and High impact at both time points. Doxycycline treatment did not significantly affect aggregate moduli. Each bar represents the mean plus 1 S.D. of $n = 6$ samples.

Chapter 5: Collagens of articular cartilage: structure, function, and their importance in tissue engineering*

Abstract

Collagen is a crucial matrix component of articular cartilage. Because articular cartilage is a load bearing tissue, developing mechanical integrity is a central goal of tissue engineering. The significant role of collagen in cartilage biomechanics necessitates creating a collagen network in tissue engineered constructs. An extensive network of collagen fibrils provides cartilage with mechanical integrity, but developing strategies to replicate this collagen network remains a challenge for articular cartilage tissue engineering efforts. To study the structure and biomechanics of the collagen network, many experimental and computational methodologies have been developed. However, despite extensive cartilage tissue engineering research, few studies have assessed collagen type, crosslinks, or fibril orientation. Further study of the collagen network, both within native tissue and engineered neotissue, will enable more robust constructs to be developed. This review focuses on the biology and biomechanics of the collagen network, relevant experimental methods for assessing the collagen network, and articular cartilage tissue engineering studies that have examined collagen.

Introduction

Due to the limited regenerative capacity and physiological importance of articular cartilage, damaged or diseased tissue needs to be replaced. Tissue

* Chapter to be submitted as Responde DJ, Natoli RM, and Athanasiou KA, "Collagens of articular cartilage: structure, function, and their importance in tissue engineering."

engineering has the potential to substantially improve treatment of cartilage defects. The matrix of cartilage, composed primarily of proteoglycans and collagen, creates the mechanical integrity of the tissue. The importance of the matrix in cartilage biomechanics, and its ability to withstand a demanding mechanical environment, necessitates producing a suitable matrix in tissue engineered constructs.

The structure of the collagen network contributes extensively to the mechanical integrity of cartilage, particularly to the tensile properties.²⁷⁴ Collagen comprises approximately two thirds of adult articular cartilage by dry weight,¹⁵⁷ making it a significant component of the extracellular matrix (ECM). Several types of collagen form a fibrillar network within the tissue. Many experimental methods exist to study the composition, structure, and crosslinking of this network. In addition, theoretical and computational models have been developed to analyze the role of collagen in articular cartilage biomechanics. Despite extensive research, tissue engineered articular cartilage tends to have significantly less collagen than native tissue.^{90,329,477} Strategies for improving this shortcoming will be needed to move closer to functional tissue engineered cartilage. This review will cover the biology and mechanics of the collagen network in articular cartilage, pertinent experimental methods for studying collagen, and results from articular cartilage tissue engineering studies. In doing so, methods and directions for advancing engineering of the articular cartilage collagen network will be highlighted and identified.

Biology of articular cartilage collagens

Types of collagen

Collagen molecules are comprised of three polypeptide chains that form a unique triple helical structure. These polypeptides contain high numbers of the repeating peptide sequence glycine-X-Y, where X and Y are frequently proline and hydroxyproline. This sequence helps stabilize the triple helix structure. Additionally, there are two short extrahelical telopeptides on each polypeptide chain which have neither the repeating peptide sequence nor a triple helical conformation. The most common types of collagen are the fibrillar molecules that self-assemble into fibrils; examples of fibrillar collagens include collagens I, II, and XI. The major collagen source within articular cartilage is a heteromer of collagen types II, IX, and XI, which is over 90% collagen II.^{157,470} This heteromer forms the fibrillar network that provides articular cartilage with its tensile strength and stiffness. As shown in figure 5-1, these fibrils have a hierarchical organization. Collagen VI is localized around the chondrocytes and contributes to mechanical properties and cell signaling. Several types of collagen, namely collagens I and X, are rarely expressed in normal articular cartilage, but do occur during development and certain pathologies. The following provides a brief synopsis of the collagens commonly studied in articular cartilage.

- Collagen II

Collagen II is only found in cartilage and the vitreous humor of the eye, and it accounts for the majority of collagen in hyaline cartilage.²⁷⁰ As the

predominant collagen of the heterofibril, collagen II is a primary indicator of hyaline cartilage differentiation. Although collagen II accounts for 75% of fetal collagen, as the tissue matures the collagen II proportion increases to 90%.¹⁵⁷ Collagen II has been shown to be expressed at higher levels by proliferating human fetal chondrocytes.⁴⁰⁷ Furthermore, creating transgenic mice that did not express collagen II resulted in chondrocyte apoptosis,⁵¹⁸ indicating the necessity of collagen II in articular cartilage.

- Collagen IX

Collagen IX forms covalent links between other collagen IX molecules and also crosslinks collagen II molecules as shown in figure 5-1B.⁵¹² Like collagen II, collagen IX can be used as a marker for cartilage differentiation. The upregulation of collagen IX during maturation also suggests it has a role in development.³⁵³ *In vivo* studies have shown that collagen IX plays a structural role in the development and integrity of articular cartilage. For instance, collagen IX knockout mice displayed irregular integrin immunostaining and abnormal columnar arrangement of chondrocytes. However, these developmental problems largely attenuated as the mice aged.¹³⁶ Other *in vivo* studies have shown the roles of collagen IX to include development of the cartilage growth plate³⁷⁸ and prevention of multiple epiphyseal dysplasia.³⁵²

- Collagen XI

Collagen XI is a fibrillar collagen that associates with collagen II. Type XI collagen comprises 10% of fetal cartilage collagen, but only 3% of adult tissue.¹⁵⁷

Collagen XI molecules crosslink primarily with other collagen XI molecules within the heterofibril.⁵¹² Additionally, collagen XI has also been shown to limit fibrillogenesis by inhibiting the growth of collagen II fibrils.²⁰⁴ This inhibition has been confirmed *in vivo* with collagen XI knockout mice that showed increased collagen fibril diameters.⁴³²

- Collagen VI

Collagen VI is localized in the matrix immediately surrounding chondrocytes, a region referred to as the pericellular matrix (PCM).³⁹² Type VI collagen contains the sequence Arg-Gly-Asp that binds to chondrocyte receptors.⁵⁸ It has been hypothesized that the close interactions between collagen VI and chondrocytes contribute to mechanotransduction,²¹³ so replicating the collagen VI structure may be important for creating an appropriate microenvironment for chondrocytes. Moreover, collagen VI mRNA is barely detectable in dedifferentiated chondrocytes, but starts to increase only six hrs following differentiation.³⁹⁸ Though mouse models have indicated that collagen VI increases as cartilage matures, it only comprises approximately 1% of adult collagen.^{157,214} Development also entails localization of collagen VI in the pericellular region; it is more widely distributed throughout the matrix prior to birth.³⁴⁵

- Collagen I

Collagen I is produced in many different connective tissues of the body, but it is not typically expressed in articular cartilage. Study of the rabbit knee joint

has shown that collagen I is expressed at the articular surface early in development, but disappears by six weeks after birth.⁵⁴ However, collagen I is abundant in fibrocartilaginous tissues such as ligament, tendon, temporomandibular joint disc, and the meniscus. Because the fibrocartilage that forms within articular cartilage is mechanically inferior, expression of collagen I is undesirable for tissue engineered articular cartilage. Culturing chondrocytes *in vitro* can result in dedifferentiation and collagen I production.^{48,123} Thus, collagen I can act as a marker for the differentiation status of chondrocytes for tissue engineering procedures.

- Collagen X

As with collagen I, collagen X is not expressed natively in hyaline cartilage. Generally, collagen X is only found near the bone, as immunohistological studies have shown that collagen X is localized in the zone of hypertrophic and calcifying cartilage.²⁸⁰ In addition, collagen X is expressed by some cells at the articular surface of maturing cartilage³⁴⁵ and in osteoarthritic cartilage.^{192,483} Collagen X has been shown to be localized at the lower growth plate of both chick embryo⁹¹ and human fetal cartilage.⁴⁰⁷ The appearance of collagen X in tissue engineered constructs can indicate hypertrophic chondrocytes.

Collagen crosslinks

Having discussed the types of collagen found in articular cartilage, we will now look at how the collagen fibrils are connected to one another. Crosslinks interconnect collagen fibrils and can be formed via various mechanisms. The

enzyme lysyl oxidase mediates normal crosslinking⁴⁴¹ and can form several types of crosslinks, including pyridinoline (Fig. 5-1C) and ketoimine linkages. In native articular cartilage, there are significantly more pyridinoline than ketoimine crosslinks, with a mean ratio of ~12 to 1.²²⁸ Crosslinks can also be formed non-enzymatically when collagen amines react with reducing sugars to form advanced glycation endproducts (AGEs).⁴⁶⁶ Many different sugars, including glucose, ribose, and threose, can play a role in AGE formation. For instance, adding ribose to adult bovine chondrocyte cultures increased the formation of AGEs.⁹⁸ In human articular cartilage, the formation of AGEs increases with advancing age.⁴⁷³ This age-dependent increase in AGE-mediated crosslinking could contribute to increasingly stiff, brittle cartilage.

Furthermore, the number and types of crosslinks change as the tissue matures. For example, as human cartilage matures, the number of crosslinks increases.^{156,270} Crosslinks increase with age in animal models as well. In bovine explants, the number of collagen crosslinks per wet weight is 730% greater in adult cartilage relative to fetal cartilage.⁴⁹⁴ AGE crosslinks also show maturation dependence, increasing linearly with age after reaching maturity.⁴⁰ After lysyl oxidase oxidizes a lysine residue, several intermediate structures form prior to forming a pyridinoline crosslink. Comparing the number of pyridinoline crosslinks to the number of crosslink intermediates provides one way of assessing tissue maturation.²²⁸ These results indicate that a tissue engineered construct may need the proper proportion of pyridinoline crosslinks to reflect native tissue.

Crosslinks play several important functional roles in cartilage. In addition to effects on the tissue mechanics (discussed below), crosslinks increase collagen retention, which could impact cell signaling. Fewer crosslinks can also increase collagen susceptibility to proteases.⁴¹³ These various functions of crosslinks show the necessity of recapitulating appropriate crosslinking in tissue engineered constructs.

Collagen fibrillogenesis

Modulation of fibril formation and degradation of fibrils control the development of the collagen network. Fibrillogenesis is a sequential process that begins when individual collagen molecules are extruded from chondrocytes. After extrusion, the collagen molecules fuse, either laterally or linearly, to form larger fibrils. Initially, this process produces small fibrils with uniform diameters that eventually interconnect to form fibrils. As the tissue matures, the diameters of the fibrils increase, and the fibril size becomes less uniform, as depicted in figure 5-2. Throughout this process, various mechanisms, such as growth inhibition and fibril degradation, regulate fibrillogenesis. The growth of fibrils is modulated at fibril interfaces by the binding of small proteoglycans.¹⁹⁶ Diffusion limitations can also inhibit fibril growth.²²⁹ Additionally, chondrocytes produce collagenases that degrade collagen molecules. Various collagenases that chondrocytes produce provide a way to finely control collagen degradation.^{155,353} In particular, cleaving regions involved in crosslinking could destabilize fibrils.

Ultrastructure of articular cartilage

- Organization of collagen

Articular cartilage has several structurally distinct regions known as the superficial, middle, deep, and calcified zones, and the properties of the collagen network vary significantly between zones (Table 5-1). In native tissue, collagen concentration is highest in the superficial zone and decreases farther from the articular surface,³⁵¹ yielding an inhomogeneous distribution (Fig. 5-2). Additionally, the organization of the collagen fibrils varies depending on the zone, and was first characterized by Benninghoff in 1925.⁴⁷ The superficial zone has fibrils oriented parallel to the articular surface. Beneath the superficial zone lies the middle zone that has larger fibrils that form interweaving arches. The deep zone contains the largest fibrils, which are oriented perpendicularly to the articular surface. The calcified layer contains the transition from the hyaline cartilage into the subchondral bone. This zonal variation can be attributed to the force distribution that cartilage experiences *in vivo*,^{341,505} yielding an anisotropic arrangement in native tissue. Generally, the fibrils have smaller diameters near the surface, with a mean fibril diameter of 35 nm in the superficial zone and 50 nm in the deep zone.²⁹⁸ Because collagen largely dictates the tensile properties, zonal variation of collagen fibril orientation and collagen content is important to consider when evaluating tensile properties of tissue samples.

Within each zone, several types of matrix exist: the pericellular matrix, the interterritorial matrix, and the territorial matrix. The territorial matrix is farthest from the chondrocytes and has less aligned collagen fibrils. Closer to the

chondrocytes, the interterritorial matrix has more oriented collagen fibers with larger diameters. The PCM immediately surrounds the chondrocytes and buffers the mechanical forces that the chondrocytes experience.^{5,6,208,210} The PCM can also impact cell-cell communication by sequestering soluble signaling molecules.⁴²²

Although the zonal organization of cartilage has been identified, considerable structural variation exists. Studies have shown differences in collagen ultrastructure based on factors like age, anatomical origin of the sample (e.g., joint and location within a joint), and variations in individual anatomy and physiology.^{125,265,351} Although collagen organization of the superficial zone is widely confirmed, the intermediate and deep zones have some conflicting results. Scanning electron microscopy (SEM) analysis has shown that intermediate fibrils actually form overlapping lamellae rather than interweaving arches.¹⁰⁴ Some studies of the deep zone have also shown divergences from the classic Benninghoff model of perpendicularly oriented fibrils. Traverse fibrils⁷⁹ and fibrils with random orientations⁴⁸⁹ have been observed, in addition to the predominant perpendicular arrangement. However, the Benninghoff model characterizes the majority of the fibrils in articular cartilage.

While the Benninghoff model describes collagen orientation through the depth of the tissue, split-lines illustrate collagen orientation in the plane of the tissue's surface. Pricking cartilage with a pin dipped in ink produces lines that correspond to fibril orientation in the superficial zone (Fig. 5-3). Electron microscopy has been used in various studies to show the correspondence

between split-lines and collagen orientation.^{79,334} Within area of the cartilage that experience the most loading, split-line patterns are highly consistent between samples.⁴⁵ The collagen orientation associated with split-lines also has significant biomechanical implications. For instance, the equilibrium modulus of the superficial layer in human patellar cartilage increased by approximately 4-fold when the samples were loaded parallel to wear-lines.³⁸ Split-lines show the importance of considering the in-plane collagen ultrastructure, in addition to the vertical variation.

- Ultrastructure development

Studies in rabbit knee joints have shown that the organization of collagen depends on age, with initial organization of the tibial plateau collagen network occurring within two weeks of birth. In particular, the orientation of collagen fibrils correlates with the acquisition of full mobility.⁵³ As the animal matures, collagen fibrils acquire increasingly vertical orientations in deeper layers (Fig. 5-2), resulting in lower tensile strength parallel to the surface.¹⁰⁵ The factors that control development of collagen orientation have not been fully elucidated, but mechanical loading appears to govern this process.¹⁷¹

Mechanical load on the tissue has been frequently proposed as the primary stimulus for collagen orientation.¹⁷¹ Additionally, theoretical modeling of cartilage development based on a loading stimulus reproduces native collagen structure.⁴⁹⁹ Although the loading hypothesis for ultrastructure development has not been fully confirmed, some experimental evidence exists. For instance, fibroblast-seeded collagen gels subjected to 2.5% cyclic strain develop fiber

alignment and mechanical anisotropy.²²³ Various studies have also shown that loading of cartilage tissue lowers the susceptibility of collagen to enzymatic degradation.^{354,488} This selective degradation has been proposed as a mechanism underlying mechanical stimulation of collagen orientation, but alternate mechanisms could also play a role.

Collagen interactions with other matrix molecules

Although the collagen network directly influences the mechanics of cartilage, interactions with other components of the matrix are also crucial. Various proteoglycans interact with collagen and, in many cases, regulate the assembly of fibrils. Reduced aggrecan deposition in mice has been shown to increase fibril diameter and alter banding patterns, suggesting interplay between aggrecan and collagen.⁴⁸⁸ Several small proteoglycans including lumican, decorin, and fibromodulin also interact with collagen. These interactions can regulate fibril diameter, fibril-fibril interactions, and susceptibility to degradation.⁴¹⁹ Knocking out perlecan, a heparan sulfate proteoglycan, reduced the size and density of collagen fibrils.^{16,111} Molecules other than proteoglycans can also influence the collagen network. For example, cartilage oligomeric matrix protein (COMP) stabilizes fibrils by binding to collagen triple helices.^{220,417} The interactions between the collagen and various matrix components play a large role in governing the size and stability of collagen fibrils.

Collagen-cell interactions

Collagen also interacts directly with chondrocytes to influence cellular function. For example, interaction with collagen increased chondrocyte

aggregation and reduced the level of chondrocyte apoptosis.^{88,518} In contrast, collagen degradation has been shown to cause apoptosis.³¹⁹ In addition to preventing apoptosis, the collagen network influences biosynthesis. For instance, inhibiting collagen crosslinking increased collagen synthesis, indicating a feedback mechanism between the collagen network and chondrocytes.⁴⁴ Collagen's influence on the survival and biosynthesis of chondrocytes shows the integral role of collagen-cell interactions in cartilage physiology.

Although the cellular interactions with collagen are not fully elucidated, many of them have been attributed to integrin- $\beta 1$ ⁸⁸ and annexin V.⁴⁶⁷ Annexin V has been shown to regulate mineralization of growth plate cartilage; it may have a role in pathological mineralization as well.²⁷⁸ Studies have suggested that annexin V influences growth plate chondrocytes by altering calcium transport across cell membranes.⁴⁸⁷ Knocking out integrins created abnormal chondrocyte shape and reduced chondrocyte proliferation.⁴⁶ The integrin receptor also mediates the differentiation of chondrocytes and appears to be critical for joint development.¹⁸⁶ These various collagen-chondrocyte interactions play a critical role in cartilage development and homeostasis.

Summary

The collagen network of articular cartilage is primarily composed of fibrils of collagens II, IX, and XI. In addition to collagen IX crosslinking, enzymatic and non-enzymatic crosslinks interconnect the fibrils. Crosslinks can impact cartilage biomechanics, collagen retention, and collagen susceptibility to proteases. As the tissue matures, collagen molecules fuse laterally or linearly to form larger fibrils

and, ultimately, fibers. Collagen exhibits zonal variation within cartilage, both in terms of amount and orientation. Additionally, several distinct levels of collagen organization exist around chondrocytes with a pericellular matrix, interterritorial matrix, and interterritorial matrix.

Collagen mechanics: theoretical, computational, and experimental insights

As discussed above, collagen in native articular cartilage is inhomogeneously dispersed and anisotropically arranged. Further, cartilage has been shown to possess tension-compression non-linearity^{235,236,453} due to the increased stiffness of collagen in tension. These features complicate theoretical and computational approaches. In this section, we will examine mechanical properties of collagen, mechanical models of articular cartilage specifically incorporating features of the collagen network, and experimental findings elucidating the varied roles of collagen in articular cartilage biomechanics.

Fibrillar and molecular stiffness of collagen

Any effort to incorporate features of the collagen network into mechanical models of articular cartilage must be informed by the mechanical properties of collagen. Researchers have investigated collagen mechanical properties within tissue and at the single molecule level. In an early study on collagenous tissue, Haut and Little²¹⁷ proposed a quasi-linear viscoelastic constitutive equation for collagen fibers from rat tails and measured the material properties via tensile stress-relaxation tests. They then used the measured material properties to

predict the tissue's behavior under constant strain-rate, hysteresis loop, and dynamic tests, finding good experimental agreement with all but the latter. The value of the material property corresponding to the elastic nature of collagen fibers was found to be 11.5 GPa. Quasi-linear viscoelasticity of collagen fibers has more recently been examined in articular cartilage. Using tensile step-wise stress relaxation testing, the instantaneous fibrillar modulus was found to be ~2.2 times the relaxed modulus ($E_{relaxed}$), the latter of which depended on applied strain (ϵ), as $E_{relaxed} = 0.5 + 250\epsilon$ MPa.³¹⁶ Another study suggests that collagen type II has an elastic modulus of 7 GPa.⁴⁴³ At the *single* molecule level, material properties of collagen type II have been measured using optical tweezers, yielding an average persistence length of 11.2 nm.³²³ Assuming a solid rod with circular cross section of diameter d , an estimate of the Young's modulus (E_Y) from the persistence length (L_P) is given by $E_Y = (64k_B T L_P) / (\pi d^4)$, where k_B is Boltzman's constant and T is the temperature.⁴⁸⁵ At room temperature (23°C), and assuming a diameter of 1 nm, $E_Y \approx 0.93$ GPa. It is important to know the stiffness of collagen fibers for implementation in mechanical models of articular cartilage, a topic which we will now discuss.

Theoretical and computational models incorporating the effects of collagen

- Fiber reinforced continuum models

While there are several ways to incorporate features of the collagen network in material models of articular cartilage, fiber reinforced continuum models (Fig. 5-4) have been the most common approach.^{159,174,185,260,286,311-}

^{313,315,317,429,437,438,444,454,496,497} However, it must be noted that the presence of

fibers within a composite does not guarantee that the mechanical behavior of the bulk material will be different than it is without the fibers. As Aspden^{24,25} points out with respect to cartilage, a collagen fiber must exceed a critical aspect ratio to have a sufficient interaction force with the rest of the ECM for the matrix to effectively transfer stress to the fiber. While collagen fibers in native tissue satisfy this aspect ratio, fiber aspect ratio may be an important consideration in tissue engineering efforts.

At the most basic level, fiber reinforced models include fibers distributed throughout the solid matrix that are predominantly active in tension (Fig. 5-4B). In an early study, Schwartz et al.⁴²⁹ related the stiffness at the continuum level to the microstructure of articular cartilage. Their microstructural model consisted of bilinear elastic fibers embedded in an elastic matrix. The fibers, representing collagen, were given a tensile modulus of 150 MPa and a compressive modulus of 2 MPa. They also allowed the fibers to have random orientation throughout the tissue. An interesting finding, which has also borne out in subsequent studies, is that re-orientation of the fibers during loading leads to increased stiffness in the direction of the applied load and a non-linear tensile stress-strain curve. Elastic fibers have also been incorporated into the linear biphasic model³⁴⁷ to overcome difficulties the homogeneous biphasic model has in fitting unconfined compression experiments.⁴⁵⁴ It was found that a fiber Young's modulus of 11 MPa best fit unconfined stress relaxation experiments. Additionally, it was discovered that different constituents in the model (e.g., fibers or the matrix) can

experience substantially different stresses in a region of identical strain. This feature is not present in homogeneous models.

The elastic fiber reinforced biphasic model has been improved upon to include cartilage inhomogeneities through the incorporation of depth-dependent material properties and anisotropy, by orienting the collagen fibers differently through the depth of the tissue.³¹¹ This model was also used to investigate the strain-rate dependent stiffness of articular cartilage, which was attributable to “self-stiffening” of fibers, with little contribution from the rest of the solid matrix.³¹⁴ In a recent study, the anisotropic nature of the collagen network was also accounted for by orienting the fibers according to their zonal structure: parallel to the articular surface in the superficial zone, random in the middle zone, and perpendicular to the subchondral bone in the deep zone.⁴³⁸ It was shown that deep vertical collagen fibers increase tissue stiffness in the transient period of loading, which the authors postulate may be mechano-protective against damage to the underlying bone. Collagen fibers in biphasic fiber reinforced models have also been treated as viscoelastic.^{260,261,496,497} These studies have also shown that collagen network architecture is important in determining the tissue's mechanical behavior. One study used sample-specific data for the tissue's composition,²⁶⁰ demonstrating the degree of specificity that can be incorporated into these models. Finally, this line of inquiry has even been extended to include hyperelastic fibers in a viscohyperelastic matrix within a biphasic framework, thereby creating a model that accounts for the non-linear nature of finite deformations.¹⁸⁵

- Other models incorporating features of the collagen network

Other methods for including aspects of the collagen network into mechanical models include transversely isotropic theories,^{109,160} conewise linear elasticity,^{234,453} and microstructural models taking into account collagen distribution, orientation, or crosslinking.^{82,95,401} With respect to articular cartilage, planes parallel to the articular surface are the transversely isotropic planes. Thus, the tissue's material properties are different perpendicular to the surface compared to parallel to the surface. It was demonstrated that a transversely isotropic, transversely homogeneous model was able to predict non-uniform behavior of the tissue, whereas the isotropic homogeneous model could not.¹⁶⁰ To account for the tension-compression non-linearity of cartilage material properties, Soltz and Ateshian⁴⁵³ developed a conewise linear elastic model within a biphasic framework. Though developed at the level of an orthotropic material, due to experimental considerations, they reduced the model to cubic symmetry. Good agreement was found between theory and experiment for both confined and unconfined compression experiments and torsional shear testing. On average, articular cartilage was ~21 times stiffer in tension than compression.

In an interesting study, Quinn and Morel⁴⁰¹ generated a model for articular cartilage mechanics using only one material property, an elastic modulus of 70 MPa for the collagen fibrils. The rest of the model was generated taking into account the molecular orientation and distribution of collagen fibers and their interaction with the proteoglycan gel. Scaling up the model allowed prediction of continuum level mechanical properties in reasonable agreement with previous

experimental measurements. The model also predicts novel matrix interactions at low compressive strains ($\sim 1\%$) where current experimental data are limited. Lastly, two studies have initiated investigation into connections within the collagen network^{82,95} (e.g., crosslinking), one of which suggests substantial differences between collagen modeled as a network than when modeled as moving in an affine manner.

Experimental findings identifying the varied roles of collagen in mechanics

- Effects of collagen amount, orientation, and intrinsic viscoelasticity on tensile properties

Turning now to predominantly experimental work, as early as 1973 the tensile properties of articular cartilage were shown to be related to collagen amount, as well as to its anisotropic and inhomogeneous arrangement within the tissue.²⁷⁴ Specifically, it was shown that cartilage is stiffer in the superficial zone compared to deeper zones (Table 5-1) and also stiffer when pulled parallel to the predominant fiber orientation (determined by split-lines, Fig. 5-3) compared to when pulled perpendicularly. Woo et al.⁵⁰⁶ found similar results to the aforementioned study by employing an exponential stress-strain law (equivalent Young's modulus ranged 1.65 to 3.5 MPa) as opposed to simply fitting the linear portion of the stress-strain curve. Results from both of these studies were additionally related to the preferred direction of collagen fibers determined by polarized light microscopy or SEM.

More recently, tension-compression non-linearity (i.e., the disparity between tensile and compressive moduli measured in articular cartilage) and

flow-independent viscoelasticity of the solid matrix (i.e., that part of the viscous behavior due solely to the solid matrix and not flow of fluid within the matrix) have been examined experimentally.^{235,236,471} Huang and associates^{235,236} employed the biphasic-conewise linearly elastic quasi-linear viscoelasticity model (B-CLE-QLV) during confined and unconfined stress-relaxation compression tests of articular cartilage at both slow and fast strain rates, finding an average aggregate modulus in tension of 8.8 MPa. The B-CLE-QLV was able to simultaneously describe the tensile and compressive behavior, performing better than the preceding biphasic-conewise linear elastic and biphasic poroviscoelastic models of articular cartilage. These findings suggest tension-compression non-linearity and flow-independent matrix viscoelasticity, both attributable to collagen, are important contributors to the transient mechanical behavior of articular cartilage. Another study examined the tensile properties as a function of strain rate, finding similar Young's moduli and ultimate tensile strengths at 1, 20, and 50% strain s^{-1} , but significantly increased properties at 70% strain s^{-1} . The authors suggest this may be a protective mechanism for cartilage to withstand sudden traumatic loads.⁴⁷¹

- Effects of crosslinking on tensile properties

While collagen content, anisotropy, and inhomogeneity are important in determining cartilage tensile properties, another important aspect is the amount of crosslinking present in the collagen network.⁷² Williamson et al.^{494,495} studied changes in collagen content and pyridinoline crosslinking as a function of age in a bovine model and related them to tissue tensile properties. They found that

both increasing collagen amount and pyridinoline crosslinking correlated with increases in equilibrium and dynamic tensile stiffnesses and tensile strength. As an alternative approach, one study inhibited crosslink formation by treatment with β -aminopropionitrile (BAPN), an inhibitor of the crosslinking enzyme lysyl oxidase, and measured tensile properties. Results showed that treated explants had significantly less crosslinking and decreased tensile properties.²² In addition, administering sugars exogenously increased the formation of AGEs and, subsequently, increased the stiffness of the tissue.⁹⁸ The biomechanical role of AGEs is unclear, if not controversial. Increased AGEs may be a way in which cartilage attempts to mitigate the decrease in mechanical properties associated with aging or, by causing cartilage to become more brittle, be an explanation for why advanced age is a risk factor for the development of osteoarthritis. Regardless, these studies, and those mentioned above, underscore the complicated role the collagen network plays with respect to the tensile mechanical properties of articular cartilage.

- The role of collagen in compression

Though it is well accepted that the GAG content of articular cartilage is essential for its compressive properties, collagen has also been shown to have a role in governing compressive behavior and, interestingly, Poisson's ratio. In articular cartilage, the negatively charged GAGs lead to substantial hydration within the tissue that induces a swelling pressure able to resist compressive loads. The swelling pressure is balanced by tensile forces within the collagen network. Kovach and Athanasiou²⁸⁷ showed that the spatial arrangement of

collagen fibers is related to the aggregate modulus measured during creep indentation. In another study, confined compression was performed to various strain levels in the presence of different saline concentrations, with the expectation that compressions greater than 5% would lead to the full load being borne by the proteoglycan osmotic pressure, which would be evidenced by equal stresses in the axial and radial directions. Contrary to the authors' expectations the axial and radial stresses were not equal, highlighting a role for the collagen network in compression.²⁷⁷ It has also been demonstrated that the function of the stiffness of the collagen network is to maintain a high concentration of proteoglycans, which is then able to resist compressive forces.⁴¹ Similar to their study of bovine cartilage tensile properties, Williamson et al.⁴⁹³ examined compressive properties as a function of age. Results showed that the compressive modulus measured in confined compression increased 180%, while tissue permeability decreased 70%, from fetus to adult. These changes were correlated with increased collagen during development, since GAG changes during this period were negligible. Finally, Kiviranata et al.²⁸² demonstrated that Poisson's ratio is negatively correlated with collagen content (i.e., increased collagen, decreased Poisson's ratio) in bovine articular cartilage. An additional unique aspect of this study was that collagen content was measured with Fourier transform infrared (FTIR) spectroscopy. Further, the effect of fiber and proteoglycan moduli on Poisson's ratio were parametrically assessed via finite element analysis, showing that the fiber modulus had far more of an effect on Poisson's ratio than the proteoglycan matrix modulus.

Summary

Collagen plays an important and varied role in articular cartilage biomechanics that has been evidenced experimentally. Further, sophisticated theoretical and computational models of collagen's biomechanical functions have reproduced experimental findings and have predicted behavior that yet remains to be verified. From a basic science standpoint, future models should continue to increase in complexity. Special focus should be placed on models informed by detailed microstructural analyses that incorporate collagen orientations and distributions with molecular physics scaling up to the tissue level and models including collagen network crosslinking. This would be a daunting challenge. At the same time that more complicated models are developed, from a functional tissue engineering approach⁸⁵ we must recognize that such a level of sophisticated understanding may not be necessary to produce a construct that can adequately function in articular cartilage's native mechanical environment. Tissue engineers and biomechanicians alike need to continue to identify the salient mechanical characteristics of tissues and constructs that are necessary for cartilage regeneration and the structure-function relationships defining them. Further, standardized testing protocols should be followed so that mechanical properties can be compared from one study to another.

Experimental methods for collagen assessment

Due to the importance of collagen in cartilage, collagen composition and ultrastructure have been examined using various experimental methods. Many of

these methods have also been used in tissue engineering studies to assess the collagen network within neotissue.

General collagen assessment

Several methods have been developed to measure collagen in articular cartilage without distinguishing among the different types of collagen. Hydroxyproline assays quantify the amount of collagen within cartilage based on the fact that hydroxyproline residues within biological tissue originate from elastin or collagen. Because articular cartilage contains negligible amounts of elastin, the amount of hydroxyproline can be used to infer the amount of collagen in the tissue. This method entails using chloramine-T to oxidize the hydroxyproline groups. Subsequently, adding Ehrlich's reagent (p-dimethyl-aminobenzaldehyde) produces a chromophore that can be quantified by assuming that 12.5% of the collagen is hydroxyproline⁴⁰⁵ or by employing a collagen standard.

Another common method is collagen staining. Sirius red, dissolved in saturated picric acid, is an anionic dye that enables selective staining of collagen. When the dye binds to collagen via the dye's sulphonic acid groups, a change in birefringence occurs that can be visualized using polarized light microscopy.²⁶² Other staining protocols can be used as well, such as Gomori or Mallory trichromes, osmium tetroxide, periodic acid-Schiff, and Van Gieson. All of these methods readily verify the presence of collagen, but do not distinguish among the various collagen types.

Immunohistochemistry (IHC) and enzyme-linked immunosorbent assays (ELISAs)

IHC provides qualitative visualization of specific collagens within cartilage. Typically, a primary antibody is used to bind a particular collagen, followed by a secondary antibody binding the primary antibody. The secondary antibody can be conjugated to enzymes, like horseradish peroxidase or alkaline phosphatase, or fluorophores to produce a product that can be visualized. Employing a monoclonal antibody rather than a polyclonal antibody can increase the specificity of the antibody binding.⁴⁰⁴ For tissue engineering applications, IHC can elucidate the localization of specific collagen types in a construct^{74,362} and characterize the phenotype of neotissue.²

ELISAs can provide highly specific, quantitative determinations of the amount of collagen within a sample. Direct ELISAs employ antibodies against collagen. Similar to the antibodies used for IHC applications, these antibodies are linked to reporter enzymes to enable quantification. Indirect ELISAs use a primary antibody to bind the collagen, followed by a secondary antibody for reporting. Alternatively, sandwich ELISAs determine the quantity of antigen between two antibody layers. The increased amplification of sandwich ELISAs is particularly valuable for samples with low amounts of collagen. Competitive ELISAs involve incubating the antigen with an unlabeled antibody. Then the antibodies are added to wells coated with the antigen. After rinsing, the secondary antibody and the substrate are added. These various ELISA methods provide a versatile array for quantitative collagen assessment.

The convenience and high sensitivity of ELISAs make them the preferred method for quantifying levels of specific collagen types. ELISAs are commonly used to determine the proportions of collagens type I and II in cartilaginous neotissue.^{409,413} The quantitative nature of ELISAs allows collagen levels to be statistically compared among treatment groups.

Electron microscopy

Electron microscopy can provide high resolution images of collagen fibril organization within cartilage. The two most common types are transmission electron microscopy (TEM) and scanning electron microscopy (SEM), both of which create images based on detecting emitted electrons. Electron microscopy has the disadvantage of requiring samples to undergo substantial preparation prior to assessment, affecting the degree to which they retain their original collagen architecture. Samples are typically stabilized by applying an oxidant (e.g., glutaraldehyde) to crosslink proteins. To more easily visualize the fibrils, bound proteoglycans are often removed with a short proteolytic digest.³⁴⁰ Subsequently, heavy salts, such as osmium tetroxide and uranyl acetate, are applied to create contrast. Next, ethanol is used to dehydrate samples prior to embedding and sectioning. Finally, the sample is permeated by a resin and then fixed. This sample preparation process, particularly the dehydration, can distort the structure of the tissue. More recently, rapid freezing has been used to prepare samples for sectioning while avoiding dehydration.¹⁵ Freezing the samples extremely quickly prevents ice crystal formation. Further, cryo-

protectants can be added to reduce the formation of ice crystals during the freezing process.

Analysis of the ultrastructure can be performed in several ways. Analyzing cross-sections of tissue can show fibril diameters and distributions, while serial sectioning can give information about the entire length of the fibril.⁵¹ In embryos, the small size of the fibrils has enabled analysis of entire fibrils, elucidating the fibrillogenesis process.¹⁹⁶ When examining sections, it is important to consider the sections location and orientation within the tissue before drawing conclusions.

- *Scanning electron microscopy (SEM)*

SEM detects electrons that are emitted from the sample surface after the primary electrons interact with the sample. Various studies have employed SEM to examine the orientation and size of collagen fibrils within articular cartilage.^{15,104,106,237,340} SEM has a lower resolution than TEM, but the depth of view is much greater. This enables SEM to provide a more three-dimensional representation of the collagen network. Cryofracture has been used to section the sample in two orthogonal planes and, subsequently, determine more about the three-dimensional collagen organization.¹⁰⁴ Prior to conducting SEM, samples must be coated with a conductive material. This coating, which is typically less than 20 nm thick, does not impair visualization of most collagen fibrils.

- *Transmission electron microscopy (TEM)*

TEM creates images based on electrons that are transmitted through thin sections of a sample. The key advantage of TEM is its high resolution. TEM can show collagen fibril morphology, fibril orientation, and fibril diameter. Furthermore, the high resolution of TEM allows imaging of detailed fibril morphology, such as banding patterns of collagen fibrils.^{267,290,379} The banding patterns indicate how the fibrils have packed together and can vary significantly, even within a single fibril. Although banding patterns reveal important structural information, aspects such as collagen quantity and collagen type provide more functionally relevant information. Many studies have employed TEM to study the collagen within cartilage and fibrils grown in vitro to examine fibril diameter and pericellular matrix organization.^{391,504}

Prior to conducting TEM, samples must be sliced into ultrathin sections approximately 50-100 nm thick. Because fibril organization is on the order of microns, TEM sections can be too thin to show tissue ultrastructure. Furthermore, treatment with heavy salts is sometimes applied to create additional contrast before microscopy. Lead citrate is commonly employed to stain biological samples for TEM. Like other lead based stains, staining intensity is heavily dependent on pH, and the tissue fixation method can also impact the staining intensity.⁴¹⁰ Because the electron density depends primarily on the amount of bound uranyl acetate, the lead is thought to bind mostly to the uranyl acetate.⁹² Additionally, conjugation of antibodies to gold particles can be used to visualize specific macromolecule localization.

Assessing collagen orientation

Polarized light microscopy measures birefringence of the sample to elucidate collagen alignment within cartilage. The polarization angle is a widely used method for quantifying collagen orientation. Additionally, orientation information can be used to infer thickness of the zones within a sample. When light passes through cartilage, it interacts with the valence electrons of collagen.¹⁹ This creates birefringence that can be detected by a polarized light microscope. In general, highly oriented fibers will increase the phase difference between the orthogonal components of light.⁵¹⁶ Collagen orientation is then deduced from the directions of the optical axes at maximal birefringence. The optical retardance, which is linearly proportional to birefringence, can also be used to infer collagen orientation. Thus, larger polarization angles are indicative of the superficial zone, while smaller polarization angles are indicative of the deep zone. Other factors, including size of the fibrils and the sample thickness, can also influence this phase difference.⁵¹⁶ This technique has been used to determine collagen fibril orientation in many studies on both native tissue^{47,516} and tissue engineered constructs.^{142,273}

Magnetic resonance can also be used to deduce the collagen fibril orientation. In particular, diffusion tensor imaging (DTI) has been applied to cartilage tissue.^{125,126,165,335} DTI measures the movement of water molecules, which is related to constraining forces within the matrix.¹²⁵ The collagen distribution within cartilage produces an anisotropic constraint on water, which allows DTI to be used to quantify collagen orientation. DTI has been shown to

reproduce the results of polarized light microscopy,¹²⁵ suggesting that DTI can provide a viable alternative for examining collagen orientation. The non-destructive nature of DTI analysis provides a key advantage. Although DTI is a powerful tool, higher costs have limited its application in the research setting.

Assessing collagen inhomogeneity

Fourier transform infrared spectroscopy (FTIR) involves detecting infrared radiation that is transmitted through a sample, the results of which can be used to quantify collagen distribution. FTIR is used to quantify the collagen content in tissue sections, providing spatial information that bulk assays such as hydroxyproline do not. This spatial resolution shows how collagen content varies with depth and location in a joint. FTIR has been used for examining collagen content in cartilage tissue.^{69,260,282,393} The data FTIR provides have functional implications, such as a correlation between the fibril network modulus and collagen content.²⁶⁰ Similarly, FTIR has been used to show the distribution of collagen in tissue engineered cartilage.³⁹³

Crosslink assessment

Methods are available to examine collagen crosslinking in articular cartilage. The amount of crosslinks can be quantified using high performance liquid chromatography (HPLC). Generally, cartilage samples are first hydrolyzed to free the crosslink residues. Then the solution is passed through an HPLC column that can separate compounds based on factors like charge, size, and polarity. The fluorescence of the eluted sample can be used to quantify the number of crosslinks by excitation/detection at 295/400 nm for pyridinolines and

328/378 nm for pentosidines. Additionally, the specific type of pyridinoline link can be determined from the elution time at peak absorbance. The high sensitivity of HPLC allows detection at the picomolar level.³⁹ More recently, mass spectrometry has been applied to yield more detailed information about crosslinking chemistry, such as glycosylation state.¹⁵⁸ As an indirect measure, lysyl oxidase activity can be used to approximate the extent of crosslinking.^{380,463} Because pyridinoline crosslinks play an important role in the mechanics of cartilage, quantifying them provides a powerful tool for assessing neotissue.

Summary

A wide variety of methods enable study of the structure and composition of collagen within cartilage samples. Techniques like IHC and histological staining can qualitatively verify the presence of collagen, which can be quantified using methods such as hydroxyproline assays and ELISAs. Electron microscopy provides information about the collagen distribution and orientation, but requires extensive sample preparation. For examining collagen orientation, traditional polarized light microscopy has been complemented by newer methods such as DTI. Additionally, HPLC can quantify the number of crosslinks, providing more information about the structure of the collagen network. Collectively, these methods can thoroughly characterize collagen within both native tissue and engineered cartilage.

Role of collagen in articular cartilage tissue engineering

Significance of collagen in tissue engineering

To produce functional cartilage constructs, tissue engineering efforts will likely need to recapitulate the collagen network of native tissue. Because the matrix plays an important role in providing mechanical integrity, it is necessary to reproduce a collagen network with appropriate composition, orientation, and crosslinking. Despite various strategies, including scaffolds, biochemical agents, and mechanical stimulation, tissue engineered constructs generally have significantly less collagen than native tissue.^{90,176,267,329,477,504} This lack of collagen is problematic because it compromises the mechanical integrity of the tissue.

Engineering the collagen network

- Collagen scaffolds for tissue engineering

Collagen has been employed as a biomaterial scaffold to promote cartilage engineering due to its natural biocompatibility, porosity, and low immunogenicity. Collagen matrices have also been found to have the proper molecular cues to stimulate collagen production.¹⁹⁷ The prevalence of collagen in the articular cartilage matrix makes collagen particularly attractive for cartilage tissue engineering applications; however, as with many natural biomaterials, collagen poses a risk for pathogen transmission. In particular, concerns have been raised about the increased frequency of prion diseases, which may be associated with collagen scaffolds.³²⁴

Despite this concern, several tissue engineering studies have examined the potential of collagen scaffolds for articular cartilage tissue engineering. Much of this work has examined chondrocytes seeded on collagen scaffolds¹⁸¹ or crosslinked collagen sponges.⁴¹⁵ Canine chondrocytes seeded on collagen II retained their chondrocytic phenotype more than cells seeded on collagen I, which is expected considering the predominance of collagen II in articular cartilage.³⁶⁰ Collagen scaffolds have been shown to increase collagen synthesis more than other common biomaterials, such as copolymers of lactic acid and glycolic acid.¹⁹⁷ To more closely replicate the cartilage matrix, collagen has been combined with other matrix molecules (e.g., GAGs).³⁷² In addition to extensive *in vitro* work, various *in vivo* studies have been conducted with collagen scaffolds, including rabbit,^{89,476} dog,^{360,361} and horse⁴²⁴ models. Similar to many other tissue engineering strategies, collagen scaffolds promote chondrocyte phenotype and matrix production without attaining native mechanical properties. For example, mesenchymal stem cells seeded on collagen gels implanted in rabbit osteochondral defects promoted hyaline cartilage formation, but failed to reproduce tissue with native mechanical values.^{89,476}

- Collagen content

Culture conditions often have a profound impact on collagen production. As summarized in Table 5-II, mechanical stimulation can be used to increase the collagen content of neotissue. For example, direct compression has been shown to increase collagen deposition.^{332,387} Hydrostatic pressure has also been shown to increase collagen gene transcription,⁴⁵⁰ collagen production,²³² and construct

tensile properties.¹⁴³ Other conditions, like cell density,^{409,492} scaffold porosity,⁵⁰⁸ and cell source,^{36,478} also modulate collagen production.

Tissue engineering studies have shown localization of collagen VI in the pericellular space. Human and bovine articular chondrocytes cultured *in vitro* exhibited chondron structures in regions displaying characteristics of hyaline cartilage.¹⁷⁵ Furthermore, confocal microscopy has shown that cultured chondrocytes sequestered type VI collagen in the pericellular space.⁹⁶ In self-assembled constructs, collagen VI localized to the pericellular region within four weeks.³⁷⁵ Type VI collagen also accumulated uniformly around cells embedded in agarose, with the rate of deposition slowing after the second week. The production of the pericellular matrix may actually be excessive in some constructs, as agarose embedded chondrocytes have exhibited collagen VI expression levels 400% higher than native values.¹³¹

Exogenous application of bioactive agents also can be used to increase collagen content. For bovine articular chondrocytes, IGF-1 increased collagen gene expression and deposition,¹²² but it did not impact the number of crosslinks.²⁵⁷ Further, TGF- β 1 promoted collagen fibril formation⁴⁵⁵ and increased the collagen weight fraction.⁵⁶ Many of the bone morphogenetic proteins (BMPs), which are part to the TGF- β superfamily, have also been shown to promote collagen synthesis. For instance, BMP-2⁴⁴⁹ and BMP-7¹⁷⁰ have been employed to increase collagen deposition. Recently, small proteoglycans in tissue engineered constructs have been shown to decrease collagen deposition. By knocking out the small leucine rich proteoglycan lumican, there was increased

collagen II deposition and increased fibril diameters.²⁶⁷ Adding various bioactive molecules, individually and in combinations, provides many opportunities for altering collagen content.

Despite many studies that demonstrate the role of growth factors, the responses to a growth factor is often difficult to predict. This is particularly true with members of the TGF- β superfamily, which have been shown to increase or decrease collagen deposition depending on the experimental system.^{56,172,182,257,397} In addition to the variation in culture systems, the developmental stage of the cell,^{206,468} zone of cell source,¹²² and the amount of ECM already deposited³⁹⁷ also influence the response to the growth factor. Synergism between growth factors can also alter their impact.¹⁴⁵ The complexity of the growth factor response makes it difficult to generalize an optimal treatment regimen.

- Crosslinking

Studies have shown that crosslinks are generally less common in tissue engineered constructs than in native tissue. For six week culture of bovine chondrocytes in a rotating bioreactor, the number of crosslinks was only 30% of native values.⁴¹³ Similarly, after four weeks of alginate bead culture, crosslinks reached only 22% of native values.⁴⁴ The inability to fully produce crosslinks in tissue engineered constructs presents a necessary area for improving tissue engineering efforts. The number of crosslinks has been found to depend on the cell source, with more crosslinks formed in constructs from full thickness cell sources compared to middle or deep zone sources.⁴⁷⁸

Various small molecules can be employed to modulate collagen crosslinking. For example, BAPN inhibits lysyl oxidase, thereby decreasing the extent of crosslinking. BAPN treatment of cartilage explants decreased tensile integrity, without altering the amounts of collagen or GAGs.²² For bovine chondrocytes cultured on alginate beads, administering BAPN reduced the amount of collagen near chondrocytes and increased collagen synthesis.⁴⁴ In another study, chondrocytes seeded on alginate beads and treated with BAPN for the first five weeks of a ten week culture exhibited increased collagen content and increased stiffness.⁴²

In contrast to inhibition, several agents can be added to increase crosslinking. Oxidative agents can be used to increase collagen crosslinking, but these compounds are not specific like lysyl oxidase. The major disadvantage of commonly used crosslinking chemicals (e.g., glutaraldehyde) is cytotoxicity. Genipin, an extract from the gardenia plant, has recently been explored as a crosslinking agent. Applying genipin to bovine articular cartilage¹⁴⁸ and human intervertebral discs¹⁰³ did not result in increased cytotoxicity, but did increase the mechanical integrity of the tissue. Alternatively, adding sugars increased collagen crosslinking by inducing AGE formation.^{98,474} Finally, though not in cartilage, applying exogenous lysyl oxidase to tissue engineered vascular constructs increased their tensile strength and elastic modulus.¹⁴¹ Interestingly, collagen crosslinks can also contribute to compressive properties, such that the proportion of mature to immature crosslinks correlated with the equilibrium modulus in unconfined compression.²⁷⁰

- Network organization

Engineering the anisotropic distribution of collagen poses another significant challenge. As a step forward, radial confinement of self-assembled constructs increased collagen organization perpendicular to the articular surface.¹⁴² In addition to confining constructs, it is possible to control the cell distribution within neotissue and, consequently, alter collagen distribution. For example, creating anisotropic pore architecture within a scaffold produced by 3D fiber deposition created zonal variation in collagen composition.⁵⁰⁸ However, this approach produced collagen levels an order of magnitude less than native tissue.

The bacterially-derived enzyme chondroitinase-ABC (C-ABC) has also been used to alter the cartilage matrix. C-ABC selectively degrades GAGs, which subsequently reduces the stress on the collagen network. C-ABC application has been shown to increase the tensile integrity of cartilage explants.²¹ C-ABC has also been used to increase tensile properties of self-assembled tissue engineered articular cartilage.³⁵⁸ Although the mechanism by which it increases tensile properties has not been characterized, it is possible that the reduced GAG content promotes crosslinking, larger fibril size, or altered fibril orientation.

Summary

Reproducing a collagen network in tissue engineered articular cartilage constructs with appropriate composition, crosslinking, and organization has proven to be a difficult task. Several strategies, including mechanical stimulation and growth factor application, have been employed to alter the collagen composition of neotissue with some success. In general, crosslinks are less

common in engineered neotissue than in native tissue. Although exogenous oxidative agents can increase crosslinking, these crosslinks are not specific like lysyl oxidase mediated crosslinking. Ultimately, it will be necessary to develop improved methods for engineering network crosslinking and organization before neotissue replicates the structure of native cartilage. By further studying the collagen network in both native tissue and engineered cartilage, it will be possible to improve the quality of tissue engineered cartilage.

Conclusions

Collagen forms a complex network within articular cartilage. The major component is the heterofibril of collagens II, IX, and XI. These fibrils are organized inhomogeneously and anisotropically within cartilage and provide mechanical integrity to the tissue. Various theoretical and computational models of cartilage biomechanics have been developed, but incorporating microstructural analyses will help improve these efforts. To better understand factors affecting the collagen network, many experimental methods are available. It is possible to readily assess the composition, crosslinking, and structure of the collagen network.

Successful articular cartilage tissue engineering will need to produce an appropriate collagen network. Studies have shown that tissue engineered cartilage generally lacks sufficient collagen, a problem that will need to be addressed. Cartilage tissue engineering studies have primarily examined the amount of collagen, with fewer studies assessing collagen type, crosslinks, or fibril orientation. By overlooking these aspects, many tissue engineering studies

do not elucidate the mechanisms that underlie observed changes in mechanical integrity. Furthermore, the interactions between collagen, proteoglycans, and chondrocytes need to be studied more extensively. Understanding properties and interactions of the collagen network will enable more robust constructs to be developed, and will subsequently improve the functionality of tissue engineered articular cartilage.

Table 5-I: Zonal variation in collagen fibril characteristics, collagen content, and mechanical properties

Characteristic/Property	Superficial zone	Deep zone
Fibril diameter ²⁹⁸	34 nm	55 nm
Fibril orientation	Parallel	Perpendicular
Collagen volume fraction ⁵¹⁵	16-31%	14-42%
Tensile modulus ³⁴⁹	15.6 - 42.2 MPa	1.1 - 2.6 MPa
Confined compressive modulus ^{97,100}	0.27 - 1.16 MPa	0.71 - 7.75 MPa

Table 5-II: Select studies showing effects of mechanical stimulation on collagen in tissue engineered cartilage

Stimulation	Effect on collagen
Shear ³³²	37% increased deposition
Direct compression ³⁸⁷	300% increased deposition
Hydrostatic pressure ²³²	17% increased deposition, 9 fold increase in type II mRNA

Figure 5-1: Hierarchical structure of a collagen fiber

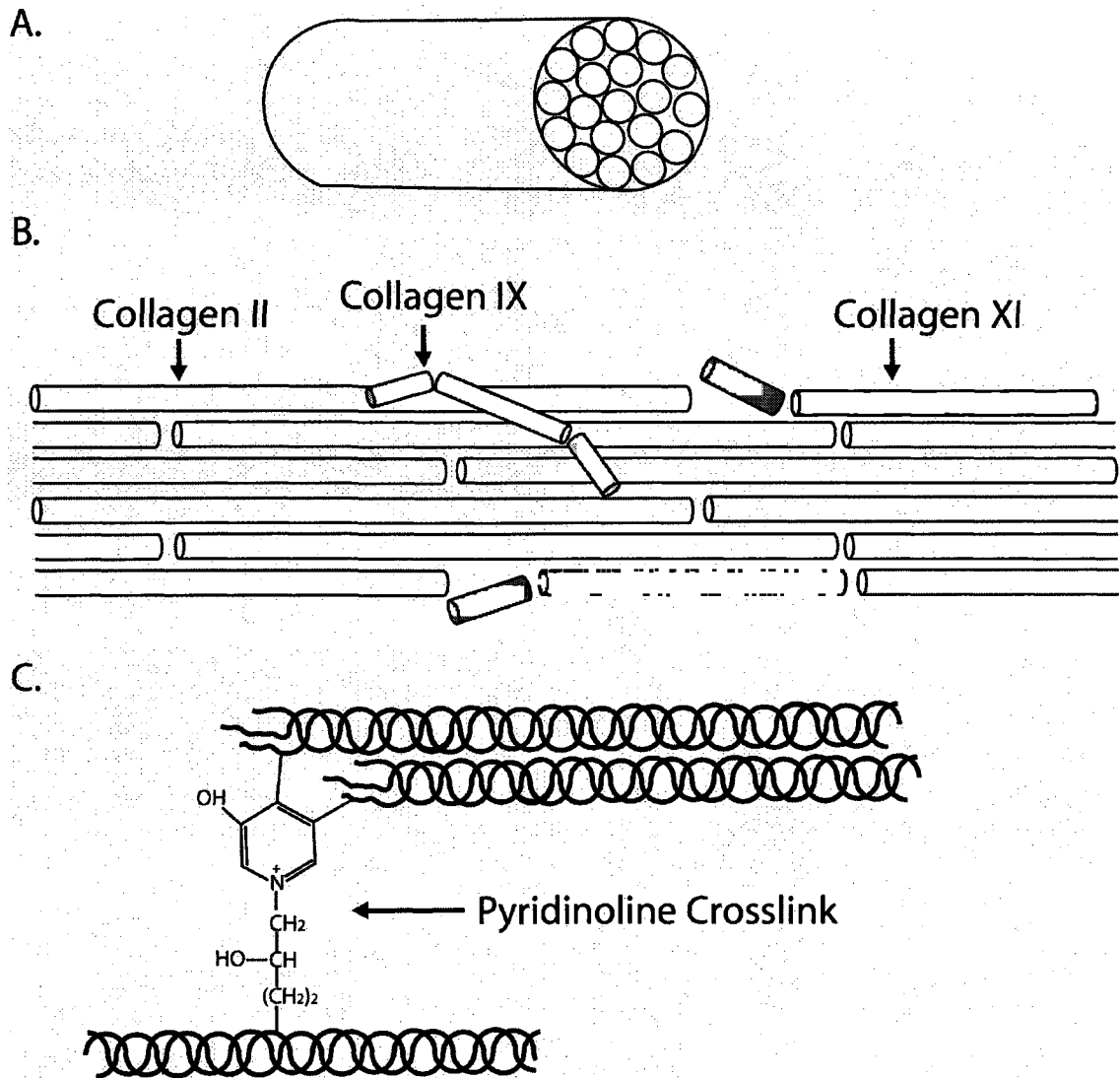


Figure 5-1. Hierarchical structure of a collagen fiber. A) A collagen fiber. A fiber is a collection of many fibrils. B) The collagen II:IX:Xl heterofibril. The fibril is formed by end-to-end and lateral fusion of collagen molecules. C) The basic triple helix structure of the collagen type II molecule. Shown out-of-scale is the molecular structure of a pyridinoline crosslink.

Figure 5-2: Development of tissue-level collagen anisotropy

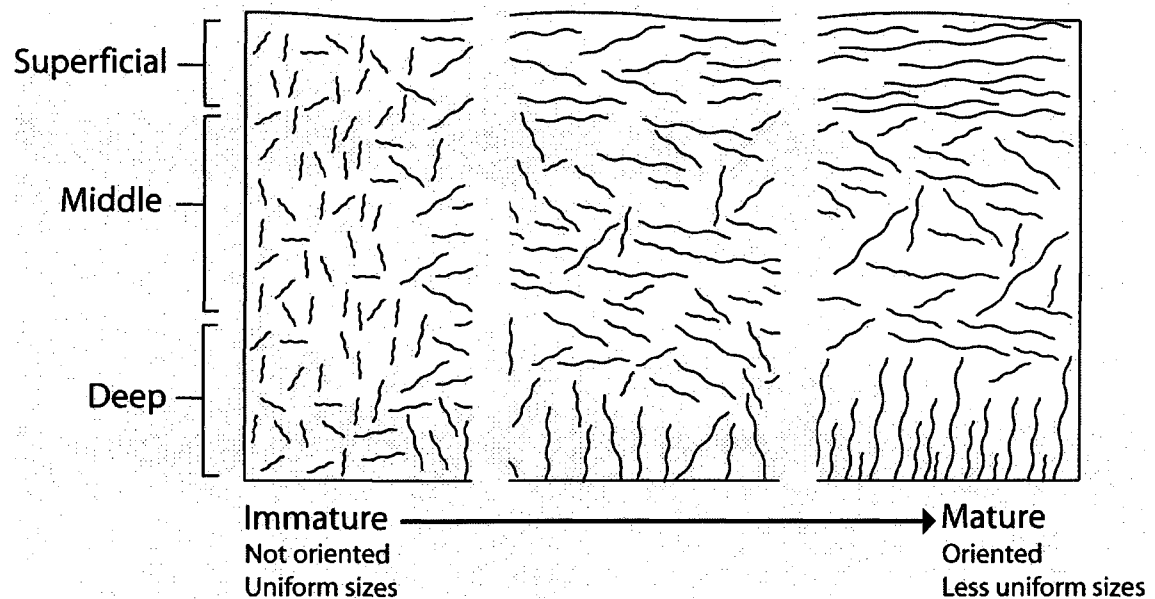


Figure 5-2. Schematic representation of how the anisotropic arrangement of collagen within articular cartilage develops over time. Immature tissue is composed of randomly oriented fibers of roughly uniform size. As the tissue matures, the characteristic collagen orientation begins to emerge. Mature tissue has horizontally oriented fibers in the superficial zone, randomly oriented fibers in the middle zone, and vertically oriented fibers in the deep zone. Mature tissue is also composed of fibers less uniform in size.

Figure 5-3: Split-lines

Figure 5-3. Demonstration of split-lines in articular cartilage covering the proximal ulna of a mature cow. Split-lines show the orientation of collagen fibers in the superficial zone. A small round pin was dipped in black ink and gently pressed into the tissue. The ink stains in the direction parallel to collagen fibers. In this picture, split-lines are running from upper left to lower right. The image was taken on a Leica MZ6 dissection scope at 4X magnification.

Figure 5-4: Mechanical models of articular cartilage incorporating collagen

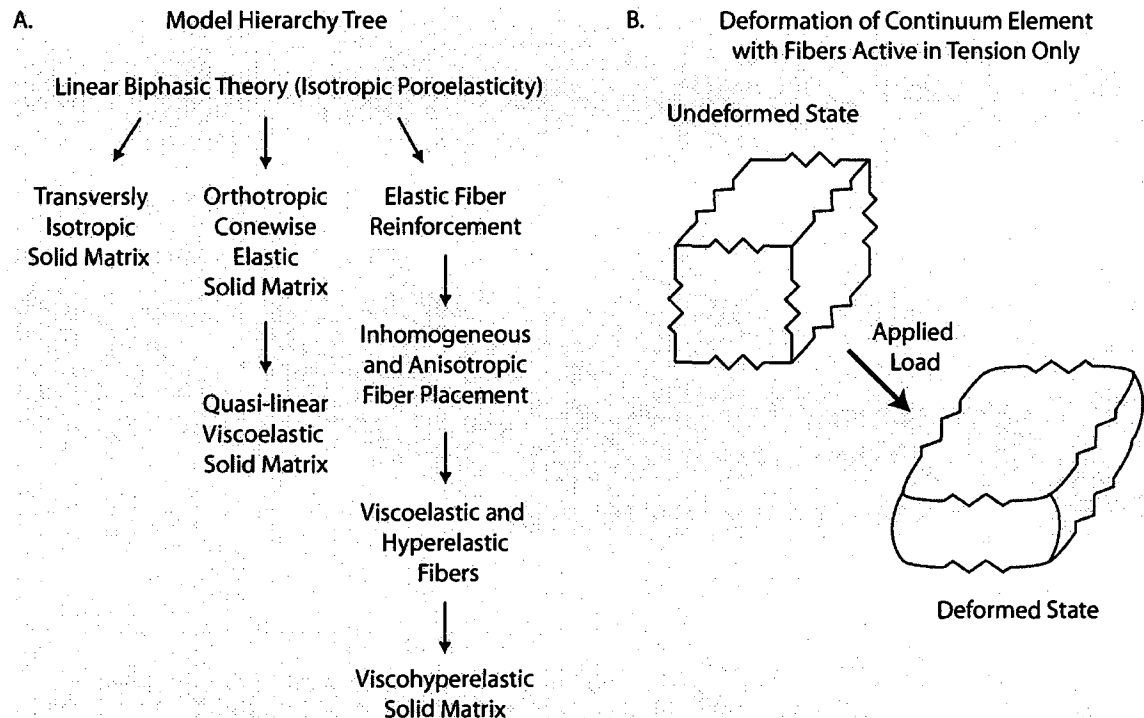


Figure 5-4. A) Hierarchy tree for models of articular cartilage incorporating features of the collagen network. The basic model is the linear biphasic theory. As one moves down the branches, the models become more complex. Each level incorporates all of the features from models above it. The most developed branch is fiber reinforcement. B) Illustration of a fiber reinforced continuum element with fibers active in tension only. An applied load causes compression of the continuum element. Members in compression are not supported by the fibers (hence the springs have been removed).

Chapter 6: Chondroitinase ABC treatment results in increased tensile properties of self-assembled tissue engineered articular cartilage*

Abstract

Compared to glycosaminoglycan (GAG) content and compressive properties, collagen and tensile properties of engineered articular cartilage have remained inferior. Based on a cartilage explant study showing increased tensile properties following chondroitinase ABC (C-ABC) treatment, C-ABC was investigated as a strategy for cartilage tissue engineering. A scaffold-less approach was employed, wherein chondrocytes were seeded into non-adherent agarose molds. C-ABC was used to deplete GAG from constructs 2 weeks after initiating culture, followed by 2 weeks culture post-treatment. Staining for GAG and type I, II, and VI collagen, quantitative total collagen, type I and II collagen, and sulfated GAG content, and compressive and tensile mechanical properties were evaluated. At 4 weeks, C-ABC treated construct ultimate tensile strength and tensile modulus increased 121% and 80% compared to untreated controls, reaching 0.5 and 1.3 MPa, respectively. This was accompanied by increased type II collagen concentration, without type I collagen. As GAG returned, compressive stiffness of C-ABC treated constructs recovered to be greater than 2 week controls. C-ABC represents a novel method for engineering functional articular cartilage by departing from conventional wisdom of employing anabolic

*Chapter under review at *Tiss Eng Part A* as Natoli RM, Revell CM, and Athanasiou KA, "Chondroitinase ABC Treatment Results in Increased Tensile Properties of Self-Assembled Tissue Engineered Articular Cartilage," August 2008.

signals. These results may be applicable to other GAG producing tissues functioning in a tensile capacity, such as musculoskeletal fibrocartilages.

Introduction

Tissue engineering replacement therapies depend on the regeneration of functional tissue.⁸⁵ While the classical paradigm of a scaffold, cells, and positive biochemical or biomechanical stimulation has led to advancements in tissue engineering, significant limitations still exist. One important limitation is engineering tissue that has mechanical properties on par with native values, such that an implanted construct could function under *in vivo* loads. With respect to articular cartilage, several groups have been able to achieve compressive properties and sulfated glycosaminoglycan (sGAG) content spanning native values using scaffolds.^{42,369,481} However, a challenge in all current articular cartilage tissue engineering strategies is obtaining collagen content and tensile properties that approach native values.³⁶⁹

A potential limitation inherent in the classical approach may be the use of scaffolds, as scaffolds pose potential problems such as stress-shielding, toxicity of degradation products, altering cellular phenotype, and initiation of inflammatory or foreign body responses.^{14,31,177,231,520} Another complication may be the interpretation of the biomechanical properties of tissue engineered constructs, as the remaining biomaterial may contribute to the measured properties. Our laboratory has recently developed a scaffold-less self-assembly approach for articular cartilage tissue engineering,²³¹ which has been enhanced through serum-free and confinement methods.¹⁴² Using this system, we have

also engineered constructs with sGAG content and compressive properties in the range of native values, due solely to the neo-tissue.

Work with cartilage explants has shown that *in vitro* growth of immature cartilage results in an imbalance of sGAG to collagen compared to the *in vivo* situation, resulting in decreased tensile properties.^{494,495} Furthermore, recent work in a cartilage explant model demonstrated that sGAG removal with chondroitinase ABC (C-ABC), followed by 2 weeks of subsequent culture, resulted in sGAG repletion and significant increases in tissue tensile modulus and ultimate tensile strength.²¹ The authors suggested that a sGAG imbalance causes pre-stress in the collagen network which prevents optimal function, a concept supported theoretically.⁴²⁹ As the collagen network is the main contributor to tensile properties, its proper control and balance within the proteoglycan gel are paramount for tensile function.^{42,401}

C-ABC is a well studied bacteria-derived enzyme that cleaves the sGAG side chains chondroitin and dermatan sulfate, as well as hyaluronic acid.^{128,394} It has been used extensively to study GAG biology,^{178,326,425} the contribution of extracellular matrix (ECM) components to tissue mechanical properties,^{286,297,412,428} and cartilage integration into defects.^{240,258,304} Therefore, following the above discussion, it stood to reason that C-ABC could be used for tissue engineering articular cartilage. As such, we chose to apply C-ABC to developing engineered constructs to cause an initial depletion of sGAG, with the hypothesis that tensile material properties would increase without permanently compromising compressive properties, ultimately leading to a more mature neo-

tissue. Moreover, we expected the tensile properties to reflect collagen content, and that collagen type I would be absent.

Materials and methods

Chondrocyte isolation, self-assembly, and culture

Bovine chondrocytes were isolated and self-assembled as previously described.^{142,231} Briefly, tissue isolated from the distal femur and patellofemoral groove of three 1 week old male calves (Research 87, Boston, MA) was digested in collagenase type II (Worthington Biochemical Corp., Lakewood, NJ) for 24 hrs. Cells were collected, counted with a hemocytometer, and frozen at -80° C. After thawing, cells were again counted and assessed for viability, before being seeded in 5 mm diameter non-adherent, cylindrical wells made of 2% agarose. Into each well, 5.5 million live cells were seeded in 150 μ L media, followed by an additional 350 μ L of culture medium 4 hrs later. Each construct was allowed to sit undisturbed for the next 20 hrs, during which the cells coalesced into free-floating constructs. A full media change was then performed. Chemically defined medium consisting of DMEM with 4.5 mg/mL glucose and L-glutamine (Biowhittaker/Cambrex, Walkersville, MD) 100 nM dexamethasone (Sigma, St. Louis, MO), 1% fungizone, 1% penicillin/streptomycin, 1% ITS+ (BD Scientific, Franklin Lakes, NJ), 50 μ g/mL ascorbate-2-phosphate, 40 μ g/mL L-proline, and 100 μ g/mL sodium pyruvate (Fisher Scientific, Pittsburgh, PA) was used throughout the study. The 500 μ L of media in each well were changed daily throughout the experiment, and all culture took place at 37°C, 10% CO₂.

At 2 weeks, all constructs were unconfined¹⁴² and transferred to tissue culture plates having only the bottom of the wells coated with a thin layer of agarose. Half of the constructs were randomly assigned to be treated with protease-free C-ABC (Sigma) at an activity of 2 U/mL media for 4 hrs at 37°C.²¹ Following treatment, constructs were thoroughly washed five times with 400 μ L of fresh media. Half of the treated constructs were returned to culture for two additional weeks, while the other half, along with untreated controls, were immediately processed for histology, quantitative biochemistry, and mechanical testing. From culture, constructs were photographed, weighed wet, and portioned for analysis. From the construct's center a 3 mm diameter punch was taken for creep indentation. The remaining outer ring was halved for biochemistry and tensile testing. Histology and immunohistochemistry (IHC) samples were prepared from additional constructs.

Gross morphology, histology, and IHC

Construct diameter was measured using ImageJ (National Institutes of Health, Bethesda, MD). For histology, constructs were cryoembedded and sectioned at 14 μ m. Samples were fixed in 10% phosphate buffered formalin and stained with Safranin O/fast green to examine GAG distribution and picrosirius red to look at collagen distribution. For IHC, after fixing with chilled acetone, slides were rinsed with IHC buffer, quenched of peroxidase activity with hydrogen peroxide/methanol, and blocked with horse serum (Vectastain ABC kit, Vector Labs, Burlingame, CA). Sections were then incubated with either mouse anti-collagen type I (Accurate Chemicals, Westbury, NY), rabbit anti-collagen type II

(Cedarlane Labs, Burlington, NC), or rabbit anti-collagen type VI (US Biological, Swampscott, MA). The secondary antibody (anti-mouse or anti-rabbit IgG, Vectastain ABC kit) was then applied, and color was developed using the Vectastain ABC reagent and DAB (Vectastain ABC kit). In addition to IHC staining of the experimental groups, bovine articular cartilage was used as a positive control for collagens type II and VI and as a negative control for type I collagen. As an additional negative control, tissue was stained as described above, but without application of the primary antibodies. Slides were examined with a light microscope.

Biochemical analysis

Samples were frozen overnight and lyophilized for 48 hrs, after which dry weights were obtained. Samples were re-suspended in 0.8 mL of 0.05 M acetic acid containing 0.5 M sodium chloride. To this suspension, 0.1 mL of a 10 mg/mL pepsin (Sigma) solution in 0.05 M acetic acid was added, and the suspension was mixed at 4°C for 96 hrs. Next, 0.1 mL of 10x Tris-buffered saline (TBS) buffer was added along with 0.1 mL pancreatic elastase (1 mg/mL dissolved in 1x TBS buffer). This suspension was mixed at 4°C overnight. This digestion protocol allows collagen epitopes to be preserved for ELISA. Following this protocol, no residual construct remained. From the digest, total cell number was determined with the Quant-iT™ PicoGreen® dsDNA Assay Kit (Invitrogen, Carlsbad, CA) assuming 7.8 pg DNA per cell.²⁷⁹ sGAG content was tested using the Blyscan™ Sulfated GAG Assay kit, which is a 1,9-dimethyl-methylene blue colorimetric assay (Accurate Chemical and Scientific Corp., Westbury, NY).

Additionally, post hydrolyzation of the digest by 2 N NaOH for 20 min at 110°C, samples were assayed for total collagen content using a chloramine-T hydroxyproline assay.⁵⁰³ SIRCOL collagen assay standard (Accurate Chemical, Westbury, NY) was used, such that the standard curve was reflective of collagen amount, eliminating the need to convert from hydroxyproline to collagen. ELISA for collagens type I and type II was performed per the manufacturer's protocol (Chondrex, Redmond, WA).

Creep indentation testing

Compressive mechanical properties were determined by creep indentation testing assuming a linear biphasic model,³⁴⁷ which determines the specimen's aggregate modulus, Poisson's ratio, and permeability. A creep indentation apparatus was used to determine the compressive creep and recovery behavior of the constructs.³⁰ Each sample was attached to a flat stainless steel surface with a thin layer of cyanoacrylate glue and equilibrated for 20 min in phosphate buffered saline. The sample was then placed into the creep indentation apparatus, which automatically loaded and unloaded the specimen while recording the tissue's creep and recovery behavior. A tare load of 0.2 g, followed by a test load of 0.7 g, was applied to all but the 2 week C-ABC treated samples with a 1 mm diameter, flat-ended, porous, rigid tip. The 2 week C-ABC treated samples were loaded with a tare of 0.05 g and test of 0.27 g due to excessive deformation resulting when these specimens were tested with the other loads. All loads were applied until equilibrium was reached. Specimen thickness was

measured using a micrometer. To calculate the specimen's material properties, a semi-analytical, semi-numeric, linear biphasic model was used.³⁴⁸

Tensile testing

Samples were cut into a dog-bone shape and affixed to paper tabs for gripping.³⁵ A micrometer was used to obtain gauge length, thickness, and width measurements for each sample. Tensile tests were performed to failure at a strain rate of 0.01 s^{-1} of gauge length on an electromechanical materials testing system (Instron Model 5565, Canton, MA). The apparent Young's modulus (E_Y) was determined by least squares fitting of the linear region of the stress-strain curve. The ultimate tensile strength (UTS) reported was the maximum stress reached during a test. All specimens failed inside the gauge length.

Statistical analysis

Five to seven samples were used for each of the four experimental groups, where the groups consisted of 2 and 4 week control and C-ABC treated constructs. For all assays, a 1-way ANOVA was run. If significance ($p < 0.05$) was found, a Student-Newman-Keuls post-hoc test was performed. As mentioned above, separate constructs were used for histology and IHC. All data are presented as mean \pm S.D.

Results

Gross characteristics

All constructs appeared hyaline-like (Fig. 6-1 A,F,K,P). Table 6-I shows growth characteristics of the constructs. For each metric (thickness, diameter,

and total wet weight), each group was significantly different from all others. C-ABC treatment resulted in an immediate and significant decrease in all of these parameters, but these effects did not negatively affect subsequent growth. Both control and C-ABC treated groups had substantial increases in thickness, diameter, and total wet weight between 2 and 4 weeks.

Histology and IHC

Following treatment with C-ABC, GAG staining was lost from the construct, but staining returned at 4 weeks (Fig. 6-1 B,G,L,Q). Collagen staining via picrosirius red showed diffuse collagen presence throughout the constructs in all groups. Examination of these slides with polarized light microscopy showed no preferential collagen orientation. There was no collagen type I staining found in any group with IHC (Fig. 6-1 C,H,M,R). In contrast, both collagen type II and type VI staining was diffuse throughout the constructs for all groups (Fig. 6-1 D,I,N,S and E,J,O,T).

sGAG content, cell number, and percent water

C-ABC treatment removed all the sGAG from the constructs, but there was robust sGAG repletion between 2 and 4 weeks. Controls also experienced an increase in sGAG from 2 to 4 weeks (Fig. 6-2A). In this figure, total sGAG content is normalized to the constructs' wet weights. Each group was significantly different from all others. Immediately following C-ABC treatment, constructs had significantly more DNA per construct than the other groups. Controls at 2 weeks, and both control and C-ABC treated constructs at 4 weeks, had similar DNA content reflective of the number of cells initially seeded. Cell numbers were $5.5 \pm$

0.3, 6.9 ± 0.8 , 5.8 ± 0.6 , and 5.0 ± 0.4 million cells for the 2 week control, 2 week C-ABC treated, 4 week control, and 4 week C-ABC treated groups, respectively. The 4 week C-ABC treated group contained $80 \pm 1\%$ water, which was significantly less than the 4 week control ($83 \pm 1\%$) and 2 week control ($84 \pm 3\%$) groups. Percent water for the 2 week C-ABC treated group was unobtainable because dry weights of these constructs were below the limits of our balance.

Total collagen and collagens type I and type II ELISAs

At 2 weeks, total collagen per wet weight as measured by hydroxyproline was significantly greater in the C-ABC treated group compared to all other groups. Total collagen per wet weight measured $12\% \pm 1.0\%$, $38\% \pm 8.5\%$, $8.1\% \pm 0.9\%$, and $11\% \pm 2.2\%$ for the 2 week control, 2 week C-ABC treated, 4 week control, and 4 week C-ABC treated groups, respectively. The large value immediately following treatment can be attributed to the significant decrease in wet weight of this group due to sGAG removal and loss of its associated water. With respect to type II collagen, each group was significantly different from all others (Fig. 6-3), with the 4 week C-ABC treated group having the most type II collagen per wet weight. Type II collagen was 65 and 61% of the total collagen for the 4 week control and C-ABC treated groups, respectively, which is similar to other articular cartilage tissue engineering efforts.^{273,413} There was no type I collagen detected by the ELISA.

Biomechanics

Figure 6-2B shows the aggregate modulus, a measure of compressive stiffness, obtained from creep indentation testing. At 2 weeks the aggregate

modulus of control constructs was significantly greater than the C-ABC treated constructs, reflecting the removal of sGAGs. The remaining stiffness (22 kPa) reflects the unique contribution of collagen to the compressive stiffness. Stiffness increased over 2 weeks of subsequent culture in both groups. Permeability was significantly increased in the 4 week control group ($84 \pm 64 \times 10^{15} \text{ N/m}^4\text{s}$) compared to all other groups. The other groups' permeabilities were $24 \pm 14 \times 10^{15}$, $16 \pm 0.7 \times 10^{15}$, and $29 \pm 0.7 \times 10^{15} \text{ N/m}^4\text{s}$ for the 2 week control, 2 week C-ABC treated, and 4 week C-ABC treated groups, respectively. Poisson's ratio was significantly decreased in the 2 week C-ABC treated group (0.02 ± 0.02) compared to all other groups. The other groups' Poisson's ratios were 0.22 ± 0.12 , 0.17 ± 0.09 , and 0.12 ± 0.09 for the 2 week control, 4 week control, and 4 week C-ABC treated groups, respectively.

Figure 6-4 shows results from construct tensile testing. At both 2 and 4 weeks UTS was significantly increased in the C-ABC treated groups. The apparent Young's modulus (E_Y) of the 4 week C-ABC treated group was significantly greater than all other groups. At 4 weeks, UTS of the C-ABC treated group was increased 121% from the control and E_Y increased 80%.

Discussion

The results of this study show that, with 2 weeks of culture following a one time C-ABC treatment of developing tissue engineered articular cartilage constructs, tensile properties were increased by 80 and 121% for the apparent Young's modulus and ultimate tensile strength, respectively. Type II collagen concentration was increased at 4 weeks in the C-ABC treated groups compared

to no treatment, though total collagen concentration was not significantly different. The increase in tensile properties could be due to increased collagen concentration, increased fibril diameter, increased crosslinking in the collagen network, or some combination of these factors, though only the first was assessed in this initial study. Further, sGAGs returned, and the compressive stiffness of treated constructs recovered to be greater than 2 week controls. These results mirror the findings of Asanbaeva et al.,²¹ which showed sGAGs returned and tensile properties increased following C-ABC treatment in a serum-based culture of cartilage explants. In that work, it was suggested that C-ABC treatment causes maturational growth of the tissue that parallels the *in vivo* situation and contrasts with expansive growth characteristic of *in vitro* culture. This study extends that work to tissue engineering in a scaffold-less, serum-free system. Furthermore, our results add compressive testing and collagen profiling, and suggest that maturational and expansive growth phases could be a framework for discussing articular cartilage tissue engineering studies.

It has been noted that low levels of collagen are associated with poor mechanical properties in most cell-seeded grafts for cartilage repair.^{267,504} To that end, several recent reports have examined potential methods for increasing collagen content or enhancing the collagen network specifically. In one study, chondrocytes seeded in hydrogels were treated with β -aminopropionitrile (BAPN), a collagen crosslinking inhibitor. It was shown that collagen fibril diameter, collagen concentration, and gene expression of cartilage specific collagens were significantly increased with BAPN treatment, though specific

protein level assessment of type I collagen was not performed.⁵⁰⁴ Another study demonstrated BAPN treatment of chondrocytes in alginate beads increased collagen amount, allowed crosslink formation, and increased compressive properties. Though some type I collagen was found, the authors contend chondrocyte phenotype was not adversely affected.⁴² Finally, Ng et al.³⁶⁹ supplemented the culture media of chondrocytes in agarose with collagen hydrosylate, due to its potential collagen type II stimulatory effect,³⁷⁴ but ultimately concluded it was not a viable long-term method for improving collagen content. The positive functional outcome and absence of type I collagen in the present study (as collagen I would suggest a shift in chondrocyte phenotype) suggest C-ABC could be an additional methodology for enhancing the collagen network in tissue engineered articular cartilage.

The biomechanical properties are the macroscopic functional representation of the tissue's underlying structure and biochemical content.^{286,401,428,429} The immediate effects of C-ABC on compressive properties and tensile strength measured in this study reflect this fact. Removal of the sGAGs resulted in an immediate decrease in compressive stiffness, since the significant decrease in fixed charge density reduces the construct's ability to support compressive load.^{205,412} The return of sGAGs at 4 weeks reflects recovery of the compressive stiffness. It has been demonstrated that the interaction of growth factors and proteoglycans can influence matrix development.¹⁶⁴ The robust sGAG repletion may be explained by the fact that chondroitin sulfate is also known to bind growth factors.³⁵⁶ Thus, once

chondroitin sulfate is removed, any endogenously produced growth factor would be available for binding its cellular receptor, as opposed to becoming bound in the developing matrix. The low Poisson's ratio seen in the 2 week C-ABC treated group may be associated with the high total collagen concentration, as Kiviranta et al.²⁸² have shown that increased collagen content correlates with a decreased Poisson's ratio in bovine articular cartilage explants. Furthermore, increased tensile strength upon sGAG depletion reflects the fact that the collagen network could become more organized upon removal of pre-stress.^{428,429}

Notably, the apparent Young's modulus at 4 weeks was significantly greater in the C-ABC treated group compared to control, and the increase in tensile strength observed immediately post treatment with C-ABC remained at 4 weeks, despite the sGAGs returning. If equal amounts of sGAG generate similar pre-stress, the fact that more sGAG and greater tensile properties are seen at 4 weeks in the C-ABC treated group compared to the 2 week controls indicates that the removal of pre-stress is not the only contribution to the increase in tensile properties. Hence, the increase in tensile properties at 4 weeks is not purely a mechanical phenomenon. An interesting biological possibility comes from the recent work of Kafienah et al.,²⁶⁷ which showed lumican protein levels were increased in engineered cartilage, and knocking down lumican expression led to increased type II collagen accumulation and increased collagen fibril diameter. It may be that C-ABC causes a temporary decrease in lumican by freeing it from the matrix post-treatment. The present study also saw a significant increase in type II collagen per wet weight (~1.3 fold compared to control at 4 weeks), which

may partially explain the increased tensile properties. Moreover, the change in type II collagen was similar in magnitude to the increase in total collagen per wet weight (~1.4 fold). It makes sense that the material properties (parameters normalized to material size) would follow biochemical properties also normalized to a measure of material size (wet weight in this case).

While increased type II collagen concentration is one possible biological explanation, other types of collagen or increased collagen crosslinking may be responsible for the increase in tensile properties. If we consider for a moment the collagen network as a polymer, then, based on the theory of rubber elasticity, an increased modulus reflects an increase in the number of crosslinks in the polymer.⁴¹⁴ Thus, when the collagen network is collapsed following C-ABC treatment, an increase in inter-collagen type II pyridinium crosslinking may occur, which has been shown to correlate to tensile properties.^{22,42,495} Additionally, collagen type IX may be playing a larger role in crosslinking the type II collagen present.⁴¹³ Supporting the idea of other collagens playing a role is the difference between total and type II collagen observed in this experiment. Finally, the order of magnitude difference between the compressive and tensile stiffness measured in our neo-tissue reflects the differences observed in native cartilage.⁹³

The present study represents a novel method toward functional tissue engineering of articular cartilage. Conventional methods used for tissue engineering articular cartilage focus on biochemical^{42,369,482} and biomechanical^{332,368,479-481} stimulation with anabolic intent. In contrast, the use of C-ABC's ECM degrading properties, while perhaps counterintuitive at first

glance, demonstrate how catabolic modulation of a particular ECM constituent can positively affect another. *In vivo* and *in vitro* studies have shown that C-ABC has minimal effects on rabbit³⁵⁵ and equine²⁴⁶ chondrocytes and has been successfully used in investigations of articular cartilage repair^{240,258,304} and central nervous system recovery following injury.¹¹³ Though there may be unknown, non-specific C-ABC activities, there is no evidence in the literature to suggest that a brief *in vitro* exposure to C-ABC causes unwanted effects. In this study, C-ABC treatment did not affect the ability of treated constructs to produce sGAG, nor did it induce type I collagen production. It is conceivable that C-ABC could be applied in tissue engineering strategies for other sGAG containing tissues, such as heart valves, ligaments, tendons, the knee meniscus, the intervertebral disc, and the temporomandibular joint disc. As it is not yet known for certain what characteristics a tissue engineered construct will need to function *in vivo*, C-ABC represents another tool for tissue engineers that may prove useful in the long run. Future studies should aim to elucidate the biological or mechanical mechanism(s) by which C-ABC treatment affects functional properties and investigate whether C-ABC can be incorporated into conventional tissue engineering strategies through combination with other stimuli. Moreover, longer time points should be investigated to see if the compressive stiffness of C-ABC treated constructs continues to increase. Ultimately, an appropriate balance of ECM components and, perhaps more importantly, tensile and compressive properties, will be needed for successful implantation and integration of tissue engineered constructs in *in vivo* models.

Table 6-I: Construct thickness, diameter, and total wet weight

Time	Treatment	Thickness (mm)	Diameter (mm)	Wet Weight (mg)
2 weeks	Control	0.38 ± 0.04^A	5.24 ± 0.09^A	8.7 ± 0.94^A
	C-ABC	0.28 ± 0.01^B	4.59 ± 0.20^B	4.8 ± 0.6^B
4 weeks	Control	0.68 ± 0.06^C	6.26 ± 0.25^C	21.31 ± 3.42^C
	C-ABC	0.44 ± 0.02^D	5.49 ± 0.15^D	11.56 ± 1.49^D

Table 6-I. Construct thickness, diameter, and total wet weight. Data are given as mean \pm S.D.

Within a column, groups not sharing a similar letter are significantly different from one another ($p < 0.05$). For each metric, each group was significantly different from all others.

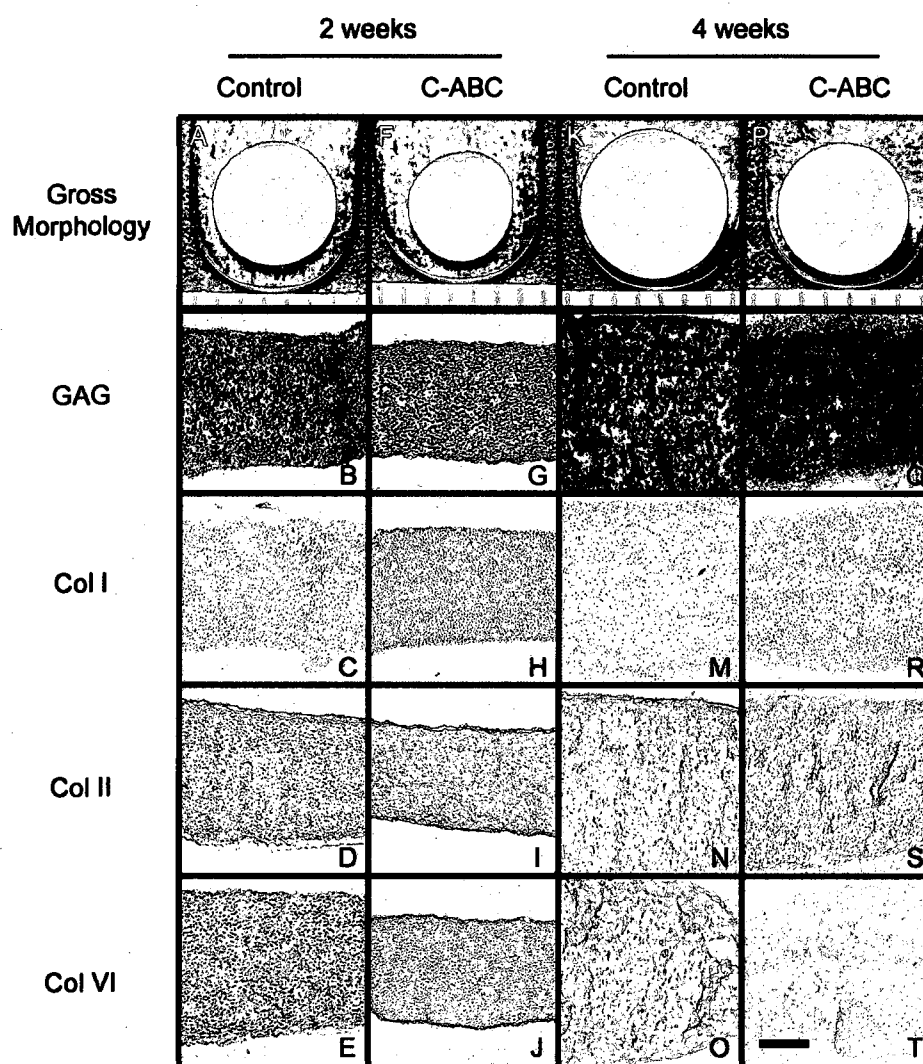
Figure 6-1: Gross morphology and histology

Figure 6-1. Representative gross and histological pictures of self-assembled tissue constructs for all groups. 2 week Control (A-E), 2 week C-ABC treated (F-J), 4 week Control (K-O), 4 week C-ABC treated (P-T). Ruler markings = 1 mm in A,F,K,P, and the scale bar = 200 μ m in T applies to all histological images. Histological images were taken at 100X and safranin-O/fast green was used to stain for GAG. Note the loss of GAG following C-ABC treatment (G), the return of GAG staining at 4 weeks (Q), and the absence of type I collagen staining in all treatment groups (C,H,M,R).

Figure 6-2: Construct sGAG concentration and compressive stiffness

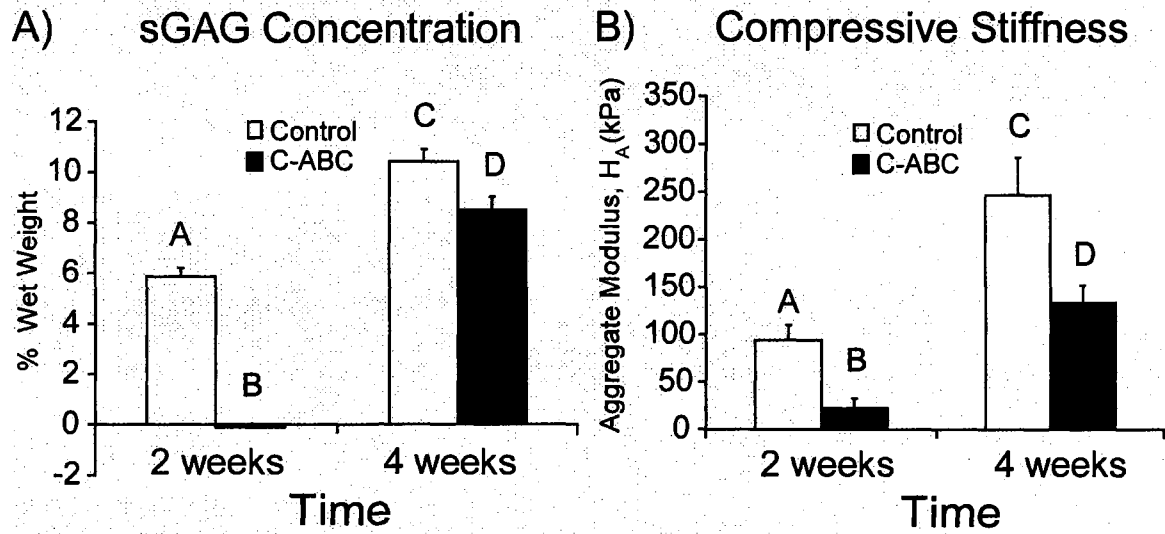


Figure 6-2. A) Construct sGAG concentration and B) compressive stiffness. Total sGAG normalized to wet weight of each group was significantly different from all others. The same was seen for the aggregate modulus. In both panels, groups not connected by the same letter are significantly different from one another ($p < 0.05$).

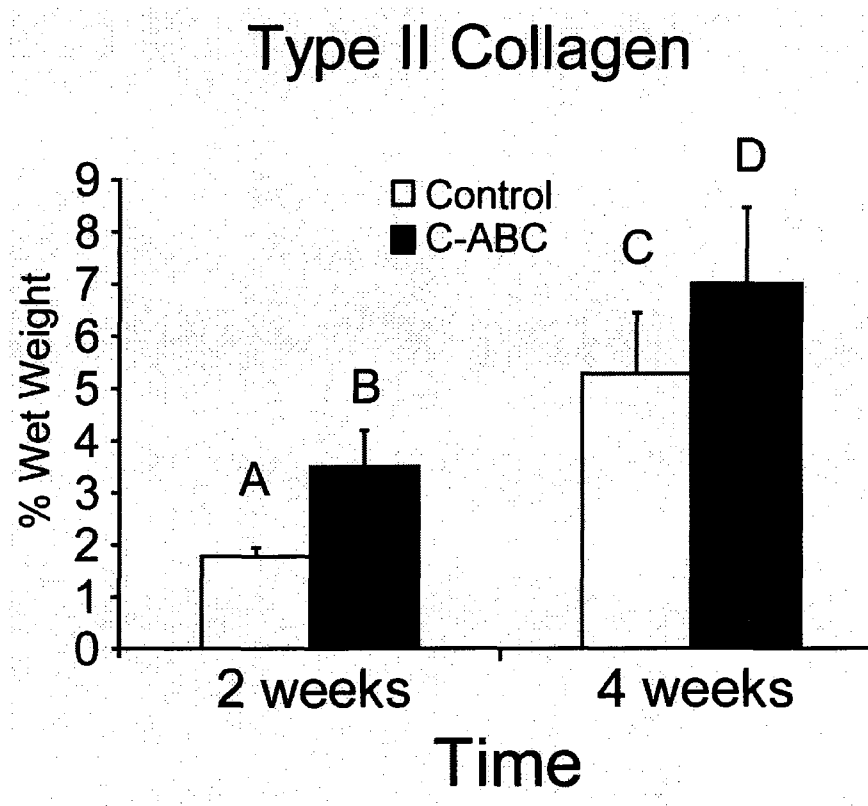
Figure 6-3: Collagen type II production

Figure 6-3. Type II collagen normalized to wet weight in the 4 week C-ABC treated group was significantly greater than in 4 week controls. Groups not connected by the same letter are significantly different from one another ($p < 0.05$).

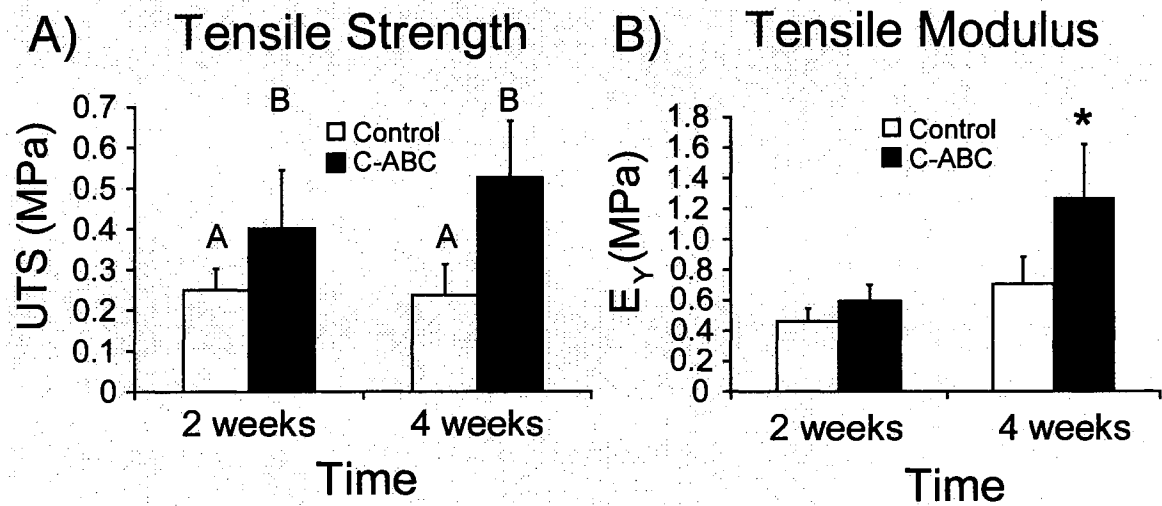
Figure 6-4: Construct tensile properties

Figure 6-4. Construct tensile properties. A) Ultimate tensile strength and B) tensile modulus. Both the ultimate tensile strength (UTS) and apparent Young's modulus (E_Y) were significantly increased at 4 weeks in the C-ABC treated group (121 and 80%, respectively). In panel A, groups not connected by the same letter are significantly different from one another. In panel B, * indicates significantly different from all other groups ($p < 0.05$).

Chapter 7: Effects of multiple chondroitinase ABC applications on tissue engineered articular cartilage*

Abstract

Increasing tensile properties and collagen content is a recognized need in articular cartilage tissue engineering. This study tested the hypothesis that multiple applications of chondroitinase ABC (C-ABC), a glycosaminoglycan (GAG) degrading enzyme, could increase construct tensile properties in a scaffold-less approach for articular cartilage tissue engineering. Developing constructs were treated with C-ABC at 2 weeks, 4 weeks, or both 2 and 4 weeks. At 4 and 6 weeks, construct sulfated GAG composition, collagen composition, and compressive and tensile biomechanical properties were assessed, along with immunohistochemistry (IHC) for collagens type I, II, and VI, and the proteoglycan decorin. At 6 weeks, the tensile modulus and ultimate tensile strength of the group treated at both 2 and 4 weeks were significantly increased over controls by 78% and 64%, reaching values of 3.4 and 1.4 MPa, respectively. Collagen concentration also increased 43%. Further, groups treated at either 2 weeks or 4 weeks alone also had increased tensile stiffness compared to controls. Surprisingly, though GAG was depleted in the treated groups, by 6 weeks there were no significant differences in compressive stiffness. IHC showed abundant collagen type II and VI in all groups, with no collagen type I. Further, decorin staining was reduced following C-ABC treatment, but returned

*Chapter in press as Natoli RM, Responde DJ, Lu BY, and Athanasiou KA, "Effects of multiple chondroitinase ABC applications on tissue engineered articular cartilage," *Journal of Orthopedic Research*, October 2008.

during subsequent culture. The results support the use of C-ABC in cartilage tissue engineering for increasing tensile properties.

Introduction

Degeneration of articular cartilage poses a significant clinical problem. The low regenerative capacity of cartilage limits healing, making the need for replacement tissue important. The primary goal of cartilage tissue engineering is to produce neotissue with sufficient mechanical properties to, when implanted, function in the native environment.

Self-assembly of chondrocytes has shown promise for cartilage tissue engineering.^{226,231} In this process, chondrocytes are cultured in non-adherent agarose wells, and inter-cellular adhesion directs self-assembly through an N-cadherin binding process.³⁷⁵ Other scaffold-less systems, such as pellet and aggregate culture, have also been used in cartilage tissue engineering.^{180,269,456} Collectively, these approaches provide potential benefits over traditional scaffold-based strategies, including increased biocompatibility and a lack of exogenous degradation products. Self-assembly has been studied with growth factors^{143,145} and mechanical stimulation,^{143,232} but efforts to-date have not produced constructs with tensile properties in the range of native tissue. Engineered constructs generally have significantly less collagen than native tissue,^{176,266,369,504} and an insufficient collagen network reduces construct functionality by impairing their tensile stiffness and resistance to proteases.⁴² One way to improve upon this limitation is application of exogenous agents that modulate the matrix of the developing tissue.

One potential exogenous agent is the glycosaminoglycan (GAG) degrading agent chondroitinase ABC (C-ABC). In a recent study, C-ABC treatment of cartilage explants followed by 2 weeks of culture resulted in reconstitution of GAG content and increased tensile properties.²¹ Moreover, C-ABC treatment of agarose encapsulated chondrocytes increased collagen concentration.⁵⁰ Cartilage grown *in vitro* tends to lack maturational growth and overproduces GAGs, resulting in an imbalance between GAG and collagen content that reduces tissue tensile properties.^{494,495} Thus, using C-ABC, which selectively degrades chondroitin and dermatan sulfates,³⁹⁵ could benefit the matrix by restoring the balance between GAG and collagen content.

The purpose of the present study was to elucidate the temporal effects of multiple C-ABC treatments on self-assembled articular cartilage constructs. To investigate this, constructs were treated with C-ABC at 2 weeks, 4 weeks, or both 2 and 4 weeks, with construct assessment at 4 and 6 weeks. We hypothesized that a single C-ABC treatment would increase tensile mechanical properties, and that multiple treatments would further enhance tensile properties. Additionally, by allowing additional culture time post-treatment, it was expected that constructs treated at 2 weeks would regain GAG content and compressive stiffness similar to untreated controls.

Materials and methods

Chondrocyte isolation and culture

Bovine chondrocytes were isolated and self-assembled as previously described.²³¹ Cartilage from the distal femur and patellofemoral groove of male calves (Research 87, Boston, MA) was digested in collagenase type II for 24 hrs. Cells were counted using a hemocytometer and then frozen at -80°C in DMEM containing 20% FBS and 10% DMSO. Within days, cells were thawed and counted. Chondrocyte viability was >90% upon thawing. Cells were then seeded at ~5 million cells in 100 μ L of media into 5 mm diameter cylindrical agarose wells. An additional 400 μ L of media was added 4 hrs later. Chondrogenic medium composed of DMEM with 4.5 mg/mL glucose and L-glutamine (Biowhittaker/Cambrex, Walkersville, MD), 100 nM dexamethasone (Sigma, St. Louis, MO), 1% fungizone, 1% penicillin/streptomycin, 1% ITS+ (BD Scientific, Franklin Lakes, NJ), 50 μ g/mL ascorbate-2-phosphate, 40 μ g/mL L-proline, and 100 μ g/mL sodium pyruvate (Fisher Scientific, Pittsburgh, PA) was used for seeding and subsequent media changes. This chondrogenic medium formulation contains no FBS and no stimulatory factors other than those listed above. The 500 μ L of media were changed daily throughout the experiment.

At 10 days, all constructs were transferred to tissue culture plates in which only the bottom of the wells was coated with a thin layer of agarose¹⁴² and randomly assigned to one of the four treatment groups. Of note, separate harvests were used for the 4 and 6 week experiments. In the 4 week experiment, cells from 3 distinct calves were used. Based on the promising results at 4

weeks, a 6 week experiment was then conducted. Cells from 4 distinct calves were used in the 6 week experiment. Separate batches of agarose wells were also fabricated for each experiment.

C-ABC treatment and construct processing

In the 4 week experiment, constructs were treated with C-ABC at 2 weeks (early), 4 weeks (late), or 2 and 4 weeks (combined). For treatment, constructs were exposed to C-ABC (Sigma or Associates of Cape Cod, Falmouth, MA) at an activity of 2 U/mL in chondrogenic media for 4 hrs at 37°C, followed by five washes in 400 μ L chondrogenic media. At 4 weeks, samples were prepared for histology, quantitative biochemistry, and mechanical testing. Hence, the late and combined groups did not have any recovery time post-treatment in the 4 week experiment. In the 6 week experiment, constructs were treated early, late, or combined, but culture duration was lengthened to 6 weeks, at which time samples were prepared for histology, quantitative biochemistry, and mechanical testing. Separate groups served as untreated controls for both experiments.

Just prior to mechanical testing, constructs were removed from culture and processed. A 3 mm diameter core was removed from the construct's center with a biopsy punch for creep indentation testing. The remaining outer ring was portioned ~60% for biochemical analysis and ~40% for tensile testing. This method of tissue processing tests tensile properties and assays the biochemical content of the outer annulus, which is presumably representative of the entire construct. However, any inhomogeneities that are specific to the annulus of tissue engineered constructs may bias the results. Indeed, inhomogeneities in

tissue engineered articular cartilage have been observed at similar time points to those investigated in this study.²⁸¹ However, as all specimens are prepared similarly, any bias is not likely to affect inter-group comparisons.

Gross morphology, histology, and immunohistochemistry (IHC)

Construct diameter was measured from digital photographs using ImageJ (National Institutes of Health, Bethesda, MD). For histology, constructs were cryoembedded and sectioned at 14 μ m. Some sections were fixed in 10% phosphate buffered formalin and stained with Safranin O/fast green for GAG content. For IHC, slides were first fixed with acetone at 4°C for 20 min. For collagens type I, II, and VI, slides were rinsed with IHC buffer, quenched of peroxidase activity, and blocked with horse serum for collagen type I and goat serum for collagens type II and VI (Vectastain ABC kit, Vector Labs, Burlingame, CA). Sections were then incubated for 1 hr with either mouse anti-collagen type I diluted 1:1000 (Accurate Chemicals, Westbury, NY), rabbit anti-collagen type II diluted 1:300 (Cedarlane Labs, Burlington, NC), or rabbit anti-collagen type VI diluted 1:300 (US Biological, Swampscott, MA). The secondary antibody, made by adding one drop of stock solution is added to 10 mL of buffer in the mixing bottle (anti-mouse or anti-rabbit IgG, Vectastain ABC kit), was then applied for 30 min, and color was developed using the Vectastain ABC reagent and 5 min exposure to DAB.

For decorin, whole rabbit serum (LF-94) was a generous gift from the laboratory of Dr. Larry W. Fisher.¹⁶⁸ Following fixation in cold acetone and peroxidase quenching, sections were treated with 0.2 U/mL protease free C-ABC

(Associates of Cape Cod) in a solution of 0.01 M Tris, 0.01 M NaCl, and 0.012 M NaAc containing 0.1% bovine serum albumin (BSA) for 1 hr at 37°C to expose the core protein. Sections were then blocked with goat serum and incubated overnight at 4°C in the presence of LF-94 diluted 1:500 in tris-buffered saline (TBS) containing 1% BSA. Finally, the secondary antibody, made as described above (anti-rabbit IgG, Vectastain ABC kit), was applied for 1 hr, and color was developed using the Vectastain ABC reagent and 5 min exposure to DAB. In addition to IHC staining of experimental groups, bovine articular cartilage was used as a positive control for collagen type II, collagen type VI, and decorin and as a negative control for type I collagen. Bovine tendon and bone were used as positive controls for collagen type I. As additional negative controls, tissues were stained for each protein as described above, but without application of the appropriate primary antibody.

Biochemical analysis

The portion of the sample assigned to biochemical analyses was weighed wet, lyophilized for 48 hrs, weighed dry, and subjected to a sequential pepsin-elastase digestion previously described.¹⁴⁵ Briefly, samples were re-suspended in 0.8 mL of 0.05 M acetic acid containing 0.5 M sodium chloride. To this suspension, 0.1 mL of a 10 mg/mL pepsin (Sigma) solution in 0.05 M acetic acid was added, and the suspension was mixed at 4°C for 96 hrs. Next, 0.1 mL of 10x TBS buffer was added along with 0.1 mL pancreatic elastase (1 mg/mL dissolved in 1x TBS buffer). This suspension was mixed at 4°C overnight. Following this protocol, no residual neo-tissue remained. DNA content was assessed with the

Quant-iT™ PicoGreen® dsDNA Assay Kit (Invitrogen, Carlsbad, CA). Following hydrolysis with 4N NaOH for 20 min at 110°C, collagen content of the samples was quantified with a modified chloramine-T hydroxyproline assay.¹¹ Finally, sulfated GAG content was quantified using the Blyscan Glycosaminoglycan Assay kit (Accurate Chemical and Scientific Corp., Westbury, NY).

Creep indentation testing

Compressive mechanical properties were determined by creep indentation testing of the central 3 mm core biopsy assuming a linear biphasic model.³⁴⁷ Thickness was measured using a micrometer, and specimens were attached to a flat stainless steel surface with a thin layer of cyanoacrylate glue. The attached specimen was then placed into the creep indentation apparatus, which was used to automatically load and unload the specimens while monitoring specimen creep and recovery. In the 4 week experiment, the late and combined treatment groups were tested using a 0.05 g tare followed by a 0.27 g test load. These lighter loads allowed control over excessive deformation that resulted immediately following GAG removal. All other specimens were tested with a tare load of 0.2 g followed by a test load of 0.7 g. The loads were applied to the specimens through a 0.8 mm diameter, flat-ended, porous tip. To determine construct mechanical properties, a semi-analytical, semi-numerical, linear biphasic model was employed,³⁴⁸ followed by a non-linear finite element optimization to refine the solution and obtain values for the aggregate modulus, permeability, and Poisson's ratio.³⁰

Tensile testing

The portion of each sample assigned to tensile testing was cut into a dog-bone shape and glued to paper tabs.³⁵ This procedure prepares specimens with slightly curved lateral edges from the outer annulus, which may introduce artifact into the testing. However, as all specimens were prepared in the same manner, this potential artifact would be evenly distributed. ImageJ was used to determine sample gauge length and width from photographs. Gauge length was defined as the distance between the paper tabs. Thickness was measured with a micrometer. Tensile tests were performed at a strain rate of 1% gauge length per second on a mechanical testing system (Instron Model 5565, Canton, MA). There was no pre-conditioning of the specimens. The Instron monitors and records displacement, which when combined with gauge length, allows strain to be calculated. Young's modulus was determined by linear regression of the linear portion of the stress-strain curve based on initial cross-sectional area. The ultimate tensile strength (UTS) was taken to be the maximal stress prior to failure.

Statistical analyses

Each group consisted of $n = 8$ samples. Two samples were randomly assigned for histology and IHC. The remaining six were used in the biochemical, compression, and tension tests. At each time point, a 2-way ANOVA based on main factors of treatment at 2 weeks or treatment at 4 weeks was performed to investigate additive or synergistic effects.⁴⁴⁷ Where warranted, the ANOVA was followed by a Student-Newman-Keuls post-hoc test on a cross of the main

factors. Significance was set at $p < 0.05$. All data are presented as mean \pm standard deviation (S.D.).

Results

4 week experiment

Figure 7-1 shows results from histology and IHC. At 4 weeks, Safranin-O/fast green staining for GAGs showed GAG presence in the control and early treatment groups, and verified GAG removal in the late and combined treatment groups. Staining for collagens type II and VI (data not shown for type VI) was evident in all constructs. With respect to collagen type VI, pericellular staining was present, but it was not exclusive. There was also diffuse staining throughout the construct. Constructs did not stain for collagen type I. Decorin stained intensely throughout constructs in the control and early treatment groups, but stained only on the perimeter of constructs in the late and combined treatment groups.

One-time treatment at 2 weeks or 4 weeks was a significant factor for diameter, wet weight (WW), and thickness. Further, with respect to decreasing WW, the interaction term was significant ($p = 0.03$). For diameter, each group was significantly different from the others, except for early and combined treatments being similar. Diameters measured 6.02 ± 0.17 , 5.45 ± 0.07 , 5.71 ± 0.18 , and 5.31 ± 0.07 mm for the control, early, late, and combined groups, respectively. For thickness, each group was significantly different from the others, except for late treatment being similar to early and combined.

Thicknesses measured 0.45 ± 0.04 , 0.36 ± 0.03 , 0.34 ± 0.05 , and 0.30 ± 0.03 mm for the control, early, late, and combined groups, respectively. For WW, each group was significantly different from the others, except for early and late treatments being similar. WWs measured 14 ± 1.7 , 9.2 ± 0.8 , 8.3 ± 1.2 , and 5.5 ± 0.6 mg for the control, early, late, and combined groups, respectively. In terms of DNA content, treatment at 4 weeks was a significant factor. Post-hoc testing showed the combined treatment group had significantly less DNA than control (30 ± 5.6 μ g per construct compared to 21 ± 1.8 μ g). The early group had 28 ± 5.2 μ g and the late group had 26 ± 6.5 μ g.

Turning to extracellular matrix (ECM) content and mechanical properties, for both GAG/WW and collagen/WW treatment at 2 weeks or treatment at 4 weeks was a significant factor. Table 7-1 shows GAG/WW and collagen/WW. Post-hoc testing of GAG/WW showed each group was significantly different from the others, except for late treatment being similar to combined. Post-hoc testing of collagen/WW showed the combined treatment group was significantly different from all others. GAG or collagen per construct can be obtained by multiplying the WW% by the total wet weight. Post-hoc testing of GAG/construct was identical to GAG/WW. Post-hoc testing of collagen/construct showed the combined treatment group was significantly different from control and the late treatment groups. In terms of compressive properties, treatment at 2 weeks or treatment at 4 weeks was a significant factor for compressive stiffness. The interaction term was also significant ($p = 0.012$). Further, treatment at 4 weeks was as significant factor for permeability. All treatment groups were significantly less stiff in

compression compared to control (Fig. 7-2A). Post-hoc testing of permeability showed an increasing trend with treatment. Permeabilities measured 3.11 ± 1.73 , 9.35 ± 5.92 , 75.5 ± 64.6 , and $86.8 \pm 85.9 \times 10^{-15} \text{ m}^4/\text{N}\cdot\text{s}$ for the control, early, late, and combined groups, respectively. Post-hoc testing of Poisson's ratio showed combined treatment was significantly greater than early or late treatment. Poisson's ratio measured 0.093 ± 0.095 , 0.035 ± 0.028 , 0.054 ± 0.039 , and 0.172 ± 0.097 for the control, early, late, and combined groups, respectively. In terms of tensile properties, treatment at 2 weeks or at 4 weeks was a significant factor for UTS, and treatment at 2 weeks was a significant factor for Young's modulus. The interaction term was also significant for Young's modulus ($p = 0.0008$). All treatment groups had significantly greater UTS than control (Fig. 7-2B). Post-hoc testing of Young's modulus showed all groups were significantly different from each other except control and early treatment. Young's modulus measured 1299 ± 101 , 1308 ± 257 , 950 ± 284 , and $1689 \pm 159 \text{ kPa}$ for the control, early, late, and combined groups, respectively.

6 week experiment

In the 6 week experiment, histology and IHC results were similar to the 4 week experiment, except GAG and decorin were present in the late and combined treatment groups (Fig. 7-1). Treatment at 4 weeks was a significant factor for diameter, WW, and thickness. Further, with respect to decreasing diameter, the interaction term was significant ($p = 0.046$). For diameter, each group was significantly different from the others, except for late and combined treatment being similar. Diameters measured 5.27 ± 0.10 , 5.14 ± 0.07 , $4.99 \pm$

0.09, and 5.00 ± 0.07 mm for the control, early, late, and combined groups, respectively. For thickness, late and combined treatments were significantly different than both control and early treatment, though the differences were small. Thicknesses measured 0.29 ± 0.03 , 0.31 ± 0.03 , 0.25 ± 0.04 , and 0.24 ± 0.02 mm for the control, early, late, and combined groups, respectively. For WW, late and combined treatments were significantly different than both control and early treatment. WWs measured 5.9 ± 0.4 , 5.7 ± 0.5 , 4.9 ± 0.3 , and 4.7 ± 0.3 mg for the control, early, late, and combined groups, respectively. DNA content at 6 weeks showed a similar trend to 4 weeks. Post-hoc testing showed the late and combined treatments had significantly less DNA than both control and early treatment.

In terms of ECM content and mechanical properties, treatment at 4 weeks was a significant factor for both GAG/WW and collagen/WW. Further, with respect to decreasing GAG/WW, the interaction term was significant ($p = 0.02$). Late or combined treatment resulted in significantly decreased GAG/WW compared to control or early treatment, while late or combined treatment resulted in significantly increased collagen/WW compared to control (Table 7-I). Post-hoc testing of GAG/construct showed each group was significantly different from the others, except for late treatment being similar to combined. There were no significant differences in collagen/construct. In terms of compressive properties, treatment at 4 weeks was a significant factor ($p = 0.048$) for compressive stiffness (Fig. 7-3A). There were no significant differences in aggregate modulus among the four groups. Post-hoc testing of permeability and Poisson's ratio also

showed no significant differences among the groups. Permeabilities measured 19.7 ± 19.8 , 17.6 ± 16.9 , 15.7 ± 8.5 , and $20.7 \pm 12.7 \times 10^{-15} \text{ m}^4/\text{N}\cdot\text{s}$ for the control, early, late, and combined groups, respectively. Poisson's ratio measured 0.138 ± 0.110 , 0.085 ± 0.119 , 0.072 ± 0.033 , and 0.133 ± 0.112 for the control, early, late, and combined groups, respectively. In terms of tensile properties, treatment at 2 weeks or at 4 weeks was a significant factor for Young's modulus, and treatment at 4 weeks was a significant factor for UTS. All treated groups had significantly greater Young's modulus than control (Fig. 7-3B). Additionally, the combined treatment group was greater than early or late treatment. Post-hoc testing of UTS showed the control and early treatment group were not significantly different, and the late and combined treatment groups were not significantly different. All other comparisons were significantly different. UTS measured 881 ± 181 , 984 ± 143 , 1343 ± 169 , and $1441 \pm 184 \text{ kPa}$ for the control, early, late, and combined groups, respectively.

Discussion

In this study, we examined the effects of multiple C-ABC applications on self-assembled tissue engineered articular cartilage constructs. Results showed that the group treated at both 2 and 4 weeks (combined) had significantly greater tensile properties (ultimate tensile strength and Young's modulus) than control in both the 4 and 6 week experiments, reaching a stiffness of 3.4 MPa at 6 weeks. Further, treating at 2 weeks (early) or at 4 weeks (late) alone resulted in significantly greater ultimate tensile strength at 4 weeks, and significantly greater Young's modulus at 6 weeks, compared to controls at these time points. Though

compressive stiffness of all treatment groups was less than control in the 4 week experiment, there were no significant differences at 6 weeks. These results support our hypotheses that multiple C-ABC treatments would further enhance tensile properties compared to a single treatment, and, given longer culture time post-treatment, the early treatment group would not have a significantly different compressive stiffness compared to untreated controls.

An interesting result of this study is that the compressive properties of all C-ABC treated groups were not significantly different from controls at 6 weeks. Furthermore sulfated GAG returned following depletion in the early treatment group over 4 weeks of culture. Additionally, though given only 2 weeks of culture post-treatment, compressive stiffness at 6 weeks of the late and combined treatment groups was not significantly different from controls, despite significantly decreased sulfated GAG content. This is potentially explained by the significantly increased collagen content in these groups compared to control, reaching 23% by WW. Indeed, collagen has been shown to have a role in the compressive behavior of articular cartilage. One study performed confined compression with the expectation that compressions greater than 5% would lead to the full load being borne by the proteoglycan osmotic pressure, evidenced by equal stresses in the axial and radial directions. However, it was found that the axial and radial stresses were not equal, highlighting a role for the collagen network in compression.²⁷⁷ Williamson *et al.*⁴⁹³ examined bovine cartilage compressive properties as a function of age, showing that the compressive modulus increased 180% from fetus to adult. This increase correlated with increased collagen during

development, as GAG content changed negligibly. These findings underscore the concept that construct material properties reflect the balance of ECM components, and both collagen and GAG contribute to compressive stiffness.

Moreover, the results of this study show C-ABC treatment increases construct tensile properties. At 4 weeks, the increase in tensile properties may be attributed to substantially decreased construct size (e.g., thickness) resulting from loss of GAG and its associated water or to increased ability of collagen to rearrange in the absence of a pre-stress generating swelling pressure.^{428,429} However, as GAG returns, differences in construct size at 6 weeks were markedly reduced. This suggests increased collagen concentration could be responsible for the increased tensile properties. Kempson *et al.*²⁷⁴ have shown that the tensile properties of articular cartilage are correlated to collagen content. However, another interesting possibility raised by results from this study is a role for the small proteoglycan decorin. Decorin is known to interact with type II collagen and has key roles in collagen fibrillogenesis, such as limiting fiber diameter.^{135,419} For example, fibroblasts seeded onto collagen scaffolds from decorin knockout mice have been shown to increase scaffold tensile properties compared to wild-type cells.¹⁶⁴ The decrease in decorin evident by IHC staining shown immediately post-treatment in the present study may allow larger diameter collagen fibers to be formed or previously blocked interactions between neighboring collagens to take place, both of which could lead to a more functional collagen network and increased tensile properties. This proposition is similar to a recently described mechanism whereby selective knockdown of the

small proteoglycan lumican led to increased collagen deposition and fibril diameter in a polyglycolic acid scaffold based approach to cartilage engineering employing bovine nasal chondrocytes.²⁶⁶ In addition to decorin and lumican, aggrecan and biglycan have a role in the observed changes. Selective modulation of small, regulatory matrix molecules could be an important consideration for future articular cartilage tissue engineering experiments.

In summary, C-ABC treatment is a promising approach for increasing tensile properties of self-assembled tissue engineered cartilage, perhaps by inducing maturational instead of expansive growth,²¹ whereby construct size changes minimally while ECM continues to be deposited. A potential limitation to scaffold-free approaches is less control over construct thickness, which is further affected by C-ABC treatment. However, construct size could be increased before treatment by using more cells⁴⁰⁹ or allowing additional culture time before C-ABC application. Using the self-assembly process, our laboratory has grown constructs greater than 1 mm thick,¹⁴³ though there is considerable biological variability. In conclusion, as hypothesized, treatment with C-ABC at both 2 and 4 weeks resulted in further enhancement of tensile properties compared to a single treatment at 2 or 4 weeks. Future experiments should probe more deeply into the mechanism as to how temporary proteoglycan depletion affects the collagen network of tissue engineered constructs by examining aspects such as fiber size and degree of crosslinking.

Table 7-I: Construct GAG and collagen content normalized to wet weight

Group	4 weeks		6 weeks	
	GAG / WW (%)	Collagen / WW (%)	GAG / WW (%)	Collagen / WW (%)
Control	6.9 ± 1.8 ^a	8.9 ± 2.1 ^a	6.3 ± 0.6 ^A	16 ± 2.1 ^A
C-ABC @ 2 weeks	4.4 ± 0.8 ^b	19 ± 3.1 ^a	5.5 ± 1.1 ^A	20 ± 4.3 ^{A,B}
C-ABC @ 4 weeks	3.1 ± 1.7 ^c	17 ± 3.4 ^a	2.7 ± 0.5 ^B	24 ± 3.9 ^B
C-ABC @ 2 & 4 weeks	1.6 ± 0.8 ^c	38 ± 15 ^b	3.3 ± 0.4 ^B	23 ± 2.0 ^B

Table 7-I. Construct GAG and collagen content normalized to wet weight. Values in table are mean ± S.D. (n = 6). WW = wet weight. Separate statistical analyses were run on each column. Within a column, groups not sharing a similar letter are significantly different from one another ($p < 0.05$ by Student-Newman-Keuls post-hoc test). At 6 weeks, the groups that had been treated at 4 weeks contained significantly less sulfated GAG/WW, but significantly more collagen/WW, than control.

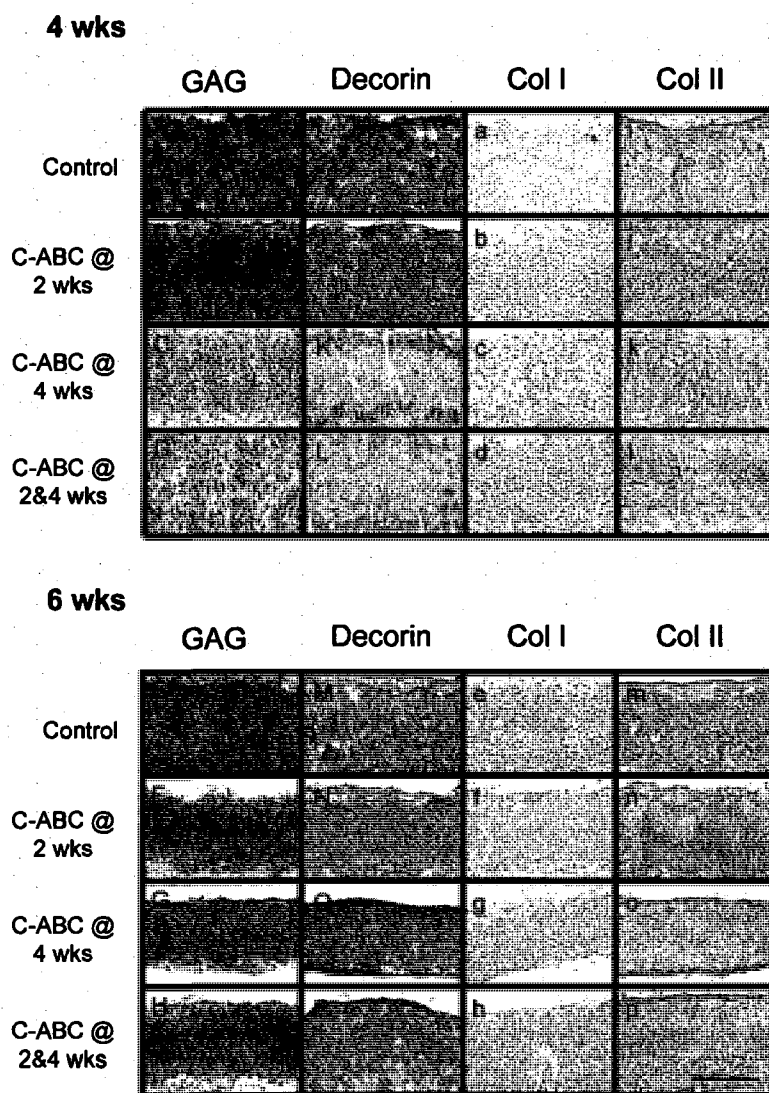
Figure 7-1: Histology and IHC

Figure 7-1. Histology and IHC. A-H) Safranin-O/fast green stain for GAGs, I-P) IHC for decorin, a-h) IHC for collagen type I, and i-p) IHC for collagen type II. At 4 weeks, note the absence of GAG and substantially decreased decorin staining immediately following C-ABC treatment in the group treated at 4 weeks and group treated at both 2 and 4 weeks (C, D, K, and L, respectively). GAG and decorin staining returned in these groups by 6 weeks (G, H, O, and P, respectively). Scale bar in P is 200 μ m.

Figure 7-2: 4 week biomechanical properties

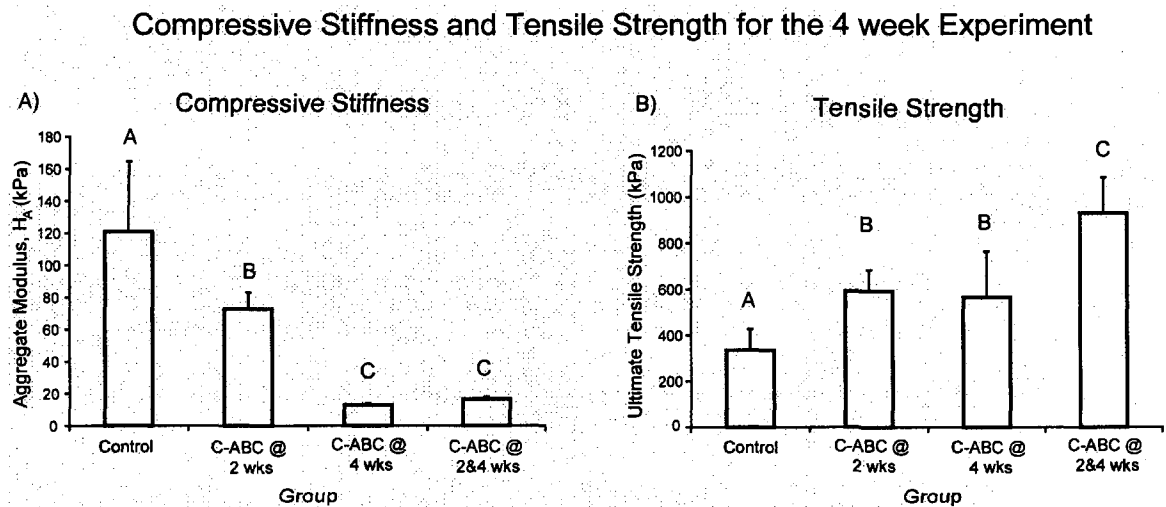


Figure 7-2. 4 week biomechanical properties. A) Compressive stiffness and B) ultimate tensile strength. Bars represent mean \pm S.D. Groups not connected by the same letter are significantly different. The aggregate modulus of all treated groups was significantly less than control. The ultimate tensile strength of all treated groups was significantly greater than control, reaching 931 ± 155 kPa in the combined group. The group treated at both 2 and 4 weeks was significantly greater than the groups treated at only 2 or 4 weeks.

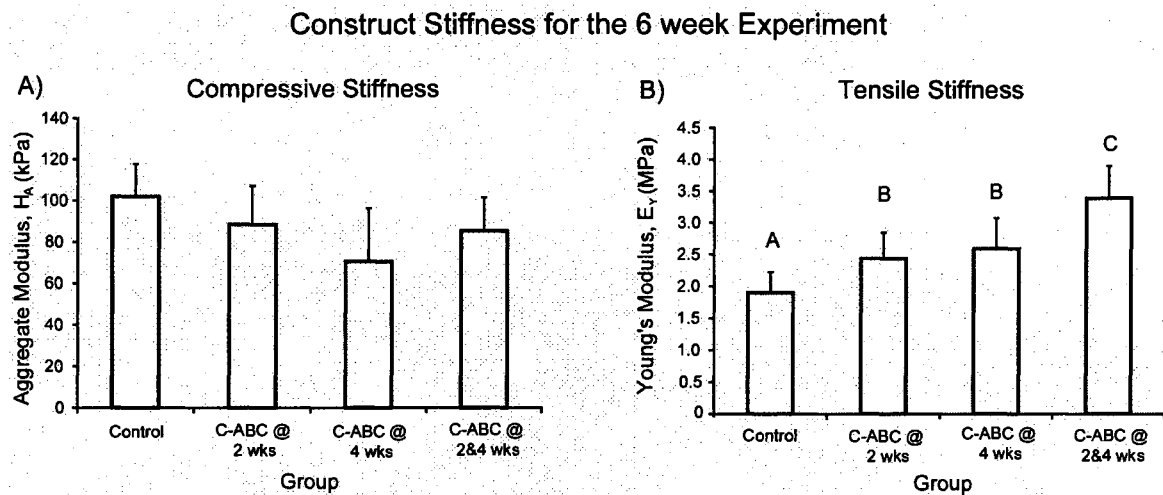
Figure 7-3: 6 week biomechanical properties

Figure 7-3. 6 week biomechanical properties. A) Compressive stiffness and B) tensile stiffness. Bars represent mean \pm S.D. Groups not connected by the same letter are significantly different. There were no significant differences in aggregate modulus. Young's modulus of all treated groups was significantly greater than control, reaching 3.4 ± 0.5 MPa in the combined group. Further, the group treated at both 2 and 4 weeks was significantly greater than the groups treated at only 2 or 4 weeks, which measured 2.4 ± 0.4 and 2.6 ± 0.5 MPa, respectively.

Conclusions and Future Directions

Arthritis is estimated to affect one in five adults.²²² Annually, our nation spends greater than \$60 billion treating aspects of this disease.⁷⁷ The last resort for patients is total joint arthroplasty,^{381,524,525} though eventual implant failure (i.e., revisions due to wear, loosening, etc.),^{49,132,250,251,259,275,291,292,363,370,388,411,452,510,511} and the morbidity (e.g., muscle weakening, infection, and thrombotic events)^{78,107,112,336,384} and mortality^{57,191,383} associated with the procedure are problematic. The difficulties associated with total joint arthroplasty and other current cartilage repair options drive the need for prevention and/or alternative treatment strategies.^{247,248,299} The challenge is that injured and/or diseased articular cartilage has a very poor healing response.^{114,367,446} This thesis identifies and develops ways to slow or prevent degenerative changes in injured tissue and to grow replacement cartilage with enhanced functional properties for future use in situations of established disease.

Mechanical injury of articular cartilage: Tissue's temporal response and amelioration of degradative changes

In the first part of this work (Chapters 2-4), articular cartilage injury was simulated through *ex vivo* impact experiments using a drop tower that employs high stress/strain rates. Post-injury, cartilage explants were then cultured for 24 hrs, or 1, 2, or 4 weeks in the presence or absence of the polymer poloxamer 188 (P188), insulin-like growth factor-I (IGF-I), and matrix metalloproteinase (MMP) inhibitor doxycycline. To determine the extent of cartilage degeneration or

success of the various interventions, gross morphology, cell viability, extracellular matrix (ECM) content and release, gene expression, and compressive biomechanical properties were assessed.

The three impact studies performed collectively delineate the tissue's response to two levels of mechanical injury. High impact (2.8 J) causes an immediate change in tissue gross morphology. By 24 hrs, there were increased cell death, increased sulfated glycosaminoglycan (sGAG) release, and decreased compressive stiffness. These degradative changes persisted at 1, 2, and 4 weeks, and were further accompanied by measurable changes in ECM biochemistry. Moreover, at 24 hrs following High impact, there were specific changes in gene expression that distinguished injured tissue from unloaded adjacent tissue. In contrast, a Low level impact (1.1 J) showed no change from control specimens immediately following impact. However, at 24 hrs or 1 week, Low impact can cause changes in gross morphology, increased sGAG release, and increased cell death. Furthermore, the significant decrease in the tissue's compressive stiffness at 4 weeks following Low impact demonstrates that Low impacted tissue exhibits a delayed biological response. This fact suggests that many cases of primary osteoarthritis, or those cases with no identifiable cause, may be due to low levels of injury thought to be unimportant by the patient or clinically undetectable.

Results of these impact studies parallel established changes from other cartilage injury experiments that have employed drop towers, as well as other systems used to induce cartilage injury, such as injurious compression or cyclical

compressive loading. Differences in the parameters assessed (e.g., cell death) can be attributed to the presence of underlying bone in the studies performed in this thesis and the high loading rates achievable in drop tower experiments, rates above those currently achievable in systems employing materials testing machines for inducing injury. More importantly, characterizing the temporal effects of impact (Chapter 2) identified cell death and sGAG release as targets for intervention.

In terms of post-injury treatment studies, following Low impact at 1 week, P188 reduced cell death 75% compared to no treatment, and IGF-I decreased sGAG release from the tissue 49% (Chapter 3). However, the combination of P188 and IGF-I did not yield additive or synergistic effects. Following High impact, 100 μ M doxycycline reduced cumulative sGAG release at 1 and 2 weeks by 30% and 38%, respectively, compared to no treatment. Interestingly, there was no difference in sGAG release comparing 2 weeks continuous doxycycline treatment with 1 week on, 1 week off (Chapter 4).

Though promising with respect to cell death and sGAG release, no treatment studied prevented the decreases in tissue stiffness. The results of the treatment studies show that established degenerative changes post-impact injury can be partially mitigated, but that to regain the loss in tissue stiffness, the most functional outcome assessed in these experiments, these treatments may need to be coupled with interventions that promote a healing response. Though the specific interventions (including time and duration of application, concentration used, etc.) considered in this thesis only lessen certain degradative changes,

different dosages, regimens, etc. may be more effective. Figure C-1 presents a working model for the tissue response and treatment of articular cartilage post-impact injury based on the work presented in this thesis.

Figure C-1: Model of articular cartilage's response to injury and treatment post-impact

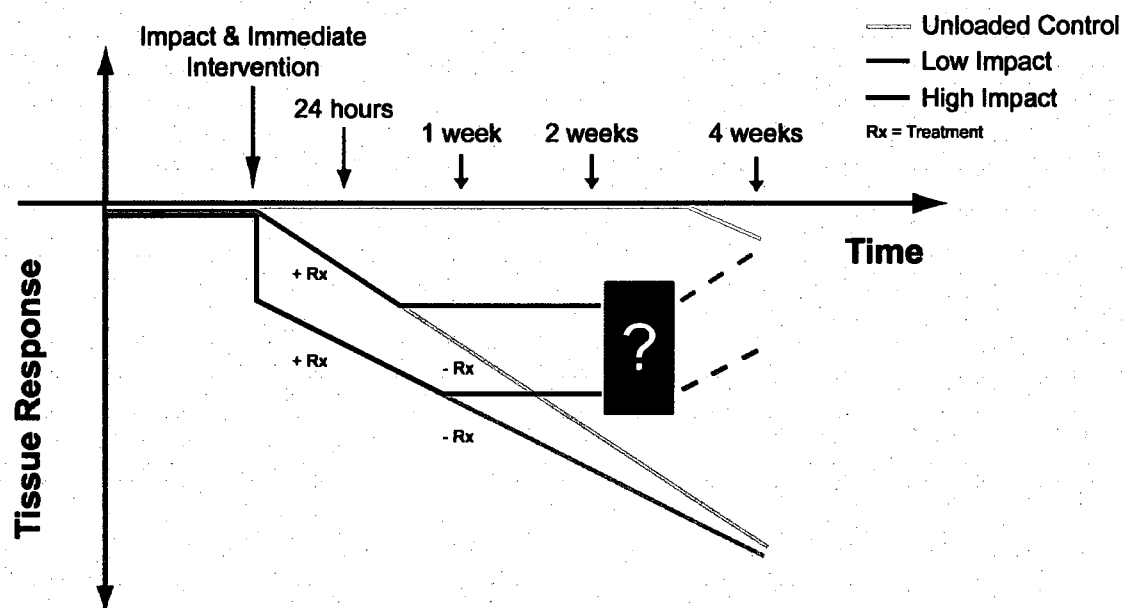


Figure C-1: A model for the tissue response and treatment of articular cartilage post-impact injury. The x-axis represents time, and the y-axis represents the tissue's response. Untreated tissue impacted at a High level shows immediate surface damage. Though Low impact does not cause immediate changes, left untreated the tissue eventually shows a tableau of degeneration similar to tissue impacted at a High level (pale lines). Additionally, given long enough, control tissue begins to degenerate due to disuse. The treatments investigated in this thesis lessened the degradative process (denoted by the flat red and blue lines), but did not recover healthy tissue. These findings suggest that the initial mechanical insult is sufficient to cause damage that cannot be reversed by the treatments studied, and highlights the need for treatment strategies that promote a healing response. The black box and dashed lines denote that the treatment studies did not go beyond 2 weeks and, hence, the uncertainty in their effects at later times.

Tissue engineering of articular cartilage: Increased functional properties with chondroitinase ABC

While the impact and treatment work of this thesis was aimed towards slowing or preventing the development of degradative changes in articular cartilage post-injury, in the case of established disease, tissue engineering of replacement articular cartilage may be a solution. Specifically, the need to create engineered neo-tissue with tensile integrity and collagen content similar to native tissue is apparent in the literature.^{176,267,369,504} The latter part of this thesis (Chapters 6 and 7) examined the use of chondroitinase ABC (C-ABC) as a novel method for increasing construct tensile properties in an *in vitro* serum-free, scaffold-less, self-assembly process for articular cartilage tissue engineering. Constructs were allowed to develop for either 2 or 4 weeks prior to C-ABC treatment and were assessed at 2, 4, and 6 weeks. Quantitatively, collagen types I and II were measured using enzyme-linked immunosorbent assay, along with total sGAG and collagen composition. Qualitatively, collagens type I, II, and VI, and the proteoglycan decorin were assessed using immunohistochemistry. Finally, constructs were mechanically tested for both compressive and tensile biomechanical properties.

In the first study (Chapter 6), treatment with C-ABC at 2 weeks resulted in increased tensile properties at 4 weeks. Specifically, construct ultimate tensile strength and tensile stiffness increased by 121% and 80% compared to untreated controls, reaching 0.5 and 1.3 MPa, respectively. These increases were accompanied by increased type II collagen concentration, without type I

collagen. Additionally, as GAG returned, compressive stiffness of C-ABC treated constructs recovered to be greater than 2 week controls, but not to the level of 4 week controls, suggesting a longer post-treatment culture time would be needed for full GAG and compressive stiffness recovery.

To test the possibility that more time was needed for GAG and compressive stiffness recovery, in the second C-ABC study (Chapter 7) culture duration post-treatment was lengthened. Further, the effects of multiple C-ABC applications were examined. In the group treated at both 2 and 4 weeks, the tensile stiffness and ultimate tensile strength were significantly increased over controls by 78% and 64% at 6 weeks, reaching values of 3.4 and 1.4 MPa, respectively. Collagen concentration also increased 43%. Furthermore, groups treated at either 2 weeks or 4 weeks alone also had increased tensile stiffness compared to controls. Surprisingly, though GAG was depleted in the treated groups, by 6 weeks there were no significant differences in compressive stiffness. Despite the potential of multiple catabolic treatments to induce chondrocyte dedifferentiation, immunohistochemistry continued to show abundant collagen type II and VI, with no collagen type I. Decorin staining was reduced following C-ABC treatment, but recovered during subsequent culture. Decorin is known to interact with collagen type II fibers, limiting their diameter. It is possible that temporary decorin depletion led to increased collagen fiber diameter, or that increased collagen crosslinking occurred, either of which can contribute to increased tensile properties.

Previous work showed C-ABC treatment improved tensile properties and altered the *in vitro* growth phenotype of cartilage explants (see Fig. C-2).²¹ The work of this thesis generalized this approach to articular cartilage tissue engineering, specifically the self-assembly process, and indicates expansive and maturational growth is an appropriate context for thinking about the tissue engineering process. These experiments also tested whether the counter-intuitive approach of catabolic modulation of developing constructs could be beneficial, showing that, at least for C-ABC, it can be. Other research has investigated how to improve tensile properties and collagen content in tissue engineered articular cartilage through means other than C-ABC;^{42,43,142,143,145,161,189,198,233,267,369,375,492} however, none to date has yielded tensile properties as high as with C-ABC treatment. Finally, based on temporary depletion of decorin, my results indicate selective modulation of small regulatory matrix molecules is an important consideration for articular cartilage tissue engineering experiments.

Figure C-2: Growth of tissue engineered articular cartilage

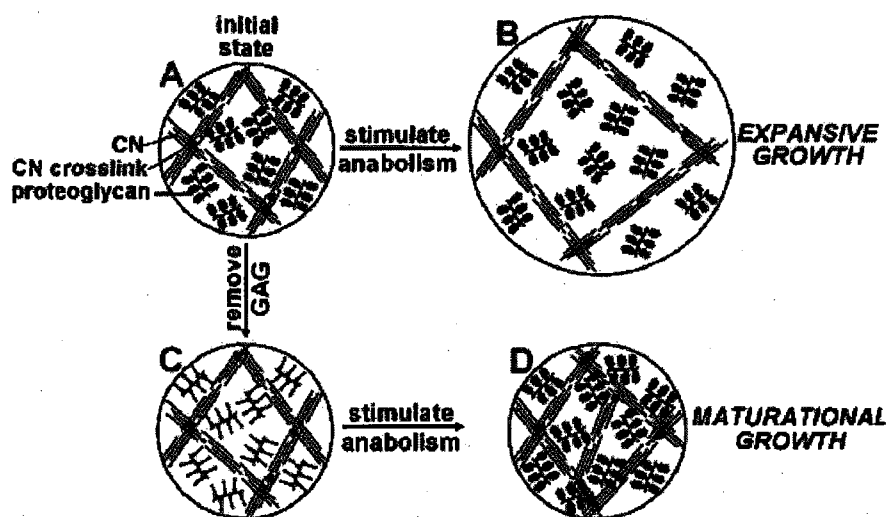


Figure C-2: This figure is taken from *Mechanisms of cartilage growth: modulation of balance between proteoglycan and collagen in vitro using chondroitinase ABC*, by Asanbaeva et al.²¹ The *in vitro* growth process begins at A (CN = collagen network). Left unaltered, cartilage explants and tissue engineered constructs continue to deposit extracellular matrix in a way whereby the growth metrics (diameter, thickness, and wet weight) of the tissue or engineered construct increase substantially (B). In contrast, removal of glycosaminoglycans through C-ABC treatment leads to a different set of initial conditions (C), from which subsequent tissue or construct growth results in extracellular matrix deposition with significantly less increase in the growth metrics (D). For tissue engineered constructs, the new growth phenotype may lead to increased tensile properties by altered collagen orientation, increased fiber diameter, and/or enhanced network crosslinking.

In summary, this thesis provides several unique contributions to the fields of articular cartilage injury and tissue engineering. First, gene expression post-impact had not previously been studied beyond 24 hrs.^{83,94,303} This work provides new data in the form of spatial and temporal gene expression patterns up to 4

weeks post-injury. With respect to the treatment studies, though P188 and IGF-I had been shown to reduce cell death *in vitro* following non-impact injuries, the effects of either of these treatments following *ex vivo* impact, or on GAG release and compressive stiffness, had not been examined.^{37,118,389,420} This thesis demonstrates that IGF-I decreases sGAG release and P188 decreases cell death. Finally, though other MMP inhibitors have been studied post-injury,¹³⁰ doxycycline had not been examined. This work shows that doxycycline decreased sGAG release following impact. Further, treatment with doxycycline for the 1st week of a 2 week culture yielded similar results to 2 weeks continuous treatment. With respect to articular cartilage tissue engineering, an innovative method for increasing neo-tissue tensile properties was developed. Conventional methods used for tissue engineering articular cartilage have focused on biochemical and biomechanical stimulation with anabolic intent. In contrast, the use of C-ABC's ECM degrading properties, while seemingly counterintuitive, demonstrate how catabolic modulation of a particular ECM constituent can positively affect another and lead to increased functional properties.

Future Directions

The exciting and promising results of this thesis present many avenues for future research. First of all, much investigation remains to be carried out with respect to basic mechanical and biological aspects of articular cartilage's response to impact injuries. Though injurious compression and cyclical mechanical loading can cause degradative changes in articular cartilage, subtle differences in results from impact experiments suggest much remains to be

uncovered of cartilage's response to high loading rates. Of particular interest would be investigation of impact levels below Low to determine the minimum impact necessary to, over time, become equivalent to High. Additionally, measurement of the tissue's tensile properties immediately post-impact and with time in culture should be performed. From the biological side, genome and proteome wide profiling of cell death, matrix breakdown, and inflammation pathways should be performed post-impact to understand the biology of cartilage injury mechanistically and to identify potential markers for disease, targets for future intervention studies, and/or measures of therapeutic success. From the mechanics side, analytical and computational models of impact need to be developed and studied. During impact experiments, only boundary conditions along the tissue are controlled. Analytical and computational models allow one to ascertain what occurs within the tissue. It is desirable to relate metrics of the impact event to the biological sequelae, as such knowledge could aid the clinical decision making processes as to when intervention is necessary.

In terms of interventions, the impact system employed in this thesis can serve as a screening tool. A logical next step would be to combine IGF-I and doxycycline treatments under the hypothesis that there could be an additive or synergistic decrease in sGAG release, as they may be acting on different intracellular pathways. Other specific experiments could investigate more concentrations of P188 and IGF-I, examine various "on/off" treatment regimens, and look at longer time points. In this thesis, the time points chosen were relatively short to establish if the treatments had efficacy. As mentioned above,

the search for interventions that promote a healing response should continue, such that the loss of tissue stiffness can be reversed and tissue function can be maintained. Finally, looking ahead, the treatment strategies employed should be considered for use in animal models, and if effective, in clinical trials.

Though C-ABC treatment is a significant stride towards achieving collagen content and tensile properties reminiscent of native tissue, much work remains. To begin, from the engineering standpoint, the minimal activity necessary to increase tensile properties should be identified. The activity used in this thesis (2 U/mL) was taken from cartilage explant experiments, which, though successful in our system, may be reducible. Optimizing the activity required will lessen the cost of this approach and may have fewer ramifications on construct GAG content, such that GAG and compressive properties could recover more quickly than 4 weeks. Additionally, longer time points post-treatment should be studied to see if the benefits seen thus far continue to be maintained and/or enhanced. Further, attempts to incorporate C-ABC treatment into the traditional biochemical (e.g., growth factors) and biomechanical (e.g., hydrostatic pressure and direct compression) approaches to cartilage tissue engineering should be undertaken. However, as a note of caution, C-ABC presents a unique case of competing ability to temporarily destroy compressive stiffness while increasing tensile stiffness. One must remember that, with the present protocol, nearly all sGAG is removed at the time of C-ABC application. So, for example, any benefit of increased GAG achieved with growth factors before C-ABC treatment will likely be rendered moot post-treatment since the "GAG clock" is apparently reset.

Finally, other bioactive agents should be investigated (e.g., the crosslinking agent genepin and/or the lysyl oxidase inhibitor BAPN) for increasing collagen and tensile properties in self-assembled tissue engineered articular cartilage independent of, and in combination with, C-ABC. Along the lines of C-ABC, more selective breakdown of GAGs with hyaluronidases, heparanases, dermatanases, and keratanases may be of interest. From the biological standpoint, the mechanism by which C-ABC increases construct tensile properties is a warranted area of investigation. Temporary decorin depletion provides only indirect, preliminary evidence that collagen fiber diameter may be changing. C-ABC should also be applied to the engineering of other tissues, such as fibrocartilages (e.g., meniscus and intervertebral disc). Finally, these tissue engineered constructs need to be examined in animal models as a true test of their ability to function in the *in vivo* environment.

References

1. Aebi, U., J. Cohn, L. Buhle, and L. Gerace. The nuclear lamina is a meshwork of intermediate-type filaments. *Nature*. 323: 560-4, 1986.
2. Aigner, J., J. Tegeler, P. Hutzler, D. Campoccia, A. Pavesio, C. Hammer, E. Kastenbauer, and A. Naumann. Cartilage tissue engineering with novel nonwoven structured biomaterial based on hyaluronic acid benzyl ester. *J Biomed Mater Res*. 42: 172-81, 1998.
3. Aigner, T. and H. A. Kim. Apoptosis and cellular vitality: issues in osteoarthritic cartilage degeneration. *Arthritis Rheum*. 46: 1986-96, 2002.
4. Akhtar, S., K. M. Meek, and V. James. Ultrastructure abnormalities in proteoglycans, collagen fibrils, and elastic fibers in normal and myxomatous mitral valve chordae tendineae. *Cardiovasc Pathol*. 8: 191-201, 1999.
5. Alexopoulos, L. G., M. A. Haider, T. P. Vail, and F. Guilak. Alterations in the mechanical properties of the human chondrocyte pericellular matrix with osteoarthritis. *J Biomech Eng*. 125: 323-33, 2003.
6. Alexopoulos, L. G., L. A. Setton, and F. Guilak. The biomechanical role of the chondrocyte pericellular matrix in articular cartilage. *Acta Biomater*. 1: 317-25, 2005.
7. Allen, K. D. and K. A. Athanasiou. A surface-regional and freeze-thaw characterization of the porcine temporomandibular joint disc. *Ann Biomed Eng*. 33: 951-62, 2005.
8. Allen, K. D. and K. A. Athanasiou. Growth factor effects on passaged TMJ disk cells in monolayer and pellet cultures. *Orthod Craniofac Res*. 9: 143-52, 2006.
9. Allison, D. D., N. Vasco, K. R. Braun, T. N. Wight, and K. J. Grande-Allen. The effect of endogenous overexpression of hyaluronan synthases on material, morphological, and biochemical properties of uncrosslinked collagen biomaterials. *Biomaterials*. 28: 5509-17, 2007.
10. Allison, D. D., T. N. Wight, N. J. Ripp, K. R. Braun, and K. J. Grande-Allen. Endogenous overexpression of hyaluronan synthases within dynamically cultured collagen gels: Implications for vascular and valvular disease. *Biomaterials*. 29: 2969-76, 2008.
11. Almarza, A. J. and K. A. Athanasiou. Seeding techniques and scaffolding choice for tissue engineering of the temporomandibular joint disk. *Tissue Eng*. 10: 1787-95, 2004.

12. Anderson, D. D., T. D. Brown, K. H. Yang, and E. L. Radin. A dynamic finite element analysis of impulsive loading of the extension-splinted rabbit knee. *J Biomech Eng.* 112: 119-28, 1990.
13. Anderson, D. D., T. D. Brown, and E. L. Radin. Stress wave effects in a finite element analysis of an impulsively loaded articular joint. *Proc Inst Mech Eng [H]*. 205: 27-34, 1991.
14. Anderson, J. M. Biological responses to materials. *Ann Rev Mat Res.* 31: 81-110, 2001.
15. ap Gwynn, I., S. Wade, K. Ito, and R. G. Richards. Novel aspects to the structure of rabbit articular cartilage. *Eur Cell Mater.* 4: 18-29, 2002.
16. Arikawa-Hirasawa, E., H. Watanabe, H. Takami, J. R. Hassell, and Y. Yamada. Perlecan is essential for cartilage and cephalic development. *Nat Genet.* 23: 354-8, 1999.
17. Armstrong, C. G. and V. C. Mow. Variations in the intrinsic mechanical properties of human articular cartilage with age, degeneration, and water content. *J Bone Joint Surg Am.* 64: 88-94, 1982.
18. Armstrong, C. G., W. M. Lai, and V. C. Mow. An analysis of the unconfined compression of articular cartilage. *J Biomech Eng.* 106: 165-73, 1984.
19. Arokoski, J. P., M. M. Hyttinen, T. Lapvetelainen, P. Takacs, B. Kosztaczky, L. Modis, V. Kovanen, and H. Helminen. Decreased birefringence of the superficial zone collagen network in the canine knee (stifle) articular cartilage after long distance running training, detected by quantitative polarised light microscopy. *Ann Rheum Dis.* 55: 253-64, 1996.
20. Arsenis, C., S. A. Moak, and R. A. Greenwald. Tetracyclines (TETs) inhibit the synthesis and/or activity of cartilage proteinases in vivo and in vitro. *Matrix Suppl.* 1: 314, 1992.
21. Asanbaeva, A., K. Masuda, E. J. Thonar, S. M. Klisch, and R. L. Sah. Mechanisms of cartilage growth: modulation of balance between proteoglycan and collagen in vitro using chondroitinase ABC. *Arthritis Rheum.* 56: 188-98, 2007.
22. Asanbaeva, A., K. Masuda, E. J. Thonar, S. M. Klisch, and R. L. Sah. Cartilage growth and remodeling: modulation of balance between proteoglycan and collagen network in vitro with beta-aminopropionitrile. *Osteoarthritis Cartilage.* 16: 1-11, 2008.

23. Ashwell, M. S., A. T. O'Nan, M. G. Gonda, and P. L. Mente. Gene expression profiling of chondrocytes from a porcine impact injury model. *Osteoarthritis Cartilage*. 16: 936-46, 2008.
24. Aspden, R. M. Fibre reinforcing by collagen in cartilage and soft connective tissues. *Proc R Soc Lond B Biol Sci*. 258: 195-200, 1994.
25. Aspden, R. M. Fibre stress and strain in fibre-reinforced composites. *Journal of Material Science*. 29: 1310-1318, 1994.
26. Aspden, R. M., J. E. Jeffrey, and L. V. Burgin. Impact loading of articular cartilage. *Osteoarthritis Cartilage*. 10: 588-9; author reply 590, 2002.
27. Ateshian, G. A., W. M. Lai, W. B. Zhu, and V. C. Mow. An asymptotic solution for the contact of two biphasic cartilage layers. *J Biomech*. 27: 1347-60, 1994.
28. Ateshian, G. A., B. J. Ellis, and J. A. Weiss. Equivalence between short-time biphasic and incompressible elastic material responses. *J Biomech Eng*. 129: 405-12, 2007.
29. Athanasiou, K. A., M. P. Rosenwasser, J. A. Buckwalter, T. I. Malinin, and V. C. Mow. Interspecies comparisons of in situ intrinsic mechanical properties of distal femoral cartilage. *J Orthop Res*. 9: 330-40, 1991.
30. Athanasiou, K. A., A. Agarwal, A. Muffoletto, F. J. Dzida, G. Constantinides, and M. Clem. Biomechanical properties of hip cartilage in experimental animal models. *Clin Orthop*. 316: 254-66, 1995.
31. Athanasiou, K. A., G. G. Niederauer, and C. M. Agrawal. Sterilization, toxicity, biocompatibility and clinical applications of polylactic acid/polyglycolic acid copolymers. *Biomaterials*. 17: 93-102, 1996.
32. Athanasiou, K. A., A. R. Shah, R. J. Hernandez, and R. G. LeBaron. Basic science of articular cartilage repair. *Clin Sports Med*. 20: 223-47, 2001.
33. Atkinson, T. S., R. C. Haut, and N. J. Altiero. An investigation of biphasic failure criteria for impact-induced fissuring of articular cartilage. *J Biomech Eng*. 120: 536-7, 1998.
34. Atkinson, T. S., R. C. Haut, and N. J. Altiero. Impact-induced fissuring of articular cartilage: an investigation of failure criteria. *J Biomech Eng*. 120: 181-7, 1998.
35. Aufderheide, A. C. and K. A. Athanasiou. Assessment of a bovine co-culture, scaffold-free method for growing meniscus-shaped constructs. *Tissue Eng*. 13: 2195-205, 2007.

36. Aydelotte, M. B. and K. E. Kuettner. Differences between sub-populations of cultured bovine articular chondrocytes. I. Morphology and cartilage matrix production. *Connect Tissue Res.* 18: 205-22, 1988.
37. Baars, D. C., S. A. Rundell, and R. C. Haut. Treatment with the non-ionic surfactant poloxamer P188 reduces DNA fragmentation in cells from bovine chondral explants exposed to injurious unconfined compression. *Biomech Model Mechanobiol.* 5: 133-9, 2006.
38. Bae, W. C., V. W. Wong, J. Hwang, J. M. Antonacci, G. E. Nugent-Derfus, M. E. Blewis, M. M. Temple-Wong, and R. L. Sah. Wear-lines and split-lines of human patellar cartilage: relation to tensile biomechanical properties. *Osteoarthritis Cartilage.* 16: 841-5, 2008.
39. Bank, R. A., B. Beekman, N. Verzijl, J. A. de Roos, A. N. Sakkee, and J. M. TeKoppele. Sensitive fluorimetric quantitation of pyridinium and pentosidine crosslinks in biological samples in a single high-performance liquid chromatographic run. *J Chromatogr B Biomed Sci Appl.* 703: 37-44, 1997.
40. Bank, R. A., M. T. Bayliss, F. P. Lafеber, A. Maroudas, and J. M. Tekoppele. Ageing and zonal variation in post-translational modification of collagen in normal human articular cartilage. The age-related increase in non-enzymatic glycation affects biomechanical properties of cartilage. *Biochem J.* 330 (Pt 1): 345-51, 1998.
41. Bassar, P. J., R. Schneiderman, R. A. Bank, E. Wachtel, and A. Maroudas. Mechanical properties of the collagen network in human articular cartilage as measured by osmotic stress technique. *Arch Biochem Biophys.* 351: 207-19, 1998.
42. Bastiaansen-Jenniskens, Y. M., W. Koevoet, A. C. de Bart, J. C. van der Linden, A. M. Zuurmond, H. Weinans, J. A. Verhaar, G. J. van Osch, and J. Degroot. Contribution of collagen network features to functional properties of engineered cartilage. *Osteoarthritis Cartilage.* 16: 359-66, 2008.
43. Bastiaansen-Jenniskens, Y. M., W. Koevoet, A. C. De Bart, A. M. Zuurmond, R. A. Bank, J. A. Verhaar, J. Degroot, and G. J. Van Osch. TGFbeta Affects Collagen Cross-Linking Independent of Chondrocyte Phenotype but Strongly Depending on Physical Environment. *Tissue Eng Part A* 2008.
44. Beekman, B., N. Verzijl, R. A. Bank, K. von der Mark, and J. M. TeKoppele. Synthesis of collagen by bovine chondrocytes cultured in alginate; posttranslational modifications and cell-matrix interaction. *Exp Cell Res.* 237: 135-41, 1997.

45. Below, S., S. P. Arnoczky, J. Dodds, C. Kooima, and N. Walter. The split-line pattern of the distal femur: A consideration in the orientation of autologous cartilage grafts. *Arthroscopy*. 18: 613-7, 2002.
46. Bengtsson, T., A. Aszodi, C. Nicolae, E. B. Hunziker, E. Lundgren-Akerlund, and R. Fassler. Loss of alpha10beta1 integrin expression leads to moderate dysfunction of growth plate chondrocytes. *J Cell Sci*. 118: 929-36, 2005.
47. Benninghoff, A. Form und Bau der Gelenkknorpel in ihren Beziehungen zur Funktion. *Cell and Tissue Research*. 2: 783-862, 1925.
48. Benya, P. D. and J. D. Shaffer. Dedifferentiated chondrocytes reexpress the differentiated collagen phenotype when cultured in agarose gels. *Cell*. 30: 215-24, 1982.
49. Best, J. T. Revision total hip and total knee arthroplasty. *Orthop Nurs*. 24: 174-9; quiz 180-1, 2005.
50. Bian, L., D. Y. Williams, D. Q. Mao, D. Xu, G. A. Ateshian, and C. T. Hung. *Influence of Temporary Chondroitinase ABC-induced GAG Suppression on Maturation of Tissue Engineered Cartilage*. in *Trans Orthopaedic Res*. 2008. San Francisco.
51. Birk, D. E., E. I. Zycband, S. Woodruff, D. A. Winkelmann, and R. L. Trelstad. Collagen fibrillogenesis in situ: fibril segments become long fibrils as the developing tendon matures. *Dev Dyn*. 208: 291-8, 1997.
52. Blanco, F. J., R. Guitian, E. Vazquez-Martul, F. J. de Toro, and F. Galdo. Osteoarthritis chondrocytes die by apoptosis. A possible pathway for osteoarthritis pathology. *Arthritis Rheum*. 41: 284-9, 1998.
53. Bland, Y. S. and D. E. Ashhurst. Development and ageing of the articular cartilage of the rabbit knee joint: distribution of the fibrillar collagens. *Anat Embryol (Berl)*. 194: 607-19, 1996.
54. Bland, Y. S. and D. E. Ashhurst. The hip joint: the fibrillar collagens associated with development and ageing in the rabbit. *J Anat*. 198: 17-27, 2001.
55. Blumberg, T. J., R. M. Natoli, and K. A. Athanasiou. Effects of doxycycline on articular cartilage GAG release and mechanical properties following impact. *Biotechnol Bioeng*. 100: 506-15, 2008.
56. Blunk, T., A. L. Sieminski, K. J. Gooch, D. L. Courter, A. P. Hollander, A. M. Nahir, R. Langer, G. Vunjak-Novakovic, and L. E. Freed. Differential effects of growth factors on tissue-engineered cartilage. *Tissue Eng*. 8: 73-84, 2002.

57. Bohm, P., T. Holy, B. Pietsch-Breitfeld, and C. Meisner. Mortality after total knee arthroplasty in patients with osteoarthritis and rheumatoid arthritis. *Arch Orthop Trauma Surg.* 120: 75-8, 2000.
58. Bonaldo, P., V. Russo, F. Bucciotti, R. Doliana, and A. Colombatti. Structural and functional features of the alpha 3 chain indicate a bridging role for chicken collagen VI in connective tissues. *Biochemistry.* 29: 1245-54, 1990.
59. Bonassar, L. J., J. L. Stinn, C. G. Paguio, E. H. Frank, V. L. Moore, M. W. Lark, J. D. Sandy, A. P. Hollander, A. R. Poole, and A. J. Grodzinsky. Activation and inhibition of endogenous matrix metalloproteinases in articular cartilage: effects on composition and biophysical properties. *Arch Biochem Biophys.* 333: 359-67, 1996.
60. Bonassar, L. J., A. J. Grodzinsky, A. Srinivasan, S. G. Davila, and S. B. Trippel. Mechanical and physicochemical regulation of the action of insulin-like growth factor-I on articular cartilage. *Arch Biochem Biophys.* 379: 57-63, 2000.
61. Bonassar, L. J., A. J. Grodzinsky, E. H. Frank, S. G. Davila, N. R. Bhaktav, and S. B. Trippel. The effect of dynamic compression on the response of articular cartilage to insulin-like growth factor-I. *J Orthop Res.* 19: 11-7, 2001.
62. Borazjani, B. H., A. C. Chen, W. C. Bae, S. Patil, R. L. Sah, G. S. Firestein, and W. D. Bugbee. Effect of impact on chondrocyte viability during insertion of human osteochondral grafts. *J Bone Joint Surg Am.* 88: 1934-43, 2006.
63. Borrelli, J., Jr., P. A. Torzilli, R. Grigienė, and D. L. Helfet. Effect of impact load on articular cartilage: development of an intra-articular fracture model. *J Orthop Trauma.* 11: 319-26, 1997.
64. Borrelli, J., Jr., M. E. Burns, W. M. Ricci, and M. J. Silva. A method for delivering variable impact stresses to the articular cartilage of rabbit knees. *J Orthop Trauma.* 16: 182-8, 2002.
65. Borrelli, J., Jr., K. Tinsley, W. M. Ricci, M. Burns, I. E. Karl, and R. Hotchkiss. Induction of chondrocyte apoptosis following impact load. *J Orthop Trauma.* 17: 635-41, 2003.
66. Borrelli, J., Jr. and W. M. Ricci. Acute effects of cartilage impact. *Clin Orthop.* 423: 33-9, 2004.
67. Borrelli, J., Jr., Y. Zhu, M. Burns, L. Sandell, and M. J. Silva. Cartilage tolerates single impact loads of as much as half the joint fracture threshold. *Clin Orthop.* 426: 266-73, 2004.

68. Boschetti, F. and G. M. Peretti. Tensile and compressive properties of healthy and osteoarthritic human articular cartilage. *Biorheology*. 45: 337-44, 2008.
69. Boskey, A. and N. Pleshko Camacho. FT-IR imaging of native and tissue-engineered bone and cartilage. *Biomaterials*. 28: 2465-78, 2007.
70. Brandt, K. D., S. A. Mazzuca, B. P. Katz, K. A. Lane, K. A. Buckwalter, D. E. Yocum, F. Wolfe, T. J. Schnitzer, L. W. Moreland, S. Manzi, J. D. Bradley, L. Sharma, C. V. Oddis, S. T. Hugenberg, and L. W. Heck. Effects of doxycycline on progression of osteoarthritis: results of a randomized, placebo-controlled, double-blind trial. *Arthritis Rheum*. 52: 2015-25, 2005.
71. Breuls, R. G., B. G. Sengers, C. W. Oomens, C. V. Bouten, and F. P. Baaijens. Predicting local cell deformations in engineered tissue constructs: a multilevel finite element approach. *J Biomech Eng*. 124: 198-207, 2002.
72. Broom, N. D. Further insights into the structural principles governing the function of articular cartilage. *J Anat*. 139 (Pt 2): 275-94, 1984.
73. Browning, J. A., R. E. Walker, A. C. Hall, and R. J. Wilkins. Modulation of Na^+ x H^+ exchange by hydrostatic pressure in isolated bovine articular chondrocytes. *Acta Physiol Scand*. 166: 39-45, 1999.
74. Bryant, S. J. and K. S. Anseth. Controlling the spatial distribution of ECM components in degradable PEG hydrogels for tissue engineering cartilage. *J Biomed Mater Res A*. 64: 70-9, 2003.
75. Buckwalter, J. A. Articular cartilage injuries. *Clin Orthop Relat Res*. 402: 21-37, 2002.
76. Buckwalter, J. A. Sports, joint injury, and posttraumatic osteoarthritis. *J Orthop Sports Phys Ther*. 33: 578-88, 2003.
77. Buckwalter, J. A., C. Saltzman, and T. Brown. The impact of osteoarthritis: implications for research. *Clin Orthop Relat Res*. 427 Suppl: S6-15, 2004.
78. Bullock, D. P., S. M. Sporer, and T. G. Shirreffs, Jr. Comparison of simultaneous bilateral with unilateral total knee arthroplasty in terms of perioperative complications. *J Bone Joint Surg Am*. 85-A: 1981-6, 2003.
79. Bullough, P. and J. Goodfellow. The significance of the fine structure of articular cartilage. *J Bone Joint Surg Br*. 50: 852-7, 1968.
80. Burgin, L. V. and R. M. Aspden. A drop tower for controlled impact testing of biological tissues. *Med Eng Phys*. 29: 525-30, 2007.

81. Burgin, L. V. and R. M. Aspden. Impact testing to determine the mechanical properties of articular cartilage in isolation and on bone. *J Mater Sci Mater Med.* 19: 703-11, 2008.
82. Bursac, P., C. V. McGrath, S. R. Eisenberg, and D. Stamenovic. A microstructural model of elastostatic properties of articular cartilage in confined compression. *J Biomech Eng.* 122: 347-53, 2000.
83. Burton-Wurster, N., R. G. Mateescu, R. J. Todhunter, K. M. Clements, Q. Sun, V. Scarpino, and G. Lust. Genes in canine articular cartilage that respond to mechanical injury: gene expression studies with Affymetrix canine GeneChip. *J Hered.* 96: 821-8, 2005.
84. Buschmann, M. D., E. B. Hunziker, Y. J. Kim, and A. J. Grodzinsky. Altered aggrecan synthesis correlates with cell and nucleus structure in statically compressed cartilage. *J Cell Sci.* 109 (Pt 2): 499-508, 1996.
85. Butler, D. L., S. A. Goldstein, and F. Guilak. Functional tissue engineering: the role of biomechanics. *J Biomech Eng.* 122: 570-5, 2000.
86. Caille, N., O. Thoumine, Y. Tardy, and J. J. Meister. Contribution of the nucleus to the mechanical properties of endothelial cells. *J Biomech.* 35: 177-87, 2002.
87. Campbell, C. J. The healing of cartilage defects. *Clin Orthop Relat Res.* 64: 45-63, 1969.
88. Cao, L., V. Lee, M. E. Adams, C. Kiani, Y. Zhang, W. Hu, and B. B. Yang. beta-Integrin-collagen interaction reduces chondrocyte apoptosis. *Matrix Biol.* 18: 343-55, 1999.
89. Caplan, A. I., M. Elyaderani, Y. Mochizuki, S. Wakitani, and V. M. Goldberg. Principles of cartilage repair and regeneration. *Clin Orthop Relat Res.* 254-69, 1997.
90. Carver, S. E. and C. A. Heath. Influence of intermittent pressure, fluid flow, and mixing on the regenerative properties of articular chondrocytes. *Biotechnol Bioeng.* 65: 274-81, 1999.
91. Castagnola, P., G. Moro, F. Descalzi-Cancedda, and R. Cancedda. Type X collagen synthesis during in vitro development of chick embryo tibial chondrocytes. *J Cell Biol.* 102: 2310-7, 1986.
92. Cattini, P. A. and H. G. Davies. Kinetics of lead citrate staining of thin sections for electron microscopy. *Stain Technol.* 58: 29-40, 1983.
93. Chahine, N. O., C. C. Wang, C. T. Hung, and G. A. Ateshian. Anisotropic strain-dependent material properties of bovine articular cartilage in the

- transitional range from tension to compression. *J Biomech.* 37: 1251-61, 2004.
94. Chan, P. S., A. E. Schlueter, P. M. Coussens, G. J. Rosa, R. C. Haut, and M. W. Orth. Gene expression profile of mechanically impacted bovine articular cartilage explants. *J Orthop Res.* 23: 1146-51, 2005.
 95. Chandran, P. L. and V. H. Barocas. Affine versus non-affine fibril kinematics in collagen networks: theoretical studies of network behavior. *J Biomech Eng.* 128: 259-70, 2006.
 96. Chang, J. and C. A. Poole. Sequestration of type VI collagen in the pericellular microenvironment of adult chondrocytes cultured in agarose. *Osteoarthritis Cartilage.* 4: 275-85, 1996.
 97. Chen, A. C., W. C. Bae, R. M. Schinagl, and R. L. Sah. Depth- and strain-dependent mechanical and electromechanical properties of full-thickness bovine articular cartilage in confined compression. *J Biomech.* 34: 1-12, 2001.
 98. Chen, A. C., M. M. Temple, D. M. Ng, N. Verzijl, J. DeGroot, J. M. TeKoppele, and R. L. Sah. Induction of advanced glycation end products and alterations of the tensile properties of articular cartilage. *Arthritis Rheum.* 46: 3212-7, 2002.
 99. Chen, C. T., N. Burton-Wurster, C. Borden, K. Hueffer, S. E. Bloom, and G. Lust. Chondrocyte necrosis and apoptosis in impact damaged articular cartilage. *J Orthop Res.* 19: 703-11, 2001.
 100. Chen, S. S., Y. H. Falcovitz, R. Schneiderman, A. Maroudas, and R. L. Sah. Depth-dependent compressive properties of normal aged human femoral head articular cartilage: relationship to fixed charge density. *Osteoarthritis Cartilage.* 9: 561-9, 2001.
 101. Chin-Purcell, M. V. and J. L. Lewis. Fracture of articular cartilage. *J Biomech Eng.* 118: 545-56, 1996.
 102. Chrisman, O. D., I. M. Ladenbauer-Bellis, M. Panjabi, and S. Goeltz. 1981 Nicolas Andry Award. The relationship of mechanical trauma and the early biochemical reactions of osteoarthritic cartilage. *Clin Orthop.* 161: 275-84, 1981.
 103. Chuang, S. Y., R. M. Odone, and T. P. Hedman. Effects of exogenous crosslinking on in vitro tensile and compressive moduli of lumbar intervertebral discs. *Clin Biomech (Bristol, Avon).* 22: 14-20, 2007.
 104. Clark, J. M. The organisation of collagen fibrils in the superficial zones of articular cartilage. *J Anat.* 171: 117-30, 1990.

105. Clark, J. M., A. Norman, and H. Notzli. Postnatal development of the collagen matrix in rabbit tibial plateau articular cartilage. *J Anat.* 191 (Pt 2): 215-21, 1997.
106. Clark, J. M. and P. T. Simonian. Scanning electron microscopy of "fibrillated" and "malacic" human articular cartilage: technical considerations. *Microsc Res Tech.* 37: 299-313, 1997.
107. Claus, A., G. Asche, J. Brade, M. Bosing-Schwenkglenks, H. Horschler, J. Muller-Farber, W. Schumm, K. Weise, and H. P. Scharf. [Risk profiling of postoperative complications in 17,644 total knee replacements]. *Unfallchirurg.* 109: 5-12, 2006.
108. Clements, K. M., N. Burton-Wurster, and G. Lust. The spread of cell death from impact damaged cartilage: lack of evidence for the role of nitric oxide and caspases. *Osteoarthritis Cartilage.* 12: 577-85, 2004.
109. Cohen, B., W. M. Lai, and V. C. Mow. A transversely isotropic biphasic model for unconfined compression of growth plate and chondroepiphysis. *J Biomech Eng.* 120: 491-6, 1998.
110. Colwell, C. W., Jr., D. D. D'Lima, H. R. Hoenecke, J. Fronek, P. Pulido, B. A. Morris, C. Chung, D. Resnick, and M. Lotz. In vivo changes after mechanical injury. *Clin Orthop.* 391 Suppl: S116-23, 2001.
111. Costell, M., E. Gustafsson, A. Aszodi, M. Morgelin, W. Bloch, E. Hunziker, K. Addicks, R. Timpl, and R. Fassler. Perlecan maintains the integrity of cartilage and some basement membranes. *J Cell Biol.* 147: 1109-22, 1999.
112. Coventry, M. B., R. D. Beckenbaugh, D. R. Nolan, and D. M. Ilstrup. 2,012 total hip arthroplasties. A study of postoperative course and early complications. *J Bone Joint Surg Am.* 56: 273-84, 1974.
113. Crespo, D., R. A. Asher, R. Lin, K. E. Rhodes, and J. W. Fawcett. How does chondroitinase promote functional recovery in the damaged CNS? *Exp Neurol.* 206: 159-71, 2007.
114. Curl, W. W., J. Krome, E. S. Gordon, J. Rushing, B. P. Smith, and G. G. Poehling. Cartilage injuries: a review of 31,516 knee arthroscopies. *Arthroscopy.* 13: 456-60, 1997.
115. Cylwik, J., K. Kita, M. Barwijuk-Machala, J. Reszec, P. Klimiuk, S. Sierakowski, and S. Sulkowski. The influence of doxycycline on articular cartilage in experimental osteoarthritis induced by iodoacetate. *Folia Morphol (Warsz).* 63: 237-9, 2004.

116. D'Lima, D. D., S. Hashimoto, P. C. Chen, C. W. Colwell, Jr., and M. K. Lotz. Human chondrocyte apoptosis in response to mechanical injury. *Osteoarthritis Cartilage*. 9: 712-9, 2001.
117. D'Lima, D. D., S. Hashimoto, P. C. Chen, C. W. Colwell, Jr., and M. K. Lotz. Impact of mechanical trauma on matrix and cells. *Clin Orthop Relat Res*. 391 Suppl: S90-9, 2001.
118. D'Lima, D. D., S. Hashimoto, P. C. Chen, M. K. Lotz, and C. W. Colwell, Jr. Prevention of chondrocyte apoptosis. *J Bone Joint Surg Am*. 83-A Suppl 2: 25-6, 2001.
119. Dahl, S. L., M. E. Vaughn, and L. E. Niklason. An ultrastructural analysis of collagen in tissue engineered arteries. *Ann Biomed Eng*. 35: 1749-55, 2007.
120. Darling, E. M. and K. A. Athanasiou. Articular cartilage bioreactors and bioprocesses. *Tissue Eng*. 9: 9-26, 2003.
121. Darling, E. M. and K. A. Athanasiou. Biomechanical strategies for articular cartilage regeneration. *Ann Biomed Eng*. 31: 1114-24, 2003.
122. Darling, E. M. and K. A. Athanasiou. Growth factor impact on articular cartilage subpopulations. *Cell Tissue Res*. 322: 463-73, 2005.
123. Darling, E. M. and K. A. Athanasiou. Rapid phenotypic changes in passaged articular chondrocyte subpopulations. *J Orthop Res*. 23: 425-432, 2005.
124. De Ceuninck, F., L. Dassencourt, and P. Anract. The inflammatory side of human chondrocytes unveiled by antibody microarrays. *Biochem Biophys Res Commun*. 323: 960-9, 2004.
125. de Visser, S. K., J. C. Bowden, E. Wentrup-Byrne, L. Rintoul, T. Bostrom, J. M. Pope, and K. I. Momot. Anisotropy of collagen fibre alignment in bovine cartilage: comparison of polarised light microscopy and spatially resolved diffusion-tensor measurements. *Osteoarthritis Cartilage*. 16: 16, 2007.
126. de Visser, S. K., R. W. Crawford, and J. M. Pope. Structural adaptations in compressed articular cartilage measured by diffusion tensor imaging. *Osteoarthritis Cartilage*. 16: 83-9, 2008.
127. Deng, Y., J. C. Hu, and K. A. Athanasiou. Isolation and chondroinduction of a dermis-isolated, aggrecan-sensitive subpopulation with high chondrogenic potential. *Arthritis Rheum*. 56: 168-76, 2007.

128. Derby, M. A. and J. E. Pintar. The histochemical specificity of *Streptomyces* hyaluronidase and chondroitinase ABC. *Histochem J.* 10: 529-47, 1978.
129. Detamore, M. S. and K. A. Athanasiou. Tensile properties of the porcine temporomandibular joint disc. *J Biomech Eng.* 125: 558-65, 2003.
130. DiMicco, M. A., P. Patwari, P. N. Siparsky, S. Kumar, M. A. Pratta, M. W. Lark, Y. J. Kim, and A. J. Grodzinsky. Mechanisms and kinetics of glycosaminoglycan release following in vitro cartilage injury. *Arthritis Rheum.* 50: 840-8, 2004.
131. Dimicco, M. A., J. D. Kisiday, H. Gong, and A. J. Grodzinsky. Structure of pericellular matrix around agarose-embedded chondrocytes. *Osteoarthritis Cartilage.* 15: 1207-16, 2007.
132. Dines, J. S., S. Fealy, E. J. Strauss, A. Allen, E. V. Craig, R. F. Warren, and D. M. Dines. Outcomes analysis of revision total shoulder replacement. *J Bone Joint Surg Am.* 88: 1494-500, 2006.
133. Donohue, J. M., D. Buss, T. R. Oegema, Jr., and R. C. Thompson, Jr. The effects of indirect blunt trauma on adult canine articular cartilage. *J Bone Joint Surg Am.* 65: 948-57, 1983.
134. Donzelli, P. S., R. L. Spilker, G. A. Ateshian, and V. C. Mow. Contact analysis of biphasic transversely isotropic cartilage layers and correlations with tissue failure. *J Biomech.* 32: 1037-47, 1999.
135. Douglas, T., S. Heinemann, S. Bierbaum, D. Scharnweber, and H. Worch. Fibrillogenesis of collagen types I, II, and III with small leucine-rich proteoglycans decorin and biglycan. *Biomacromolecules.* 7: 2388-93, 2006.
136. Dreier, R., A. Opolka, J. Grifka, P. Bruckner, and S. Grassel. Collagen IX-deficiency seriously compromises growth cartilage development in mice. *Matrix Biol.* 30: 30, 2008.
137. Duda, G. N., M. Eilers, L. Loh, J. E. Hoffman, M. Kaab, and K. Schaser. Chondrocyte death precedes structural damage in blunt impact trauma. *Clin Orthop.* 393: 302-9, 2001.
138. Eberhardt, A. W., L. M. Keer, J. L. Lewis, and V. Vithoontien. An analytical model of joint contact. *J Biomech Eng.* 112: 407-13, 1990.
139. Eberhardt, A. W., J. L. Lewis, and L. M. Keer. Normal contact of elastic spheres with two elastic layers as a model of joint articulation. *J Biomech Eng.* 113: 410-7, 1991.

140. Eberhardt, A. W. and S. Peri. A Vertical Surface Breaking Crack in Normal and Sliding Joint Contact. *Journal of Biomechanical Engineering*. 117: 153-155, 1995.
141. Elbjeirami, W. M., E. O. Yonter, B. C. Starcher, and J. L. West. Enhancing mechanical properties of tissue-engineered constructs via lysyl oxidase crosslinking activity. *J Biomed Mater Res A*. 66: 513-21, 2003.
142. Elder, B. D. and K. A. Athanasiou. Effects of confinement on the mechanical properties of self-assembled articular cartilage constructs in the direction orthogonal to the confinement surface. *J Orthop Res*. 26: 238-46, 2008.
143. Elder, B. D. and K. A. Athanasiou. Synergistic and additive effects of hydrostatic pressure and growth factors on tissue formation. *PLoS ONE*. 3: e2341, 2008.
144. Elder, B. D. and K. A. Athanasiou, "Paradigms of Tissue Engineering with Applications to Cartilage Regeneration." In: *Musculoskeletal Tissue Regeneration: Biological Materials and Methods*, edited by W.S. Pietrzak. Totowa, NJ: Humana Press, 2008.
145. Elder, B. D. and K. A. Athanasiou. Systematic assessment of growth factor treatment on biochemical and biomechanical properties of engineered articular cartilage constructs. *Osteoarthritis Cartilage* 2008.
146. Elliott, D. M., F. Guilak, T. P. Vail, J. Y. Wang, and L. A. Setton. Tensile properties of articular cartilage are altered by meniscectomy in a canine model of osteoarthritis. *J Orthop Res*. 17: 503-8, 1999.
147. Elliott, D. M., D. A. Narmoneva, and L. A. Setton. Direct measurement of the Poisson's ratio of human patella cartilage in tension. *J Biomech Eng*. 124: 223-8, 2002.
148. Englert, C., T. Blunk, R. Muller, S. S. von Glasser, J. Baumer, J. Fierlbeck, I. M. Heid, M. Nerlich, and J. Hammer. Bonding of articular cartilage using a combination of biochemical degradation and surface cross-linking. *Arthritis Res Ther*. 9: R47, 2007.
149. Ewers, B. J. and R. C. Haut. Polysulphated glycosaminoglycan treatments can mitigate decreases in stiffness of articular cartilage in a traumatized animal joint. *J Orthop Res*. 18: 756-61, 2000.
150. Ewers, B. J., W. N. Newberry, and R. C. Haut. Chronic softening of cartilage without thickening of underlying bone in a joint trauma model. *J Biomech*. 33: 1689-94, 2000.

151. Ewers, B. J., D. Dvoracek-Driksna, M. W. Orth, and R. C. Haut. The extent of matrix damage and chondrocyte death in mechanically traumatized articular cartilage explants depends on rate of loading. *J Orthop Res.* 19: 779-84, 2001.
152. Ewers, B. J., V. M. Jayaraman, R. F. Banglmaier, and R. C. Haut. Rate of blunt impact loading affects changes in retropatellar cartilage and underlying bone in the rabbit patella. *J Biomech.* 35: 747-55, 2002.
153. Ewers, B. J., B. T. Weaver, and R. C. Haut. Impact orientation can significantly affect the outcome of a blunt impact to the rabbit patellofemoral joint. *J Biomech.* 35: 1591-8, 2002.
154. Ewers, B. J., B. T. Weaver, E. T. Sevensma, and R. C. Haut. Chronic changes in rabbit retro-patellar cartilage and subchondral bone after blunt impact loading of the patellofemoral joint. *J Orthop Res.* 20: 545-50, 2002.
155. Eyre, D. Collagen of articular cartilage. *Arthritis Res.* 4: 30-5, 2002.
156. Eyre, D. R., I. R. Dickson, and K. Van Ness. Collagen cross-linking in human bone and articular cartilage. Age-related changes in the content of mature hydroxypyridinium residues. *Biochem J.* 252: 495-500, 1988.
157. Eyre, D. R., M. A. Weis, and J. J. Wu. Articular cartilage collagen: an irreplaceable framework? *Eur Cell Mater.* 12: 57-63, 2006.
158. Eyre, D. R., M. A. Weis, and J. J. Wu. Advances in collagen cross-link analysis. *Methods.* 45: 65-74, 2008.
159. Farquhar, T., P. R. Dawson, and P. A. Torzilli. A microstructural model for the anisotropic drained stiffness of articular cartilage. *J Biomech Eng.* 112: 414-25, 1990.
160. Federico, S., A. Grillo, G. La Rosa, G. Giaquinta, and W. Herzog. A transversely isotropic, transversely homogeneous microstructural-statistical model of articular cartilage. *J Biomech.* 38: 2008-18, 2005.
161. Fedewa, M. M., T. R. Oegema, Jr., M. H. Schwartz, A. MacLeod, and J. L. Lewis. Chondrocytes in culture produce a mechanically functional tissue. *J Orthop Res.* 16: 227-36, 1998.
162. Fehrenbacher, A., E. Steck, M. Rickert, W. Roth, and W. Richter. Rapid regulation of collagen but not metalloproteinase 1, 3, 13, 14 and tissue inhibitor of metalloproteinase 1, 2, 3 expression in response to mechanical loading of cartilage explants in vitro. *Arch Biochem Biophys.* 410: 39-47, 2003.

163. Felson, D. T., R. C. Lawrence, P. A. Dieppe, R. Hirsch, C. G. Helmick, J. M. Jordan, R. S. Kington, N. E. Lane, M. C. Nevitt, Y. Zhang, M. Sowers, T. McAlindon, T. D. Spector, A. R. Poole, S. Z. Yanovski, G. Ateshian, L. Sharma, J. A. Buckwalter, K. D. Brandt, and J. F. Fries. Osteoarthritis: new insights. Part 1: the disease and its risk factors. *Ann Intern Med.* 133: 635-46, 2000.
164. Ferdous, Z., V. M. Wei, R. Iozzo, M. Hook, and K. J. Grande-Allen. Decorin-transforming Growth Factor- Interaction Regulates Matrix Organization and Mechanical Characteristics of Three-dimensional Collagen Matrices. *J Biol Chem.* 282: 35887-98, 2007.
165. Filidoro, L., O. Dietrich, J. Weber, E. Rauch, T. Oerther, M. Wick, M. F. Reiser, and C. Glaser. High-resolution diffusion tensor imaging of human patellar cartilage: feasibility and preliminary findings. *Magn Reson Med.* 53: 993-8, 2005.
166. Finlay, J. B. and R. U. Repo. Instrumentation and procedure for the controlled impact of articular cartilage. *IEEE Trans Biomed Eng.* 25: 34-9, 1978.
167. Finlay, J. B. and R. U. Repo. Impact characteristics of articular cartilage. *ISA Trans.* 17: 29-34, 1978.
168. Fisher, L. W., J. T. Stubbs, 3rd, and M. F. Young. Antisera and cDNA probes to human and certain animal model bone matrix noncollagenous proteins. *Acta Orthop Scand Suppl.* 266: 61-5, 1995.
169. Flachsman, E. R., N. D. Broom, and A. Oloyede. A biomechanical investigation of unconstrained shear failure of the osteochondral region under impact loading. *Clin Biomech (Bristol, Avon).* 10: 156-165, 1995.
170. Flechtenmacher, J., K. Huch, E. J. Thonar, J. A. Mollenhauer, S. R. Davies, T. M. Schmid, W. Puhl, T. K. Sampath, M. B. Aydelotte, and K. E. Kuettner. Recombinant human osteogenic protein 1 is a potent stimulator of the synthesis of cartilage proteoglycans and collagens by human articular chondrocytes. *Arthritis Rheum.* 39: 1896-904, 1996.
171. Foolen, J., C. van Donkelaar, N. Nowlan, P. Murphy, R. Huiskes, and K. Ito. Collagen orientation in periosteum and perichondrium is aligned with preferential directions of tissue growth. *J Orthop Res.* 26: 1263-8, 2008.
172. Fortier, L. A., A. J. Nixon, H. O. Mohammed, and G. Lust. Altered biological activity of equine chondrocytes cultured in a three-dimensional fibrin matrix and supplemented with transforming growth factor beta-1. *Am J Vet Res.* 58: 66-70, 1997.

173. Fortier, L. A., H. O. Mohammed, G. Lust, and A. J. Nixon. Insulin-like growth factor-I enhances cell-based repair of articular cartilage. *J Bone Joint Surg Br.* 84: 276-88, 2002.
174. Fortin, M., J. Soulhat, A. Shirazi-Adl, E. B. Hunziker, and M. D. Buschmann. Unconfined compression of articular cartilage: nonlinear behavior and comparison with a fibril-reinforced biphasic model. *J Biomech Eng.* 122: 189-95, 2000.
175. Fraser, S. A., A. Crawford, A. Frazer, S. Dickinson, A. P. Hollander, I. M. Brook, and P. V. Hatton. Localization of type VI collagen in tissue-engineered cartilage on polymer scaffolds. *Tissue Eng.* 12: 569-77, 2006.
176. Freed, L. E., A. P. Hollander, I. Martin, J. R. Barry, R. Langer, and G. Vunjak-Novakovic. Chondrogenesis in a cell-polymer-bioreactor system. *Exp Cell Res.* 240: 58-65, 1998.
177. Frenkel, S. R. and P. E. Di Cesare. Scaffolds for articular cartilage repair. *Ann Biomed Eng.* 32: 26-34, 2004.
178. Front, P., F. Aprile, D. R. Mitrovic, and D. A. Swann. Age-related changes in the synthesis of matrix macromolecules by bovine articular cartilage. *Connect Tissue Res.* 19: 121-33, 1989.
179. Fung, Y. C., *Biomechanics Mechanical Properties of Living Tissues*. 2nd ed. 1993, New York: Springer Verlag.
180. Furukawa, K. S., H. Suenaga, K. Toita, A. Numata, J. Tanaka, T. Ushida, Y. Sakai, and T. Tateishi. Rapid and large-scale formation of chondrocyte aggregates by rotational culture. *Cell Transplant.* 12: 475-9, 2003.
181. Fuss, M., E. M. Ehlers, M. Russlies, J. Rohwedel, and P. Behrens. Characteristics of human chondrocytes, osteoblasts and fibroblasts seeded onto a type I/III collagen sponge under different culture conditions. A light, scanning and transmission electron microscopy study. *Ann Anat.* 182: 303-10, 2000.
182. Galera, P., F. Redini, D. Vivien, J. Bonaventure, H. Penfornis, G. Loyau, and J. P. Pujol. Effect of transforming growth factor-beta 1 (TGF-beta 1) on matrix synthesis by monolayer cultures of rabbit articular chondrocytes during the dedifferentiation process. *Exp Cell Res.* 200: 379-92, 1992.
183. Garcia, J. J., N. J. Altiero, and R. C. Haut. An approach for the stress analysis of transversely isotropic biphasic cartilage under impact load. *J Biomech Eng.* 120: 608-13, 1998.

184. Garcia, J. J., N. J. Altiero, and R. C. Haut. Estimation of in situ elastic properties of biphasic cartilage based on a transversely isotropic hypo-elastic model. *J Biomech Eng.* 122: 1-8, 2000.
185. Garcia, J. J. and D. H. Cortes. A biphasic viscohyperelastic fibril-reinforced model for articular cartilage: formulation and comparison with experimental data. *J Biomech.* 40: 1737-44, 2007.
186. Garciadiego-Cazares, D., C. Rosales, M. Katoh, and J. Chimal-Monroy. Coordination of chondrocyte differentiation and joint formation by alpha5beta1 integrin in the developing appendicular skeleton. *Development.* 131: 4735-42, 2004.
187. Gelse, K., S. Soder, W. Eger, T. Diemtar, and T. Aigner. Osteophyte development--molecular characterization of differentiation stages. *Osteoarthritis Cartilage.* 11: 141-8, 2003.
188. Gelse, K., K. von der Mark, T. Aigner, J. Park, and H. Schneider. Articular cartilage repair by gene therapy using growth factor-producing mesenchymal cells. *Arthritis Rheum.* 48: 430-41, 2003.
189. Gemmiti, C. V. and R. E. Guldberg. Fluid flow increases type II collagen deposition and tensile mechanical properties in bioreactor-grown tissue-engineered cartilage. *Tissue Eng.* 12: 469-79, 2006.
190. Gerber, B. E., D. Robinson, Z. Nevo, T. Brosh, H. Ash, A. Yaron, and D. Aviezer. Mechanical resistance of biological repair cartilage: comparative in vivo tests of different surgical repair procedures. *Int J Artif Organs.* 25: 1109-15, 2002.
191. Gill, G. S., D. Mills, and A. B. Joshi. Mortality following primary total knee arthroplasty. *J Bone Joint Surg Am.* 85-A: 432-5, 2003.
192. Girkontaite, I., S. Frischholz, P. Lammi, K. Wagner, B. Swoboda, T. Aigner, and K. Von der Mark. Immunolocalization of type X collagen in normal fetal and adult osteoarthritic cartilage with monoclonal antibodies. *Matrix Biol.* 15: 231-8, 1996.
193. Glasson, S. S., R. Askew, B. Sheppard, B. Carito, T. Blanchet, H. L. Ma, C. R. Flannery, D. Peluso, K. Kanki, Z. Yang, M. K. Majumdar, and E. A. Morris. Deletion of active ADAMTS5 prevents cartilage degradation in a murine model of osteoarthritis. *Nature.* 434: 644-8, 2005.
194. Golub, L., R. Greenwald, N. Ramamurthy, S. Zucker, L. Ramsammy, and T. McNamara. Tetracyclines (TCs) inhibit matrix metalloproteinases (MMPs): in vivo effects in arthritic and diabetic rats and new in vitro studies. *Matrix Suppl.* 1: 315-6, 1992.

195. Golub, L. M., H. M. Lee, M. E. Ryan, W. V. Giannobile, J. Payne, and T. Sorsa. Tetracyclines inhibit connective tissue breakdown by multiple non-antimicrobial mechanisms. *Adv Dent Res.* 12: 12-26, 1998.
196. Graham, H. K., D. F. Holmes, R. B. Watson, and K. E. Kadler. Identification of collagen fibril fusion during vertebrate tendon morphogenesis. The process relies on unipolar fibrils and is regulated by collagen-proteoglycan interaction. *J Mol Biol.* 295: 891-902, 2000.
197. Grande, D. A., C. Halberstadt, G. Naughton, R. Schwartz, and R. Manji. Evaluation of matrix scaffolds for tissue engineering of articular cartilage grafts. *J Biomed Mater Res.* 34: 211-20, 1997.
198. Gratz, K. R., V. W. Wong, A. C. Chen, L. A. Fortier, A. J. Nixon, and R. L. Sah. Biomechanical assessment of tissue retrieved after in vivo cartilage defect repair: tensile modulus of repair tissue and integration with host cartilage. *J Biomech.* 39: 138-46, 2006.
199. Green, D. M., P. C. Noble, J. S. Ahuero, and H. H. Birdsall. Cellular events leading to chondrocyte death after cartilage impact injury. *Arthritis Rheum.* 54: 1509-17, 2006.
200. Greenebaum, B., K. Blossfield, J. Hannig, C. S. Carrillo, M. A. Beckett, R. R. Weichselbaum, and R. C. Lee. Poloxamer 188 prevents acute necrosis of adult skeletal muscle cells following high-dose irradiation. *Burns.* 30: 539-47, 2004.
201. Greenwald, R. A., L. M. Golub, B. Lavietes, N. S. Ramamurthy, B. Gruber, R. S. Laskin, and T. F. McNamara. Tetracyclines inhibit human synovial collagenase in vivo and in vitro. *J Rheumatol.* 14: 28-32, 1987.
202. Greenwald, R. A., S. A. Moak, N. S. Ramamurthy, and L. M. Golub. Tetracyclines suppress matrix metalloproteinase activity in adjuvant arthritis and in combination with flurbiprofen, ameliorate bone damage. *J Rheumatol.* 19: 927-38, 1992.
203. Greenwald, R. A., L. M. Golub, N. S. Ramamurthy, M. Chowdhury, S. A. Moak, and T. Sorsa. In vitro sensitivity of the three mammalian collagenases to tetracycline inhibition: relationship to bone and cartilage degradation. *Bone.* 22: 33-8, 1998.
204. Gregory, K. E., J. T. Oxford, Y. Chen, J. E. Gambee, S. P. Gygi, R. Aebbersold, P. J. Neame, D. E. Mechling, H. P. Bachinger, and N. P. Morris. Structural organization of distinct domains within the non-collagenous N-terminal region of collagen type XI. *J Biol Chem.* 275: 11498-506, 2000.

205. Gu, W. Y. and H. Yao. Effects of hydration and fixed charge density on fluid transport in charged hydrated soft tissues. *Ann Biomed Eng.* 31: 1162-70, 2003.
206. Guerne, P. A., A. Sublet, and M. Lotz. Growth factor responsiveness of human articular chondrocytes: distinct profiles in primary chondrocytes, subcultured chondrocytes, and fibroblasts. *J Cell Physiol.* 158: 476-84, 1994.
207. Guilak, F., A. Ratcliffe, and V. C. Mow. Chondrocyte deformation and local tissue strain in articular cartilage: a confocal microscopy study. *J Orthop Res.* 13: 410-21, 1995.
208. Guilak, F., W. R. Jones, H. P. Ting-Beall, and G. M. Lee. The deformation behavior and mechanical properties of chondrocytes in articular cartilage. *Osteoarthritis Cartilage.* 7: 59-70, 1999.
209. Guilak, F. The deformation behavior and viscoelastic properties of chondrocytes in articular cartilage. *Biorheology.* 37: 27-44, 2000.
210. Guilak, F. and V. C. Mow. The mechanical environment of the chondrocyte: a biphasic finite element model of cell-matrix interactions in articular cartilage. *J Biomech.* 33: 1663-73, 2000.
211. Guilak, F., J. R. Tedrow, and R. Burgkart. Viscoelastic properties of the cell nucleus. *Biochem Biophys Res Commun.* 269: 781-6, 2000.
212. Guilak, F., B. Fermor, F. J. Keefe, V. B. Kraus, S. A. Olson, D. S. Pisetsky, L. A. Setton, and J. B. Weinberg. The role of biomechanics and inflammation in cartilage injury and repair. *Clin Orthop Relat Res:* 17-26, 2004.
213. Guilak, F., L. G. Alexopoulos, M. L. Upton, I. Youn, J. B. Choi, L. Cao, L. A. Setton, and M. A. Haider. The pericellular matrix as a transducer of biomechanical and biochemical signals in articular cartilage. *Ann N Y Acad Sci.* 1068: 498-512, 2006.
214. Hagiwara, H., C. Schroter-Kermani, and H. J. Merker. Localization of collagen type VI in articular cartilage of young and adult mice. *Cell Tissue Res.* 272: 155-60, 1993.
215. Hall, A. C. Differential effects of hydrostatic pressure on cation transport pathways of isolated articular chondrocytes. *J Cell Physiol.* 178: 197-204, 1999.
216. Hasler, E. M., W. Herzog, J. Z. Wu, W. Muller, and U. Wyss. Articular cartilage biomechanics: theoretical models, material properties, and biosynthetic response. *Crit Rev Biomed Eng.* 27: 415-88, 1999.

217. Haut, R. C. and R. W. Little. A constitutive equation for collagen fibers. *J Biomech.* 5: 423-30, 1972.
218. Haut, R. C. Contact pressures in the patellofemoral joint during impact loading on the human flexed knee. *J Orthop Res.* 7: 272-80, 1989.
219. Hayman, D. M., T. J. Blumberg, C. C. Scott, and K. A. Athanasiou. The effects of isolation on chondrocyte gene expression. *Tissue Eng.* 12: 2573-81, 2006.
220. Hedbom, E., P. Antonsson, A. Hjerpe, D. Aeschlimann, M. Paulsson, E. Rosa-Pimentel, Y. Sommarin, M. Wendel, A. Oldberg, and D. Heinegard. Cartilage matrix proteins. An acidic oligomeric protein (COMP) detected only in cartilage. *J Biol Chem.* 267: 6132-6, 1992.
221. Hedbom, E. and H. J. Hauselmann. Molecular aspects of pathogenesis in osteoarthritis: the role of inflammation. *Cell Mol Life Sci.* 59: 45-53, 2002.
222. Helmick, C. G., D. T. Felson, R. C. Lawrence, S. Gabriel, R. Hirsch, C. K. Kwoh, M. H. Liang, H. M. Kremers, M. D. Mayes, P. A. Merkel, S. R. Pillemer, J. D. Reveille, and J. H. Stone. Estimates of the prevalence of arthritis and other rheumatic conditions in the United States. Part I. *Arthritis Rheum.* 58: 15-25, 2008.
223. Henshaw, D. R., E. Attia, M. Bhargava, and J. A. Hannafin. Canine ACL fibroblast integrin expression and cell alignment in response to cyclic tensile strain in three-dimensional collagen gels. *J Orthop Res.* 24: 481-90, 2006.
224. Henson, F. M., E. A. Bowe, and M. E. Davies. Promotion of the intrinsic damage-repair response in articular cartilage by fibroblastic growth factor-2. *Osteoarthritis Cartilage.* 13: 537-44, 2005.
225. Hering, T. M., J. Kollar, T. D. Huynh, J. B. Varelans, and L. J. Sandell. Modulation of extracellular matrix gene expression in bovine high-density chondrocyte cultures by ascorbic acid and enzymatic resuspension. *Arch Biochem Biophys.* 314: 90-8, 1994.
226. Hoben, G. M., J. C. Hu, R. A. James, and K. A. Athanasiou. Self-assembly of fibrochondrocytes and chondrocytes for tissue engineering of the knee meniscus. *Tissue Eng.* 13: 939-46, 2007.
227. Hoben, G. M. and K. A. Athanasiou. Creating a spectrum of fibrocartilages through different cell sources and biochemical stimuli. *Biotechnol Bioeng.* 100: 587-98, 2008.
228. Hollander, A. P., S. C. Dickinson, T. J. Sims, P. Brun, R. Cortivo, E. Kon, M. Marcacci, S. Zanasi, A. Borriore, C. De Luca, A. Pavesio, C. Soranzo,

- and G. Abatangelo. Maturation of tissue engineered cartilage implanted in injured and osteoarthritic human knees. *Tissue Eng.* 12: 1787-98, 2006.
229. Holmes, D. F., H. K. Graham, J. A. Trotter, and K. E. Kadler. STEM/TEM studies of collagen fibril assembly. *Micron.* 32: 273-85, 2001.
 230. Hu, J. C. and K. A. Athanasiou, "Structure and function of articular cartilage." In: *Handbook of Histology Methods for Bone and Cartilage*, edited by Y.H. An and K.L. Martin. Totowa, NJ: Humana Press Inc., 2003.
 231. Hu, J. C. and K. A. Athanasiou. A self-assembling process in articular cartilage tissue engineering. *Tissue Eng.* 12: 969-79, 2006.
 232. Hu, J. C. and K. A. Athanasiou. The effects of intermittent hydrostatic pressure on self-assembled articular cartilage constructs. *Tissue Eng.* 12: 1337-44, 2006.
 233. Huang, A. H., M. Yeger-McKeever, A. Stein, and R. L. Mauck. Tensile properties of engineered cartilage formed from chondrocyte- and MSC-laden hydrogels. *Osteoarthritis Cartilage.* 16: 1074-82, 2008.
 234. Huang, C. Y., V. C. Mow, and G. A. Ateshian. The role of flow-independent viscoelasticity in the biphasic tensile and compressive responses of articular cartilage. *J Biomech Eng.* 123: 410-7, 2001.
 235. Huang, C. Y., M. A. Soltz, M. Kopacz, V. C. Mow, and G. A. Ateshian. Experimental verification of the roles of intrinsic matrix viscoelasticity and tension-compression nonlinearity in the biphasic response of cartilage. *J Biomech Eng.* 125: 84-93, 2003.
 236. Huang, C. Y., A. Stankiewicz, G. A. Ateshian, and V. C. Mow. Anisotropy, inhomogeneity, and tension-compression nonlinearity of human glenohumeral cartilage in finite deformation. *J Biomech.* 38: 799-809, 2005.
 237. Hughes, L. C., C. W. Archer, and I. ap Gwynn. The ultrastructure of mouse articular cartilage: collagen orientation and implications for tissue functionality. A polarised light and scanning electron microscope study and review. *Eur Cell Mater.* 9: 68-84, 2005.
 238. Hung, C. T., R. L. Mauck, C. C. Wang, E. G. Lima, and G. A. Ateshian. A paradigm for functional tissue engineering of articular cartilage via applied physiologic deformational loading. *Ann Biomed Eng.* 32: 35-49, 2004.
 239. Hunter, W. Of the structure and diseases of articulating cartilages. *Philos Trans R Soc.* 43: 514-521, 1743.

240. Hunziker, E. B. and E. Kapfinger. Removal of proteoglycans from the surface of defects in articular cartilage transiently enhances coverage by repair cells. *J Bone Joint Surg Br.* 80: 144-50, 1998.
241. Hunziker, E. B. Articular cartilage repair: are the intrinsic biological constraints undermining this process insuperable? *Osteoarthritis Cartilage.* 7: 15-28, 1999.
242. Huser, C. A. and M. E. Davies. Validation of an in vitro single-impact load model of the initiation of osteoarthritis-like changes in articular cartilage. *J Orthop Res.* 24: 725-32, 2006.
243. Huser, C. A., M. Peacock, and M. E. Davies. Inhibition of caspase-9 reduces chondrocyte apoptosis and proteoglycan loss following mechanical trauma. *Osteoarthritis Cartilage.* 14: 1002-10, 2006.
244. Huser, C. A. and M. E. Davies. Calcium signaling leads to mitochondrial depolarization in impact-induced chondrocyte death in equine articular cartilage explants. *Arthritis Rheum.* 56: 2322-34, 2007.
245. Huser, C. A. and M. E. Davies. Effect of a glucosamine derivative on impact-induced chondrocyte apoptosis in vitro. A preliminary report. *Osteoarthritis Cartilage.* 16: 125-8, 2008.
246. Iqbal, J., J. L. Bird, A. P. Hollander, and M. T. Bayliss. Effect of matrix depleting agents on the expression of chondrocyte metabolism by equine chondrocytes. *Res Vet Sci.* 77: 249-56, 2004.
247. Jackson, D. W. and T. M. Simon. Tissue engineering principles in orthopaedic surgery. *Clin Orthop Relat Res.* S31-45, 1999.
248. Jackson, D. W., M. J. Scheer, and T. M. Simon. Cartilage substitutes: overview of basic science and treatment options. *J Am Acad Orthop Surg.* 9: 37-52, 2001.
249. Jackson, D. W., T. M. Simon, and H. M. Aberman. Symptomatic articular cartilage degeneration: the impact in the new millennium. *Clin Orthop.* 391 Suppl: S14-25, 2001.
250. Jacobsson, S. A., K. Djerf, and O. Wahlstrom. A comparative study between McKee-Farrar and Charnley arthroplasty with long-term follow-up periods. *J Arthroplasty.* 5: 9-14, 1990.
251. Jacobsson, S. A., K. Djerf, and O. Wahlstrom. Twenty-year results of McKee-Farrar versus Charnley prosthesis. *Clin Orthop Relat Res.* S60-8, 1996.

- 252. Janusz, M. J., E. B. Hookfin, S. A. Heitmeyer, J. F. Woessner, A. J. Freemont, J. A. Hoyland, K. K. Brown, L. C. Hsieh, N. G. Almstead, B. De, M. G. Natchus, S. Pikul, and Y. O. Taiwo. Moderation of iodoacetate-induced experimental osteoarthritis in rats by matrix metalloproteinase inhibitors. *Osteoarthritis Cartilage*. 9: 751-60, 2001.
- 253. Jeffrey, J. E., D. W. Gregory, and R. M. Aspden. Matrix damage and chondrocyte viability following a single impact load on articular cartilage. *Arch Biochem Biophys*. 322: 87-96, 1995.
- 254. Jeffrey, J. E., L. A. Thomson, and R. M. Aspden. Matrix loss and synthesis following a single impact load on articular cartilage in vitro. *Biochim Biophys Acta*. 1334: 223-32, 1997.
- 255. Jeffrey, J. E. and R. M. Aspden. The biophysical effects of a single impact load on human and bovine articular cartilage. *Proc Inst Mech Eng [H]*. 220: 677-86, 2006.
- 256. Jeffrey, J. E. and R. M. Aspden. Cyclooxygenase inhibition lowers prostaglandin E2 release from articular cartilage and reduces apoptosis but not proteoglycan degradation following an impact load in vitro. *Arthritis Res Ther*. 9: R129, 2007.
- 257. Jenniskens, Y. M., W. Koevoet, A. C. de Bart, H. Weinans, H. Jahr, J. A. Verhaar, J. DeGroot, and G. J. van Osch. Biochemical and functional modulation of the cartilage collagen network by IGF1, TGFbeta2 and FGF2. *Osteoarthritis Cartilage*. 14: 1136-46, 2006.
- 258. Jo, C. H., E. M. Kim, H. J. Ahn, H. J. Kim, S. C. Seong, and M. C. Lee. Degree of degeneration and chondroitinase ABC treatment of human articular cartilage affect adhesion of chondrocytes. *Tissue Eng*. 12: 167-76, 2006.
- 259. Joshi, A. B., M. L. Porter, I. A. Trail, L. P. Hunt, J. C. Murphy, and K. Hardinge. Long-term results of Charnley low-friction arthroplasty in young patients. *J Bone Joint Surg Br*. 75: 616-23, 1993.
- 260. Julkunen, P., P. Kiviranta, W. Wilson, J. S. Jurvelin, and R. K. Korhonen. Characterization of articular cartilage by combining microscopic analysis with a fibril-reinforced finite-element model. *J Biomech*. 40: 1862-70, 2007.
- 261. Julkunen, P., R. K. Korhonen, W. Herzog, and J. S. Jurvelin. Uncertainties in indentation testing of articular cartilage: a fibril-reinforced poroviscoelastic study. *Med Eng Phys*. 30: 506-15, 2008.
- 262. Junqueira, L. C., G. Bignolas, and R. R. Brentani. Picrosirius staining plus polarization microscopy, a specific method for collagen detection in tissue sections. *Histochem J*. 11: 447-55, 1979.

263. Junquiera, L. C., J. Carneiro, and R. O. Kelley, *Basic Histology*. Ninth ed. 1998, Stamford, Connecticut: Appleton and Lange. 494.
264. Jurvelin, J. S., D. J. Muller, M. Wong, D. Studer, A. Engel, and E. B. Hunziker. Surface and subsurface morphology of bovine humeral articular cartilage as assessed by atomic force and transmission electron microscopy. *J Struct Biol*. 117: 45-54, 1996.
265. Kaab, M. J., I. A. Gwynn, and H. P. Notzli. Collagen fibre arrangement in the tibial plateau articular cartilage of man and other mammalian species. *J Anat*. 193 (Pt 1): 23-34, 1998.
266. Kafienah, W., F. L. Cheung, T. Sims, I. Martin, S. Miot, C. V. Ruhland, P. J. Roughley, and A. P. Hollander. Lumican inhibits collagen deposition in tissue engineered cartilage. *Matrix Biol* 2008.
267. Kafienah, W., F. L. Cheung, T. Sims, I. Martin, S. Miot, C. V. Ruhland, P. J. Roughley, and A. P. Hollander. Lumican inhibits collagen deposition in tissue engineered cartilage. *Matrix Biol*. 27: 526-34, 2008.
268. Kafka, V. Surface fissures in articular cartilage: new concepts, hypotheses and modeling. *Clin Biomech (Bristol, Avon)*. 17: 73-80, 2002.
269. Kandel, R. A., H. Chen, J. Clark, and R. Renlund. Transplantation of cartilagenous tissue generated in vitro into articular joint defects. *Artif Cells Blood Substit Immobil Biotechnol*. 23: 565-77, 1995.
270. Kelly, D. J., A. Crawford, S. C. Dickinson, T. J. Sims, J. Mundy, A. P. Hollander, P. J. Prendergast, and P. V. Hatton. Biochemical markers of the mechanical quality of engineered hyaline cartilage. *J Mater Sci Mater Med*. 18: 273-81, 2007.
271. Kelly, P. A. and J. J. O'Connor. Transmission of rapidly applied loads through articular cartilage. Part 2: Cracked cartilage. *Proc Inst Mech Eng [H]*. 210: 39-49, 1996.
272. Kelly, P. A. and J. J. O'Connor. Transmission of rapidly applied loads through articular cartilage. Part 1: Uncracked cartilage. *Proc Inst Mech Eng [H]*. 210: 27-37, 1996.
273. Kelly, T. A., K. W. Ng, C. C. Wang, G. A. Ateshian, and C. T. Hung. Spatial and temporal development of chondrocyte-seeded agarose constructs in free-swelling and dynamically loaded cultures. *J Biomech*. 39: 1489-97, 2006.
274. Kempson, G. E., H. Muir, C. Pollard, and M. Tuke. The tensile properties of the cartilage of human femoral condyles related to the content of

- collagen and glycosaminoglycans. *Biochim Biophys Acta*. 297: 456-72, 1973.
275. Kerboull, L., M. Hamadouche, J. P. Courpied, and M. Kerboull. Long-term results of Charnley-Kerboull hip arthroplasty in patients younger than 50 years. *Clin Orthop Relat Res*: 112-8, 2004.
 276. Kevorkian, L., D. A. Young, C. Darrah, S. T. Donell, L. Shepstone, S. Porter, S. M. Brockbank, D. R. Edwards, A. E. Parker, and I. M. Clark. Expression profiling of metalloproteinases and their inhibitors in cartilage. *Arthritis Rheum*. 50: 131-41, 2004.
 277. Khalsa, P. S. and S. R. Eisenberg. Compressive behavior of articular cartilage is not completely explained by proteoglycan osmotic pressure. *J Biomech*. 30: 589-94, 1997.
 278. Kim, H. J. and T. Kirsch. Collagen/annexin V interactions regulate chondrocyte mineralization. *J Biol Chem*. 283: 10310-7, 2008.
 279. Kim, Y. J., R. L. Sah, J. Y. Doong, and A. J. Grodzinsky. Fluorometric assay of DNA in cartilage explants using Hoechst 33258. *Anal Biochem*. 174: 168-76, 1988.
 280. Kirsch, T. and K. von der Mark. Isolation of human type X collagen and immunolocalization in fetal human cartilage. *Eur J Biochem*. 196: 575-80, 1991.
 281. Kisiday, J. D., B. Kurz, M. A. DiMicco, and A. J. Grodzinsky. Evaluation of medium supplemented with insulin-transferrin-selenium for culture of primary bovine calf chondrocytes in three-dimensional hydrogel scaffolds. *Tissue Eng*. 11: 141-51, 2005.
 282. Kiviranta, P., J. Rieppo, R. K. Korhonen, P. Julkunen, J. Toyras, and J. S. Jurvelin. Collagen network primarily controls Poisson's ratio of bovine articular cartilage in compression. *J Orthop Res*. 24: 690-9, 2006.
 283. Koay, E. J., G. M. Hoben, and K. A. Athanasiou. Tissue engineering with chondrogenically differentiated human embryonic stem cells. *Stem Cells*. 25: 2183-90, 2007.
 284. Koay, E. J., G. Ofek, and K. A. Athanasiou. Effects of TGF-beta1 and IGF-I on the compressibility, biomechanics, and strain-dependent recovery behavior of single chondrocytes. *J Biomech*. 41: 1044-52, 2008.
 285. Komistek, R. D., T. R. Kane, M. Mahfouz, J. A. Ochoa, and D. A. Dennis. Knee mechanics: a review of past and present techniques to determine in vivo loads. *J Biomech*. 38: 215-28, 2005.

286. Korhonen, R. K., M. S. Laasanen, J. Toyras, R. Lappalainen, H. J. Helminen, and J. S. Jurvelin. Fibril reinforced poroelastic model predicts specifically mechanical behavior of normal, proteoglycan depleted and collagen degraded articular cartilage. *J Biomech.* 36: 1373-9, 2003.
287. Kovach, I. S. and K. A. Athanasiou. Small-angle HeNe laser light scatter and the compressive modulus of articular cartilage. *J Orthop Res.* 15: 437-41, 1997.
288. Krueger, J. A., P. Thisse, B. J. Ewers, D. Dvoracek-Driksna, M. W. Orth, and R. C. Haut. The extent and distribution of cell death and matrix damage in impacted chondral explants varies with the presence of underlying bone. *J Biomech Eng.* 125: 114-9, 2003.
289. Kuo, C. H. and L. M. Keer. Contact Stress and Fracture Analysis of Articular Cartilage. *Bimod Eng Appl Basis Comm.* 5: 515-521, 1993.
290. Kuo, S. M., Y. J. Wang, C. L. Weng, H. E. Lu, and S. J. Chang. Influence of alginate on type II collagen fibrillogenesis. *J Mater Sci Mater Med.* 16: 525-31, 2005.
291. Kurtz, S., F. Mowat, K. Ong, N. Chan, E. Lau, and M. Halpern. Prevalence of primary and revision total hip and knee arthroplasty in the United States from 1990 through 2002. *J Bone Joint Surg Am.* 87: 1487-97, 2005.
292. Kurtz, S., K. Ong, E. Lau, F. Mowat, and M. Halpern. Projections of primary and revision hip and knee arthroplasty in the United States from 2005 to 2030. *J Bone Joint Surg Am.* 89: 780-5, 2007.
293. Kurz, B., M. Jin, P. Patwari, D. M. Cheng, M. W. Lark, and A. J. Grodzinsky. Biosynthetic response and mechanical properties of articular cartilage after injurious compression. *J Orthop Res.* 19: 1140-6, 2001.
294. Kurz, B., A. K. Lemke, J. Fay, T. Pufe, A. J. Grodzinsky, and M. Schunke. Pathomechanisms of cartilage destruction by mechanical injury. *Ann Anat.* 187: 473-85, 2005.
295. Kutner, M. H., C. J. Nachtsheim, J. Neter, and L. William, *Applied Linear Statistical Models*. Fifth ed. 2005, New York, NY: McGraw-Hill. 1396.
296. Kwan, M. K., W. M. Lai, and V. C. Mow. Fundamentals of fluid transport through cartilage in compression. *Ann Biomed Eng.* 12: 537-58, 1984.
297. Laasanen, M. S., J. Toyras, J. Hirvonen, S. Saarakkala, R. K. Korhonen, M. T. Nieminen, I. Kiviranta, and J. S. Jurvelin. Novel mechano-acoustic technique and instrument for diagnosis of cartilage degeneration. *Physiol Meas.* 23: 491-503, 2002.

298. Langsjo, T. K., M. Hyttinen, A. Pelttari, K. Kiraly, J. Arokoski, and H. J. Helminen. Electron microscopic stereological study of collagen fibrils in bovine articular cartilage: volume and surface densities are best obtained indirectly (from length densities and diameters) using isotropic uniform random sampling. *J Anat.* 195 (Pt 2): 281-93, 1999.
299. Laurencin, C. T., A. M. Ambrosio, M. D. Borden, and J. A. Cooper, Jr. Tissue engineering: orthopedic applications. *Annu Rev Biomed Eng.* 1: 19-46, 1999.
300. Lawrence, R. C., C. G. Helmick, F. C. Arnett, R. A. Deyo, D. T. Felson, E. H. Giannini, S. P. Heyse, R. Hirsch, M. C. Hochberg, G. G. Hunder, M. H. Liang, S. R. Pillemer, V. D. Steen, and F. Wolfe. Estimates of the prevalence of arthritis and selected musculoskeletal disorders in the United States. *Arthritis Rheum.* 41: 778-99, 1998.
301. Lawrence, R. C., D. T. Felson, C. G. Helmick, L. M. Arnold, H. Choi, R. A. Deyo, S. Gabriel, R. Hirsch, M. C. Hochberg, G. G. Hunder, J. M. Jordan, J. N. Katz, H. M. Kremers, and F. Wolfe. Estimates of the prevalence of arthritis and other rheumatic conditions in the United States. Part II. *Arthritis Rheum.* 58: 26-35, 2008.
302. Lee, D. A., M. M. Knight, J. F. Bolton, B. D. Idowu, M. V. Kayser, and D. L. Bader. Chondrocyte deformation within compressed agarose constructs at the cellular and sub-cellular levels. *J Biomech.* 33: 81-95, 2000.
303. Lee, J. H., J. B. Fitzgerald, M. A. Dimicco, and A. J. Grodzinsky. Mechanical injury of cartilage explants causes specific time-dependent changes in chondrocyte gene expression. *Arthritis Rheum.* 52: 2386-95, 2005.
304. Lee, M. C., K. L. Sung, M. S. Kurtis, W. H. Akeson, and R. L. Sah. Adhesive force of chondrocytes to cartilage. Effects of chondroitinase ABC. *Clin Orthop Relat Res:* 286-94, 2000.
305. Legler, F. and K. Schwemmler. [Studies on doxycycline levels in human tissues after i.v. administration (author's transl)]. *Arzneimittelforschung.* 25: 1965-7, 1975.
306. Leipzig, N. D. and K. A. Athanasiou. Unconfined creep compression of chondrocytes. *J Biomech.* 38: 77-85, 2005.
307. Leipzig, N. D. and K. A. Athanasiou. Static compression of single chondrocytes catabolically modifies single-cell gene expression. *Biophys J.* 94: 2412-22, 2008.

308. Levin, A., N. Burton-Wurster, C. T. Chen, and G. Lust. Intercellular signaling as a cause of cell death in cyclically impacted cartilage explants. *Osteoarthritis Cartilage*. 9: 702-11, 2001.
309. Levin, A. S., C. T. Chen, and P. A. Torzilli. Effect of tissue maturity on cell viability in load-injured articular cartilage explants. *Osteoarthritis Cartilage*. 13: 488-96, 2005.
310. Lewis, J. L., L. B. Deloria, M. Oyen-Tiesma, R. C. Thompson, M. Ericson, and T. R. Oegema. Cell death after cartilage impact occurs around matrix cracks. *J Orthop Res*. 21: 881-7, 2003.
311. Li, L., A. Shirazi-Adl, and M. D. Buschmann. Investigation of mechanical behavior of articular cartilage by fibril reinforced poroelastic models. *Biorheology*. 40: 227-33, 2003.
312. Li, L. P., J. Soulhat, M. D. Buschmann, and A. Shirazi-Adl. Nonlinear analysis of cartilage in unconfined ramp compression using a fibril reinforced poroelastic model. *Clin Biomech (Bristol, Avon)*. 14: 673-82, 1999.
313. Li, L. P., M. D. Buschmann, and A. Shirazi-Adl. A fibril reinforced nonhomogeneous poroelastic model for articular cartilage: inhomogeneous response in unconfined compression. *J Biomech*. 33: 1533-41, 2000.
314. Li, L. P., M. D. Buschmann, and A. Shirazi-Adl. Strain-rate dependent stiffness of articular cartilage in unconfined compression. *J Biomech Eng*. 125: 161-8, 2003.
315. Li, L. P. and W. Herzog. Strain-rate dependence of cartilage stiffness in unconfined compression: the role of fibril reinforcement versus tissue volume change in fluid pressurization. *J Biomech*. 37: 375-82, 2004.
316. Li, L. P. and W. Herzog. The role of viscoelasticity of collagen fibers in articular cartilage: theory and numerical formulation. *Biorheology*. 41: 181-94, 2004.
317. Li, L. P., R. K. Korhonen, J. Iivarinen, J. S. Jurvelin, and W. Herzog. Fluid pressure driven fibril reinforcement in creep and relaxation tests of articular cartilage. *Med Eng Phys*. 30: 182-9, 2008.
318. Li, X., R. C. Haut, and N. J. Altiero. An analytical model to study blunt impact response of the rabbit P-F joint. *J Biomech Eng*. 117: 485-91, 1995.

319. Lo, M. Y. and H. T. Kim. Chondrocyte apoptosis induced by collagen degradation: inhibition by caspase inhibitors and IGF-1. *J Orthop Res.* 22: 140-4, 2004.
320. Lohmander, L. S., T. Saxne, and D. K. Heinegard. Release of cartilage oligomeric matrix protein (COMP) into joint fluid after knee injury and in osteoarthritis. *Ann Rheum Dis.* 53: 8-13, 1994.
321. Lohmander, L. S., M. Ionescu, H. Jugessur, and A. R. Poole. Changes in joint cartilage aggrecan after knee injury and in osteoarthritis. *Arthritis Rheum.* 42: 534-44, 1999.
322. Lohmander, L. S., A. Ostenberg, M. Englund, and H. Roos. High prevalence of knee osteoarthritis, pain, and functional limitations in female soccer players twelve years after anterior cruciate ligament injury. *Arthritis Rheum.* 50: 3145-52, 2004.
323. Luo, Z. P., Y. L. Sun, T. Fujii, and K. N. An. Single molecule mechanical properties of type II collagen and hyaluronan measured by optical tweezers. *Biorheology.* 41: 247-54, 2004.
324. Lupi, O. Prions in dermatology. *J Am Acad Dermatol.* 46: 790-3, 2002.
325. Malesud, C. J., R. Shuckett, and V. M. Goldberg. Changes in proteoglycans of human osteoarthritic cartilage maintained in explant culture: implications for understanding repair in osteoarthritis. *Scand J Rheumatol Suppl.* 77: 7-12, 1988.
326. Malesud, C. J., R. S. Papay, T. M. Hering, D. Holderbaum, V. M. Goldberg, and T. M. Haqqi. Phenotypic modulation of newly synthesized proteoglycans in human cartilage and chondrocytes. *Osteoarthritis Cartilage.* 3: 227-38, 1995.
327. Maniotis, A. J., C. S. Chen, and D. E. Ingber. Demonstration of mechanical connections between integrins, cytoskeletal filaments, and nucleoplasm that stabilize nuclear structure. *Proc Natl Acad Sci U S A.* 94: 849-54, 1997.
328. Marks, J. D., C. Y. Pan, T. Bushell, W. Cromie, and R. C. Lee. Amphiphilic, tri-block copolymers provide potent membrane-targeted neuroprotection. *Faseb J.* 15: 1107-9, 2001.
329. Martin, I., B. Obradovic, S. Treppo, A. J. Grodzinsky, R. Langer, L. E. Freed, and G. Vunjak-Novakovic. Modulation of the mechanical properties of tissue engineered cartilage. *Biorheology.* 37: 141-7, 2000.
330. Martin, J. A. and J. A. Buckwalter. Post-traumatic osteoarthritis: the role of stress induced chondrocyte damage. *Biorheology.* 43: 517-21, 2006.

331. Maskarinec, S. A., J. Hannig, R. C. Lee, and K. Y. Lee. Direct observation of poloxamer 188 insertion into lipid monolayers. *Biophys J.* 82: 1453-9, 2002.
332. Mauck, R. L., M. A. Soltz, C. C. Wang, D. D. Wong, P. H. Chao, W. B. Valhmu, C. T. Hung, and G. A. Ateshian. Functional tissue engineering of articular cartilage through dynamic loading of chondrocyte-seeded agarose gels. *J Biomech Eng.* 122: 252-60, 2000.
333. McCutchen, C. W. Cartilage is poroelastic, not viscoelastic (including an exact theorem about strain energy and viscous loss, and an order of magnitude relation for equilibration time). *J Biomech.* 15: 325-7, 1982.
334. Meachim, G., D. Denham, I. H. Emery, and P. H. Wilkinson. Collagen alignments and artificial splits at the surface of human articular cartilage. *J Anat.* 118: 101-18, 1974.
335. Meder, R., S. K. de Visser, J. C. Bowden, T. Bostrom, and J. M. Pope. Diffusion tensor imaging of articular cartilage as a measure of tissue microstructure. *Osteoarthritis Cartilage.* 14: 875-81, 2006.
336. Meier, W., R. L. Mizner, R. L. Marcus, L. E. Dibble, C. Peters, and P. C. Lastayo. Total knee arthroplasty: muscle impairments, functional limitations, and recommended rehabilitation approaches. *J Orthop Sports Phys Ther.* 38: 246-56, 2008.
337. Mengshol, J. A., K. S. Mix, and C. E. Brinckerhoff. Matrix metalloproteinases as therapeutic targets in arthritic diseases: bull's-eye or missing the mark? *Arthritis Rheum.* 46: 13-20, 2002.
338. Milentijevic, D., I. F. Rubel, A. S. Liew, D. L. Helfet, and P. A. Torzilli. An in vivo rabbit model for cartilage trauma: a preliminary study of the influence of impact stress magnitude on chondrocyte death and matrix damage. *J Orthop Trauma.* 19: 466-73, 2005.
339. Milentijevic, D. and P. A. Torzilli. Influence of stress rate on water loss, matrix deformation and chondrocyte viability in impacted articular cartilage. *J Biomech.* 38: 493-502, 2005.
340. Minns, R. J. and F. S. Steven. The collagen fibril organization in human articular cartilage. *J Anat.* 123: 437-57, 1977.
341. Moger, C. J., R. Barrett, P. Bleuet, D. A. Bradley, R. E. Ellis, E. M. Green, K. M. Knapp, P. Muthuvelu, and C. P. Winlove. Regional variations of collagen orientation in normal and diseased articular cartilage and subchondral bone determined using small angle X-ray scattering (SAXS). *Osteoarthritis Cartilage.* 15: 682-7, 2007.

342. Morel, V. and T. M. Quinn. Cartilage injury by ramp compression near the gel diffusion rate. *J Orthop Res.* 22: 145-51, 2004.
343. Morel, V. and T. M. Quinn. Short-term changes in cell and matrix damage following mechanical injury of articular cartilage explants and modelling of microphysical mediators. *Biorheology.* 41: 509-19, 2004.
344. Morel, V., A. Mercay, and T. M. Quinn. Prestrain decreases cartilage susceptibility to injury by ramp compression in vitro. *Osteoarthritis Cartilage.* 13: 964-70, 2005.
345. Morrison, E. H., M. W. Ferguson, M. T. Bayliss, and C. W. Archer. The development of articular cartilage: I. The spatial and temporal patterns of collagen types. *J Anat.* 189 (Pt 1): 9-22, 1996.
346. Mow, V. C., S. C. Kuei, W. M. Lai, and C. Armstrong. Biphasic creep and stress relaxation of articular cartilage: theory and experiments. *J Biomech Eng.* 102: 73-84, 1980.
347. Mow, V. C., S. C. Kuei, W. M. Lai, and C. G. Armstrong. Biphasic creep and stress relaxation of articular cartilage in compression? Theory and experiments. *J Biomech Eng.* 102: 73-84, 1980.
348. Mow, V. C., M. C. Gibbs, W. M. Lai, W. B. Zhu, and K. A. Athanasiou. Biphasic indentation of articular cartilage--II. A numerical algorithm and an experimental study. *J Biomech.* 22: 853-61, 1989.
349. Mow, V. C., A. Ratcliffe, and A. R. Poole. Cartilage and diarthrodial joints as paradigms for hierarchical materials and structures. *Biomaterials.* 13: 67-97, 1992.
350. Mrosek, E. H., A. Lahm, C. Erggelet, M. Uhl, H. Kurz, B. Eissner, and J. C. Schagemann. Subchondral bone trauma causes cartilage matrix degeneration: an immunohistochemical analysis in a canine model. *Osteoarthritis Cartilage.* 14: 171-8, 2006.
351. Muir, H., P. Bullough, and A. Maroudas. The distribution of collagen in human articular cartilage with some of its physiological implications. *J Bone Joint Surg Br.* 52: 554-63, 1970.
352. Muragaki, Y., E. C. Mariman, S. E. van Beersum, M. Perala, J. B. van Mourik, M. L. Warman, B. R. Olsen, and B. C. Hamel. A mutation in the gene encoding the alpha 2 chain of the fibril-associated collagen IX, COL9A2, causes multiple epiphyseal dysplasia (EDM2). *Nat Genet.* 12: 103-5, 1996.
353. Mwale, F., E. Tchetina, C. W. Wu, and A. R. Poole. The assembly and remodeling of the extracellular matrix in the growth plate in relationship to

- mineral deposition and cellular hypertrophy: an in situ study of collagens II and IX and proteoglycan. *J Bone Miner Res.* 17: 275-83, 2002.
354. Nabeshima, Y., E. S. Grood, A. Sakurai, and J. H. Herman. Uniaxial tension inhibits tendon collagen degradation by collagenase in vitro. *J Orthop Res.* 14: 123-30, 1996.
 355. Nahir, A. M., D. Shomrat, and M. Awad. Chondroitinase ABC affects the activity of intracellular enzymes in rabbit articular cartilage chondrocytes. *J Rheumatol.* 22: 702-7, 1995.
 356. Nandini, C. D. and K. Sugahara. Role of the sulfation pattern of chondroitin sulfate in its biological activities and in the binding of growth factors. *Adv Pharmacol.* 53: 253-79, 2006.
 357. Natoli, R. M. and K. A. Athanasiou. P188 Reduces Cell Death and IGF-I Reduces GAG Release Following Single-Impact Loading of Articular Cartilage. *J Biomech Eng.* 130: 041012, 2008.
 358. Natoli, R. M., C. M. Revell, and K. A. Athanasiou. *Chondroitinase ABC Treatment Results in Increased Tensile Properties in a Scaffold-less, Serum-free Model of Articular Cartilage Tissue Engineering.* in *Trans Orthopaedic Res.* 2008. San Francisco.
 359. Natoli, R. M., C. C. Scott, and K. A. Athanasiou. Temporal effects of impact on articular cartilage cell death, gene expression, matrix biochemistry, and biomechanics. *Ann Biomed Eng.* 36: 780-92, 2008.
 360. Nehrer, S., H. A. Breinan, A. Ramappa, S. Shortkroff, G. Young, T. Minas, C. B. Sledge, I. V. Yannas, and M. Spector. Canine chondrocytes seeded in type I and type II collagen implants investigated in vitro. *J Biomed Mater Res.* 38: 95-104, 1997.
 361. Nehrer, S., H. A. Breinan, A. Ramappa, H. P. Hsu, T. Minas, S. Shortkroff, C. B. Sledge, I. V. Yannas, and M. Spector. Chondrocyte-seeded collagen matrices implanted in a chondral defect in a canine model. *Biomaterials.* 19: 2313-28, 1998.
 362. Nettles, D. L., S. H. Elder, and J. A. Gilbert. Potential use of chitosan as a cell scaffold material for cartilage tissue engineering. *Tissue Eng.* 8: 1009-16, 2002.
 363. Neumann, L., K. G. Freund, and K. H. Sorensen. Total hip arthroplasty with the Charnley prosthesis in patients fifty-five years old and less. Fifteen to twenty-one-year results. *J Bone Joint Surg Am.* 78: 73-9, 1996.

364. Newberry, W. N., D. K. Zukosky, and R. C. Haut. Subfracture insult to a knee joint causes alterations in the bone and in the functional stiffness of overlying cartilage. *J Orthop Res.* 15: 450-5, 1997.
365. Newberry, W. N., J. J. Garcia, C. D. Mackenzie, C. E. Decamp, and R. C. Haut. Analysis of acute mechanical insult in an animal model of post-traumatic osteoarthritis. *J Biomech Eng.* 120: 704-9, 1998.
366. Newberry, W. N., C. D. Mackenzie, and R. C. Haut. Blunt impact causes changes in bone and cartilage in a regularly exercised animal model. *J Orthop Res.* 16: 348-54, 1998.
367. Newman, A. P. Articular cartilage repair. *Am J Sports Med.* 26: 309-24, 1998.
368. Ng, K. W., R. L. Mauck, L. Y. Statman, E. Y. Lin, G. A. Ateshian, and C. T. Hung. Dynamic deformational loading results in selective application of mechanical stimulation in a layered, tissue-engineered cartilage construct. *Biorheology.* 43: 497-507, 2006.
369. Ng, K. W., J. D. Saliman, E. Y. Lin, L. Y. Statman, L. E. Kugler, S. B. Lo, G. A. Ateshian, and C. T. Hung. Culture duration modulates collagen hydrolysate-induced tissue remodeling in chondrocyte-seeded agarose hydrogels. *Ann Biomed Eng.* 35: 1914-23, 2007.
370. Nich, C., J. P. Courpied, M. Kerboull, M. Postel, and M. Hamadouche. Charnley-Kerboull total hip arthroplasty for osteonecrosis of the femoral head a minimal 10-year follow-up study. *J Arthroplasty.* 21: 533-40, 2006.
371. Nixon, A. J., R. A. Saxer, and B. D. Brower-Toland. Exogenous insulin-like growth factor-I stimulates an autoinductive IGF-I autocrine/paracrine response in chondrocytes. *J Orthop Res.* 19: 26-32, 2001.
372. O'Brien, F. J., B. A. Harley, I. V. Yannas, and L. J. Gibson. The effect of pore size on cell adhesion in collagen-GAG scaffolds. *Biomaterials.* 26: 433-41, 2005.
373. Oegema, T. R., Jr., J. L. Lewis, and R. C. Thompson, Jr. Role of acute trauma in development of osteoarthritis. *Agents Actions.* 40: 220-3, 1993.
374. Oesser, S. and J. Seifert. Stimulation of type II collagen biosynthesis and secretion in bovine chondrocytes cultured with degraded collagen. *Cell Tissue Res.* 311: 393-9, 2003.
375. Ofek, G., C. M. Revell, J. C. Hu, D. D. Allison, K. J. Grande-Allen, and K. A. Athanasiou. Matrix development in self-assembly of articular cartilage. *PLoS ONE.* 3: e2795, 2008.

376. Oloyede, A., R. Flachsman, and N. D. Broom. The dramatic influence of loading velocity on the compressive response of articular cartilage. *Connect Tissue Res.* 27: 211-24, 1992.
377. Olson, S. A. and F. Guilak. From articular fracture to posttraumatic arthritis: a black box that needs to be opened. *J Orthop Trauma.* 20: 661-2, 2006.
378. Opolka, A., S. Ratzinger, T. Schubert, H. U. Spiegel, J. Grifka, P. Bruckner, A. Probst, and S. Grassel. Collagen IX is indispensable for timely maturation of cartilage during fracture repair in mice. *Matrix Biol.* 26: 85-95, 2007.
379. Ortolani, F., M. Giordano, and M. Marchini. A model for type II collagen fibrils: distinctive D-band patterns in native and reconstituted fibrils compared with sequence data for helix and telopeptide domains. *Biopolymers.* 54: 448-63, 2000.
380. Palamakumbura, A. H. and P. C. Trackman. A fluorometric assay for detection of lysyl oxidase enzyme activity in biological samples. *Anal Biochem.* 300: 245-51, 2002.
381. Palm, T. M., K. Kaarela, M. S. Hakala, H. J. Kautiainen, H. P. Kroger, and E. A. Belt. Need and sequence of large joint replacements in rheumatoid arthritis. A 25-year follow-up study. *Clin Exp Rheumatol.* 20: 392-4, 2002.
382. Park, K., J. Huang, F. Azar, R. L. Jin, B. H. Min, D. K. Han, and K. Hasty. Scaffold-free, engineered porcine cartilage construct for cartilage defect repair--in vitro and in vivo study. *Artif Organs.* 30: 586-96, 2006.
383. Parvizi, J., T. A. Sullivan, R. T. Trousdale, and D. G. Lewallen. Thirty-day mortality after total knee arthroplasty. *J Bone Joint Surg Am.* 83-A: 1157-61, 2001.
384. Patel, V. P., M. Walsh, B. Sehgal, C. Preston, H. DeWal, and P. E. Di Cesare. Factors associated with prolonged wound drainage after primary total hip and knee arthroplasty. *J Bone Joint Surg Am.* 89: 33-8, 2007.
385. Patwari, P., M. N. Cook, M. A. DiMicco, S. M. Blake, I. E. James, S. Kumar, A. A. Cole, M. W. Lark, and A. J. Grodzinsky. Proteoglycan degradation after injurious compression of bovine and human articular cartilage in vitro: interaction with exogenous cytokines. *Arthritis Rheum.* 48: 1292-301, 2003.
386. Patwari, P., V. Gaschen, I. E. James, E. Berger, S. M. Blake, M. W. Lark, A. J. Grodzinsky, and E. B. Hunziker. Ultrastructural quantification of cell death after injurious compression of bovine calf articular cartilage. *Osteoarthritis Cartilage.* 12: 245-52, 2004.

387. Pei, M., L. A. Solchaga, J. Seidel, L. Zeng, G. Vunjak-Novakovic, A. I. Caplan, and L. E. Freed. Bioreactors mediate the effectiveness of tissue engineering scaffolds. *Faseb J.* 16: 1691-4, 2002.
388. Petersen, S. A. and R. J. Hawkins. Revision of failed total shoulder arthroplasty. *Orthop Clin North Am.* 29: 519-33, 1998.
389. Phillips, D. M. and R. C. Haut. The use of a non-ionic surfactant (P188) to save chondrocytes from necrosis following impact loading of chondral explants. *J Orthop Res.* 22: 1135-42, 2004.
390. Pickvance, E. A., T. R. Oegema, Jr., and R. C. Thompson, Jr. Immunolocalization of selected cytokines and proteases in canine articular cartilage after transarticular loading. *J Orthop Res.* 11: 313-23, 1993.
391. Poole, C. A., M. H. Flint, and B. W. Beaumont. Morphological and functional interrelationships of articular cartilage matrices. *J Anat.* 138 (Pt 1): 113-38, 1984.
392. Poole, C. A., S. Ayad, and J. R. Schofield. Chondrons from articular cartilage: I. Immunolocalization of type VI collagen in the pericellular capsule of isolated canine tibial chondrons. *J Cell Sci.* 90 (Pt 4): 635-43, 1988.
393. Potter, K., L. H. Kidder, I. W. Levin, E. N. Lewis, and R. G. Spencer. Imaging of collagen and proteoglycan in cartilage sections using Fourier transform infrared spectral imaging. *Arthritis Rheum.* 44: 846-55, 2001.
394. Prabhakar, V., R. Raman, I. Capila, C. J. Bosques, K. Pojasek, and R. Sasisekharan. Biochemical characterization of the chondroitinase ABC I active site. *Biochem J.* 390: 395-405, 2005.
395. Prabhakar, V., I. Capila, R. Raman, A. Srinivasan, C. J. Bosques, K. Pojasek, M. A. Wruck, and R. Sasisekharan. The catalytic machinery of chondroitinase ABC I utilizes a calcium coordination strategy to optimally process dermatan sulfate. *Biochemistry.* 45: 11130-9, 2006.
396. Pylawka, T. K., M. Wimmer, B. J. Cole, A. S. Viridi, and J. M. Williams. Impaction affects cell viability in osteochondral tissues during transplantation. *J Knee Surg.* 20: 105-10, 2007.
397. Qi, W. N. and S. P. Scully. Effect of type II collagen in chondrocyte response to TGF-beta 1 regulation. *Exp Cell Res.* 241: 142-50, 1998.
398. Quarto, R., B. Dozin, P. Bonaldo, R. Cancedda, and A. Colombatti. Type VI collagen expression is upregulated in the early events of chondrocyte differentiation. *Development.* 117: 245-51, 1993.

399. Quinn, T. M., A. J. Grodzinsky, E. B. Hunziker, and J. D. Sandy. Effects of injurious compression on matrix turnover around individual cells in calf articular cartilage explants. *J Orthop Res.* 16: 490-9, 1998.
400. Quinn, T. M., R. G. Allen, B. J. Schalet, P. Perumbuli, and E. B. Hunziker. Matrix and cell injury due to sub-impact loading of adult bovine articular cartilage explants: effects of strain rate and peak stress. *J Orthop Res.* 19: 242-9, 2001.
401. Quinn, T. M. and V. Morel. Microstructural modeling of collagen network mechanics and interactions with the proteoglycan gel in articular cartilage. *Biomech Model Mechanobiol.* 6: 73-82, 2007.
402. Radin, E. L. and I. L. Paul. Importance of bone in sparing articular cartilage from impact. *Clin Orthop.* 78: 342-4, 1971.
403. Radin, E. L., M. G. Ehrlich, R. Chernack, P. Abernethy, I. L. Paul, and R. M. Rose. Effect of repetitive impulsive loading on the knee joints of rabbits. *Clin Orthop.* 131: 288-93, 1978.
404. Ramos-Vara, J. A. Technical aspects of immunohistochemistry. *Vet Pathol.* 42: 405-26, 2005.
405. Reddy, G. K. and C. S. Enwemeka. A simplified method for the analysis of hydroxyproline in biological tissues. *Clin Biochem.* 29: 225-9, 1996.
406. Reginster, J. Y. The prevalence and burden of arthritis. *Rheumatology (Oxford).* 41 Supp 1: 3-6, 2002.
407. Reichenberger, E., T. Aigner, K. von der Mark, H. Stoss, and W. Bertling. In situ hybridization studies on the expression of type X collagen in fetal human cartilage. *Dev Biol.* 148: 562-72, 1991.
408. Repo, R. U. and J. B. Finlay. Survival of articular cartilage after controlled impact. *J Bone Joint Surg Am.* 59: 1068-76, 1977.
409. Revell, C. M., C. E. Reynolds, and K. A. Athanasiou. Effects of initial cell seeding in self assembly of articular cartilage. *Ann Biomed Eng.* 36: 1441-8, 2008.
410. Reynolds, E. S. The use of lead citrate at high pH as an electron-opaque stain in electron microscopy. *J Cell Biol.* 17: 208-12, 1963.
411. Riaz, S. and M. Umar. Revision knee arthroplasty. *J Pak Med Assoc.* 56: 456-60, 2006.
412. Rieppo, J., J. Toyras, M. T. Nieminen, V. Kovanen, M. M. Hyttinen, R. K. Korhonen, J. S. Jurvelin, and H. J. Helminen. Structure-function

relationships in enzymatically modified articular cartilage. *Cells Tissues Organs*. 175: 121-32, 2003.

413. Riesle, J., A. P. Hollander, R. Langer, L. E. Freed, and G. Vunjak-Novakovic. Collagen in tissue-engineered cartilage: types, structure, and crosslinks. *J Cell Biochem*. 71: 313-27, 1998.
414. Rodriguez, F., *Principles of Polymer Systems*. 4th ed. 1996, Philadelphia: Taylor & Francis.
415. Ronziere, M. C., S. Roche, J. Gouttenoire, O. Demarteau, D. Herbage, and A. M. Freyria. Ascorbate modulation of bovine chondrocyte growth, matrix protein gene expression and synthesis in three-dimensional collagen sponges. *Biomaterials*. 24: 851-61, 2003.
416. Roos, H., T. Adalberth, L. Dahlberg, and L. S. Lohmander. Osteoarthritis of the knee after injury to the anterior cruciate ligament or meniscus: the influence of time and age. *Osteoarthritis Cartilage*. 3: 261-7, 1995.
417. Rosenberg, K., H. Olsson, M. Morgelin, and D. Heinegard. Cartilage oligomeric matrix protein shows high affinity zinc-dependent interaction with triple helical collagen. *J Biol Chem*. 273: 20397-403, 1998.
418. Roth, V. and V. C. Mow. The intrinsic tensile behavior of the matrix of bovine articular cartilage and its variation with age. *J Bone Joint Surg Am*. 62: 1102-17, 1980.
419. Roughley, P. J. and E. R. Lee. Cartilage proteoglycans: structure and potential functions. *Microsc Res Tech*. 28: 385-97, 1994.
420. Rundell, S. A., D. C. Baars, D. M. Phillips, and R. C. Haut. The limitation of acute necrosis in retro-patellar cartilage after a severe blunt impact to the in vivo rabbit patello-femoral joint. *J Orthop Res*. 23: 1363-9, 2005.
421. Rundell, S. A. and R. C. Haut. Exposure to a standard culture medium alters the response of cartilage explants to injurious unconfined compression. *J Biomech*. 39: 1933-8, 2006.
422. Ruoslahti, E. and Y. Yamaguchi. Proteoglycans as modulators of growth factor activities. *Cell*. 64: 867-9, 1991.
423. Sah, R. L., S. B. Trippel, and A. J. Grodzinsky. Differential effects of serum, insulin-like growth factor-I, and fibroblast growth factor-2 on the maintenance of cartilage physical properties during long-term culture. *J Orthop Res*. 14: 44-52, 1996.
424. Sams, A. E., R. R. Minor, J. A. Wootton, H. Mohammed, and A. J. Nixon. Local and remote matrix responses to chondrocyte-laden collagen scaffold

- implantation in extensive articular cartilage defects. *Osteoarthritis Cartilage*. 3: 61-70, 1995.
425. Sandy, J. D., H. L. Brown, and D. A. Lowther. Control of proteoglycan synthesis. Studies on the activation of synthesis observed during culture of articular cartilages. *Biochem J*. 188: 119-30, 1980.
 426. Sandy, J. D. A contentious issue finds some clarity: on the independent and complementary roles of aggrecanase activity and MMP activity in human joint aggrecanolysis. *Osteoarthritis Cartilage*. 14: 95-100, 2006.
 427. Sato, T., K. Konomi, S. Yamasaki, S. Aratani, K. Tsuchimochi, M. Yokouchi, K. Masuko-Hongo, N. Yagishita, H. Nakamura, S. Komiya, M. Beppu, H. Aoki, K. Nishioka, and T. Nakajima. Comparative analysis of gene expression profiles in intact and damaged regions of human osteoarthritic cartilage. *Arthritis Rheum*. 54: 808-17, 2006.
 428. Schmidt, M. B., V. C. Mow, L. E. Chun, and D. R. Eyre. Effects of proteoglycan extraction on the tensile behavior of articular cartilage. *J Orthop Res*. 8: 353-63, 1990.
 429. Schwartz, M. H., P. H. Leo, and J. L. Lewis. A microstructural model for the elastic response of articular cartilage. *J Biomech*. 27: 865-73, 1994.
 430. Scott, C. and K. A. Athanasiou. Mechanical impact and articular cartilage. *Crit Rev Biomed Eng*. 34: 347-78, 2006.
 431. Scott, C. C. and K. A. Athanasiou. Design, validation, and utilization of an articular cartilage impact instrument. *Proc Inst Mech Eng [H]*. 220: 845-55, 2006.
 432. Seegmiller, R., F. C. Fraser, and H. Sheldon. A new chondrodystrophic mutant in mice. Electron microscopy of normal and abnormal chondrogenesis. *J Cell Biol*. 48: 580-93, 1971.
 433. Serbest, G., J. Horwitz, M. Jost, and K. Barbee. Mechanisms of cell death and neuroprotection by poloxamer 188 after mechanical trauma. *Faseb J*. 20: 308-10, 2006.
 434. Serink, M. T., A. Nachemson, and G. Hansson. The effect of impact loading on rabbit knee joints. *Acta Orthop Scand*. 48: 250-62, 1977.
 435. Shieh, A. C. and K. A. Athanasiou. Biomechanics of single zonal chondrocytes. *J Biomech*. 39: 1595-602, 2006.
 436. Shieh, A. C., E. J. Koay, and K. A. Athanasiou. Strain-dependent Recovery Behavior of Single Chondrocytes. *Biomech Model Mechanobiol*. 5: 172-9, 2006.

437. Shirazi, R. and A. Shirazi-Adl. Analysis of articular cartilage as a composite using nonlinear membrane elements for collagen fibrils. *Med Eng Phys.* 27: 827-35, 2005.
438. Shirazi, R. and A. Shirazi-Adl. Deep vertical collagen fibrils play a significant role in mechanics of articular cartilage. *J Orthop Res.* 26: 608-15, 2008.
439. Shlopov, B. V., G. N. Smith, Jr., A. A. Cole, and K. A. Hasty. Differential patterns of response to doxycycline and transforming growth factor beta1 in the down-regulation of collagenases in osteoarthritic and normal human chondrocytes. *Arthritis Rheum.* 42: 719-27, 1999.
440. Shlopov, B. V., J. M. Stuart, M. L. Gumanovskaya, and K. A. Hasty. Regulation of cartilage collagenase by doxycycline. *J Rheumatol.* 28: 835-42, 2001.
441. Siegel, R. C. Collagen cross-linking. Synthesis of collagen cross-links in vitro with highly purified lysyl oxidase. *J Biol Chem.* 251: 5786-92, 1976.
442. Silver, F. H., G. Bradica, and A. Tria. Relationship among biomechanical, biochemical, and cellular changes associated with osteoarthritis. *Crit Rev Biomed Eng.* 29: 373-91, 2001.
443. Silver, F. H., G. Bradica, and A. Tria. Elastic energy storage in human articular cartilage: estimation of the elastic modulus for type II collagen and changes associated with osteoarthritis. *Matrix Biol.* 21: 129-37, 2002.
444. Simha, N. K., M. Fedewa, P. H. Leo, J. L. Lewis, and T. Oegema. A composites theory predicts the dependence of stiffness of cartilage culture tissues on collagen volume fraction. *J Biomech.* 32: 503-9, 1999.
445. Simon, S. R., E. L. Radin, I. L. Paul, and R. M. Rose. The response of joints to impact loading. II. In vivo behavior of subchondral bone. *J Biomech.* 5: 267-72, 1972.
446. Simon, T. M. and D. W. Jackson. Articular cartilage: injury pathways and treatment options. *Sports Med Arthrosc.* 14: 146-54, 2006.
447. Slinker, B. K. The statistics of synergism. *J Mol Cell Cardiol.* 30: 723-31, 1998.
448. Smith, G. N., Jr., E. A. Mickler, K. A. Hasty, and K. D. Brandt. Specificity of inhibition of matrix metalloproteinase activity by doxycycline: relationship to structure of the enzyme. *Arthritis Rheum.* 42: 1140-6, 1999.
449. Smith, P., F. D. Shuler, H. I. Georgescu, S. C. Ghivizzani, B. Johnstone, C. Niyibizi, P. D. Robbins, and C. H. Evans. Genetic enhancement of

matrix synthesis by articular chondrocytes: comparison of different growth factor genes in the presence and absence of interleukin-1. *Arthritis Rheum.* 43: 1156-64, 2000.

450. Smith, R. L., J. Lin, M. C. Trindade, J. Shida, G. Kajiyama, T. Vu, A. R. Hoffman, M. C. van der Meulen, S. B. Goodman, D. J. Schurman, and D. R. Carter. Time-dependent effects of intermittent hydrostatic pressure on articular chondrocyte type II collagen and aggrecan mRNA expression. *J Rehabil Res Dev.* 37: 153-61, 2000.
451. Smith, R. L., D. R. Carter, and D. J. Schurman. Pressure and shear differentially alter human articular chondrocyte metabolism: a review. *Clin Orthop Relat Res.* 427 Suppl: S89-95, 2004.
452. Sochart, D. H. and M. L. Porter. The long-term results of Charnley low-friction arthroplasty in young patients who have congenital dislocation, degenerative osteoarthritis, or rheumatoid arthritis. *J Bone Joint Surg Am.* 79: 1599-617, 1997.
453. Soltz, M. A. and G. A. Ateshian. A Conewise Linear Elasticity mixture model for the analysis of tension-compression nonlinearity in articular cartilage. *J Biomech Eng.* 122: 576-86, 2000.
454. Soulhat, J., M. D. Buschmann, and A. Shirazi-Adl. A fibril-network-reinforced biphasic model of cartilage in unconfined compression. *J Biomech Eng.* 121: 340-7, 1999.
455. Sporn, M. B., A. B. Roberts, L. M. Wakefield, and R. K. Assoian. Transforming growth factor-beta: biological function and chemical structure. *Science.* 233: 532-4, 1986.
456. Stewart, M. C., K. M. Saunders, N. Burton-Wurster, and J. N. Macleod. Phenotypic stability of articular chondrocytes in vitro: the effects of culture models, bone morphogenetic protein 2, and serum supplementation. *J Bone Miner Res.* 15: 166-74, 2000.
457. Sugimoto, K., T. Iizawa, H. Harada, K. Yamada, M. Katsumata, and M. Takahashi. Cartilage degradation independent of MMP/aggrecanases. *Osteoarthritis Cartilage.* 12: 1006-14, 2004.
458. Sweigart, M. A., C. F. Zhu, D. M. Burt, P. D. DeHoll, C. M. Agrawal, T. O. Clanton, and K. A. Athanasiou. Intraspecies and interspecies comparison of the compressive properties of the medial meniscus. *Ann Biomed Eng.* 32: 1569-79, 2004.
459. Tchetverikov, I., L. S. Lohmander, N. Verzijl, T. W. Huizinga, J. M. TeKoppele, R. Hanemaaijer, and J. DeGroot. MMP protein and activity

- levels in synovial fluid from patients with joint injury, inflammatory arthritis, and osteoarthritis. *Ann Rheum Dis.* 64: 694-8, 2005.
460. Thompson, R. C., Jr., T. R. Oegema, Jr., J. L. Lewis, and L. Wallace. Osteoarthrotic changes after acute transarticular load. An animal model. *J Bone Joint Surg Am.* 73: 990-1001, 1991.
 461. Thompson, R. C., Jr., M. J. Vener, H. J. Griffiths, J. L. Lewis, T. R. Oegema, Jr., and L. Wallace. Scanning electron-microscopic and magnetic resonance-imaging studies of injuries to the patellofemoral joint after acute transarticular loading. *J Bone Joint Surg Am.* 75: 704-13, 1993.
 462. Torzilli, P. A., R. Grigienė, J. Borrelli, Jr., and D. L. Helfet. Effect of impact load on articular cartilage: cell metabolism and viability, and matrix water content. *J Biomech Eng.* 121: 433-41, 1999.
 463. Trackman, P. C., C. G. Zoski, and H. M. Kagan. Development of a peroxidase-coupled fluorometric assay for lysyl oxidase. *Anal Biochem.* 113: 336-42, 1981.
 464. Trickey, W. R., G. M. Lee, and F. Guilak. Viscoelastic properties of chondrocytes from normal and osteoarthritic human cartilage. *J Orthop Res.* 18: 891-8, 2000.
 465. Trickey, W. R., F. P. Baaijens, T. A. Laursen, L. G. Alexopoulos, and F. Guilak. Determination of the Poisson's ratio of the cell: recovery properties of chondrocytes after release from complete micropipette aspiration. *J Biomech.* 39: 78-87, 2006.
 466. Ulrich, P. and A. Cerami. Protein glycation, diabetes, and aging. *Recent Prog Horm Res.* 56: 1-21, 2001.
 467. van der Kraan, P. M., P. Buma, T. van Kuppevelt, and W. B. van den Berg. Interaction of chondrocytes, extracellular matrix and growth factors: relevance for articular cartilage tissue engineering. *Osteoarthritis Cartilage.* 10: 631-7, 2002.
 468. van Osch, G. J., S. W. van der Veen, P. Buma, and H. L. Verwoerd-Verhoef. Effect of transforming growth factor-beta on proteoglycan synthesis by chondrocytes in relation to differentiation stage and the presence of pericellular matrix. *Matrix Biol.* 17: 413-24, 1998.
 469. Varga, F., M. Drzik, M. Handl, J. Chlpik, P. Kos, E. Filova, M. Rampichova, A. Necas, T. Trc, and E. Amler. Biomechanical characterization of cartilages by a novel approach of blunt impact testing. *Physiol Res.* 56 Suppl 1: S61-8, 2007.

470. Vaughan, L., M. Mendler, S. Huber, P. Bruckner, K. H. Winterhalter, M. I. Irwin, and R. Mayne. D-periodic distribution of collagen type IX along cartilage fibrils. *J Cell Biol.* 106: 991-7, 1988.
471. Verteramo, A. and B. B. Seedhom. Zonal and directional variations in tensile properties of bovine articular cartilage with special reference to strain rate variation. *Biorheology.* 41: 203-13, 2004.
472. Verteramo, A. and B. B. Seedhom. Effect of a single impact loading on the structure and mechanical properties of articular cartilage. *J Biomech.* 40: 3580-9, 2007.
473. Verzijl, N., J. DeGroot, E. Oldehinkel, R. A. Bank, S. R. Thorpe, J. W. Baynes, M. T. Bayliss, J. W. Bijlsma, F. P. Lafeber, and J. M. Tekoppele. Age-related accumulation of Maillard reaction products in human articular cartilage collagen. *Biochem J.* 350 Pt 2: 381-7, 2000.
474. Verzijl, N., J. DeGroot, Z. C. Ben, O. Brau-Benjamin, A. Maroudas, R. A. Bank, J. Mizrahi, C. G. Schalkwijk, S. R. Thorpe, J. W. Baynes, J. W. Bijlsma, F. P. Lafeber, and J. M. TeKoppele. Crosslinking by advanced glycation end products increases the stiffness of the collagen network in human articular cartilage: a possible mechanism through which age is a risk factor for osteoarthritis. *Arthritis Rheum.* 46: 114-23, 2002.
475. Vrahas, M. S., K. Mithoefer, and D. Joseph. The long-term effects of articular impaction. *Clin Orthop Relat Res.* 423: 40-3, 2004.
476. Wakitani, S., T. Goto, S. J. Pineda, R. G. Young, J. M. Mansour, A. I. Caplan, and V. M. Goldberg. Mesenchymal cell-based repair of large, full-thickness defects of articular cartilage. *J Bone Joint Surg Am.* 76: 579-92, 1994.
477. Waldman, S. D., M. D. Gryn timer, R. M. Pilliar, and R. A. Kandel. Characterization of cartilaginous tissue formed on calcium polyphosphate substrates in vitro. *J Biomed Mater Res.* 62: 323-30, 2002.
478. Waldman, S. D., M. D. Gryn timer, R. M. Pilliar, and R. A. Kandel. The use of specific chondrocyte populations to modulate the properties of tissue-engineered cartilage. *J Orthop Res.* 21: 132-8, 2003.
479. Waldman, S. D., C. G. Spiteri, M. D. Gryn timer, R. M. Pilliar, and R. A. Kandel. Long-term intermittent shear deformation improves the quality of cartilaginous tissue formed in vitro. *J Orthop Res.* 21: 590-6, 2003.
480. Waldman, S. D., C. G. Spiteri, M. D. Gryn timer, R. M. Pilliar, and R. A. Kandel. Long-term intermittent compressive stimulation improves the composition and mechanical properties of tissue-engineered cartilage. *Tissue Eng.* 10: 1323-31, 2004.

481. Waldman, S. D., D. C. Couto, M. D. Gryn timer, R. M. Pilliar, and R. A. Kandel. A single application of cyclic loading can accelerate matrix deposition and enhance the properties of tissue-engineered cartilage. *Osteoarthritis Cartilage*. 14: 323-30, 2006.
482. Waldman, S. D., Y. Usmani, M. Y. Tse, and S. C. Pang. Differential Effects of Natriuretic Peptide Stimulation on Tissue-Engineered Cartilage. *Tissue Eng* 2007.
483. Walker, G. D., M. Fischer, J. Gannon, R. C. Thompson, Jr., and T. R. Oegema, Jr. Expression of type-X collagen in osteoarthritis. *J Orthop Res*. 13: 4-12, 1995.
484. Wang, C. C., X. E. Guo, D. Sun, V. C. Mow, G. A. Ateshian, and C. T. Hung. The functional environment of chondrocytes within cartilage subjected to compressive loading: a theoretical and experimental approach. *Biorheology*. 39: 11-25, 2002.
485. Wang, M. D., H. Yin, R. Landick, J. Gelles, and S. M. Block. Stretching DNA with optical tweezers. *Biophys J*. 72: 1335-46, 1997.
486. Wang, N., J. P. Butler, and D. E. Ingber. Mechanotransduction across the cell surface and through the cytoskeleton. *Science*. 260: 1124-7, 1993.
487. Wang, W., J. Xu, and T. Kirsch. Annexin V and terminal differentiation of growth plate chondrocytes. *Exp Cell Res*. 305: 156-65, 2005.
488. Watanabe, H., Y. Yamada, and K. Kimata. Roles of aggrecan, a large chondroitin sulfate proteoglycan, in cartilage structure and function. *J Biochem*. 124: 687-93, 1998.
489. Weiss, C., L. Rosenberg, and A. J. Helfet. An ultrastructural study of normal young adult human articular cartilage. *J Bone Joint Surg Am*. 50: 663-74, 1968.
490. Wilder, F. V., B. J. Hall, J. P. Barrett, Jr., and N. B. Lemrow. History of acute knee injury and osteoarthritis of the knee: a prospective epidemiological assessment. The Clearwater Osteoarthritis Study. *Osteoarthritis Cartilage*. 10: 611-6, 2002.
491. Wilkins, R. J., J. A. Browning, and J. P. Urban. Chondrocyte regulation by mechanical load. *Biorheology*. 37: 67-74, 2000.
492. Williams, G. M., T. J. Klein, and R. L. Sah. Cell density alters matrix accumulation in two distinct fractions and the mechanical integrity of alginate-chondrocyte constructs. *Acta Biomater*. 1: 625-33, 2005.

493. Williamson, A. K., A. C. Chen, and R. L. Sah. Compressive properties and function-composition relationships of developing bovine articular cartilage. *J Orthop Res.* 19: 1113-21, 2001.
494. Williamson, A. K., A. C. Chen, K. Masuda, E. J. Thonar, and R. L. Sah. Tensile mechanical properties of bovine articular cartilage: variations with growth and relationships to collagen network components. *J Orthop Res.* 21: 872-80, 2003.
495. Williamson, A. K., K. Masuda, E. J. Thonar, and R. L. Sah. Growth of immature articular cartilage in vitro: correlated variation in tensile biomechanical and collagen network properties. *Tissue Eng.* 9: 625-34, 2003.
496. Wilson, W., C. C. van Donkelaar, B. van Rietbergen, K. Ito, and R. Huiskes. Stresses in the local collagen network of articular cartilage: a poroviscoelastic fibril-reinforced finite element study. *J Biomech.* 37: 357-66, 2004.
497. Wilson, W., C. C. van Donkelaar, B. van Rietbergen, and R. Huiskes. A fibril-reinforced poroviscoelastic swelling model for articular cartilage. *J Biomech.* 38: 1195-204, 2005.
498. Wilson, W., C. C. van Donkelaar, R. van Rietbergen, and R. Huiskes. The role of computational models in the search for the mechanical behavior and damage mechanisms of articular cartilage. *Med Eng Phys.* 27: 810-26, 2005.
499. Wilson, W., N. J. Driessen, C. C. van Donkelaar, and K. Ito. Prediction of collagen orientation in articular cartilage by a collagen remodeling algorithm. *Osteoarthritis Cartilage.* 14: 1196-202, 2006.
500. Wilson, W., C. van Burken, C. van Donkelaar, P. Buma, B. van Rietbergen, and R. Huiskes. Causes of mechanically induced collagen damage in articular cartilage. *J Orthop Res.* 24: 220-8, 2006.
501. Wilson, W., J. M. Huyghe, and C. C. van Donkelaar. Depth-dependent compressive equilibrium properties of articular cartilage explained by its composition. *Biomech Model Mechanobiol.* 6: 43-53, 2007.
502. Wluka, A. E., Y. Wang, S. R. Davis, and F. M. Cicuttini. Tibial plateau size is related to grade of joint space narrowing and osteophytes in healthy women and in women with osteoarthritis. *Ann Rheum Dis.* 64: 1033-7, 2005.
503. Woessner, J. F., Jr. The determination of hydroxyproline in tissue and protein samples containing small proportions of this imino acid. *Arch Biochem Biophys.* 93: 440-7, 1961.

504. Wong, M., M. Siegrist, V. Gaschen, Y. Park, W. Graber, and D. Studer. Collagen fibrillogenesis by chondrocytes in alginate. *Tissue Eng.* 8: 979-87, 2002.
505. Wong, M. and D. R. Carter. Articular cartilage functional histomorphology and mechanobiology: a research perspective. *Bone.* 33: 1-13, 2003.
506. Woo, S. L., W. H. Akeson, and G. F. Jemmott. Measurements of nonhomogeneous, directional mechanical properties of articular cartilage in tension. *J Biomech.* 9: 785-91, 1976.
507. Woo, S. L., P. Lubock, M. A. Gomez, G. F. Jemmott, S. C. Kuei, and W. H. Akeson. Large deformation nonhomogeneous and directional properties of articular cartilage in uniaxial tension. *J Biomech.* 12: 437-46, 1979.
508. Woodfield, T. B., C. A. Van Blitterswijk, J. De Wijn, T. J. Sims, A. P. Hollander, and J. Riesle. Polymer scaffolds fabricated with pore-size gradients as a model for studying the zonal organization within tissue-engineered cartilage constructs. *Tissue Eng.* 11: 1297-311, 2005.
509. Wright, V. Post-traumatic osteoarthritis--a medico-legal minefield. *Br J Rheumatol.* 29: 474-8, 1990.
510. Wroblewski, B. M. and P. D. Siney. Charnley low-friction arthroplasty of the hip. Long-term results. *Clin Orthop Relat Res.* 191-201, 1993.
511. Wroblewski, B. M., P. D. Siney, and P. A. Fleming. Charnley low-frictional torque arthroplasty in young rheumatoid and juvenile rheumatoid arthritis: 292 hips followed for an average of 15 years. *Acta Orthop.* 78: 206-10, 2007.
512. Wu, J. J., P. E. Woods, and D. R. Eyre. Identification of cross-linking sites in bovine cartilage type IX collagen reveals an antiparallel type II-type IX molecular relationship and type IX to type IX bonding. *J Biol Chem.* 267: 23007-14, 1992.
513. Wu, J. Z., W. Herzog, and J. Ronsky. Modeling axi-symmetrical joint contact with biphasic cartilage layers--an asymptotic solution. *J Biomech.* 29: 1263-81, 1996.
514. Wu, J. Z. and W. Herzog. Finite element simulation of location- and time-dependent mechanical behavior of chondrocytes in unconfined compression tests. *Ann Biomed Eng.* 28: 318-30, 2000.
515. Wu, J. Z. and W. Herzog. Elastic anisotropy of articular cartilage is associated with the microstructures of collagen fibers and chondrocytes. *J Biomech.* 35: 931-42, 2002.

- 516. Xia, Y. Averaged and depth-dependent anisotropy of articular cartilage by microscopic imaging. *Semin Arthritis Rheum.* 37: 317-27, 2008.
- 517. Yagi, R., D. McBurney, D. Lavery, S. Weiner, and W. E. Horton, Jr. Intrajoint comparisons of gene expression patterns in human osteoarthritis suggest a change in chondrocyte phenotype. *J Orthop Res.* 23: 1128-38, 2005.
- 518. Yang, C., S. W. Li, H. J. Helminen, J. S. Khillan, Y. Bao, and D. J. Prockop. Apoptosis of chondrocytes in transgenic mice lacking collagen II. *Exp Cell Res.* 235: 370-3, 1997.
- 519. Yelin, E., "The economics of osteoarthritis." In: *Osteoarthritis*, edited by K.D. Brandt, M. Doherty, and L.S. Lohmander. New York: Oxford University Press, 1998, pp. 23-30.
- 520. Yoon, D. M. and J. P. Fisher. Chondrocyte signaling and artificial matrices for articular cartilage engineering. *Adv Exp Med Biol.* 585: 67-86, 2006.
- 521. Yu, L. P., Jr., G. N. Smith, Jr., K. A. Hasty, and K. D. Brandt. Doxycycline inhibits type XI collagenolytic activity of extracts from human osteoarthritic cartilage and of gelatinase. *J Rheumatol.* 18: 1450-2, 1991.
- 522. Yu, L. P., Jr., G. N. Smith, Jr., K. D. Brandt, S. L. Myers, B. L. O'Connor, and D. A. Brandt. Reduction of the severity of canine osteoarthritis by prophylactic treatment with oral doxycycline. *Arthritis Rheum.* 35: 1150-9, 1992.
- 523. Zhang, H., C. C. Liew, and K. W. Marshall. Microarray analysis reveals the involvement of beta-2 microglobulin (B2M) in human osteoarthritis. *Osteoarthritis Cartilage.* 10: 950-60, 2002.
- 524. Zhang, W., R. W. Moskowitz, G. Nuki, S. Abramson, R. D. Altman, N. Arden, S. Bierma-Zeinstra, K. D. Brandt, P. Croft, M. Doherty, M. Dougados, M. Hochberg, D. J. Hunter, K. Kwok, L. S. Lohmander, and P. Tugwell. OARSI recommendations for the management of hip and knee osteoarthritis, part I: critical appraisal of existing treatment guidelines and systematic review of current research evidence. *Osteoarthritis Cartilage.* 15: 981-1000, 2007.
- 525. Zhang, W., R. W. Moskowitz, G. Nuki, S. Abramson, R. D. Altman, N. Arden, S. Bierma-Zeinstra, K. D. Brandt, P. Croft, M. Doherty, M. Dougados, M. Hochberg, D. J. Hunter, K. Kwok, L. S. Lohmander, and P. Tugwell. OARSI recommendations for the management of hip and knee osteoarthritis, Part II: OARSI evidence-based, expert consensus guidelines. *Osteoarthritis Cartilage.* 16: 137-62, 2008.

Appendix 1: *In situ* mechanical properties of the chondrocyte cytoplasm and nucleus*

Abstract

The way in which the nucleus experiences mechanical forces has important implications for understanding mechanotransduction. Knowledge of nuclear material properties and, specifically, their relationship to the properties of the bulk cell can help determine if the nucleus directly experiences mechanical load, or if it is signal transduction secondary to cell membrane deformation that leads to altered gene expression. Prior work measuring nuclear material properties using micropipette aspiration suggests that the nucleus is substantially stiffer than the bulk cell,²¹¹ whereas recent work with unconfined compression of single chondrocytes showed a nearly one-to-one correlation between cellular and nuclear strains.³⁰⁷ In this communication, a linearly elastic finite element model of the cell with a nuclear inclusion was used to simulate the unconfined compression data. Cytoplasmic and nuclear stiffnesses were varied from 1 to 7 kPa for several combinations of cytoplasmic and nuclear Poisson's ratios. It was found that the experimental data were best fit when the ratio of cytoplasmic to nuclear stiffness was 1.4, and both cytoplasm and nucleus were modeled as incompressible. The cytoplasmic to nuclear stiffness ratio is significantly lower than prior reports for isolated nuclei. These results suggest the nucleus may behave mechanically different *in situ* than when isolated.

*Appendix under review at *J Biomech* as Ofek G, Natoli RM, and Athanasiou KA, "*In situ* Mechanical Properties of the Chondrocyte Cytoplasm and Nucleus," August 2008.

Introduction

How mechanical forces are experienced by the nucleus has important consequences for understanding mechanotransduction.⁴⁸⁶ Mechanotransduction is the process by which mechanical loads induce changes in the gene expression profile of a cell, which can ultimately alter cellular physiology and homeostasis. It has also been shown that alterations in the physical dimensions of the nucleus, resulting from an applied load on the tissue⁸⁴ or single cell,³⁰⁷ correlate with changes in gene regulation. Previous investigation into mechanical characteristics of isolated nuclei suggest they behave like a viscoelastic material and are significantly stiffer than the cell as a whole.^{86,211} However, these results are possibly influenced by the fact that the nuclei were removed from their *in situ* environment. The nuclear lamina, the framework for nuclear structure, is intimately linked to intermediate filaments positioned throughout the cytoplasm.³²⁷ Thus, mechanical properties of the nucleus may change when these connections are disrupted and the nucleus undergoes structural reorganization.

In this communication, a finite element modeling approach was employed to obtain cytoplasmic and nuclear stiffness values which best match previously reported cellular and nuclear axial and lateral strains obtained during unconfined compression of single attached chondrocytes.³⁰⁷ Based on the nearly one-to-one correlation of cellular and nuclear strains observed in that study, we hypothesized the *in situ* nuclear stiffness is similar to that of the cytoplasm. Further, effects of changing both cytoplasmic and nuclear Poisson's ratios were

explored to investigate the validity of the commonly used assumption of cellular incompressibility.

Materials and methods

An axisymmetric model of the chondrocyte (height = 10 μm , width = 12 μm) with a nuclear inclusion (radius = 2.5 μm) was created using ABAQUS 6.7.1 (Fig. A1-1). The aforementioned geometric parameters were chosen to closely resemble an attached chondrocyte seeded for 3 hrs.^{284,306} Both nucleus and cytoplasm were modeled as isotropic linearly elastic solids. This elastic model was chosen since the experimental data for cytoplasmic and nuclear strains were reported at equilibrium,³⁰⁷ corresponding to long-time behavior of a viscoelastic solid.³⁰⁶ Along the cell bottom, 4 μm of membrane was placed in frictionless contact with a rigid substrate. Preliminary analysis showed substrate adhesiveness had no effect on the cytoplasmic and nuclear mechanical properties determined. Finally, the cell membrane was placed in frictionless contact with the compression platen. A reference point was created for the platen to which a 25 nN load was applied. The cytoplasm and nucleus consisted of 522 and 144 axially symmetric four node reduced integration continuum elements (CAX4R), respectively. This was determined sufficient for convergence, as a model containing 2123 and 561 elements (cytoplasm and nucleus, respectively) yielded identical results.

To determine the combination of cytoplasmic and nuclear stiffnesses and Poisson's ratios that best matched observed cytoplasmic and nuclear strains,³⁰⁷ a root-mean-square difference cost function was used, defined as:

$$\delta_{RMS} = \sqrt{\left(\varepsilon_{Axial}^{Model}(Nuc) - \varepsilon_{Axial}^{Experimental}(Nuc)\right)^2 + \left(\varepsilon_{Axial}^{Model}(Cyto) - \varepsilon_{Axial}^{Experimental}(Cyto)\right)^2 + \left(\varepsilon_{Lateral}^{Model}(Nuc) - \varepsilon_{Lateral}^{Experimental}(Nuc)\right)^2 + \left(\varepsilon_{Lateral}^{Model}(Cyto) - \varepsilon_{Lateral}^{Experimental}(Cyto)\right)^2}$$

δ_{RMS} was calculated for each combination of material properties. Lower values of δ_{RMS} indicate model output more closely matched the previously reported data.

In an initial coarse search, cytoplasmic and nuclear Young's moduli were varied parametrically at 0.5 kPa increments from 1 to 7 kPa for combinations of Poisson's ratios shown in Table A1-I. These search parameters were guided by literature values for Poisson's ratios and cellular stiffness,^{306,307,435,465} as well as preliminary analyses confirming Young's moduli less than 1 kPa and Poisson's ratios less than 0.3 yielded higher δ_{RMS} values.

Based on results from the coarse search, Young's moduli were refined to increment 0.25 kPa from 3 to 5.5 kPa for $\nu_{Cyto} = \nu_{Nuc} = 0.5$ and $\nu_{Cyto} = 0.4$, $\nu_{Nuc} = 0.5$. Simulations were also performed for the cell without a nuclear inclusion to examine the contribution of the nucleus. For these cases, the cell was considered to be an isotropic linearly elastic solid with the same initial physical dimensions as before. For the cell model, cost function values were calculated using only cytoplasmic axial and lateral strains.

Results

Table A1-I shows minimum values computed from the cost function for each combination of Poisson's ratios, and the values of cytoplasmic and nuclear Young's moduli for which the minimum was obtained. From the initial coarse search, the ratio of cytoplasmic to nuclear stiffness was either ~ 1.4 ($E_Y^{Cyto} = 3.5$

kPa, $E_Y^{\text{Nuc}} = 5$ kPa) or ~ 1.1 ($E_Y^{\text{Cyto}} = 4$ kPa, $E_Y^{\text{Nuc}} = 4.5$ kPa) depending upon Poisson's ratios used. The minimum δ_{RMS} , or case most closely matching the experimental data, occurred for $\nu_{\text{Cyto}} = \nu_{\text{Nuc}} = 0.5$, i.e., both cytoplasm and nucleus incompressible. Figure A1-1 shows the cell in its undeformed and deformed states for this minimum δ_{RMS} case. Comparing cases where cytoplasmic and nuclear Poisson's ratios were held equal, there was little effect of Poisson's ratio on δ_{RMS} , though the $\nu_{\text{Cyto}} = \nu_{\text{Nuc}} = 0.3$ case had different "best fit" Young's moduli than the $\nu_{\text{Cyto}} = \nu_{\text{Nuc}} = 0.4$ or $\nu_{\text{Cyto}} = \nu_{\text{Nuc}} = 0.5$ cases.

Figure A1-2 shows a 3-D plot of δ_{RMS} as a function of E_Y^{Cyto} and E_Y^{Nuc} for $\nu_{\text{Cyto}} = \nu_{\text{Nuc}} = 0.5$. In this refined search, the minimum Young's moduli were determined to be $E_Y^{\text{Cyto}} = 3.75$ kPa and $E_Y^{\text{Nuc}} = 5.25$ kPa, with $\delta_{\text{RMS}} = 0.02276$. In the refined search for $\nu_{\text{Cyto}} = 0.4$ and $\nu_{\text{Nuc}} = 0.5$, minimum Young's moduli were determined to be $E_Y^{\text{Cyto}} = 4.0$ kPa and $E_Y^{\text{Nuc}} = 4.75$ kPa, with $\delta_{\text{RMS}} = 0.02572$. Without a nuclear inclusion, $E_Y^{\text{Cell}} = 4.25$ kPa, which did not change for $\nu_{\text{Cell}} = 0.4$ or 0.5 .

Discussion

Using a finite element approach, this study investigated *in situ* mechanical properties of the nucleus. Young's moduli and Poisson's ratio were parametrically changed for the cytoplasm and nucleus, and predicted cellular and nuclear strains were compared to known experimental results during unconfined cytocompression.³⁰⁷ It was found that the experimental data were best matched when $E_Y^{\text{Cyto}} = 3.75$ kPa, $E_Y^{\text{Nuc}} = 5.25$ kPa, and both cytoplasm and nucleus were incompressible. These results suggest the ratio of nuclear to cytoplasmic

stiffness is less than previously reported for single cells.^{86,209} Moreover, changing Poisson's ratio had little effect on the model.

Examining nuclear mechanical properties is an important step toward understanding cellular mechanotransduction. Nuclear physical characteristics change in response to an applied load on native tissue²⁰⁷ or tissue engineered constructs.³⁰² Enclosed within the nucleus, chromatin is organized by the nuclear lamina.¹ Due to cellular deformations, mechanical linkages between cytoskeleton and nuclear lamina may lead to changes in chromatin conformation/alignment and/or 3-D spatial orientation of transcription factors. Thus, understanding how the nucleus senses and responds to forces provides insight into possible gene regulatory mechanisms.

The results presented in this communication have applicability to current finite element models of cell – matrix interactions. These models predict the local mechanical environment of chondrocytes under various loading conditions.^{71,210,484,514} When considering the cell without a nuclear inclusion, cellular Young's modulus was minimally greater than the cytoplasm itself. Moreover, the *in situ* difference between cytoplasmic and nuclear stiffnesses during compression is small, and variations in Poisson's ratio had little effect on Young's moduli (i.e. $E_Y^{\text{Cyto}} = 3.75 \text{ kPa}$, $E_Y^{\text{Nuc}} = 5.25 \text{ kPa}$ for $\nu_{\text{Cyto}} = \nu_{\text{Nuc}} = 0.5$ versus $E_Y^{\text{Cyto}} = 4 \text{ kPa}$, $E_Y^{\text{Nuc}} = 4.75 \text{ kPa}$ for $\nu_{\text{Cyto}} = 0.4$, $\nu_{\text{Nuc}} = 0.5$). These results suggest that assumptions of cellular homogeneity and incompressibility may be valid simplifications for theoretical models describing chondrocytes.

Several explanations exist for why our results differ from previously reported nuclear and cellular stiffnesses. We observed a nuclear to cytoplasmic stiffness ratio of ~ 1.1 or ~ 1.4 depending on the assumed combination of Poisson's ratios, whereas prior results from micropipette aspiration testing of chondrocytes and isolated nuclei suggest this ratio is 3 to 4.²¹¹ However, in comparison to the free-floating state in micropipette aspiration, cytoskeletal rearrangements during cell attachment for unconfined cytocompression may cause alterations in nuclear structure and decreased stiffness. Moreover, when tested *in situ*, connections between the nuclear lamina and cytoskeleton are intact, resulting in a more integrated mechanical framework between the cytoplasm and nucleus. Additionally, the predicted stiffness value of the overall cell using our model is 2 to 3 times greater than previous unconfined compression results for single chondrocytes.^{306,435} Since our finite element model represents the cell as an ellipsoid, more accurately resembling the geometry of attached chondrocytes than a cylinder,⁴³⁶ the increased stiffness is likely an effect of modeling changing contact surface area. Smaller contact area results in increased stress and, hence, greater cell stiffness. Finally, the cellular stiffness under compression is greater than previous micropipette aspiration results with single chondrocytes,⁴⁶⁴ in which tensile forces dominate.

In conclusion, this study elucidated a combination of chondrocyte cytoplasmic and nuclear stiffnesses and Poisson's ratios which simulated previous results for unconfined cytocompression. *In situ*, nuclear stiffness was determined to be 40% more than the cytoplasm, which is lower than previously

reported.^{86,211} Moreover, little effect of Poisson's ratio on the model's behavior was observed, and the incompressible case best matched the prior experimental data. These results have implications in understanding the basis of cellular mechanotransduction.

Table A1-I: Effect of Poisson's ratio combinations on cytoplasmic and nuclear stiffnesses for the initial coarse search

Poisson's Ratio		"Best fit" Stiffness		
Cytoplasm	Nucleus	Cytoplasm (kPa)	Nucleus (kPa)	δ_{RMS}
0.3	0.3	4	4.5	0.03770
0.3	0.4	4	4.5	0.03360
0.4	0.3	3.5	5	0.03357
0.4	0.4	3.5	5	0.03018
0.4	0.5	4	4.5	0.02595
0.5	0.4	3.5	5	0.02627
0.5	0.5	3.5	5	0.02279

Table A1-I. Effect of Poisson's ratio combinations on cytoplasmic and nuclear stiffnesses for the initial coarse search. In the coarse search, cytoplasmic and nuclear stiffness values were each varied parametrically from 1 to 7 kPa, resulting in 169 different stiffness combinations for each set of Poisson's ratio values. In the coarse search, it was observed that the $\nu_{Cyt} = \nu_{Nuc} = 0.5$ combination best fit the experimental data with the lowest cost function value, resulting in $E_Y^{Cyt} = 3.5$ kPa, $E_Y^{Nuc} = 5$ kPa. The similarity of "best fit" stiffnesses and cost function demonstrate that Poisson's ratio had little effect on the ratio of cytoplasmic to nuclear stiffness.

Figure A1-1: Axisymmetric finite element model of chondrocyte and nucleus

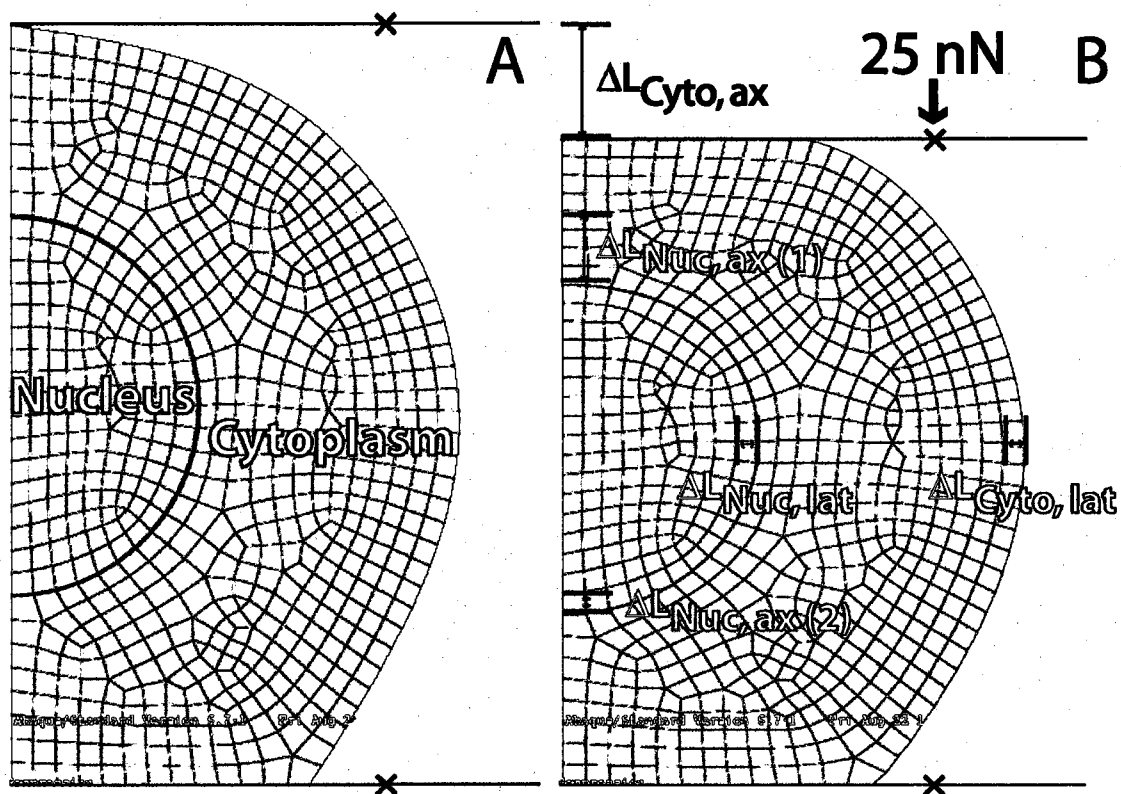


Figure A1-1. Axisymmetric finite element depiction of a chondrocyte, with distinct nuclear and cytoplasmic regions, undergoing unconfined compression. In its undeformed state (A), the cell is considered to be 10 μm tall and 12 μm wide, with a spherical nuclear inclusion of radius 2.5 μm . The lateral and axial deformations of both the cytoplasm and nucleus were measured in response a 25 nN load applied onto the cell (B). The linear elastic mechanical properties of the cytoplasm and nucleus were varied parametrically, and a cost function (δ_{RMS}) value was calculated for each case in comparison to known experimental data.³⁰⁷ (ax = axial; lat = lateral)

Figure A1-2: Cost function (δ_{RMS}) plots

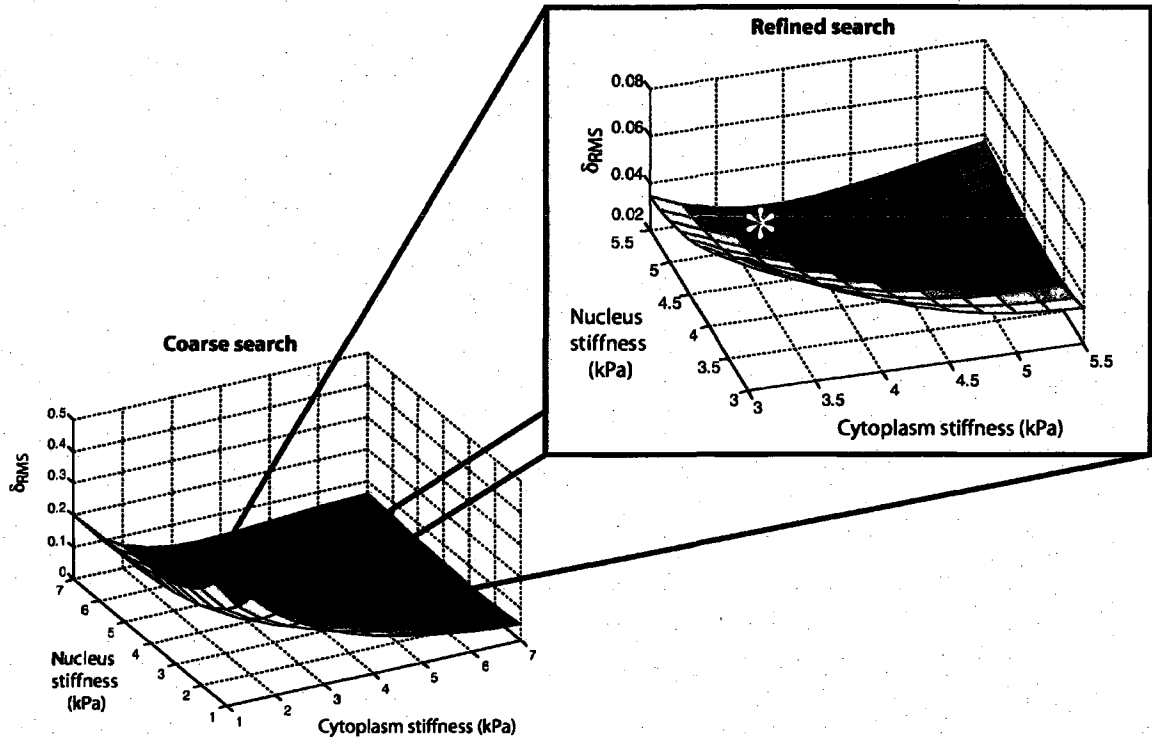


Figure A1-2. Cost function (δ_{RMS}) plots for the case of $\nu_{Cyt} = \nu_{Nuc} = 0.5$. In the initial coarse search, the elastic moduli of the cytoplasm and nucleus were varied from 1 kPa to 7 kPa, at 0.5 kPa increments. In the exploded view, the search was refined to range from 3 kPa to 5.5 kPa, at 0.25 kPa increments. A global minimum for δ_{RMS} was observed at $E_Y^{Cyt} = 3.75$ kPa, $E_Y^{Nuc} = 5.25$ kPa (indicated by the asterisk).

Appendix 2: Validation, pilot, and supplemental data for various articular cartilage impact experiments*

Introduction

This appendix provides supplemental data for the articular cartilage impact work contained in this thesis. First, data are presented that validate the manual compression protocol used in Chapter 3. In that chapter, P188 was applied to articular cartilage explants post-injury. Prior work with P188^{37,389} suggested that compression was necessary for P188 to decrease cell death, presumably by assisting P188's entry into the tissue. However, no description of the compression protocol was provided. In this thesis the compression protocol used was 10 manual compressions of ~1 MPa at 0.1 Hz using a custom made stainless steel non-porous platen, where a cycle consisted of ~2 sec of load followed by ~8 sec recovery.

In Chapter 4, 50 and 100 μ M doxycycline were delivered in the media post-injury. Choosing doxycycline concentrations for explants was complicated since previous studies used cells or animal models.^{439,440,448} This appendix provides data from a pilot study that guided our decision to use 50 and 100 μ M.

Finally, in all the impact studies contained in this thesis (Chapters 2-4), sulfated glycosaminoglycan (sGAG) release post-injury was investigated. However, hyaluronic acid (HA), another important GAG in articular cartilage, is not sulfated. It was hypothesized that HA release to the media would also be

*I acknowledge Dr. Nic Liepzig for fabricating the compression device and Dr. Jane Grande-Allen and Dr. David Allison for assisting with the FACE procedure and data analysis.

increased post-injury. Fluorophore assisted carbohydrate electrophoresis (FACE) was used to test this hypothesis.

Methods

Compression device fabrication and validation

The compression device was made from type 309 heat-resistant austenitic stainless steel (J & L Specialty Steel, Pittsburgh, PA). Knowing the density allowed calculation of the volume of steel required to produce a 19.7 N load, which, when applied to a circular area 5 mm in diameter, delivers 1 MPa. The device was designed with the sketching capability of SolidWorks 3D computer aided design software and then machined to specification.

Validation of manual compression to 1 MPa load at 0.1 Hz, where a cycle consisted of ~2 sec of load followed by ~8 sec recovery, was accomplished as follows: the load cell of an electromechanical materials testing system (Instron Model 5565, Canton, MA) was turned upside down on a flat surface. Articular cartilage explants were then placed in a petri dish atop the load cell sensor. A digital timer was used to keep time as the explant was manually loaded and unloaded in the petri dish. This procedure was repeated on five different explants. Finally, load versus time data collected by the Instron was imported into Matlab for statistical analysis.

Doxycycline pilot experiment

Four bovine ulnas were obtained and impacted with 1.1 J as described in Chapter 4. Unimpacted control explants (5 mm) were taken from the same joints.

Explants were cultured for 1 week in the presence of 100 or 300 μM doxycycline. 300 μM doxycycline was chosen because it is well above the concentration at which the activity of matrix metalloproteinases-1 (MMP-1) is inhibited by 50%;²⁰³ 100 μM is below this level. Medium was changed and collected on days 1, 3, 5, and 7 and subsequently pooled for analysis of sGAG with the DMMB assay. On day 7, explant culture was terminated. The central 3 mm core of the explant was tested under creep indentation; the outer annulus underwent processing for PCR as described in Chapter 2. Gene expression of MMP-1, tissue inhibitor of MMP-1 (TIMP-1), and GAPDH was assessed.

FACE analysis of culture media post-injury

Media collected over 1 week from nine uncompressed, untreated explants that were part of Chapter 3 were assessed as previously described.^{9,10} Three unimpacted control, three Low impact, and three High impact specimens were assayed.

Results

Compression device fabrication and validation

The manual compression protocol was robust. Figure A2-1 shows that 19.7 N was readily achievable in a cyclical manner. Tolerance in the statistical analysis was set to be $1 \text{ MPa} \pm 0.05 \text{ MPa}$. The analysis showed that the stress was within this range $1.76 \pm 0.15 \text{ s}$ (mean \pm 98% confidence interval) of every 10 s period.

Doxycycline pilot experiment

It was found that doxycycline was readily soluble in phosphate buffered saline, but not in DMEM. While 300 μ M doxycycline dissolved in DMEM, it formed a yellow, crystalline “slurry” in media over 2 days. This was not the case for 100 μ M doxycycline. Treatment with either doxycycline concentration yielded an ~30% decrease in sGAG released from explants for each impact level (Fig. A2-2). There were no differences in the tissue’s aggregate modulus, Poisson’s ratio, or permeability. There were also no differences in GAPDH, MMP-1, or TIMP-1 gene expression. However, the TIMP-1/MMP-1 ratio was over 2.5 times greater in the Low impact, 100 μ M doxycycline group compared to all others.

FACE analysis of culture media post-injury

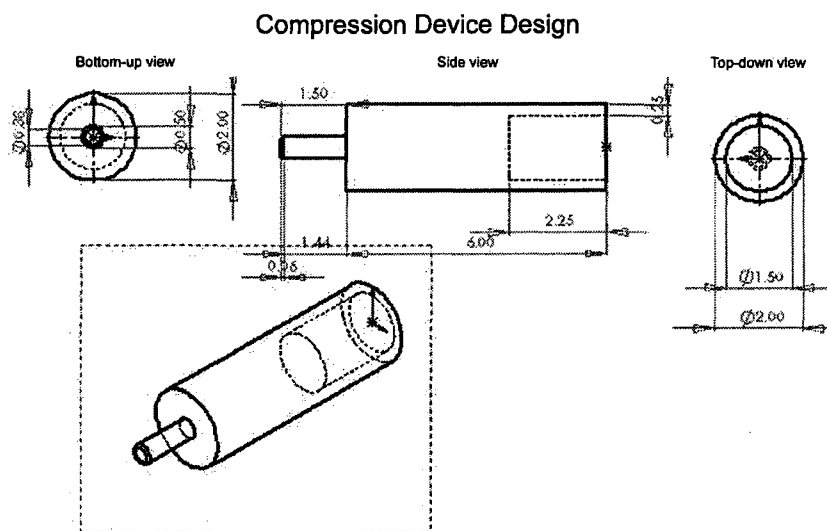
In general, the intensity of the bands in sample lanes increased from control to Low to High (Fig. A2-3). This observation was congruent with data from the DMMB assay, which showed impact caused an increased amount of sGAG release from explants (Chapter 3). HA was not found in any sample tested.

Summary

This appendix provides several pieces of data related to the impact work of this thesis. First, the manual compression protocol used in Chapter 3 was validated. Second, 100 μ M doxycycline was shown to have similar capability as 300 μ M doxycycline with respect to decreasing sGAG release from articular cartilage explants. However, since the media were pooled, statistical comparison was not possible. Nevertheless, based on this observation, and the fact that the TIMP-1/MMP-1 ratio was increased, 100 μ M doxycycline was chosen as one

concentration for use in Chapter 4. To investigate if a lower concentration could also be effective, 50 μ M doxycycline was also investigated. Finally, whether HA is released from articular cartilage following impact loading was assessed. HA was not seen in media assayed with FACE analysis, suggesting that HA is not released in the first week post-injury. This may also suggest that hyaluronidase is not part of the early response of cartilage to injury.

Figure A2-1: Compression device design and validation data



Representative data obtained from Instron

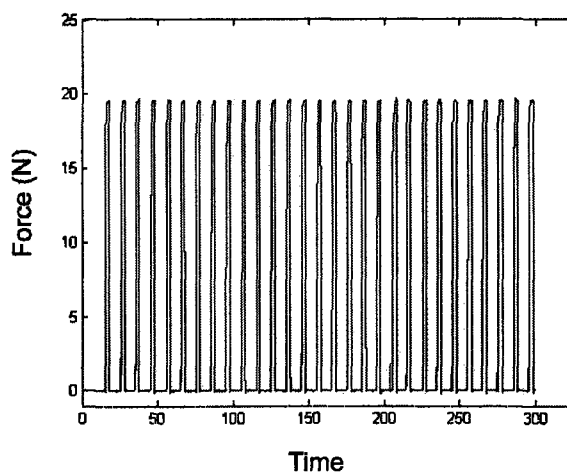


Figure A2-1: Compression device design and validation data. Sketch dimensions are in inches. Note how the graph demonstrates the ability to manually deliver 1 MPa (19.7 N over a circular area 5 mm in diameter) cyclically in a consistent manner.

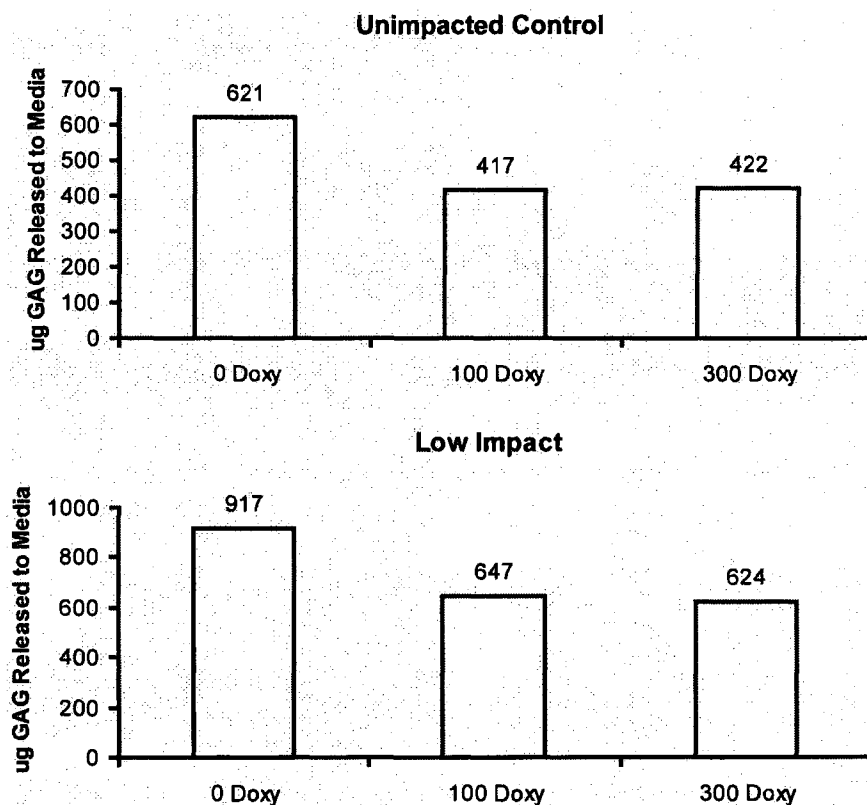
Figure A2-2: sGAG release data from doxycycline pilot

Figure A2-2: Total μg of sulfated glycosaminoglycan (sGAG) released over 7 days from 5 mm diameter cartilage explants ($n = 4$, pooled). Unimpacted controls or Low impact specimens were cultured in the presence of 100 or 300 μM doxycycline. There was an $\sim 30\%$ decrease in sGAG released from explants in the treated groups for each impact level.

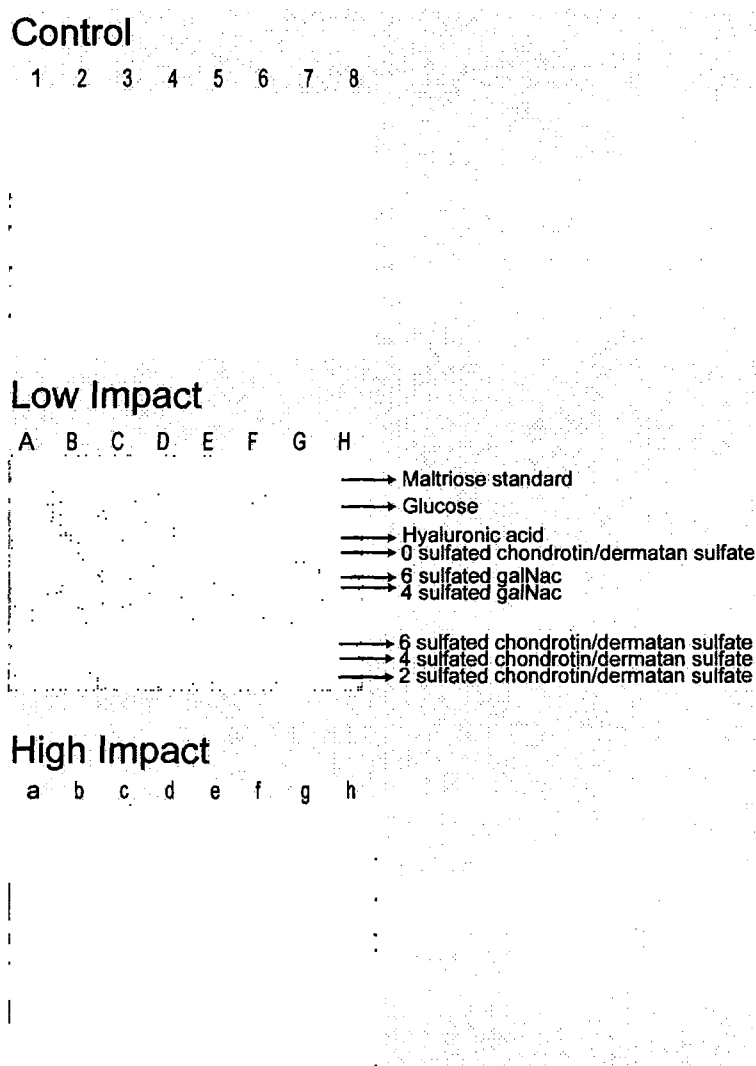
Figure A2-3: Data for HA release post-impact injury

Figure A2-3: Fluorophore assisted carbohydrate electrophoresis (FACE) gels for collected media samples from unimpacted control, Low impact, and High impact specimens (n = 3 in duplicate). Lanes 1, 8, A, H, a, and h are ladder lanes. The bands of the ladder are labeled in the Low impact gel. Lanes 2 and 3, 4 and 5, and 6 and 7 represent control samples #1, 2, and 3, respectively. Lanes B-G and b-g are interpreted similarly for Low and High impact samples. Notice that hyaluronic acid (HA) was not released to the media from any of the samples investigated. The maltriose standard row can be used for quantification, though this was not necessary since HA was absent.

Appendix 3: Mechanical properties of immature bovine articular cartilage and mechanical testing of self-assembled articular cartilage constructs*

Introduction

Inherent in functional tissue engineering of articular cartilage is measurement of the biomechanical properties of engineered constructs and comparison of these values to native tissue values.⁸⁵ The results presented in this appendix 1) provide data on the mechanical properties of immature, bovine articular cartilage explants from the patellofemoral groove (one of the locations from which cells were harvested for the tissue engineering studies contained in this thesis) for comparison with results from tissue engineering efforts and 2) serve as pilot experiments for several hypotheses about the mechanical testing and behavior of self-assembled articular cartilage constructs. In terms of compressive stiffness, it was hypothesized that self-assembled constructs would demonstrate a strain dependent increase in aggregate modulus (H_A), and, secondly, that the tare load used during testing can affect the measured value of H_A . To test these hypotheses, three combinations of tare load and test load were used during creep indentation testing. With respect to the tensile behavior, it was hypothesized that constructs would exhibit viscoelastic behavior, demonstrated by strain-rate dependent stiffness and stress-relaxation. To test these hypotheses, constructs were pulled in tension to failure at three strain-rates and

*I acknowledge Kerem Kalpacki for help with stress-relaxation data analysis and Ke Xun Chen for performing the creep indentation tests.

tested under incremental stepwise stress-relaxation. Additionally, a methodology is described for determining Poisson's ratio during tension.

Methods

Tissue acquisition and mechanical testing of cartilage explants

For explants, cartilage from the patellofemoral groove of male calves (Research 87, Boston, MA) was obtained with a 5 mm dermal biopsy punch. The explant was then trimmed manually with a scalpel to generate a thickness of ~1.5 mm. Following trimming, the central region of the explant was removed with a 3 mm biopsy punch, yielding an inner core and an outer annulus. The inner core was used for creep indentation testing. The outer annulus was prepared for tensile testing by first cutting it in half to yield two crescent shaped specimens, and then sectioning the crescent with a scalpel into three specimens each of ~0.5 mm thick. The middle of these three specimens was then cut into a dog bone shape. This final step generated the specimen used for tensile testing.

Compressive mechanical properties were determined by creep indentation testing of the central 3 mm core assuming a linear biphasic model.³⁴⁷ Thickness was measured using a micrometer, and specimens were attached to a flat stainless steel surface with a thin layer of cyanoacrylate glue and submersed in phosphate buffered saline. The attached specimen was then placed into the creep indentation apparatus, which was used to automatically load and unload the specimens while monitoring specimen creep and recovery. Specimens were tested with a tare load of 0.2 g followed by a test load of 0.7 g. The loads were

applied to the specimens through a 1 mm diameter, flat-ended, porous tip. To determine construct mechanical properties, a semi-analytical, semi-numerical, linear biphasic model was employed,³⁴⁸ followed by a non-linear finite element optimization to refine the solution and obtain values for the aggregate modulus, permeability, and Poisson's ratio.³⁰

For tensile testing, ImageJ was used to determine sample width from photographs. Thickness was measured with a micrometer. The specimen was then loaded into a mechanical testing system (Instron Model 5565, Canton, MA) that had its zero position point pre-determined. The sample was pulled until a 0.08 N pre-load was reached. Displacement from the zero position to the point at which the pre-load was reached defined the sample's gauge length. This methodology differs from that for testing self-assembled constructs because tissue was determined to be too strong for the gluing to paper method (see below). The specimen was then pulled at a rate of 1% gauge length per second. During testing, the Instron monitored and recorded displacement, which when combined with gauge length, allowed strain to be calculated. Young's modulus was determined by linear regression of the linear portion of the stress-strain curve based on initial cross-sectional area. The ultimate tensile strength (UTS) was taken to be the maximal stress prior to failure.

Generation of self-assembled constructs for mechanical testing

Bovine chondrocytes were isolated and self-assembled as previously described.²³¹ Cartilage from the distal femur and patellofemoral groove of male calves (Research 87, Boston, MA) was digested in collagenase type II for 24 hrs.

Cells were counted using a hemocytometer and trypan blue staining and then frozen at -80°C . Within days, cells were thawed and counted again. Cells were then seeded at ~ 5.5 million live cells in $100\ \mu\text{L}$ of media into 5 mm diameter cylindrical agarose wells. An additional $400\ \mu\text{L}$ of media was added 4 hrs later. Chondrogenic medium composed of DMEM with 4.5 mg/mL glucose and L-glutamine (Biowhittaker/Cambrex, Walkersville, MD), 100 nM dexamethasone (Sigma, St. Louis, MO), 1% fungizone, 1% penicillin/streptomycin, 1% ITS+ (BD Scientific, Franklin Lakes, NJ), $50\ \mu\text{g/mL}$ ascorbate-2-phosphate, $40\ \mu\text{g/mL}$ L-proline, and $100\ \mu\text{g/mL}$ sodium pyruvate (Fisher Scientific, Pittsburgh, PA) was used for seeding and subsequent media changes. The $500\ \mu\text{L}$ of media were changed daily throughout the experiment. At 10 days, all constructs were transferred to tissue culture plates in which only the bottom of the wells was coated with a thin layer of agarose¹⁴² and randomly assigned to either 1, 5, or 10% strain-rate tensile testing to failure or to stress-relaxation tensile testing. Constructs were cultured for four weeks. Just prior to mechanical testing, constructs were removed from culture and processed. A 3 mm diameter core was removed from the construct's center with a biopsy punch for creep indentation testing. The remaining outer ring was portioned $\sim 60\%$ for biochemical analysis and $\sim 40\%$ for tensile testing. The biochemical samples were used for an experiment that was not part of this study.

Construct compressive testing

Creep indentation compression testing was performed as described above with the following notable exceptions: 1) the indenter tip had a diameter of 0.8

mm and 2) tare/test load combinations were 0.2 g/ 0.7 g ("Gold Standard" used to test self-assembled constructs in our laboratory), 0.05 g/ 0.7 g ("Low"), and 0.05 g/ 2.0 g ("High"). The first two groups test the effect of tare load, while the latter two groups test the effect of test load. The samples tested were the central 3 mm cores obtained from the 1, 5, and 10% strain-rate tensile testing to failure groups.

Construct tensile testing to failure

The portion of each sample assigned to tensile testing was cut into a dog-bone shape and glued to paper tabs.³⁵ ImageJ was used to determine sample gauge length and width from photographs. Gauge length was defined as the distance between the paper tabs. Thickness was measured with a micrometer. Tensile tests were performed at strain-rates of 1, 5, or 10% gauge length per second on a mechanical testing system (Instron Model 5565, Canton, MA). There was no pre-conditioning of the specimens. Young's modulus and UTS were obtained as described above for tissue (see Fig. A3-2A).

Additionally, Poisson's ratio was determined for the specimens tested at 1% gauge length per second (our laboratory's typical testing method). Poisson's ratio is defined as the negative of the ratio of lateral to axial strain, i.e., $-(\text{lateral strain})/(\text{axial strain})$. Axial strain data were acquired via the Instron. Lateral strain was acquired via digital image analysis as follows. First, free downloadable software was added to a digital camera to enable time-lapse videography. The software script was set such that the camera would take a photograph at 2 s, and every 4.5 s thereafter. These settings were validated by running the script while

photographing a digital timer. Just before beginning a tensile test, a photograph of the specimen loaded into the Instron was taken. This image defined time zero ($t = 0$; Fig. A3-2B). The camera script and tensile test were then begun simultaneously, such that the acquired images corresponded to the Instron data in time. During tensile data analysis, the pictures were matched in time to the linear portion of the stress-strain curve. In the example of figure A3-2, the linear portion begins at $t = 15.5$ s and ends at 38 s. Using ImageJ, the lateral strain was then determined. The width of the specimen in pixels from the $t = 0$ picture determined the "lateral gauge length." Width in pixels was measured in subsequent pictures corresponding to the linear portion of the stress-strain curve, allowing lateral strain to be calculated. Figure A3-2C shows a plot of axial strain versus $-(\text{lateral strain})$. Linear regression of this plot yields Poisson's ratio.

Construct stress-relaxation tensile testing

The tensile stress-relaxation apparatus consisted of a custom-made bath grip system used within the Instron.¹²⁹ Samples were prepared and fixed to paper tabs as described above, loaded into the system, and allowed to equilibrate for 10 min. After 10 min, a 0.02 N tare load was applied. The distance of separation between the top and bottom grips at this point was taken to be the initial specimen length. Immediately following application of the tare load, the samples were preconditioned through application of cyclical 5% strain at a strain rate of 10 mm/min for 15 cycles. After preconditioning, successive step strains were applied at 5% increments beginning with 10% and going up to 40%. Between these steps, the samples were allowed to relax for 10 min. If the sample did not fail

during application of these strains, the sample was pulled at a constant rate of 0.1 mm/s until failure. Figure A3-4 shows a representative stress-relaxation curve generated using this protocol. Note that the strains reported in figure A3-4 use the gauge length measured via Image J as separation between the paper tabs, and not the gauge length determined by the 0.02 N tare load. The instantaneous modulus was determined by linear regression of peak stress versus strain plot; the relaxed modulus was determined by linear regression of relaxed stress versus strain plot. Though not performed, fitting of the transient portion of the curve assuming a standard linear solid viscoelastic material model would yield the construct's apparent viscosity.⁷

Statistics

All data are presented as mean \pm S.D. A one-way ANOVA was run on material properties and test strain obtained from creep indentation testing of self-assembled constructs based on tare/test load combination. A one-way ANOVA was also run on the material properties obtained from tensile testing to failure of self-assembled constructs at different strain-rates based on strain-rate. If significance was found, a Student-Newman-Keuls post-hoc test was performed. Significance was set at $p < 0.05$. An $n = 6-7$ explants were used for tissue characterization. An $n = 4-5$ specimens were used for testing of self-assembled constructs.

Results

Tissue explants

The method of trimming to the desired thickness was robust, yielding explants with thicknesses of 1.50 ± 0.11 mm. The strain under the test load measured $1.41 \pm 0.43\%$, well within the limits of linear theory. Table A3-I contains the results from creep indentation and tensile testing to failure at 1% of gauge length per second for tissue explants. About half of the specimens (4 of 7) broke at the specimen-clamp interface during tensile testing, which may affect the UTS data. The others broke in the middle of the gauge length.

Construct creep indentation testing

Tare/test load combination and test strain were significant based on the ANOVA ($p = 0.02$ and 0.01 , respectively). Post-hoc testing showed that the aggregate modulus of the Low tare/test combination was significantly less than the aggregate modulus of the High and Gold Standard tare/test combinations. Test strain in the Gold Standard and Low groups was significantly less than test strain in the High group. There were no significant differences in thickness among the groups. The average thickness was 0.56 ± 0.03 mm. Further, there were no significant differences in permeability or Poisson's ratio among the groups. Permeabilities measured 46.7 ± 31.1 , 95.1 ± 64.1 , and 39.7 ± 26.8 $\text{m}^4/\text{N}\cdot\text{s} \times 10^{-15}$ for the Gold Standard, Low, and High groups, respectively. Poisson's ratios were 0.236 ± 0.081 , 0.158 ± 0.133 , and 0.212 ± 0.147 for the Gold Standard, Low, and High groups, respectively.

Construct tensile testing to failure

Figure A3-3 shows the results of tensile testing to failure at 1, 5, or 10% gauge length per second. Tensile testing at these particular strain rates did not significantly affect either Young's modulus or UTS. The average Young's modulus of all specimens was 997 ± 265 kPa. For UTS, the average was 458 ± 143 kPa.

Due to the few number of points obtained at 5 and 10% gauge length per second, Poisson's ratio was only able to be measured for the group tested at 1% gauge length per second. Poisson's ratio measured 0.39 ± 0.09 for these constructs.

Construct stress-relaxation tensile testing

Figure A3-4 shows a representative stress-relaxation curve. Only three of four tests were of sufficient quality to be analyzed. A fifth sample failed during mounting. The three analyzed constructs all demonstrated stress-relaxation viscoelastic behavior, but *a posteriori* strain calculations based on gauge length measured via Image J were greater than anticipated based on the Instron program. Instantaneous moduli were found to be 1150, 1470, and 1116 kPa for samples one, two, and three, respectively, while relaxed moduli of samples one, two, and three were 1047, 1690, and 1001 kPa, respectively.

Discussion

This appendix provides data on the biomechanical properties of immature, native bovine articular cartilage and demonstrates that self-assembled articular

cartilage constructs exhibit the viscoelastic behavior of stress-relaxation. However, strain-rate dependent stiffness was not observed for the small range and magnitudes of rates examined (1-10% of gauge length per second). Further, it was shown that the tare/test load combination used during creep indentation can significantly affect the measured value of the construct's aggregate modulus.

Several studies have assessed the biomechanical properties of immature bovine articular cartilage. Hu and Athanasiou²³¹ report an aggregate modulus of 139 ± 41 kPa, permeability of $42 \pm 28 \text{ m}^4/\text{N}\cdot\text{s} \times 10^{-15}$, and Poisson's ratio of 0.01 ± 0.01 using creep indentation. Values from the present experiment are slightly greater for the aggregate modulus and less for the permeability. When tested in confined compression, the aggregate modulus measured 270 ± 20 kPa and the permeability measured was on the order of $O(10^{-14}-10^{-15})$.⁴⁹³ The study also showed that the aggregate modulus increases and the permeability decreases with increasing strain. Hung and colleagues²³⁸ give ~ 277 kPa for the tissue's compressive Young's modulus measured in unconfined compression.

Turning to tension, Williamson et al.⁴⁹⁵ report an equilibrium modulus of ~ 2.75 MPa and strength of ~ 4 MPa using a modified stress relaxation test. In more recent study, a ramp modulus of ~ 7.5 MPa was measured (average of d0 S&M in figure 6 of the referenced paper).²¹ In a related study, the ramp modulus was $\sim 10-11$ MPa and the strength was $\sim 5-6$ MPa (average of d0 S&M in figure 5 of the referenced paper).²² In these latter two studies, samples were tested to failure at a strain-rate of $\sim 1.3\%$ of gauge length per second (gauge length = 4 mm, elongation at 5 mm/min). Hence, by comparison with these reports, the

values given in Table A3-I are in reasonable agreement with previously published results, providing a solid benchmark for measuring articular cartilage tissue engineering efforts.

The biomechanical behavior of articular cartilage is complicated, exhibiting viscoelastic behavior in both tension and compression.³⁴⁹ Further, in compression the material properties are known to depend on strain^{97,493,501} in addition to strain rate.^{314,315,376} Specifically, stiffness increases and permeability decreases as strain and strain rate increase. The data in this appendix suggest that our self-assembled constructs have strain dependent stiffness. Test strain was significantly greater in the High tare/test load combination compared to Low, accompanied by an almost 1-fold increase in stiffness.

Perhaps more interesting is the effect of tare load on testing of self-assembled constructs. Increasing the tare load for a constant test load yielded a 60% increase in the measured aggregate modulus (Low versus Gold Standard groups). Additionally, despite the total load (test + tare) being greater in the Gold Standard group compared to Low, the test strains were not significantly different. It is possible that greater displacement beneath the tare load results in testing of a deeper, stiffer region of the construct. The purpose of the tare load is to ensure tissue contact with the indenter; however, this could potentially be accomplished by other means. To remove the potential effects of a tare load, future work in this area should seek to develop a compressive testing methodology that does not involve a tare load. Then, a series of test loads that impart significantly different

test strains could be used to establish the degree of strain dependent stiffness present in self-assembled constructs.

Tensile Poisson's ratio for articular cartilage tissue has been measured,^{93,147,236,418,507} yielding a wide range of values. The values are often greater than 0.5, demonstrating the anisotropic nature of native tissue. A unique aspect of the present work is measurement of Poisson's ratio of tissue engineered constructs during tension. Compared to compression, few cartilage tissue engineering studies have assessed tensile properties,^{142,143,145,161,189,198,233,375,492} and none to our knowledge has measured Poisson's ratio. The methodology described in this appendix is robust, but can be improved by increasing both the frequency of image acquisition and the resolution.

Furthermore, as hypothesized, self-assembled constructs exhibited stress-relaxation (Fig. A3-4). Interestingly, there does not appear to be much difference between the instantaneous and equilibrium moduli, or comparing these moduli to Young's modulus from tests to failure at 1, 5, and 10% gauge length per second. As mentioned above, Young's modulus and UTS were not rate dependent. This is similar to observations from articular cartilage tissue, where rate-dependent effects were not observed until 70% gauge length per second.⁴⁷¹

The protocol used for stress-relaxation testing of constructs in this appendix is probably non-optimal, as it was adapted straight from protocols used to test tissue. While it was capable of demonstrating the stress-relaxation behavior of self-assembled constructs, optimization of the testing protocol is

needed. For example, the strains shown in figure A3-4 (calculated from gauge length measured by ImageJ) do not match the strains that were expected from the Instron program. Further, there are few data points during the transition from one strain level to the next. These observations suggest that the sensitivity and speed of data acquisition of the system may need to be increased. Another consideration is the pre-conditioning step. The number of cycles, frequency, strain, and strain-rate needed for adequate pre-conditioning should be investigated. Pre-conditioning is important for viscoelastic testing to remove hysteresis, thereby reaching a limiting value.¹⁷⁹ Whether pre-conditioning has a role in tensile tests to failure should also be studied.

In conclusion, biomechanical properties of immature, native bovine articular cartilage tissue were measured that are in agreement with previously published data. Comparing these data to the properties of the self-assembled constructs, we see that constructs are in the range of biphasic compressive properties, and moving in the right direction with respect to tensile properties. Further, self-assembled constructs exhibit more complicated mechanical behavior similar to native tissue, such as strain-dependent stiffness and tensile stress relaxation. Perhaps more importantly, the data in this appendix show that a proper tare load/test load combination that yields consistency in the measured values of the compressive stiffness is needed for compressive testing. A compressive test should utilize a minimum tare load (ideally none at all), and the test load should yield similar strains among all groups tested within an experiment and from one experiment to the next. However, the inherent

biological variability of the system may make the latter unrealistic. Further development of testing methods for and characterization of the mechanical behavior of self-assembled constructs will enable more in depth comparison with what us known about native tissue.

Table A3-I: Mechanical properties of immature bovine articular cartilage

Compression			Tension	
Aggregate Modulus (kPa)	Permeability ($\text{m}^4/\text{N}\cdot\text{s} \times 10^{-15}$)	Poisson's Ratio	Young's Modulus (MPa)	Ultimate Tensile Strength (MPa)
238 ± 72	6.59 ± 6.32	0.06 ± 0.05	4.8 ± 2.6	$4.0 \pm 2.2^*$

Table A3-I: Mechanical properties of immature. The values in this table represent mean \pm S.D. of explants from the patellofemoral groove of 1-3 week old male calves measured under creep indentation and tensile testing to failure at 1% of gauge length (n = 6-7 from four distinct animals). The * indicates that not all specimens broke in the middle of the gauge length.

Figure A3-1: Aggregate modulus resulting from different tare/test loads

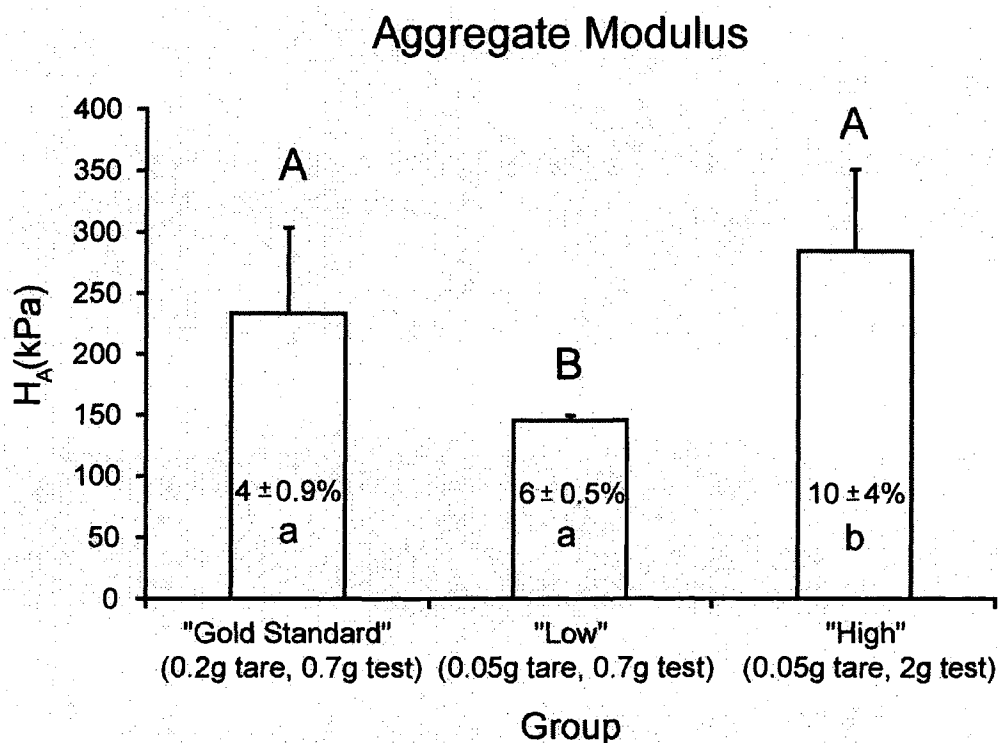


Figure A3-1: The aggregate modulus (H_A) of self-assembled constructs tested under different tare load/test load combinations. Bars represent mean \pm S.D. for H_A ($n = 4-5$). Values within the bars are mean \pm S.D. of the test strains for that group. The uppercase letters above the bar reflect results from post-hoc testing on H_A , while the lowercase letters within the bars reflect results from post-hoc testing on test strain. In either case, groups not connected by a similar letter are significantly different from one another. There is a significant, nearly 1-fold increase in H_A comparing the 0.05 g tare/0.7 g test load combination to the 0.05 g tare/2.0 g test load combination, accompanied by significantly increased test strain. Interestingly, there is a significant decrease in H_A for the group tested with the 0.05 g tare/0.7 g test compared to the "gold standard" even though test strains between the two groups are similar. This last result suggests the tare load affects the measured stiffness.

Figure A3-2: Representative data for tensile test to failure

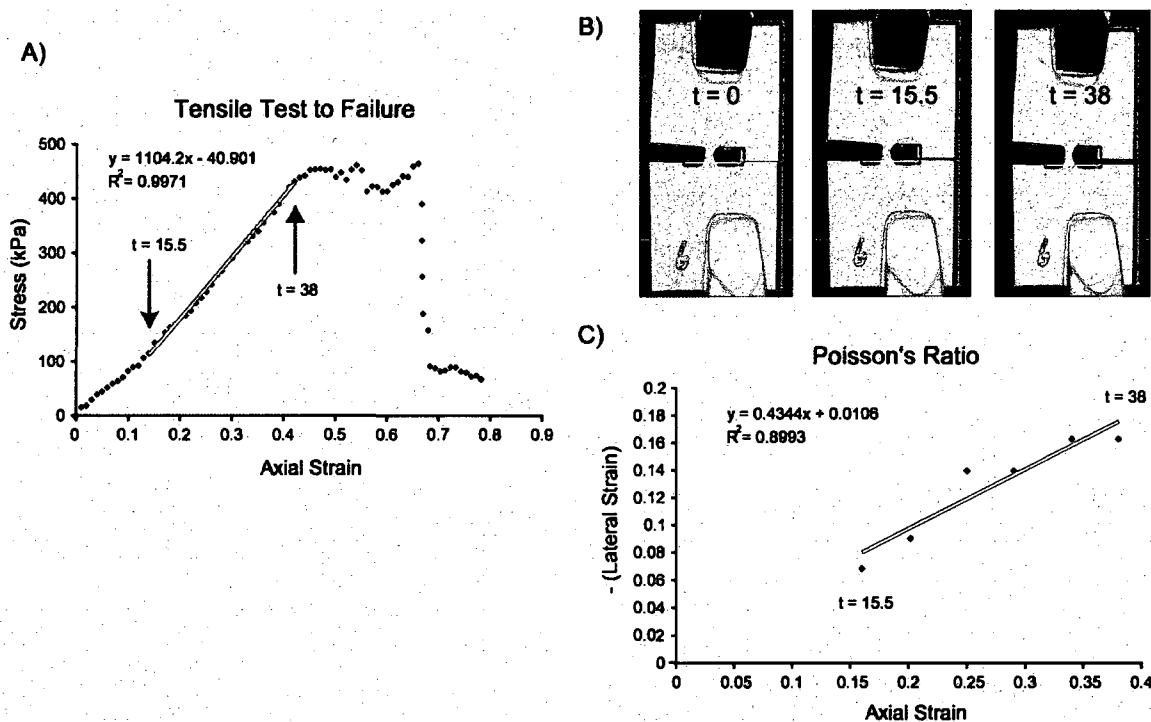


Figure A3-2: Representative data from a tensile test to failure at a strain-rate of 1% of gauge length. A) Stress versus axial strain, B) digital images taken during the test for determination of Poisson's ratio, and C) linear regression of axial strain versus negative of the lateral strain demonstrating how Poisson's ratio is obtained. In B, note the subtle decrease in the lateral dimension of construct. "Time-stamps" are provided in each subfigure to demonstrate the way in which lateral strain is matched in time to axial strain.

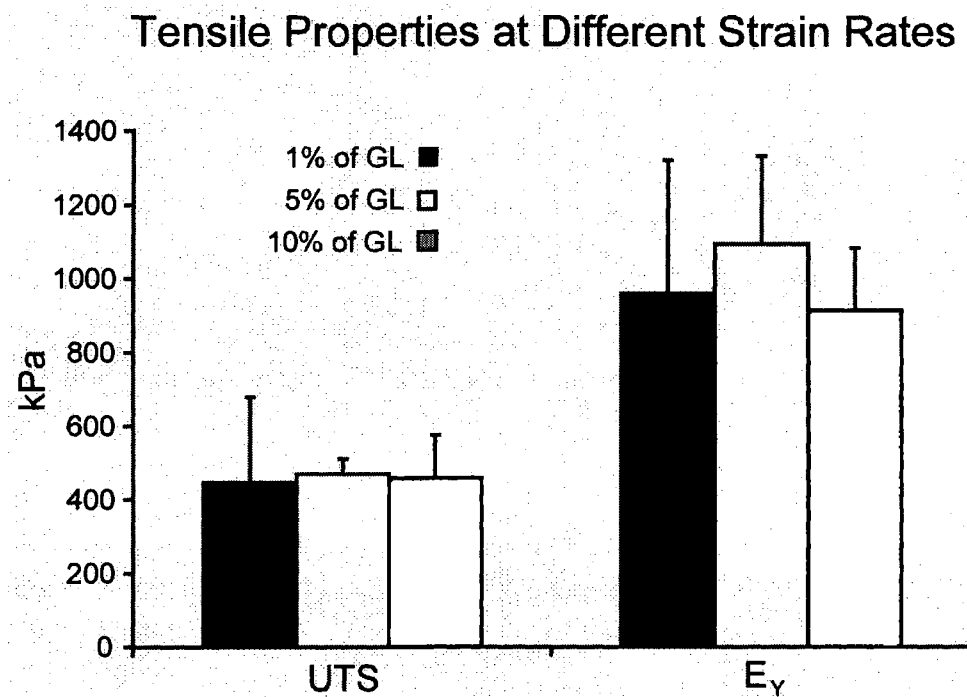
Figure A3-3: Construct tensile properties at different strain rates

Figure A3-3: Comparison of construct ultimate tensile strength (UTS) and Young's modulus (E_Y) at three different strain rates (1%, 5%, and 10% of gauge length). Bars represent mean \pm S.D. ($n = 4-5$). There were no significant differences due to strain rate for either material property.

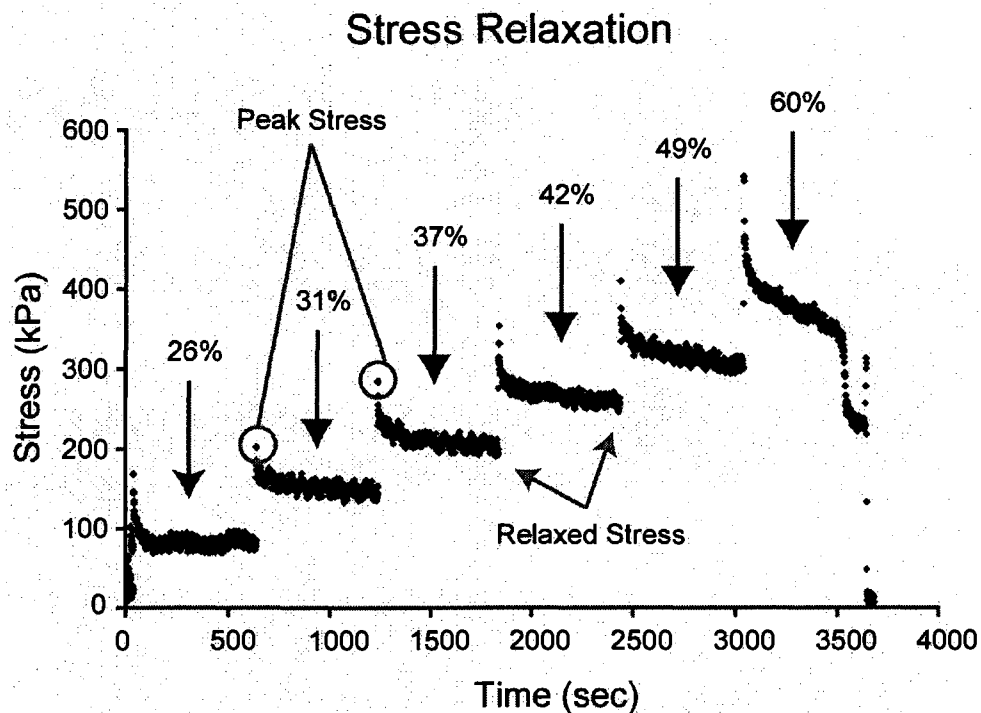
Figure A3-4: Stress-relaxation of a self-assembled construct

Figure A3-4: Representative stress-relaxation curve for a self-assembled construct. The arrows denote the part of the test for which the strain was held constant at the value given above the arrow. Peak stresses are plotted against strain level to obtain the instantaneous modulus, while relaxed stresses are plotted against strain level to obtain the relaxed modulus.

Appendix 4: Transmission electron microscopy images of self-assembled constructs*

Introduction

In this thesis it was demonstrated that chondroitinase-ABC (C-ABC) treatment of self-assembled articular cartilage tissue engineered constructs leads to increased tensile properties (Chapters 6 and 7). However, the mechanism by which this occurs remains unknown. One possibility is that C-ABC treatment leads to increased collagen fiber size or orientation. To investigate these possibilities, transmission electron microscopy (TEM) was performed on constructs from the first C-ABC study (Chapter 6).

Methods

Tissue processing of self-assembled constructs

Constructs were grown as described in Chapter 6. Samples for TEM were obtained from two separate constructs from each group, where the groups were 2 week control, 2 week C-ABC treatment, 4 week control, 4 week C-ABC treatment at 2 weeks. Briefly, 1.5 mm diameter punches were taken from the outer annulus remaining after coring out the 3 mm diameter center used for indentation testing. The 1.5 mm diameter punches were then fixed with a solution containing 3% glutaraldehyde plus 2% paraformaldehyde in 0.1 M cacodylate buffer, pH 7.3. The large difference between the punch diameter and construct thickness allowed orientation to be maintained such that samples could

*I acknowledge the Institutional Core Grant #CA16672 High Resolution Electron Microscopy Facility, UTMDACC and Kenneth Dunner, who prepared and imaged the samples.

be sectioned and examined in both longitudinal and cross-sectional orientations. Fixed samples were stained overnight with 1% cupromeronic blue (US Biological, Swampscott, MA) in 0.2 M acetate buffer (pH 5.6) containing 0.3 M MgCl_2 . Following rinsing in the acetate buffer, specimens were placed in 0.5% Na_2WO_4 overnight.

Transmission electron microscopy

Samples were dehydrated in increasing concentrations of ethanol and then infiltrated and embedded in LX-112 medium. The samples were then polymerized in a 70°C oven for 2 days. Ultrathin sections were cut in a Leica Ultracut microtome (Leica, Deerfield, IL), stained with uranyl acetate and lead citrate in a Leica EM Stainer, and examined in a JEM 1010 transmission electron microscope (JEOL, USA, Inc., Peabody, MA) at an accelerating voltage of 80 kV. Digital images were obtained using AMT Imaging System (Advanced Microscopy Techniques Corp, Danvers, MA).

Results

Figure A4-1 shows representative TEM images. Going across the page are images of increasing magnification. Going down the page are the four groups examined in this study. With the exception of the 2 week C-ABC treated group, the black staining of glycosaminoglycans (GAGs) by cupromeronic blue is evident. Collagen molecules were also present in all groups, but collagen fibers, determined by the presence of banding (Fig. A4-2), were extremely rare, making

measurement of diameters impractical. Further, there were no discernable differences between longitudinal and cross-sectional orientations.

Discussion

This appendix examined whether TEM could be used to uncover differences in collagen fiber diameter or collagen orientation in self-assembled constructs following C-ABC treatment. Collagen molecules were present in all images, but overt fibers were rare. Further, the lack of differences between the cross-sectional and longitudinal sections suggests that orientation was not present at this scale. Despite these findings, the TEM images were useful in demonstrating that GAG is depleted by C-ABC treatment and returns with additional time in culture. These data corroborate the histological and quantitative biochemical findings of Chapters 6 and 7.

TEM has been used to study collagen fiber diameter and orientation in tissue^{4,133,264} and tissue engineered constructs.^{119,161,267,504} With respect to articular cartilage tissue engineering, studies have shown effects on collagen diameter by modulation of culture conditions. Treatment of articular chondrocytes cultured in alginate with β -aminopropionitrile (BAPN; an inhibitor of the crosslinking enzyme lysyl oxidase) increased collagen fiber diameter from 62 nm to 109 nm,⁵⁰⁴ and knockdown of the small proteoglycan lumican with antisense RNA increased collagen diameter from 27 nm to 31 nm in polyglycolic acid (PGA) scaffolds seeded with bovine nasal chondrocytes.²⁶⁷ The high density of GAG staining in the present study may have precluded successful visualization

of some elements of the collagen network. Future work should examine longer time points to see if collagen fibers develop.

Figure A4-1: Representative TEM images

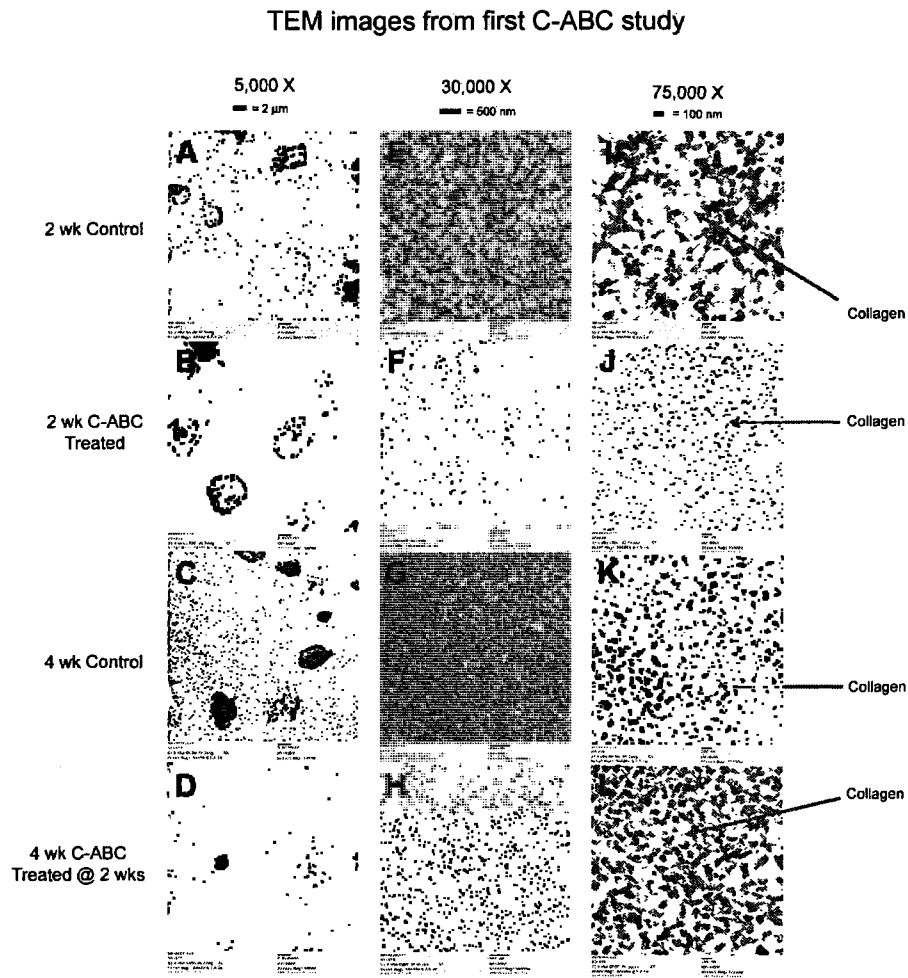


Figure A4-1: Representative TEM images for the first C-ABC study. 2 week control (A, E, I), 2 week C-ABC treatment (B, F, J), 4 week control (C, G, K), 4 week C-ABC treatment at 2 weeks (D, H, L). A-D magnification 5,000 X, E-H magnification 30,000 X, I-L magnification 75,000 X. Cupromeronic blue stains glycosaminoglycans (GAGs) black. At 2 weeks, C-ABC treated specimens show GAG loss and a denser collagenous matrix. Between 2 and 4 weeks, the constructs deposit extracellular matrix, resulting in increased spacing between cells (A & B versus C & D). Additionally, GAG staining returns to the matrix in the C-ABC treated group over 2 weeks of culture (F & J versus H & L). Collagen molecules are evident in each group (grayish members indicated by red arrows).

Figure A4-2: Select TEM image showing a collagen fiber

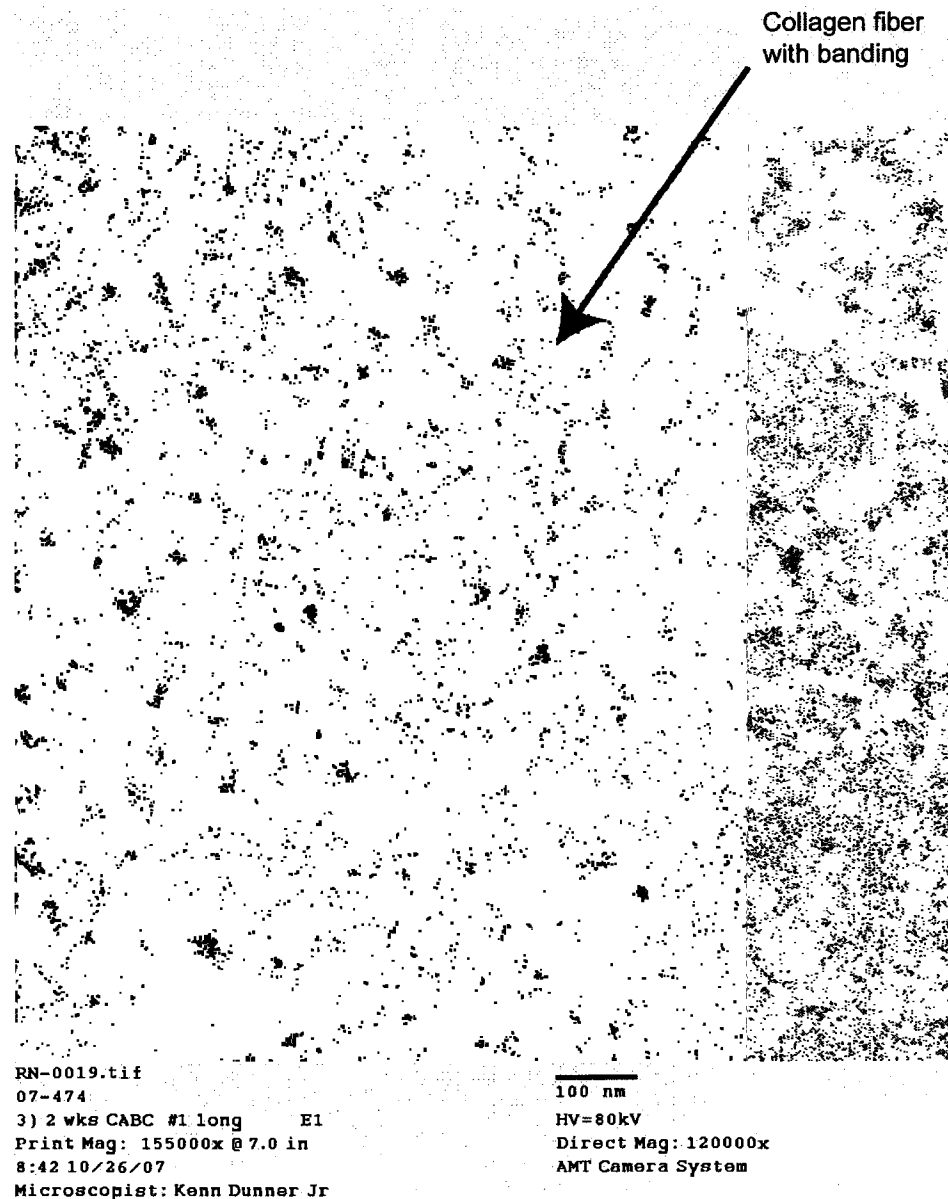


Figure A4-2: Select TEM image from the 2 week C-ABC treated group showing a collagen fiber demonstrating the typical banding pattern. In general, collagen fibers were not found. (Magnification = 120,000 X; scale bar 100 nm)